Australian Government

Australian Centre for International Agricultural Research

Australian Aid

# Population Structure of Yellowfin Tuna (*Thunnus albacares*) and Bigeye Tuna (*T. obesus*) in the Indonesian Region

## FINAL REPORT

## ACIAR Project FIS/2009/059

KEMENTERIAN KELAUTAN DAN PERIKANAN

CSL central science laboratory

UNIVERSITY of TASMANIA

CODES ARC CENTRE OF EXCELLENCE IN ORE DEPOSITS

THE UNIVERSITY OF QUEENSLAND AUSTRALIA

Pacific Community Communauté du Pacifique

CSIRO

The Australian Centre for International Agricultural Research (ACIAR) was established in June 1982 by an Act of the Australian Parliament. Its mandate is to help identify agricultural problems in developing countries and to commission collaborative research between Australian and developing country researchers in fields where Australia has special research competence.

Australian Centre for International Agricultural Research
GPO Box 1571, Canberra, Australia 2601
www.aciar.gov.au

This publication is an output of ACIAR Project FIS/2009/059:
*Developing research capacity for management of Indonesia's pelagic fisheries resources.*

**Suggested citation:**

Proctor C. H., Lester R. J. G., Clear N. P., Grewe P. M., Moore B. R., Eveson J. P., Lestari P., Wujdi A., Taufik M., Wudianto, Lansdell M. J., Hill P. L., Dietz C., Thompson J. M., Cutmore S. C., Foster S. D, Gosselin T. and Davies C. R. (2019). Population structure of yellowfin tuna (*Thunnus albacares*) and bigeye tuna (*T. obesus*) in the Indonesian region. Final Report as output of ACIAR Project FIS/2009/059. Australian Centre for International Agricultural Research, Canberra. 139 pp.

ISBN: 978-0-646-80325-8

## Author affiliations

Commonwealth and Scientific and Industrial Research Organisation (CSIRO), Australia:

Craig Proctor, Naomi Clear, Peter Grewe, Paige Eveson, Matt Lansdell, Peta Hill (formerly CSIRO, now UTas), Campbell Davies

Centre for Fisheries Research, Indonesia:

Wudianto

Research Institute for Marine Fisheries, MMAF, Indonesia:

Pratiwi Lestari, Muhammad Taufik

Research Institute for Tuna Fisheries, MMAF, Indonesia:

Arief Wujdi

School of Biological Sciences, University of Queensland, Australia:

Robert Lester, Scott Cutmore

Central Science Laboratory, University of Tasmania, Australia:

Chris Dietz

Centre for Ore Deposit and Earth Sciences, University of Tasmania, Australia:

Jay Thompson

Pacific Community (SPC), New Caledonia:

Brad Moore (also affiliated with University of Tasmania)

Department of Biology, Laval University, Quebec, Canada:

Thierry Gosselin

## Acronyms

| | |
|---|---|
| AMAFRAD | Agency for Marine and Fisheries Research and Development (Indonesia) |
| AMAFRHR | Agency for Marine and Fisheries Research and Human Resources (Indonesia) |
| BET | Bigeye Tuna |
| CFR | Centre for Fisheries Research |
| CODES | Centre for Ore Deposit and Earth Sciences (University of Tasmania) |
| CSL | Central Science Laboratory (University of Tasmania) |
| DGCF | Directorate General of Capture Fisheries (Indonesia) |
| FMA | Fisheries Management Area |
| IBIS | Institute for Integrative Biology and Systems, Laval University, Canada |
| IO | Indian Ocean |
| IOTC | Indian Ocean Tuna Commission |
| NGO | Non Government Organisation |
| RFMO | Regional Fisheries Management Organisation |
| RIMF | Research Institute for Marine Fisheries (Indonesia) |
| RITF | Research Institute for Tuna Fisheries (Indonesia) |
| RIFEC | Research Institute for Fisheries Enhancement and Conservation (Indonesia) |
| RCFMC | Research Centre for Fisheries Management and Conservation (Indonesia) |
| RCCF | Research Centre for Capture Fisheries (Indonesia) |
| SPC | Secretariat of the Pacific Community |
| WCPFC | Western and Central Pacific Fisheries Commission |
| WCPO | Western and Central Pacific Ocean |
| YFT | Yellowfin Tuna |

# Contents

## Acknowledgements

Firstly, we wish to thank the many staff of Port Authority Offices and local fisheries offices (Offices of *Dinas Kelautan dan Perikanan*) in Indonesia who assisted in the two rounds of sampling for this project's population structure study. We are also grateful to all in the tuna fishing industry who provided assistance in the purchase of the fish and also to the vessel owners, skippers and traders who provided information on catch locations.

We are similarly grateful to Mr Ahmed Riyaz Jauhary, Ms Shafiya Naeem, and Dr Shiham Adam of Marine Research Centre, Malé, The Maldives, and to Ms Cynthia Wickham, Ms June Kwanairara, Mr John Teri and Mr Adrian Wickham and other staff of the Tri Marine Group and affiliated National Fisheries Developments Ltd (NFD) in Noro, Solomon Islands, for assistance for the tuna sampling. Dr Mike Batty, Director of Fisheries Development at the Forum Fisheries Agency and Mr Simon Diffey, former Institutional Development Advisor for the Mekem Strong Solomon Islands Fisheries Programme, are also thanked for their invaluable assistance for the Solomon Islands sampling.

The following scientists are thanked for their participation in the field sampling: Prof. Wudianto (CFR), Mr Anung Agustinus Widodo (CFR), Mr Mohamad Natsir, Mr Mahiswara (RIMF), Mr Irwan Jatmiko (RITF), Dr Erfind Nurdin (RIMF), Mr Mujiyanto (RIFEC), and Dr Dale Kolody (CSIRO).

We thank Mr Scott Cooper (CSIRO) for his assistance in establishing a relational database for accommodating all the data related to the many samples collected and analysed.

Ms Prihatiningsih, Ms Pustika Ratnawati, Ms Wahyuni Nasution, Ms. Atiah and Ms. Arlini Batubara (all scientific staff of RIMF), Ms. Astri Wulandri (RIFEC), and Ms. Fenni Eddrisea (coordinator of Training, RIMF) are thanked for their assistance in the dissections for parasite investigations.

The following current and former Directors and Heads of the Indonesian research institutes are thanked for their roles and contributions to the project (institutions at time of involvement in parentheses): Dr Toni Ruchimat (CFR), Dr Purwanto (RCFMC), Dr Duto Nugroho (RCFMC), Prof. Hari Eko Irianto (CFRD), Dr Ali Suman (RIMF), Dr Fayakun Satria (RIMF), Mr Zulkarnaen Fahmi (RITF) and Mr Budi Nugraha (RITF). We also thank Dr Subhat Nurhakim (former Director of RCCF) and to Dr Chris Barlow (former ACIAR Fisheries Program Manager) for their contributions to the planning of the project and to Dr Barlow for his support through the project's course.

We thank Prof. Leonid Danyushevsky of the laser-ablation ICP-MS laboratory at Centre for Ore Deposits and Earth Sciences at University of Tasmania (UTas) for his inputs and assistance for the elemental analyses of the tuna otoliths. We are also grateful to Ms. Christine Cook of the Isotope Ratio Mass Spectrometry laboratory, Central Science Laboratory, University of Tasmania (UTas), for her assistance with the stable isotope analyses of the otoliths. Assoc. Prof. Thomas Cribb and Dr Russell Yong of the School of Biological Sciences, University of Queensland, are thanked for their contributions to the parasites component of the population structure study including their inputs into training provided to our parasites research trainee, Ms Pratiwi Lestari (RIMF).

Finally, we thank Ms. Mirah Nuryati, Ms Maria Ludwina, and Ms. Fitri Apriliyani of ACIAR Country Office and Ms. Sunny Apriyani of CFR for their assistance through this project and particularly for guidance and assistance through the arduous process of RISTEK Foreign Researcher Permit and KITAS visa applications.

# 1. Executive summary

***The study:*** Population structure of yellowfin tuna (*Thunnus albacares*) and bigeye tuna (*T. obesus*) in the Indonesian region.

### *Key issues*

Indonesia's pelagic fisheries resources are of considerable importance to the nation's economy and as an important source of protein for Indonesia's large population of 261 million people. Two species of critical importance to Indonesia and to neighbouring countries in the Indian and Western Pacific Ocean regions are yellowfin tuna (*Thunnus albacares*) and bigeye tuna (*Thunnus obesus*), and together accounted for around 6.3% of total value of Indonesia's capture fisheries commodities in 2015 (MMAF 2016). Current assessments and management strategies are based on assumptions of single, separate Indian Ocean and Western Pacific Ocean stocks of both species. Understanding of connectivity of these species across the Indonesian archipelago and adjoining oceans was considered a high priority for improved management.

### *Primary objective*

The overall objective of the 'mother project'[1], of which the population structure study was one of two main components, was to improve Indonesia's capacity to assess and manage its tuna fisheries by addressing key information gaps, particularly for yellowfin tuna (YFT) and bigeye tuna (BET), and to improve Indonesia's pelagic fisheries research capacity. The immediate objective of this study was to define the population structures of YFT and BET in Indonesia's archipelagic waters and connectivity with adjoining regions; and to communicate the study's findings and recommendations to the Indonesian and international science and policy communities.

### *Methodologies*

Three independent, complementary techniques – genetics (next generation sequencing and Single Nucleotide Polymorphism markers), otolith chemistry[2] (analyses of stable isotopes and elements) and occurrence of parasites – were used to determine the degree of population structure and connectivity of YFT and BET between the central Indian Ocean, Indonesian archipelagic waters (IAW) and Western Pacific Ocean.

### *Study outcomes*

The three techniques provided outcomes that were consistent with the inference of multiple populations for YFT and BET across the geographic range of the project. The outcomes of the genetics analyses suggested at least 2 or 3 genetic groupings for both species, with clines of genetic variation across the geographic range. The patterns of distribution of parasites suggested limited movement of fish (both species) westwards from the IAW into the eastern Indian Ocean, and also little movement from the Western Pacific Ocean westwards into the Indonesian archipelago, at least for the sizes examined (typically 30 – 50 cm fork length). The overall outcome from the otolith chemistry analyses was that the YFT and BET had not moved large distances in their first 4 – 6 months of life. These results suggest that the current national and regional governance arrangements are likely to be consistent with the structure and connectivity of YFT and BET populations. The study achieved capacity development

---

[1] *ACIAR Project FIS/2009/059 Developing research capacity for management of Indonesia's pelagic fisheries resources.*

[2] *Otoliths are structures in the inner ear that can be 'read', similar to the growth rings of trees, to determine factors such as the fish's age. The chemical composition of specific sections can be compared with geographic variation in ocean chemistry to indicate location at known ages and thus movement through time.*

for Indonesian scientists in the analytical fields of three techniques, in addition to skills associated with the large-scale sampling program.

### *Impacts anticipated*

The population structure study, albeit a 'first-look' investigation involving only the juvenile life-history stages of the two species, has outcomes that will be a valuable contribution to current considerations by Indonesia and Regional Fisheries Management Organisations (including as inputs into the structure of regional stock assessments) on appropriate management for these globally significant resources. The study's results will play a key role in defining future research activities to further investigate the degree of connectivity of the tuna populations in IAW and adjoining oceans, in particular the level of exchange with the WCPO. The capacity developments achieved in the project will ensure Indonesia's fisheries scientists play key, prominent roles[3] in the future research.

### *Recommendations*

This project demonstrated that the question of connectivity between IAW and adjacent oceans can be addressed through a combination of populations structure methods. Refining and extending these result through multi-year sampling of spawning adults and/or larvae and use of methods that provide more direct estimates of annual exchange between areas, such as close-kin Mark Recapture, should be a high priority for future work.

There is an ongoing need for capacity development for Indonesia's fisheries scientists in population/stock structure research, to build on what has been achieved in this study.

[3] *Several of the Indonesian scientists who were involved in this study have been applying the capacity they received in a current project: Population structure of IOTC species in the Indian Ocean: Estimation with Next Generation Sequencing Technologies and Otolith Microchemistry (Project PSTBS-IO) (funded by the European Union through FAO and IOTC).*

# Ringkasan eksekutif (Bahasa Indonesia)

***Studi:*** Struktur populasi madidihang (*Thunnus albacares*) dan tuna mata besar (*T. obesus*) di wilayah Indonesia.

## *Isu kunci*

Sumber daya perikanan pelagis merupakan sumber daya yang sangat penting bagi perekonomian dan sebagai sumber protein bagi penduduk Indonesia yang berjumlah sangat besar sekitar 261 juta orang. Terdapat 2 jenis ikan tuna yang sangat penting bagi Indonesia dan negara-negara tetangga di kawasan Samudra Hindia dan Pasifik Barat yaitu madidihang (*Thunnus albacares*) dan tuna mata besar (*Thunnus obesus*), dimana keduanya menyumbang sekitar 6,3% dari total nilai komoditas perikanan tangkap Indonesia pada tahun 2015 (KKP, 2016). Kajian dan strategi pengelolaan saat ini didasarkan pada asumsi bahwa untuk kedua jenis ikan tuna tersebut masing-masing memiliki stok yang berbeda untuk perairan Samudra Hindia dan Samudra Pasifik Barat.. Pemahaman tentang konektivitas spesies-spesies ini di seluruh perairan kepulauan Indonesia dan samudra yang berdampingan dianggap sebagai prioritas penting bagi peningkatan pengelolaan jenis ikan tuna tersebut.

## *Tujuan utama*

Tujuan menyeluruh dari 'proyek induk', di mana studi struktur populasi merupakan salah satu dari dua komponen utama, yang mana untuk meningkatkan kapasitas Indonesia dalam mengkaji dan mengelola perikanan tuna dengan cara mengurangi kesenjangan informasi kunci, terutama untuk madidihang (YFT) dan tuna mata besar (BET), dan untuk meningkatkan kapasitas penelitian perikanan pelagis di Indonesia. Tujuan langsung dari penelitian ini adalah untuk menentukan struktur populasi madidihang (YFT)dan tuna mata besar (BET) di perairan kepulauan Indonesia (IAW) dan konektivitasnya dengan wilayah perairan samudera yang berdampingan; dan untuk mengkomunikasikan temuan-temuan dan rekomendasi penelitian kepada komunitas ilmiah dan penentu kebijakan baik di Indonesia maupun internasional.

## *Metodologi*

Tiga metode analisis independen, yang saling melengkapi - genetika (“next generation sequencing” dan “Single Nucleotide Polymorphism markers”), kimia otolit (analisis isotop dan elemen yang stabil) dan keberadaan parasit - digunakan untuk menentukan tingkat struktur populasi dan konektivitas/keterkaitan ikan YFT dan BET yang berada di Samudra Hindia tengah, perairan kepulauan Indonesia (IAW) dan Samudra Pasifik Barat.

## *Hasil studi*

Tiga teknik analisis memberikan hasil yang konsisten dengan inferensi beberapa populasi untuk YFT dan BET di seluruh rentang geografis proyek ini. Hasil dari analisis genetika menyarankan setidaknya terdapat 2 atau 3 pengelompokan genetik untuk kedua spesies, dengan garis keturunan variasi genetik di seluruh rentang geografis. Pola distribusi parasit mengidikasikan terjadi pergerakan terbatas kedua spesies ikan (YFT dan BET) ke arah barat dari IAW ke Samudra Hindia bagian timur, dan juga sedikit pergerakan dari Samudra Pasifik Barat ke barat ke perairan kepulauan Indonesia, setidaknya untuk ukuran yang diteliti (panjangnya 30 - 50 cm FL). Hasil keseluruhan dari analisis kimia otolit menunjukan bahwa YFT dan BET tidak bergerak jarak jauh dalam 4 - 6 bulan pertama kehidupan mereka. Hasil ini menunjukkan bahwa pengaturan tata kelola nasional dan regional saat ini masih konsisten dengan struktur dan konektivitas populasi YFT dan BET. Studi ini dapat meningkatkan kemampuan (kapasitas) bagi para peneliti Indonesia di bidang tiga teknik analisis, dan juga keterampilan yang terkait dengan program pengambilan sampel skala besar.

### *Dampaknya sudah diantisipasi*

Studi struktur populasi, meskipun investigasi 'pandangan pertama' yang hanya melibatkan tahap sejarah kehidupan juvenil dari dua spesies, memiliki hasil yang akan memberikan kontribusi berharga bagi pertimbangan saat ini bagi Indonesia dan Organisasi Manajemen Perikanan Regional/RFMO (termasuk sebagai masukan ke dalam struktur kajian stok regional) tentang pengelolaan yang tepat untuk sumber daya perikanan yang signifikan secara global. Hasil penelitian ini akan memainkan peran kunci dalam menentukan tahapan kegiatan penelitian di masa depan untuk meneliti lebih lanjut tingkat konektivitas populasi tuna di IAW dan samudera yang berdekatan, khususnya tingkat pertukaran/percampuran dengan WCPO. Pengembangan kapasitas yang dicapai dalam proyek ini akan memastikan para peneliti perikanan Indonesia memainkan peran penting dalam penelitian di masa mendatang.

### *Rekomendasi*

Proyek ini menunjukkan bahwa pertanyaan tentang konektivitas antara IAW dan perairan samudera yang berdekatan dapat dijelaskan melalui kombinasi metode penentuan struktur populasi. Memperbaiki dan memperluas hasil kajian ini melalui pengambilan sampel beberapa tahun untuk ikan dewasa yang telah melakukan pemijahan dan / atau larva dan penggunaan metode yang memberikan perkiraan lebih langsung dari pertukaran tahunan antar perairan, seperti “Close-Kin Mark Recapture”, harus menjadi prioritas tinggi untuk pekerjaan di masa depan.

Terdapat kebutuhan yang berkelanjutan/terus menerus untuk pengembangan kapasitas bagi para peneliti perikanan Indonesia dalam penelitian struktur populasi / stok, untuk membangun/meningkatkan apa yang telah dicapai dalam penelitian ini.

# 2. Introduction

Indonesia's tuna fisheries resources are of high importance to the nation's economy and as a domestic food resource, and includes production from several gear types in both commercial and small-scale/artisanal sectors. The Indonesian tuna fisheries span a broad geographical range including the eastern and north eastern Indian Ocean, the Indonesian archipelago, and into the Western Pacific Ocean. Combined overall catch of the four most important tuna species - skipjack (*Katsuwonus pelamis*), yellowfin tuna (*Thunnus albacares*), bigeye tuna (*T. obesus*) and albacore tuna (*T. alalunga*) - in 2016 was 657,582 tonnes[4], based on combined figures of Indonesia's reports to the Scientific Committees of Indian Ocean Tuna Commission (IOTC) and Western and Central Pacific Fisheries Commission (WCPFC) in 2017 (Ruchimat et al. 2017; MMAF-RI 2017). Both in terms of catch volume of these *large pelagic fish* (as they are referred to Indonesian fisheries statistics) and fleet size (all gears combined), Indonesia is one of the largest tuna fishing nations in the world.

In 2015, the combined value of Indonesian production of yellowfin tuna (YFT) and bigeye tuna (BET), to both export and domestic markets, amounted to IDR 6,897 billion (~AU$690 mill.), around 6.3% of total value of Indonesia's capture fisheries commodities (MMAF 2016). These two species are also important to fisheries of country neighbours in the Indian Ocean (IO) and Western and Central Pacific Ocean (WCPO) regions. Stock assessments in these regions at time of development of this project (2010 – 2012) were that both YFT and BET, although overall were not overfished, may have been overfished in some areas (Langley et al. 2009; IOTC 2010; WCPFC 2010; Davies et al. 2011). IOTC and WCPFC had recommended there needed to be appropriate control of fishing pressures, and that accurate assessments of the stocks were difficult to make because of a serious lack of high-quality, validated information on the true scale of the catches of these tunas (juveniles in particular) by the Indonesian and Philippine fishing fleets. In keeping with Indonesia's increased participation in both RFMOs at that time, the (Indonesian) Agency for Marine and Fisheries Research and Development[5] (AMAFRAD) identified that filling information gaps surrounding these two important species in Indonesian waters, and the fisheries based on them, as high priority for the next phase of Indonesia–Australia collaboration on pelagic fisheries research. This was vital for developing Indonesia's internal fisheries management plans of action as well as making major contributions to the regional strategies developed through the RFMOs.

In considering the high priorities for achieving improved management of Indonesia's tuna fisheries, Indonesia's Ministry of Marine Affairs and Fisheries (MMAF), through the Directorate General of Capture Fisheries (DGCF) and AMAFRAD, identified the need for a better understanding of the amount of mixing between tuna stocks/populations across Indonesia's eleven Fisheries Management Areas (FMAs), and the degree of connectivity to stocks/populations in the IO and WCPO. YFT and BET were identified as the two highest priority species; research with high national importance for domestic fisheries management but also of international importance, for assisting improved assessments by the RFMOs.

Stock assessments for YFT and BET at time of development of this project were based on assumptions of separate, biologically distinct stocks of both species in the Indian Ocean and WCPO (Chiang et al. 2008; Davies et al. 2011; IOTC 2011; Langley et al. 2011) and those assumptions currently remain unchanged (Grewe et al. 2016; McKechnie et al. 2017; Tremblay-Boyer et al. 2017). The YFT and BET caught in Indonesian waters were treated as IO fish if landed at ports and landing places within the IOTC Statistical Area (principally western Indonesia) and as WCPO fish is landed at ports within the

*[4] This combined catch figure excludes albacore caught by Indonesian vessels in the WCPFC statistical area, as the albacore catch has been under review (MMAF 2017a).*

*[5] AMAFRAD is now AMAFRHRD (Agency for Marine and Fisheries Research and Human Resources Development) is the research arm of Indonesia's Ministry of Marine Affairs and Fisheries.*

WCPFC Statistical Area (principally eastern Indonesia). However, the results of some genetic (Grewe et al. 2000; Appleyard et al. 2002; Dammannagoda et al. 2008) and otolith chemistry (Wells et al. 2012) investigations began to question the validity of these assumptions, suggesting meta-population structure across relatively small spatial scales. Tagging studies in Hawaiian Islands region had demonstrated retentive behaviours of YFT and suggested that long-distance (>1000 km) movements by this species were rare (Itano and Holland 2000).Tagging of both YFT and BET in the WPO, including in eastern Indonesian archipelagic waters (SPC 2012) in 2009 – 2010, also suggested the extent of spatial movements and regional mixing by these tuna species may not be as extensive as earlier thought.

With advances in genetic analytical techniques and emergence of next generation sequencing (Allendorf et al. 2010; Davey et al. 2011; Nielsen et al. 2012; Peterson et al. 2012), there was strong agreement on both Indonesian and Australian sides that this next phase project should examine the level of heterogeneity across the region. However, in recognition of the strengths in using a multi-technique approach to elucidating stock/population structures for fish species, we decided on using not only the new genetic technologies but also otolith chemistry analyses and parasites characterisation. These two latter techniques had proven their worth in investigations of stock structures of other species (Lester et al. 2001; Rooker et al. 2003; Rooker et al. 2008; Lester and MacKenzie 2009; Schloesser et al. 2010; Zeigler and Whitledge 2011; Moore et al. 2012) and, in some earlier studies of pelagic species, the three techniques had been used together, drawing on the strengths of each but also recognising their respective limitations (Gunn et al. 2002; Buckworth et al. 2007; Welch et al. 2009). The key advantage of using a multi-technique approach is that each method is informative about the fish's life history at different spatial and temporal scales. Genetics has the potential to inform about the evolutionary patterns as well as rates of mixing of fish from different regions, whereas parasites and otolith chemistry are directly influenced by factors including the environment and individual fish physiology and so have potential to inform about the patterns of movement during the fishes lifetime. Growth patterns are influenced by both genetic and environmental factors. Due to these differences, the use of these techniques in a holistic approach increases the chance of detecting different stocks where they exist (Buckworth et al. 2007; Welch et al. 2009).

At time of this project's initiation, two key developments had yet to emerge; developments that would greatly increase the potential for transition of this study's outputs to more highly significant impacts:

1. The "*Strategic plan for ACIAR engagement in capture fisheries research and capacity development in Indonesia, 2015–25*", developed by ACIAR and AMAFRAD in collaboration with ABARES and CSIRO (ACIAR Project FIS/2011/030). The plan was developed during 2012 – 2014 and released in 2015 (P4KSI and ACIAR 2015), and;
2. Harvest Strategy development for Indonesia's tuna fisheries. The development process commenced in late 2014.

This population structure study for YFT and BET comprised essentially half of the large ACIAR project FIS/2009/059, *Developing research capacity for management of Indonesia's pelagic fisheries resources.* The other half of the project was a study focused on various aspects of Indonesia's FAD[6]-based tuna fisheries, the outcomes of which are covered in a separate Final Report (Proctor et al. in prep).

The overall aim of project FIS/2009/059 was to improve Indonesia's pelagic fisheries research capacity, especially that related to management of its important tuna fisheries resources, and in

[6] *Fish Aggregating Devices – referring specifically to deepwater anchored FADs.*

particular in relation to YFT and BET. The immediate objectives of the project fell within three primary components: 1. defining the population structures of YFT and BET in Indonesia's archipelagic waters and connectivity to populations in adjoining regions; 2. assessing and characterising Indonesia's tuna fisheries that are based around FADs, and 3. the communication of the project's findings and recommendations.

## References (cited in Introduction)

Allendorf F. W., Hohenlohe P. A. and Luikart G. (2010). Genomics and the future of conservation genetics. Nat. Rev. Genet. 11, 697–709.

Appleyard S. A., Ward R. D., and Grewe P. M. (2002). Genetic stock structure of bigeye tuna in the Indian Ocean using mitochondrial DNA and microsatellites. J. Fish Biol. 60, 767–770.

Buckworth R. C., Newman S. J., Ovenden J. R., Lester R. J. G. and McPherson G. R. (2007). The stock structure of northern and western Australian Spanish mackerel. Final report, Fisheries Research and Development Corporation Project 1998/159. Department of Primary Industry, Fisheries & Mines, Northern Territory Government, Australia. Fishery Report 88, i–vi, 225 pp.

Chiang H-C., Hsu C-C., Wu G. C-C., Chang S-K. and Yang H-Y. (2008). Population structure of bigeye tuna (*Thunnus obesus*) in the Indian Ocean inferred from mitochondrial DNA. Fish. Res. 90, 305–312.

Dammannagoda S. T., Hurwood D. A. and Mather P. B. (2008). Evidence for fine geographical scale heterogeneity in gene frequencies in yellowfin tuna (*Thunnus albacares*) from the north Indian Ocean around Sri Lanka. Fish. Res. 90, 147–157.

Davies N., Hoyle S., Harley S., Langley A., Kleiber P., and Hampton J. (2011). Stock assessment of bigeye tuna in the Western and Central Pacific Ocean. Report to Scientific Committee of Western and Central Pacific Fisheries Commission, 7th Regular Session, 9 – 17 August 2011, Pohnpei, FSM. WCPFC-SC7-2011/SA-WP-02, 133 pp.

Davey J. W., Hohenlohe P. A., Etter P. D., Boone J. Q., Catchen J. M. and Baxter M. L. (2011). Genome-wide genetic marker discovery and genotyping using next-generation sequencing. Nat. Rev. Genet. 12, 499–510.

Grewe P. M., Appleyard S. A. and Ward R. D. (2000). Determining genetic stock structure of bigeye tuna in the Indian Ocean using mitochondrial DNA and DNA microsatellites. Report for the Fisheries Research and Development Corporation FRDC No. 97/122. Hobart: FRDC.

Grewe P. M., Irianto H. E., Proctor C. H., Adam M. S, Jauhary A. R., Schafer K., Itano D., Evans K., Killian A. and Davies C. R. (2016). Population structure and provenance of tropical tunas: recent results from high throughput genotyping and potential implications for monitoring and assessment. Submitted to the 12th Scientific Committee Meeting of Western and Central Pacific Fisheries Commission, Bali, 3 – 11 August 2016. WCPFC-SC12-2016-SA WP-01. 6 pp.

Gunn J. S., Clear N. P., Ward R. D., Appleyard S. A., Grewe P. M. and Innes B. H. (2002). The origins of recruits to the east coast yellowfin tuna fishery and the delineation of the structure of yellowfin stocks in the western Pacific. Final Report to the Fisheries Research Development Corporation, FRDC Project 94/022, 141 pp.

Itano D. G. and Holland K. N. (2000). Movement and vulnerability of bigeye (*Thunnus obesus*) and yellowfin tuna (*Thunnus albacares*) in relation to FADs and natural aggregation points. Aquatic Living Resources 13, 213–223.

IOTC (2010). Report of the Thirteenth Session of the IOTC Scientific Committee. Victoria, Seychelles, 6 – 10 December 2010. IOTC–2010–SC13–R: 224 pp.

IOTC (2011). Report of the Fourteenth Session of the IOTC Scientific Committee. Mahé, Seychelles, 12–17 December 2011. IOTC–2011–SC14–R[E]: 259 pp.

Langley A., Harley S., Hoyle S., Davies N., Hampton J. and Kleiber P. (2009). Stock assessment of yellowfin tuna in the western and central Pacific Ocean. Submitted to 5th Regular Session of the Scientific Committee of Western and Central Pacific Fisheries Commission, 10 – 21 August 2009, Port Vila, Vanuatu. WCPFC-SC5-2005/SA-WP-03. 125 pp.

Langley A., Hoyle S., and Hampton J. (2011). Stock assessment of yellowfin tuna in the Western and Central Pacific Ocean. Report to Scientific Committee of Western and Central Pacific Fisheries Commission, 7th Regular Session, 9 – 17 August 2011, Pohnpei, FSM. WCPFC-SC7-2011/SA-WP-03, 132 pp.

Lester R. J. G., Thompson C., Moss H. and Barker S. C. (2001). Movement and stock structure of narrow-barred Spanish mackerel as indicated by parasites. J. Fish Biol. 59, 833–842.

Lester R. J. G. and MacKenzie K. (2009). The use and abuse of parasites as stock markers for fish. Fish. Res. 97, 1–2.

MMAF – RI (2016). Capture Fisheries Statistics of Indonesia by Province, 2015. Publication of Directorate General of Capture Fisheries, Ministry of Marine Affairs and Fisheries, Indonesia. 401 pp.

MMAF – RI (2017). Indonesia's Annual Report to the Western and Central Pacific Fisheries Commission. Submitted to the 12th Regular Session of the WCPFC Scientific Committee. Rarotonga, Cook Island, 9 - 17 August 2017. 34 pp.

McKechnie S., Pilling G., and Hampton J. (2017). Stock assessment of bigeye tuna in the western and central Pacific Ocean. Report to Scientific Committee of Western and Central Pacific Fisheries Commission, 13th Regular Session, 9 – 17 August 2017, Rarotonga, Cook Islands. WCPFC-SC13-2017/SA-WP-05, 149 pp.

Moore B. R., Welch D. J., Newman S. J. and Lester R. J. G. (2012). Parasites as indicators of movement and population connectivity of a non-diadromous, tropical estuarine teleost: king threadfin *Polydactylus macrochir*. J. Fish Biol. 81, 230–252.

Nielsen E. E., Cariani A., Aoidh E. M., Maes G. E., Milano I., Ogden R., Taylor M., Hemmer-Hansen J., Babbucci M., Bargelloni L., Bekkevold D., Diopere E., Grenfell L., Helyar S., Limborg M. T., Martinsohn J. T., McEwing R., Panitz F., Patarnello T., Tinti F., Van Houdt J. K. J., Volckaert F. A. M., Waples R. S., FishPopTrace c., Albin J. E. J., Vieites Baptista J. M., Barmintsev V., Bautista J. M., Bendixen C., Bergé J.-P., Blohm D., Cardazzo B., Diez A., Espiñeira M., Geffen A.J., Gonzalez E., González-Lavín N., Guarniero I., Jeráme M., Kochzius M., Krey G., Mouchel O., Negrisolo E., Piccinetti C., Puyet A., Rastorguev S., Smith J. P., Trentini M., Verrez-Bagnis V., Volkov A., Zanzi A., and Carvalho G. R. (2012). Gene-associated markers provide tools for tackling illegal fishing and false eco-certification. Nature Communications 3, 851.

Peterson B. K., Weber J. N., Kay E. H., Fisher H. S. and Hoekstra H. E. (2012). Double Digest RADseq: An inexpensive method for DeNovo SNP discovery and genotyping in model and non-model species. Plos One 7, e37135.

P4KSI and ACIAR (Centre for Fisheries Research and Development, Indonesia, and Australian Centre for International Agricultural Research) (2015). Strategic plan for ACIAR engagement in capture fisheries research and capacity development in Indonesia, 2015–25. ACIAR Technical Reports No. 88. ACIAR: Canberra. 28 pp.

Rooker J. R., Secor D. H., Zdanowicz V. S., De Metrio G., Relini L. O. (2003). Identification of Atlantic bluefin tuna (*Thunnus thynnus*) stocks from putative nurseries using otolith chemistry. Fish. Oceanogr. 12, 75–84.

Rooker J. R., Secor D. H., DeMetrio G., Kaufman A. J., Rios A. B. and Ticina V. (2008). Evidence of trans-Atlantic movement and natal homing of bluefin tuna from stable isotopes in otoliths. Mar. Ecol. Prog. Ser. 368, 231–239.

Ruchimat T., Wudianto, Fahmi Z., Setyadji B. and Sadiyah L. (2017). Indonesia National Report to the Scientific Committee of the Indian Ocean Tuna Commission. IOTC-2017-SC20-NR09.

Schloesser R. W., Neilson J. D., Secor D. H., and Rooker J. R. (2010). Natal origin of Atlantic bluefin tuna (*Thunnus thynnus*) from the Gulf of St. Lawrence based on d13C and d18O in otoliths. Can. J. Fish. Aquat. Sci., 67, 563–569.

SPC (2012). Indonesian Tagging Report. Unpublished. 31 pp.

Tremblay-Boyer L., McKechnie S., Pilling G. and Hampton J. (2017). Stock assessment of yellowfin tuna in the western and central Pacific Ocean. Report to Scientific Committee of Western and Central Pacific Fisheries Commission, 13th Regular Session, 9 – 17 August 2017, Rarotonga, Cook Islands. WCPFC-SC13-2017/SA-WP-06, 125 pp.

WCPFC (2010). Summary Report of the Sixth Regular Session of the Scientific Committee of Commission for the Conservation and Management of Highly Migratory Fish Stocks in the Western and Central Pacific Ocean. Nuku'alofa, Tonga, 10–19 August 2010, 169 pp.

Welch D. J., Buckworth R. C., Ovenden J. R., Newman S. J., Broderick D., Lester R. J. G., Ballagh A. C., Stapley J. M., Charters R. A. and Gribble N. A. (2009). Determination of management units for grey mackerel fisheries in northern Australia. Final Report, Fisheries Research and Development Corporation Project 2005/010, Fishing & Fisheries Research Centre Technical report No. 4, Fishing & Fisheries Research Centre, James Cook University, Townsville, Australia, 158 pp.

Wells R. J. D., Rooker J. R. and Itano D. G. (2012). Nursery origin of yellowfin tuna in the Hawaiian Islands. Marine Ecology Progress Series 461, 187–196.

Zeigler J. M. and Whitledge G. W. (2011). Otolith trace element and stable isotopic compositions differentiate fishes from the Middle Mississippi River, its tributaries, and floodplain lakes. Hydrobiologia 661, 289–302.

# 3. Objectives

The primary research questions of this study can be generically summarised as follows:

1. Is there evidence of population structure in yellowfin tuna (YFT) and bigeye tuna (BET) across the Indonesian archipelago to the extent of justifying regional assessment and regional management?;
2. What is the level of connectivity between the tunas in eastern Indonesia waters and those in western Indonesia waters, and between those in Indonesian waters and those in adjacent oceanic regions—Western Pacific Ocean and Indian Ocean?

The specific objectives for the population structure study were:

1. Using three independent, complementary techniques (genetics, otolith chemistry and parasite loads), to determine the degree of population structure and connectivity of YFT and BET over a wide geographical range;
2. Advise, in consultation with the relevant RFMOs, on the implications of the results of the above investigation for approaches to assessment and management of fisheries harvesting these stocks;
3. Provide capacity development for Indonesian scientists in the aforementioned analytical techniques.

# 4. Sampling strategy

The following sections detail the field sampling of fish that provided the biological samples for the analyses of the three techniques – parasites, otolith chemistry and genetics, the fish dissection procedures, and direct age estimates on a subsample of the fish. Following these sections (Sections 4.1 – 4.3), the three techniques are presented as separate chapters (Sections 5 – 7).

## 4.1 Fish sampling

The YFT and BET upon which the genetics, otolith chemistry and parasites analyses were based, were sampled in two periods: late April – mid June 2013, and early June – late July 2014; periods that were sufficiently similar in season to enable an inter-annual comparison of 'signals' from the three techniques, without the impacts from seasonal differences. The samples were obtained from 11 fishing ports: 9 locations across the Indonesian archipelago and 2 'outlier' locations for comparison – the Maldives and the Solomon Islands. The Indonesian sampling ports (Figure 1) were Padang (West Sumatera), Palabuhanratu (West Java), Prigi (southern East Java), Kendari (SE Sulawesi), Gorontalo (North Sulawesi), Bitung (North Sulawesi), Ambon (Maluku), Sorong (West Papua), and Jayapura (Papua). Malé and Noro were the sampling ports for the Maldives and Solomon Islands respectively. The choice of ports for Indonesia was largely based on what would provide good representation across the nation's Fisheries Management Areas (FMAs) in which tuna fishing activity was known to occur. There were other areas that could have been included if budget and sufficient time had been available, including ports in provinces of Bali, West Nusa Tenggara, East Nusa Tenggara, and other locations in the provinces of Maluku and North Maluku.

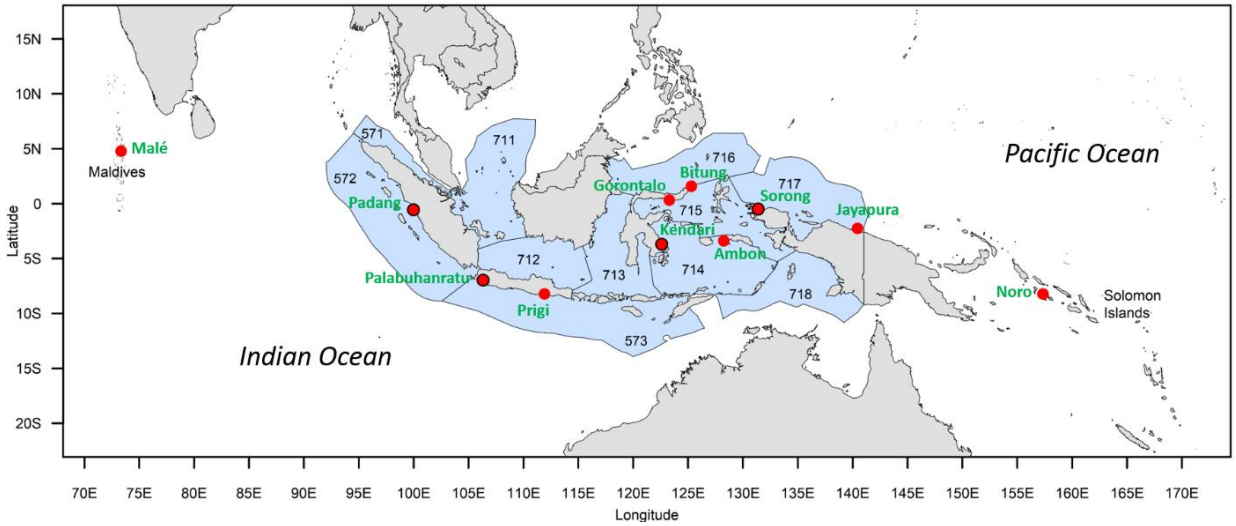


Figure 4.1. Map showing the location of fishing ports (red circles) where sampling was conducted for juvenile YFT and BET in 2013 and 2014. The four ports which were also location of enumeration for the FAD fisheries study are shown by red circles with black outline. The blue shaded areas with three digit numbers represent the 11 Indonesian Fisheries Management Areas (FMAs).

In both rounds of sampling, 2013 and 2014, the sampling strategy was the same. A protocol was drafted for the sampling in 2013 and used as the guideline for training for the sampling teams. The protocol (Appendix 1) was subsequently revised prior to the 2014 sampling. The target size range of fish sampled, for both YFT and BET, was 25 – 50cm FL. This size and age of fish (4 to 6 months – see below) was considered appropriate for this first look at population structure, as it was unlikely the fish would have moved large distances from their spawning locations. It is also a size of fish that is commonly landed by Indonesian purse-seine, pole and line, handline/troll-line and gill-net vessels, and so we had confidence that we could achieve the required samples at all sampling locations. This size of fish was also chosen because the juvenile YFT and BET were an important component of the

Indonesian fisheries and achieving more clarity around the true scale of catch of the juveniles had been voiced as a high priority by both IOTC and WCPFC. In an ideal world, this project would have sampled other size classes, including larvae and spawning adults, but largely for budget and time reasons, this was not possible.

Three sampling teams, each comprised of 3 scientists from Indonesia's fisheries research institutes[7] and/or CSIRO, left Jakarta simultaneously to sample at 3 Indonesian locations each, with 3 – 4 days required in each location. Assistance in procuring the fish in the Indonesian locations was provided by local Port Authorities and local fisheries officers. The Maldives and Solomon Islands were sampled by teams of 2 scientists, with assistance from staff of Marine Research Centre in Malé, Maldives, and staff of the companies Tri Marine and Kitano Cold Storage in Noro, Solomon Islands, respectively. The fish were sourced direct from fishing vessels at time of catch unloading, at point of sale (in fish auction places and from stalls in fish markets), or from distribution companies, and were hand-picked to achieve as best quality (in terms of fish condition) as possible.

The sampling teams were instructed, to as best as possible, spread the sampling across catches from multiple vessels during the 3 – 5 days of sampling at each location. This was aimed at achieving a representative sample for the landings of juvenile YFT and juvenile BET for each region. In general this was achieved, and the total sampled fish from each location were comprised of multiple "batches", with a "batch" being a sample from one vessel, or, in some cases, a sample from a fish distributor ('middle-man'). A negative aspect of this sampling strategy was the higher than expected variation in fishing locations among vessels at some ports, such as Kendari, resulting in samples from widely separated catch locations (Figure 5.2). Effort was made to obtain as best information as possible on the actual catch location of the fish sampled. This ranged from the most precise – latitude and longitude positions as provided by the GPS waypoints of skippers, to the least precise – approximate catch areas provided by skippers, vessel owners, fish distributors or agents.

## 4.2 Numbers of samples achieved and size distribution of fish

The original target for the sampling of this study was 100 YFT and 100 BET from each of the 11 sampling locations in the size range 25 – 50 cm FL. The size frequencies for the fish sampled and the numbers of fish sampled in both rounds of sampling (2013 and 2014) are presented in Figure 4.2 and Table 4.1 a & b respectively. For YFT this target was achieved, and in many cases surpassed (> 100 fish), at almost all locations in both rounds of sampling. Among the few cases where less than 100 YFT were sampled, the minimum was 73 (in Maldives in 2013). Achieving the target of 100 fish sampled for BET proved far more difficult than for YFT, at many of the 11 locations. Only on 4 of the 22 sampling visits to ports, across the two rounds of sampling, was the target achieved, with several of the locations in eastern Indonesia proving particularly difficult (e.g. Biting in 2013 and Gorontalo in 2014, with less than 5 BET able to be sampled).

[7] *Research Centre for Fisheries Management and Conservation (Jakarta) (now Centre for Fisheries Research), Research Institute for Marine Fisheries (Jakarta), Research Institute for Tuna Fisheries (Bali), and Research Institute for Fisheries Enhancement and Conservation (Jatiluhur).*

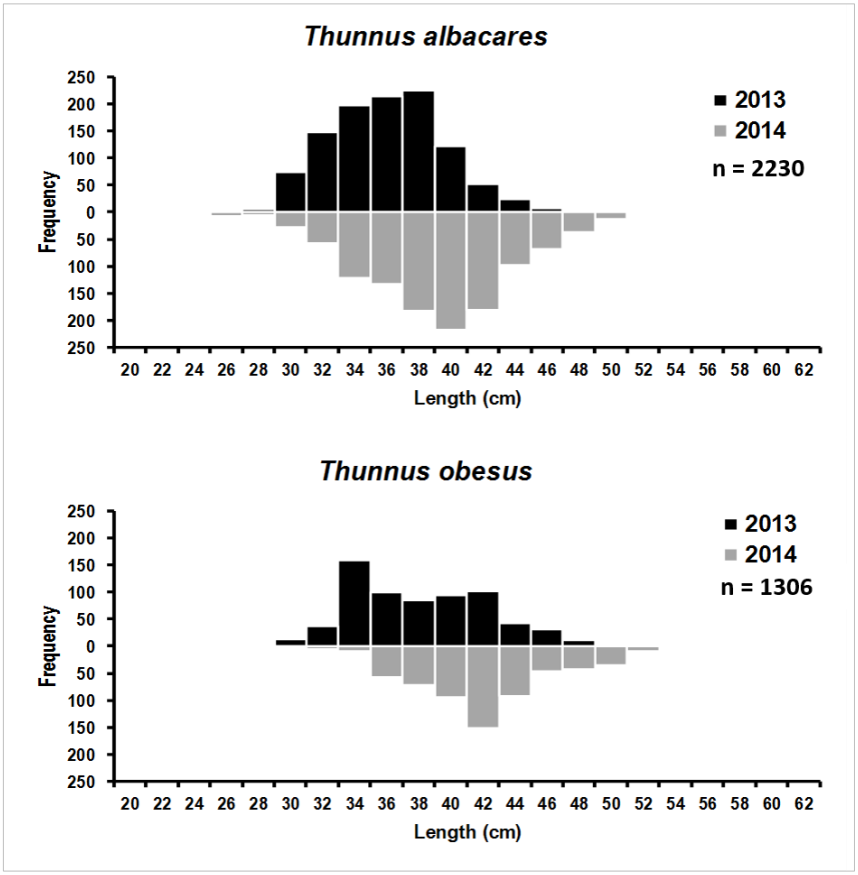


Figure 4.2. Length frequency distributions of YFT (*T. albacares*), and BET (*T. obesus*) sampled for this study, in 2013 (black) and 2014 (grey). Source: Sulistyaningsih (2017)[8].

Table 4.1.a. Numbers (n) of BET sampled for this study, by species and by year, for each sampling location.

| BET | | 2013 | 2013 | 2014 | 2014 |
|---|---|---|---|---|---|
| Location | Place | Length | n | Length | n |
| 1 | Padang | 32.5 - 40.0 | 124 | 30.0 - 50.0 | 97 |
| 2 | Palabuhanratu | 30.0 - 41.0 | 102 | 29.0 - 43.5 | 103 |
| 3 | Prigi | 28.0 - 42.0 | 36 | 30.5 - 45.0 | 43 |
| 4 | Kendari | 30.0 - 54.5 | 52 | 38.5 - 49.0 | 93 |
| 5 | Gorontalo | 34.5 - 58.5 | 68 | 46.0 | 1 |
| 6 | Bitung | 33.5 - 46.5 | 4 | 39.5 - 49.0 | 23 |
| 7 | Ambon | 32.0 - 48.5 | 57 | 39.0 - 47.0 | 60 |
| 8 | Sorong | 39.0 - 48.0 | 100 | 37.0 - 51.0 | 71 |
| 9 | Jayapura | 33.0 - 49.0 | 17 | 38.0 - 50.0 | 35 |
| 12 | Maldives | 34.0 - 43.5 | 44 | 26.0 - 62.0 | 49 |
| 13 | Solomon Is. | 35.0 - 48.5 | 75 | 38.0 - 54.0 | 52 |

[8] *Sulistyaningsih, R.K. (2017) The use of otolith shape to infer population structure of bigeye tuna, Thunnus obesus, and yellowfin tuna, Thunnus albacares, within the Indonesian archipelago and adjacent locations. Master of Applied Sciences thesis. Institute for Marine and Antarctic Studies, University of Tasmania, 2017. 49 pp.*

Table 4.1.b. Numbers (n) of YFT sampled for this study, by species and by year, for each sampling location.

| YFT | | 2013 | 2013 | 2014 | 2014 |
|---|---|---|---|---|---|
| Location | Place | Length | n | Length | n |
| 1 | Padang | 30.0 - 40.0 | 102 | 30.5 - 47.0 | 102 |
| 2 | Palabuhanratu | 29.5 - 43.0 | 102 | 30.0 - 46.5 | 100 |
| 3 | Prigi | 29.0 - 42.0 | 97 | 27.0 - 46.5 | 106 |
| 4 | Kendari | 30.5 - 50.0 | 100 | 34.5 - 47.5 | 105 |
| 5 | Gorontalo | 30.5 - 44.5 | 100 | 29.0 - 49.5 | 88 |
| 6 | Bitung | 29.0 - 56.0 | 100 | 29.5 - 48.0 | 104 |
| 7 | Ambon | 31.5 - 44.5 | 100 | 38.0 - 47.0 | 104 |
| 8 | Sorong | 36.5 - 44.0 | 100 | 39.0 - 50.0 | 106 |
| 9 | Jayapura | 31.0 - 42.5 | 100 | 34.0 - 47.0 | 108 |
| 12 | Maldives | 30.0 - 45.0 | 73 | 20.5 - 49.0 | 112 |
| 13 | Solomon Is. | 31.0 - 45.5 | 99 | 32.5 - 50.5 | 122 |

## 4.3 Fish dissection procedure

The dissection procedure was standard for both rounds of sampling of the juvenile YFT and BET. More detail, with illustrations, is available in the project's sampling protocol (Appendix 1). Following purchase, fish were placed on ice and taken to the place of processing (in some cases a lab provided by Port Authority, and in other cases a make-shift 'lab' at the local fisheries office. The fish were then processed individually, in form of a processing line, and beginning with confirmation of the species. Examination of the liver confirmed either YFT with one long liver lobe and no striations, or BET with no long liver lobe and presence of striations. The liver and other viscera (including stomach, intestines and pyloric caeca) were removed and placed together into a zip-lock plastic bag, and frozen for subsequent inspection for parasites. Fork length (FL) was then recorded for each fish to the nearest 0.5 cm, unless damaged. Otoliths (sagittae) were then removed with stainless steel forceps, using the "lifting the lid" technique (i.e. accessing the otoliths via removal of the top of the head). The otoliths were wiped clean with tissue and placed into individual, pre-labelled polyurethane vials. Left and right otoliths were placed together i.e. not into separate vials. Later in the day or evening, the lids of the vials were left open for 12 – 15 hrs to allow air drying.

Following otolith removal, a sample of muscle tissue was obtained from the upper body. The method of tissue sampling differed between years, but in both cases was designed to minimise risk of cross-contamination through inadvertent inclusion of fish 'slime' from the external body surface . In 2013, after cleaning the body surface with water and tissues, a scalpel was used to remove an ~ 1 $cm^2$ square of skin, and a cube of ~1 $cm^3$ of muscle tissue removed. In 2014, after cleaning the body surface, a sharp knife was used to take a thin slice of muscle tissue and the mouth of the vial used as a 'cookie-cutter' to achieve a small round of tissue of 9 mm diameter and approximately 4 – 5 mm in depth. In both years the tissue samples were placed into pre-labelled cryo-vials (2 ml, CRYO.S™, Greiner Bio-One) and preserved in RNAlater (an aqueous, non-toxic tissue and cell storage reagent that stabilizes and protects cellular RNA in intact, unfrozen tissue and cell samples), made to the recipe given in Appendix 2. The final step in processing was the removal of the gill 'basket', placed into a zip-lock plastic bag, and frozen for subsequent inspection for parasites.

## 4.4 Direct age estimates

### *4.4.1 Methods*

To determine the age of the fish collected for the study, and their approximate spawning dates, a subset of otoliths were selected for daily ageing. This is a direct method for determining age. Indirect methods, such as converting length to age using length-at-age keys, are subject to more uncertainties. Nineteen of the fish selected were between 39 and 42 cm FL, around the mean of the fish sampled and indicative of the length range of fish analysed for otolith chemistry. Four larger fish were selected for daily ageing, representing the largest fish among those sampled (Table 4.2).

Otoliths were prepared and read by Fish Ageing Services Pty Ltd. Thin, transverse sections of otoliths for daily age reading were prepared in a 4-step process. Firstly, the otolith was fixed on the edge (end) of a slide using thermoplastic mounting media (*crystalbond 509*) with the anterior side of the otolith hanging over the edge. Care was taken to ensure that the primordium was just on the inside of the glass edge. The correct alignment is critical to the quality of the section. If the primordium is too close to the slide edge there is a risk that the primordium may be removed in the initial grind and if set too far from the edge then there is a high chance that the primordium will be ground through in step 3. The otolith was then ground down to the edge using 400 and 800 grit wet and dry paper. The slide was then reheated and the otolith was removed and placed (ground side down) on another slide and the crystalbond was allowed to cool. Once cooled the otolith section was ground horizontally to the grinding surface using varying grades (800 & 1200 grit) of wet and dry sandpaper and finally 5um lapping film (Figure 4.3). During this process the otolith preparation was continuously checked and where necessary flipped to ensure that thickness was reached that allowed for the interpretation of the daily zones and that the remaining section still contained the primordium.

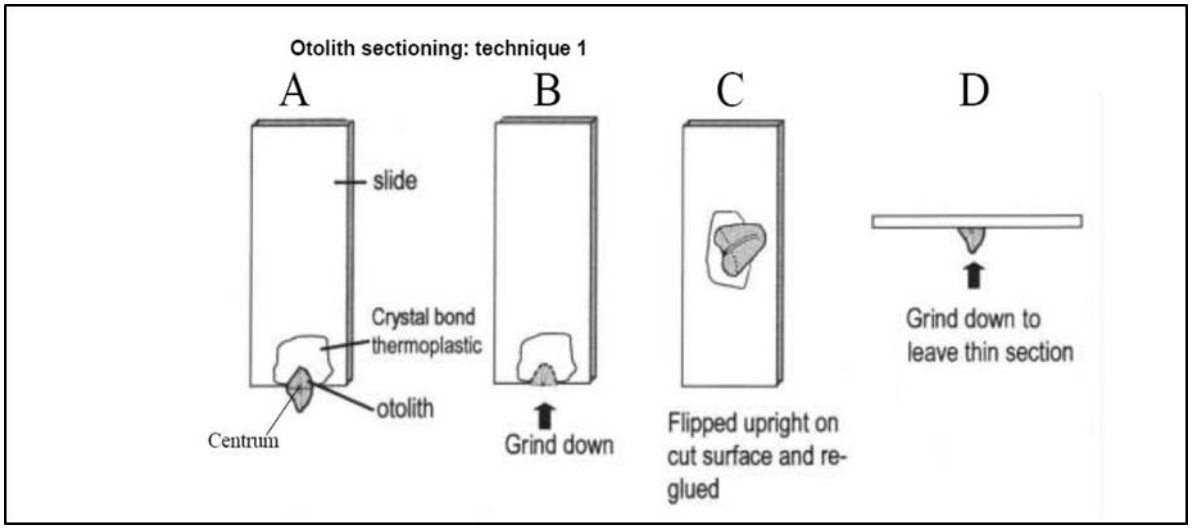


Figure 4.3. Illustration of the grinding process for preparation of transverse otolith thin sections (Source: Robbins and Choat[9], 2002).

Otoliths were viewed at between 100 to 400x magnification using a compound microscope illuminated with transmitted light. To conceal scratches and improve the clarity of the preparations, a small amount of immersion oil was first used to cover the top surface of the preparation.

For daily-age estimation, each otolith section was read at least twice by an experienced principal reader, and the average of the counts was used as the final age estimate, i.e. the age the fish was at capture. Counts were made from the primordium along the ventral (longer) arm of the section to the

[9] *Robbins, W.D. and Choat, J.H. (2002) Age-based dynamics of tropical reef fishes; A guide to the processing, analysis and interpretation of tropical fish otoliths. Townsville, Australia, p 1-39.*

margin (Figure 4.4) to produce an age in days. A readability score from 1 (poor) to 5 (excellent) was assigned by the otolith reader.

Zones widths were measured at four spots on the otolith (Figure 3) pertaining to the otolith chemistry analysis. These were:

Point 1 - 65 um out from primordia on ventral side;

Point 2 - first inflection, 30um from ventral edge;

Point 3 - 60 um in from margin;

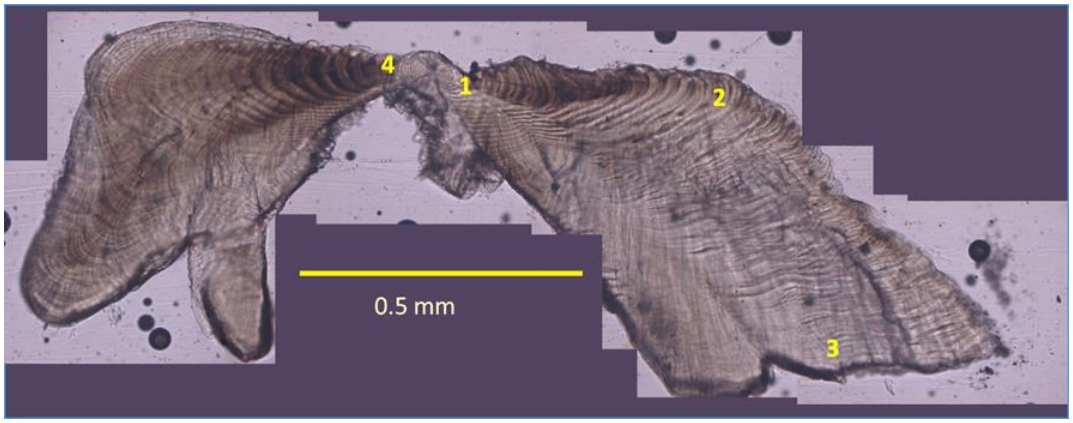


Figure 4.4. Counts of daily increments were made from the primordium along the ventral arm; and from the primordium to 4 points: 65 microns either side of the primordium (1 and 4), point 2 was at the first inflection, point 3 at the margin.

A customised image analysis system was used to age and measure zone widths. This system counts and measures manually marked increments and collects an image from each sample aged.

A CCD digital camera mounted onto the dissecting microscope (Leica MZ80) displayed a live image on the monitor. Using a customised image analysis system, a transect was drawn on the otolith image from the primordium to the desired end point. In this case two transects were drawn for each sample. One running from the primordium out to the first inflection and the second running from the primordium to a similar position on the dorsal side. The positions of the opaque zones along each transect were marked with a screen cursor and the numbers of zones marked and the subsequent distance between each mark along the transect was exported to a Microsoft database. The otolith image was automatically captured and exported, along with *x-y* coordinates of the marked zones, into the database. Two examples from the same specimen are shown below in Figure 4.5.

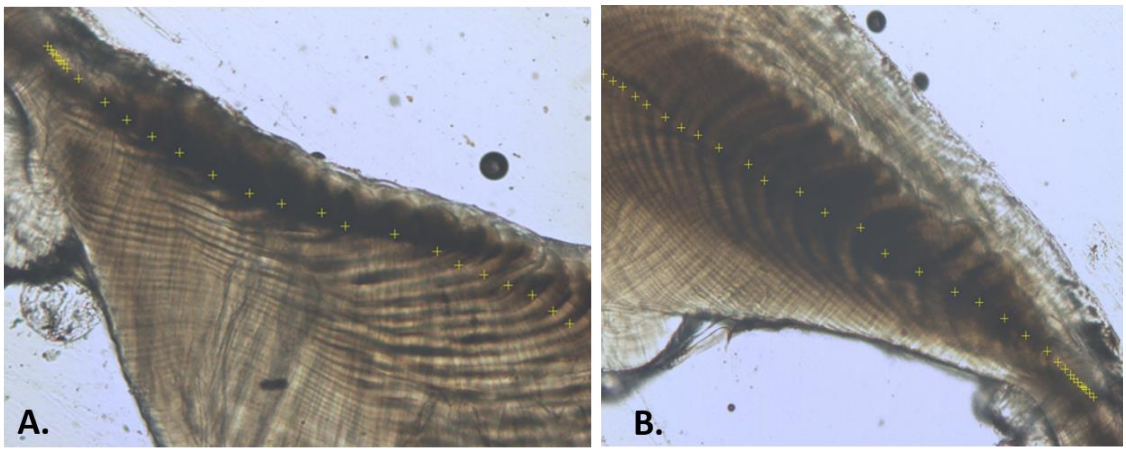


Figure 4.5 A) Positions of increments on the ventral side of the primordium of a BET otolith section and B) positions of increments on dorsal side of the same BET section, at 100 x magnification.

### 4.4.2 Results

Direct age estimates were made by counting daily increments on otolith sections. For the 9 bigeye that were chosen for daily ageing, fish lengths were 40-42 cm (approximating the length range chosen for elemental chemistry and stable isotope analysis) and the mean age was 135 days, or 4.5 months (see Table 4.2 and Figure 4.6). For the 10 yellowfin, fish lengths were 39-41 cm and the mean age was 118 days, or 3.9 months. The larger bigeye were 56.5 and 58.5 cm and aged at 234 days and 159 days respectively. The larger yellowfin were 53 cm and 56 cm and were aged at 205 days and 233 days.

Results of the examination of the otoliths at 4 spots are reported in the otolith chemistry section (Section 6).

Table 4.2. Samples from which daily age counts were made, daily age estimates and back-calculated spawning dates. LCF= Length to Caudal Fork.

| | species | LCF (cm) | sampling date | sampling location | increment count (days) | age (months) | back-calculated spawning date |
|---|---|---|---|---|---|---|---|
| 1 | yellowfin | 39 | 30/04/2013 | Padang | 107 | 3.6 | 13/01/2013 |
| 2 | yellowfin | 40 | 29/04/2013 | Padang | 108 | 3.6 | 11/01/2013 |
| 3 | yellowfin | 40 | 30/04/2013 | Sorong | 137 | 4.6 | 14/12/2012 |
| 4 | yellowfin | 40 | 30/04/2013 | Sorong | 113 | 3.8 | 7/01/2013 |
| 5 | yellowfin | 40 | 30/04/2013 | Sorong | 111 | 3.7 | 9/01/2013 |
| 6 | yellowfin | 53 | 30/04/2013 | Bitung | 205 | 6.8 | 7/10/2012 |
| 7 | yellowfin | 56 | 30/04/2013 | Bitung | 233 | 7.8 | 9/09/2012 |
| 8 | yellowfin | 40 | 24/06/2014 | Padang | 116 | 3.9 | 28/02/2014 |
| 9 | yellowfin | 40 | 25/06/2014 | Padang | 115 | 3.8 | 2/03/2014 |
| 10 | yellowfin | 40 | 25/06/2014 | Padang | 122 | 4.1 | 23/02/2014 |
| 11 | yellowfin | 40 | 17/06/2014 | Sorong | 117 | 3.9 | 20/02/2014 |
| 12 | yellowfin | 40 | 12/06/2014 | Jayapura | 130 | 4.3 | 2/02/2014 |
| 13 | bigeye | 41 | 3/05/2013 | Sorong | 132 | 4.4 | 22/12/2012 |
| 14 | bigeye | 41 | 4/05/2013 | Palabuhanratu | 124 | 4.1 | 31/12/2012 |
| 15 | bigeye | 41 | 30/04/2013 | Sorong | 146 | 4.9 | 5/12/2012 |
| 16 | bigeye | 42 | 25/04/2013 | Prigi | 143 | 4.8 | 3/12/2012 |
| 17 | bigeye | 57 | 25/04/2013 | Gorontalo | 159 | 5.3 | 17/11/2012 |
| 18 | bigeye | 59 | 25/04/2013 | Gorontalo | 234 | 7.8 | 3/09/2012 |
| 19 | bigeye | 40 | 23/06/2014 | Padang | 137 | 4.6 | 6/02/2014 |
| 20 | bigeye | 40 | 23/06/2014 | Padang | 136 | 4.5 | 7/02/2014 |
| 21 | bigeye | 40 | 25/06/2014 | Padang | 130 | 4.3 | 15/02/2014 |
| 22 | bigeye | 41 | 24/06/2014 | Ambon | 147 | 4.9 | 28/01/2014 |
| 23 | bigeye | 41 | 17/06/2014 | Sorong | 129 | 4.3 | 8/02/2014 |

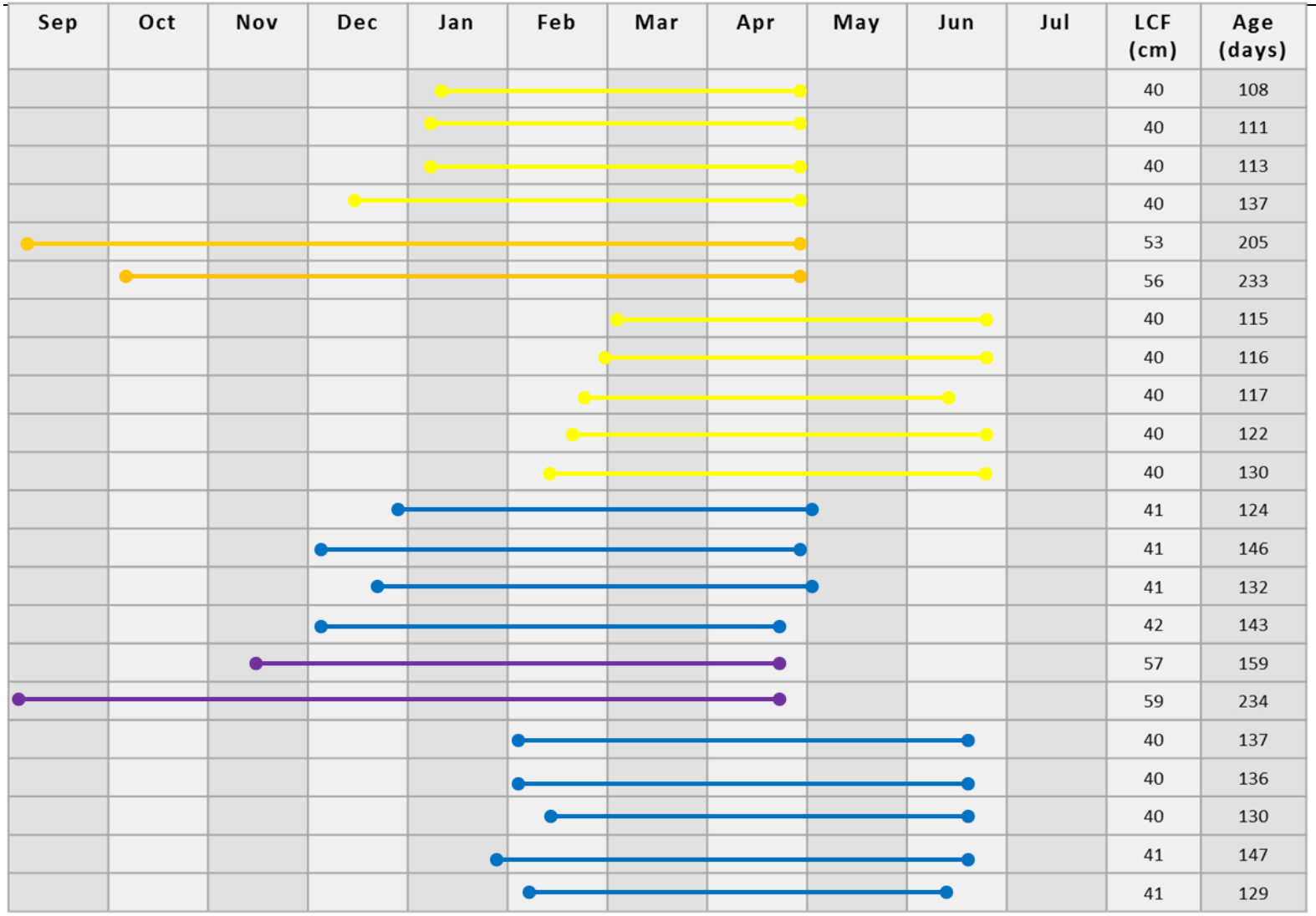


Figure 4.6. Spawning dates back-calculated using daily age estimates for 12 yellowfin tuna (yellow and orange lines) and 11 bigeye tuna (blue and purple lines). Samples were collected in 2013 between late May and early April. Samples were collected in 2014 during June.

## 4.5 Data management

A Microsoft Access database was established to manage data associated with the stock structure component of the ACIAR project.

The three components of the stock structure project -- parasites, genetics and otolith chemistry – all analysed samples collected from the same fish, so each component needed to access the same information on fishing operations, port sampling and biological data. These data were stored in tables within the database (Figure 4.7) and, as they were stored in only one place, discrepancies and errors were minimised.

Data recorded in the field were entered into the database after checking for inconsistencies between the samples and field data by comparing field data sheets against received samples. A universal reference number (URN) was assigned to each fish.

Database tables linked via primary keys were designed to minimise repetition of data in multiple tables and to allow easy retrieval of data (see the relationships diagram, Figure 4.7). Separate tables were established to hold the data for the samples analysed as part of each of the three components; these tables were designed specifically to fulfil the requirements of each component. For example, for the genetics component, external service providers were involved in parts of the genetics preparation and analysis therefore sample tracking was very important to ensure careful management and exchange of data so no mistakes were made. For the otolith chemistry component, the two otoliths from each fish were analysed using different techniques so there was an emphasis on being able to collate results from the same fish.

The database was designed to also store metadata of samples, which allowed users to keep track of which samples had been collected, where they were at any time and which had been analysed by each of the three techniques. An important part of the project was comparing results from the three components, and the database allowed those links between results from the same samples. The user-friendly interface allowed easy querying for choosing the subset of analysed samples according to, for example, catch date, location, and fish size. Data summaries, maps, graphs and analysis using Excel and R were facilitated by the smooth interface that the ACIAR database had with those applications.

The ACIAR database has the flexibility to grow as more data are sourced. As example, in 2017, ACIAR John Allwright Fellow, Ms Ririk Sulistyaningsih (Research Institute for Tuna Fisheries, Bali), conducted a study of otolith shape on a subset of the otoliths collected for this project for her Masters degree at University of Tasmania. The otolith shape data are now stored in the ACIAR database and hence linked to the other results on the stock structure.

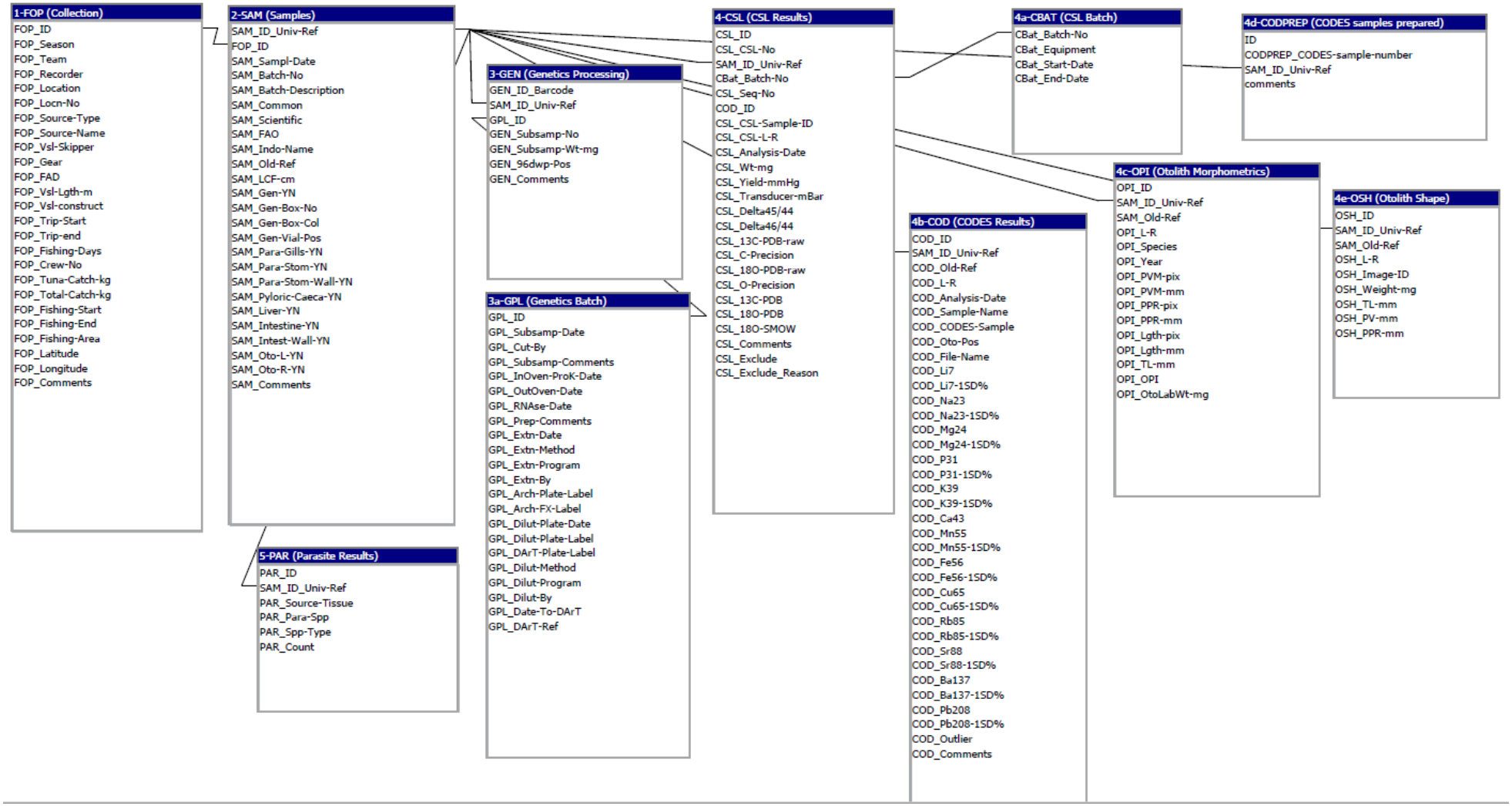


Figure 4.7 Relationship diagram for the ACIAR project's database.

# 5. Technique 1: Parasites

**Parasites as indicators of movement of juvenile bigeye tuna (*Thunnus obesus*) and yellowfin tuna (*Thunnus albacares)* in Indonesian waters**

Team: Pratiwi Lestari[1], Brad R. Moore[2,3], Scott C. Cutmore[4] and Robert. J. G. Lester[4]

[1]Research Institute for Marine Fisheries, Cibinong, West Java, Indonesia

[2]Coastal Fisheries Programme, Pacific Community (SPC), New Caledonia

[3]Institute for Marine and Antarctic Studies, University of Tasmania, Australia

[4]School of Biological Sciences, The University of Queensland, Australia

*Note: The Tables and Figures for this chapter follow as Sections 5.6 and 5.7 respectively, following the Discussion (Section 5.5).*

## 5.1 Summary

Bigeye tuna (*Thunnus obesus*; BET) and yellowfin tuna (*Thunnus albacares*; YFT) are important components of commercial and artisanal fisheries in Indonesia and globally. The degree of movement and mixing of these species among different regions in Indonesian waters and Indonesia and adjacent nations is largely unquantified. Here, we use spatial and temporal patterns of parasites to provide information on movement of juvenile BET and YFT among six Indonesian Fisheries Management Areas (FMAs), and among Indonesian waters and two nearby nations: Maldives in the Indian Ocean and Solomon Islands in the western Pacific Ocean. Both tuna species had different parasite compositions in the nearby nations compared to Indonesia suggesting little exchange. In Indonesia, both tuna species showed differences among FMAs, especially between fish caught within the Indonesian archipelago and those caught outside. Within the archipelago both tuna species frequently carried an internal gill fluke, *Didymozoon longicolle*. This parasite was almost absent from fish captured from the Eastern Indian Ocean (FMAs 572 and 573) suggesting that few BET or YFT had moved from the archipelago to the eastern Indian Ocean. Tuna captured off West Papua in the western Pacific Ocean (FMA 717) had significantly higher numbers of several parasites compared to those within the archipelago, suggesting limited movement of these young fish from West Papua into the archipelago.

## 5.2 Introduction

The use of parasites as biological tags for determining patterns of movement and stock structure of aquatic organisms is a well-established technique. The principle of the approach is that where the parasite fauna of two samples is the same, those samples have either grown in a similar environment or share a common history. Where the parasite faunas are different, the history of the samples is different according to the parasite's residence time in or on the samples, with parasites with short residence times providing information on recent history, and parasites with long residence times providing information on long-term history (Lester and MacKenzie 2009; Lester and Moore 2015). Parasites have been used to elucidate movements in fishes and invertebrates from a range of environments, including estuarine (Moore et al. 2012), coastal and nearshore (Lester et al. 2001), deep-sea (Lester et al. 1988) and oceanic waters (Lester et al. 1985; Jones 1991).

In this report, parasites are used to provide information on the degree of movement and mixing of juvenile BET and YFT among six Indonesian FMAs, and among Indonesia and adjacent nations. In addition to examining spatial patterns (i.e. among and within FMAs), we also explore temporal patterns (i.e. between two sampling years) in parasite fauna of the two tuna species, to assess whether observed patterns are stable over time.

## 5.3 Methods

### 5.3.1 Sample collection and examination

BET and YFT samples were collected in 2013 and 2014 from nine ports in six FMAs within Indonesia: Padang, Prigi, Palabuhanratu, Bitung, Gorontalo, Kendari, Ambon, Sorong, and Jayapura, and two 'outlier' areas: Maldives in the Indian Ocean and Solomon Islands in the western Pacific Ocean (Table 5.1, Figures 5.1 and 5.2).

Samples were obtained directly from fishers, or from local fish markets and fish distribution companies. The catch areas of the fish were determined as best as possible from information provided by vessel skippers. In most cases fresh, whole fish were purchased, with fish having been stored on ice from time of capture to unloading in port. To reduce the effect of fish age on the analyses, fish selected for parasite examination were generally between 30 cm and 50 cm fork length (FL). The age of fish were in the range of 3 to 5 months (see Section 4.4 above), based on age estimates made from daily growth band readings on otolith sections from 11 YFT and 13 BET (Kyne Krusic-Golub, Fish Ageing Services, pers. comm.). Gills and viscera were removed, placed into individual plastic bags with a label giving location, date and time of capture and caudal fork length (LF), and then frozen. In 2013 the gill and viscera samples became separated and only one of the pair was examined in some cases. In 2014 gills and viscera from the same fish were kept together and both were dissected. Approximately 10 fresh fish of each species were examined at the start of the project to detect and identify parasites that would be useful in the project.

For parasitological examination frozen tissues were thawed, the gill arches opened and external and internal gill surfaces examined under a dissecting microscope. The viscera were separated into stomach, pyloric caeca, intestine and liver, and scanned individually under a dissecting microscope. Parasites found were removed, identified, counted, and preserved in 70% alcohol. All counts were performed by the one person (Pratiwi Lestari), and samples were not dissected in any particular order.

### 5.3.2 Molecular sequencing and phylogenetic analysis of parasite DNA

To help clarify parasite identity, the Polymerase Chain Reaction (PCR) was used to amplify and compare the ITS2 region of the genome of 25 didymozoid individuals. Total genomic DNA was extracted using phenol/chloroform extraction techniques (Sambrook and Russell 2001). The ITS2 region was amplified using the primers 3S (3S: 5'-GGT ACC GGT GGA TCA CGT GGC TAG TG-3'; Morgan and Blair 1995) and ITS2.2 (5'-CCT GGT TAG TTT CTT TTC CTC CGC-3'; Cribb et al. 1998). PCR was performed with a total volume of 20 µl consisting of 5 µl of 5x MyTaq Reaction Buffer (Bioline), 0.75 µl of each primer (10 pmols), 0.25 µl of Taq polymerase (Bioline MyTaq™ DNA Polymerase) and 2 µl of DNA template (approximately 10 ng), made up to 20 µl with Invitrogen™ ultraPURE™ distilled water. Amplification was carried out on a MJ Research PTC-150 thermocycler. The following profile was used to amplify the ITS2 region: an initial single cycle of 95°C denaturation for 3 min, 45°C annealing for 2 min, 72°C extension for 90 s, followed by 4 cycles of 95°C denaturation for 45 s, 50°C annealing for 45 s, 72°C extension for 90 s, followed by 30 cycles of 95°C denaturation for 20 s, 52°C annealing for 20 s, 72°C extension for 90 s, followed by a final 72°C extension for 5 min. Amplified DNA was purified using a Bioline ISOLATE II PCR and Gel Kit according to the manufacturer's protocol. Cycle sequencing of purified DNA was carried out at the Australian Genome Research Facility using ABI Big Dye™ v.3.1 chemistry following the manufacturer's recommendations, with the primers used for PCR amplification as well as the additional internal primer GA1 (5'-AGA ACA TCG ACA TCT TGA AC-3'; Anderson and Barker 1998). Sequencher™ version 4.5 (GeneCodes Corp.) was used to assemble and edit contiguous sequences. The start and the end of the ITS2 region were determined by annotation through the ITS2 Database (Keller et al. 2009; Ankenbrand et al. 2015) using the 'Metazoa' model.

New sequence data generated during this studied were aligned with those available on GenBank using MUSCLE (Edgar 2004) implemented in MEGA version 6.06 (Tamura et al. 2013), with UPGMA clustering for iterations 1 and 2. The resultant alignments were refined by eye and Neighbor-joining analyses were conducted in MEGA version 6.06 using the following parameters: "Model/Method =No. of differences", "Substitutions to include = Transitions + Transversions" and "Gaps/Missing Data Treatment = Pairwise deletion". *Neometadidymozoon polymorphis* (AJ224760) and *Indodidymozoon lesteri* (AJ224751) were designated as functional outgroup taxa.

### 5.3.3 Statistical analysis of parasite abundances

**a) Movement and mixing among Fisheries Management Areas**

The data were initially analysed with reference to FMAs using results from all parasitological examinations. Subsequent more detailed analyses excluded fish which lacked data from either gill or viscera. Summary statistics were compiled for each tuna species by collection year and source FMA, and included mean abundance (total number of individuals of a particular parasite per sample divided by the total number of hosts examined, including uninfected hosts) and prevalence (number of hosts infected with a particular parasite divided by number of hosts examined, expressed as a percentage) for each parasite species deemed suitable for use as a biological tag, following the terminology of Bush et al. (1997). Shapiro-Wilk's tests revealed that the frequency distributions of the parasite species were not normal ($p < 0.05$). In general, the abundance data for each parasite of both YFT had two components: one which could be approximated by a negative binomial distribution and a second component consisting of a large zero category, presumably arising because some fish had not been exposed to infection. The natural log of the parasite + 1 (Ln[x + 1]) was used to minimise the variance of the abundance data. These transformed data was used throughout the univariate and multivariate analyses.

Transformed abundance data for those species with a prevalence of > 10% in at least one of the samples (component species; Bush et al. 1997) were compared among FMAs using a series of one-way permutational analysis of variance using the *vegan* package (Oksanen et al. 2017) in R version 3.3.10 (R Core Team 2016). Each permutational analysis of variance was based on a Euclidean distance similarity matrix and 999 permutations of the data. A p-value of < 0.01 was considered significant for all tests. Samples of BET from FMA716 in 2013 and the Maldives in 2014 were excluded from these analyses due to small sample sizes (n=2 and 5, respectively).

Linear discriminant analysis (LDA), non-metric multi-dimensional scaling (MDS) and canonical analysis of principal coordinates (CAP) were performed to provide a visual indication of the similarities in parasite community assemblages among FMAs in each collection year. LDA was performed using the *MASS* package (Ripley et al. 2016) in R. Results of the LDA were plotted as graphs of the first and second discriminant axes, with 95% confidence interval ellipses established around the mean canonical score of each sample group. Non-metric MDS and CAP analyses were performed using Primer v. 6 and PERMANOVA+ (Primer-E, Plymouth, UK) and were based on a Euclidean distance similarity coefficient. As the results for the LDA, MDS and CAP were in close agreement, only the LDA results are presented here. Broadscale patterns in spatial structuring of Indonesian samples were further examined via random forests using the *randomForest* package (Liaw and Wiener 2002) in R version 3.5.0 (R Core Team 2018). Samples from collection FMAs within Indonesia were grouped into three regions for the random forest analyses: eastern Indian Ocean (encompassing samples from FMAs 572 and 573), archipelagic waters (FMAs 714, 715 and 716) and western Pacific Ocean (FMA 717). The R package *randomForest* is a type of ensemble learning method, where an ensemble of classification trees is aggregated for prediction (Cutler et al. 2007). Component species were used as predictor variables in each random forest model, and 10000 trees were used. Different random seed values were applied for each tuna species to ensure stability in predictions and variable importance. Detailed descriptions of random forests and their application can be found in Breiman (2001), Cutler et al. (2007) and Strobl et al. (2009).

**b) Movement and mixing within Fisheries Management Areas**

Data from groups of fish caught in the same month from different locations within individual Indonesian FMAs allowed an examination of the potential degree of mixing within FMAs. Differences in parasite community assemblages among groups were examined using permutational multivariate analyses of variance using the *vegan* package (Oksanen et al. 2017) in R. As with the univariate tests described above, each permutational multivariate analysis of variance was based on a Euclidean distance similarity matrix and 999 permutations of the data. Comparisons were only conducted on those groups where large numbers (typically > 15) of fish with both gill and viscera material were available in either group. Only component species (i.e. those species with a prevalence of > 10% in at least one of the samples for each comparison) were included in the analyses. A p-value of < 0.01 was considered significant for all tests.

## 5.4 Results

### *5.4.1 Parasite characterisations*

Based on morphology, eleven parasite species or species complexes were identified in the two tuna species. Of these, nine were used in the analyses. The two omitted were the copepod *Hatschekia* sp. and the digenean *Hirudinella* sp. They were considered to have a possibly short residence times in the fish and therefore might be lost as fish moved from one area to another. Didymozoids were considered permanent parasites. They were within the tissues of the fish and hence are not easily dislodged. Though some are known to be lost annually or at spawning, the tuna sampled were all less than one year old and likely immature (Itano 2000; Farley et al. 2010) so it was assumed no didymozoids had been lost. Juvenile acanthocephalans were embedded in tissue and also considered permanent parasites.

The parasites counted and their tentative identifications are in Table 5.2. The DNA sequences used to clarify parasite taxonomy showed that of those samples processed, three of the didymozoids occurred in both tuna species. These were *Didymocystis* sp. 1, *Wedlia globosa* and *Wedlia* sp. 2 (Table 5.2 and Figure 5.3). Sequence data revealed that the parasite morphological types sometimes constituted more than one species of didymozoid. In yellowfin tuna for example, our *Koellikeria* type 1 apparently constituted at least three species of didymozoid, and *Koellikeria* type 4 constituted two species (Table 5.2). These species could not be reliably differentiated during the routine dissections. A more accurate identification may have improved the resolving power of the analyses but though these counts may be a composite they nevertheless represent a feature of the parasite fauna potentially valuable in host discrimination and hence were used as species complexes in the analyses.

Summaries of the mean abundances of the most commonly observed permanent parasites and the fish sample sizes by FMA are in Table 5.3. Of the nine parasite species (or species complexes) that were considered to have long-residence times in or on the fish and therefore appropriate for use as biological tags, seven were observed with a prevalence of > 10% in at least one of the samples in either of the collection years. Five of the seven parasites were tissue-dwelling adult didymozoid digeneans. The sixth (*Bolbosoma* sp.) was a juvenile acanthocephalan, adults of which are found in cetaceans, and the seventh, juvenile *Rhadinorhynchus* sp., were found attached in the gut wall.

### 5.4.2 Movement and mixing among Fisheries Management Areas

#### *Thunnus obesus* (BET)

**Patterns in individual parasite species**

The abundances of several component species infecting BET were different among FMAs. Table 5.3 gives overall average numbers of component parasite species in all BET dissected. Table 5.4 presents data by year and is restricted to fish that had both gill and viscera examinations. Permutational analyses of variance showed that many of differences among FMAs were significant (Table 5.5).

BET from the Maldives had high numbers of *Didymozoon longicolle* (D2), an average of 3.22 individuals per fish (Tables 5.3 and 5.4). This parasite was largely absent from fish in the neighbouring Indonesian FMAs of 572 and 573 which had averages of 0.25 and 0. That the differences were statistically significant is demonstrated in Table 5.5. Maldives fish also had significantly higher numbers of *Koellikeria* type 3 (6.24 per fish) compared to FMA 572 (0.28 per fish) (Table 5.5). These results show that the Maldives fish had a very different history from the neighbouring Indonesian fish.

BET from the Solomon Islands had high numbers of *Koellikeria* type 3, 2.24 per fish (Table 5.3) versus 0.47 per fish in the neighbouring Indonesian area (FMA 717) a difference significant in both years (Table 5.5). They also showed significant differences in numbers of *Didymocystis bifurcata* (D1) and *Didymozoon longicolle* (D2) in 2013 though this was less evident in the sample taken in 2014. The differences indicate that the Solomon Island fish sampled had a different history from the neighbouring Indonesian fish in both years.

In Indonesian waters two trends stand out. Samples taken from FMAs 572 and 573 in the Indian Ocean had very low numbers and a low prevalence of *Didymozoon longicolle* (D2) and *Bolbosoma* sp. compared to fish within the archipelago (Tables 5.3, 5.4 and 5.5; Figure 5.5). In addition, FMA 572 had very low numbers of *Didymocystis bifurcata* (D1). The general absence of these parasites from FMAs 572 and 573 and their abundance in the archipelago suggests limited movement from the archipelago into the Indian Ocean.

BET from outside the archipelago to the east, FMA 717, had higher numbers and greater prevalence of *Didymozoon longicolle* (D2) than those within the archipelago (Table 5.3; Figure 5.5). Within the archipelago there were few or no consistent differences detected among the FMAs.

**Patterns in parasite community assemblages in BET**

The combined results from all component parasites may be best visualised in the Linear Discriminant Analysis (LDA; Figure 5.6, top left and right). BET with zero or few parasites are clustered near the axis origins. Such fish occurred in almost all samples so that ellipses derived from parasite abundances tend to be centred near the axis origins. The purple ellipse in each figure represents parasites in the Maldives fish. In both 2013 and 2014 samples they are greatly elongated. They should be compared to data from nearest Indonesian samples, i.e. fish from FMAs 572 and 573, which are represented by orange and yellow ellipses. These are relatively compact and quite distinct from the purple ellipses. This suggests that the Maldives BET had a very different parasite fauna from those from FMAs 572 and 573 in both years.

Solomon Island samples are represented by the two ellipses in pink. Their nearest FMA is FMA 717, the blue ellipse. In both years the results suggest that the parasite fauna of BET from Solomon Islands differs from that of FMA 717.

The three FMAs within the Indonesian archipelago, 714, 715 and 716, are represented by light green, dark green and aquamarine ellipses in 2013 and 2014 (Figure 5.5, top left and top right; aquamarine absent from top left due to small sample size). The ellipses are of similar size, shape and position

suggesting little discrimination between the parasite faunas within the archipelago, though they are clearly more diverse than samples from the Indonesian southwest coast (FMAs 572 and 573). The differentiation of samples from FMAs 572 and 573 (i.e. eastern Indian Ocean) from other Indonesian locations was further supported by the results of the random forests, with a high classification success for fish from FMAs 572 and 573 in both years (Table 5.6). Poor classification success was observed for samples from FMA 717 in both years (Table 5.6), with uninfected fish generally aligning with those from the eastern Indian Ocean, and those from Sorong 'A' aligning more closely with those from within the archipelago than those caught off Jayapura within the same FMA, a result that was also evident from the within-FMA analyses (see below).

## *Thunnus albacares* (YFT)

### Patterns in individual parasite species

The results for YFT (Tables 5.3 and 5.7) show some similarity to those for BET but show a greater degree of discrimination among areas, with the abundances of more parasite species being significantly different among FMAs in YFT compared to BET (cf. Tables 5.5 and 5.8).

Fish from the Maldives had higher numbers of *D. longicolle* (D2, average 3.96) and *Koellikeria* type 1 (average 2.08) than fish from adjacent Indonesian waters (FMAs 572 and 573, Tables 5.3 and 5.6) indicating that they had a different history from the Indonesian fish. Those from the Solomon Islands differed from Indonesian fish in their numbers of D1 and D2 in most comparisons (Table 5.8), again suggesting little mixing between the two regions.

Within Indonesia, YFT from the eastern Indian Ocean, FMAs 572 and 573, had few *D. longicolle* compared to those from within the archipelago (Tables 5.3, 5.7 and 5.8). Like the BET result, this suggests that there was little movement from the archipelago into the Indian Ocean. Also like the BET result, a comparison of parasite abundances between FMA 717 in the east outside the archipelago with those within the archipelago show significant differences but in the case of YFT they are more extreme. FMA 717 had high numbers of *D. longicolle* (D2), *Bolbosoma* sp. and other parasites compared to fish sampled within the archipelago (Tables 5.3, 5.7 and 5.8), and a greater prevalence of *D. longicolle* in both 2013 and 2014 (Figure 5.5), again indicating that these fish had a different history to the bulk of fish in the archipelago. An additional insight is that fish from the Celebes Sea in FMA 716 had significantly higher abundances of *D. bifurcata* (D1) compared to those from all other FMAs (Tables 5.3, 5.7 and 5.8) suggesting they may form a distinct group.

### Patterns in parasite community assemblages in YFT

In the Linear Discriminant Analyses (LDAs) for YFT, Maldives samples are again represented by purple ellipses (Figure 5.6, bottom left and right). Though the resulting ellipses differ in size between years, they are much larger than the orange and red ellipses representing the nearest Indonesian FMAs (572 and 573), suggesting these fish have a different history.

The Solomon Island samples differed between years (pink/crimson ellipses, Figure 5.5 bottom, left versus right). In the first year relatively few parasites were found resulting in a compact ellipse. Greater numbers of parasites and larger within-sample variability in parasite numbers were observed in the second year, resulting in a much larger confidence ellipse. In both years however, there is a clear difference between the Solomon samples and the nearest Indonesian area, FMA 717 (blue ellipse, Figure 5.5 bottom left and right). In turn, yellowfin tuna from FMA 717 were largely distinct from those from within the Indonesian archipelago, with many samples pulling out to the right-hand side of the LDA plots in both 2013 and 2014 (Figure 5.6), again suggesting a different history.

Samples from FMAs within the Indonesian archipelago, FMAs 714, 715 and 716 (light green, dark green and aquamarine ellipses in Figure 5.6, respectively) are of similar size shape and position suggesting much similarity in their parasite fauna. Grouped together, yellowfin tuna from these FMAs clearly harboured a more diverse parasite community assemblage than those from the eastern Indian Ocean (Figure 5.6). The differentiation of samples from FMAs 572 and 573 (i.e. eastern Indian Ocean) in 2013 from other Indonesian locations was further supported by the results of the random forests, with a high classification success for observed in this year (Table 5.6). In 2014, classification success from the random forest models was low across all regions, owing to a larger number of uninfected and lightly infected fish in this year (evident from the large number of samples clustered near the axis origins in Figure 5.6, bottom right).

### 5.4.3 Movement and mixing within Fisheries Management Areas

In a few cases it was possible to compare the parasite faunas of groups of fish caught in the same month in different locations within individual Indonesian FMAs (Table 5.9). This provided an indication of the degree of homogeneity with an FMA. The most striking differences occurred in YFT from FMA 717 between Sorong 'A' at the western limit and Jayapura in the east. Jayapura had very high numbers of D1, D2, K1, K3 and K4 and *Bolbosoma* sp. compared to Sorong 'A'. Differences were evident in BET but were less marked. This result suggests that even within this FMA considerable group fidelity had occurred in both species.

In 2013, both BET and YFT from Kendari 'A' differed from BET and YFT from Ambon (Table 5.9). For both tuna species, samples from Kendari 'A' contained a parasite fauna that was more characteristic of samples from the Indian Ocean than Ambon, with low abundances of *Didymozoon longicolle* and *Koellikeria* type 1.

For BET, samples collected in 2013 from Palabuhanratu 'A' differed to those from Prigi 'A' in FMA 573. The differences were not observed when slightly different locations (Palabuhanratu 'B' and Prigi 'B') were sampled in 2014 (Table 5.9). Other comparisons yielded non-significant results, suggesting fish from these groups shared a common history or resided in a similar environment, or that the variability in the parasite data obscured any differences.

## 5.5 Discussion

The technique of using parasites to discriminate between stocks ideally requires abundant parasites. Many fish examined in the present study had zero or very few parasites so that on the LDA graphs these fish tended to be grouped together regardless of which area they had come from. An effective analytical technique employed in other studies is to assign individual fish to area according to their parasites (Moore et al. 2012, Poulin and Kamiya 2015) and compare the results with actual collection site. This was not feasible here because the absence of a key parasite such as *D. longicolle* in an individual fish automatically assigned the fish to the Indonesian Indian Ocean FMAs where this parasite appeared largely absent even though the fish had been caught in a school with a rich parasite fauna.

Prior to the study, the fish to be sampled had been estimated to be up to a year old (Eveson et al. 2015). Subsequent ageing from daily rings in the otoliths of sampled fish showed that the fish were only a few months old (Kyne Krusic-Golub, Fish Ageing Services pers. comm.) and thus had had little time to accumulate parasites.

A key assumption in using didymozoids as biological tags was that they had been in the fish for several months. While most adult didymozoids have life spans of about a year, and/or are lost during spawning, they were considered as permanent parasites in the current study as the fish sampled were less than 6 months old and likely immature (Itano, 2000; Farley et al. 2010). While the lifecycles

of didymozoids used as biological tags in the current study are largely undefined, it is likely that the tuna pick them up by feeding on a small forage fish. Thus, the parasite data reflects movement of the two tuna species since the acquisition of a piscivorous diet. While the feeding ecology of juvenile bigeye tuna is poorly quantified, skipjack tuna (*Katsuwonus pelamis*) have been shown to be piscivorous from a very early age (Tanabe 2001). Assuming BET and YFT are similar, the parasite signal likely represents several months of the fishes' lives.

The parasite data suggest little similarity in the histories of BET from the Maldives compared to BET from neighbouring Indonesian waters. Within Indonesia, the low numbers of parasites from the Indian Ocean, especially *D. longicolle,* is consistent with the possibility of movement of BET from the Indian Ocean to within the archipelago which had higher numbers of these parasites. If eastward movement was occurring, the fish could have been accumulating parasites en route. The reverse was unlikely, however, because of the long-term residence time of the parasites in the fish. Within the archipelago there was little evidence of discrete groups of BET. This is in general agreement with tagging data. Of approximately 100 BET that were tagged within the Indonesia archipelago in the Pacific Tuna Tagging Program (2008 and 2009) that were recaptured and tags recovered, 12 had moved over 500 nmi (SPC unpublished data). All 12 had moved east or northeast into the Western Pacific Ocean. Most fish were recaptured close to the area in which they were tagged suggesting some regional fidelity. Of 5807 BET tagged in the open waters of the tropical Pacific and recovered, 71% had moved east (Schaefer et al. 2015).

Similarly for YFT, the parasite data suggest that YFT within the Indonesian archipelago were distinct from those in the Indian Ocean because of the low numbers of *D. longicolle* in the Indian Ocean samples. Due to low numbers of this parasite species in the Indian Ocean samples it is unlikely YFT move from the archipelago to the Indian Ocean. Fish from the Celebes Sea and eastern Indonesia had even higher numbers of several didymozoids compared to the archipelago suggesting these fish are either resident in these areas or if they have moved from the archipelago they have moved east and acquired more parasites en route.

As with BET, the movements patterns inferred for YFT from the parasite data are largely consistent with those observed from observations of tagged fish. Of the YFT tagged by the PTTP both within and outside the Indonesian archipelago in 2008 and subsequently recaptured and tags recovered, 56 were recaptured over 500 nmi away, and almost all had moved in an easterly direction (SPC unpublished data). Of the 30 YFT tagged in 2009 and recaptured > 500 nmi away, almost all individuals had moved further east into the Pacific. Overall, of the approximately 1262 YFT tagged within the Indonesian Exclusive Economic Zone, 160 were recovered outside the zone while the vast majority (1102) had remained within suggesting limited movement of many of the fish (SPC unpublished data).

Differences in parasite abundance among FMAs were greater for juvenile YFT than for BET. It may be that juvenile YFT are more site-attached than BET. However, many more YFT were dissected than BET, and parasites were slightly less common in BET compared to YFT, so the larger data set from YFT may be reason for the apparently greater differences between areas in YFT compared with BET rather than differences in the ranges of individual fish.

Of the parasite types used as biological tags, *D. longicolle* provided the greatest discrimination between areas, separating eastern Indian Ocean locations from elsewhere. *Didymozoon longicolle* has been previously reported from a wide range of tuna species, including skipjack tuna, Pacific Bluefin tuna (*Thunnus orientalis*) and chub mackerel (*Scomber japonicus*) from Japan (Ishii 1935), bigeye tuna and yellowfin tuna from Hawaii (Yamaguti 1970), yellowfin tuna in the Gulf of Guinea (Baudin-Laurencin 1971), chub mackerel and yellowfin tuna from Massachusetts and the Gulf of Mexico, respectively (Williams Jr and Bunkley-Williams 1996) skipjack tuna and albacore (*Thunnus alalunga*) from the western Mediterranean, (Mele et al. 2010; 2012), and blackfin tuna (*Thunnus atlanticus*), bigeye tuna and skipjack tuna off the coast of Brazil (Nascimento-Justo and Kohn 2012).

The observation of *D. longicolle* in both bigeye tuna and yellowfin tuna from the Indian Ocean (Maldives), through the Indonesia archipelago, to the western Pacific Ocean extends the known distribution of this species, and suggests a widespread geographic distribution of this parasite in scombrid species across temperate to tropical waters worldwide. While the lifecycle of *D. longicolle* is presently undefined, it is likely that the species utilises a pelagic mollusc such as a heteropod or pteropod (Vande Vusse 1980; Lester and Newman 1986) and a copepod (Køie and Lester 1985) as first and second intermediate hosts, and a small teleost fish as the third intermediate hosts from the which the tuna acquire the parasite. The near absence of the parasite in FMAs 572 and 573 may reflect the limited availability of one of the intermediate hosts or a low density of the tuna final host in these areas.

The limited movement from the Indonesia archipelago into the eastern Indian Ocean and from the western Pacific Ocean into the archipelago inferred from the parasite data likely reflects local oceanographic conditions, habitat preferences, and availability of prey resources of the collection areas (Rooker et al. 2016; Weng et al. 2017). Sampling sites within the Indonesian archipelago fall within the Banda, Ceram, Halmahera, Molucca and eastern Celebes Seas, which that encompass a wide variety of bathymetric features (including coral reefs, seamounts, banks, basins and ridges), exhibit cyclical patterns in seasonal sea surface currents within their boundaries and lay east of the cool, low salinity waters of Indonesian Throughflow, with limited direct flow to the eastern Indian Ocean (Gordon 2005; Dao et al. 2015). These seas experience stable sea surface temperatures (SSTs) commonly ranging between approximately 26–30°C annually (Tadjuddah 2016; Kusuma et al. 2017). These local conditions likely create optimal habitat for juvenile tuna within the archipelago, with little requirement to move outside to waters of preferred temperature or for foraging.

Historically, both BET and YFT were considered to be highly mobile and thought to form single stocks for assessment purposes in each of the IO and WCPO. The parasite results are consistent with other recent lines of evidence suggest that at least YFT may form multiple populations, or stocks, within both of these oceans and possibly within Indonesia itself. Based on an examination of mtDNA, Dammannagoda et al. (2008) concluded there may be genetically discrete populations of YFT tuna in the waters around Sri Lanka. Similarly, Aguila et al. (2015) found evidence of genetic differences between YFT from the Philippines and the Bismarck Sea, Papua New Guinea, while Grewe et al. (2015), using next generation sequencing technology, found evidence of genetic differences among YFT samples from three widely spaced locations in the tropical Pacific. For such differences to occur populations must be non-mixing throughout the duration of their life history, or display strong spawning site fidelity assuming sampling was conducted during spawning. While our parasite results are consistent with the occurrence of distinct groups of both BET and YFT across the locations sampled, examination was limited to only small, young fish. Parasitological examination of older fish, of both BET and YFT, would provide much more parasite data to inform on how movement varies with ontogeny.

## 5.6 Tables

Table 5.1. Approximate sources of Indonesian samples, by year and by FMA. Collection locations are based on best available catch information.

| Year | FMA | Sample name | Collection location | | No. fish by year | | No. fish, all years | |
|---|---|---|---|---|---|---|---|---|
| | | | Latitude | Longitude | BET | YFT | BET | YFT |
| **2013** | FMA572 | Padang A | -1.27°S | 99.20°E | 97 | 101 | | |
| | | **FMA572 total** | | | **97** | **101** | **158** | **137** |
| | FMA573 | Palabuhanratu A | -7.62°S | 105.79°E | 52 | 71 | | |
| | | Prigi A | -11.07°S | 111.59°E | 36 | 95 | | |
| | | **FMA573 total** | | | **88** | **166** | **168** | **287** |
| | FMA714 | Kendari A | -2.35°S | 124.39°E | 21 | 24 | | |
| | | Kendari D | -2.25°S | 122.25°E | 4 | 0 | | |
| | | Gorontolo D | -2.35°S | 124.39°E | 3 | 6 | | |
| | | Ambon | -3.86°S | 128.09°E | 58 | 115 | | |
| | | **FMA714 total** | | | **86** | **145** | **157** | **255** |
| | FMA715 | Gorontolo A | 0.22°N | 121.82°E | 17 | 0 | | |
| | | Gorontolo B | 0.31°N | 122.22°E | 2 | 63 | | |
| | | Gorontalo C | -0.61°S | 123.61°E | 22 | 0 | | |
| | | Bitung F | 1.46°N | 125.34°E | 2 | 3 | | |
| | | Bitung H | 0.47°N | 126.74°E | 0 | 6 | | |
| | | Sorong B | -2.10°S | 129.26°E | 6 | 5 | | |
| | | Sorong C | -3.45°S | 132.13°E | 16 | 10 | | |
| | | **FMA715 total** | | | **65** | **87** | **92** | **193** |
| | FMA716 | Bitung A | 4.15°N | 126.06°E | 0 | 19 | | |
| | | Bitung D | 2.25°N | 125.43°E | 2 | 15 | | |
| | | **FMA716 total** | | | **2** | **34** | **22** | **74** |
| | FMA717 | Sorong A | 0.25°N | 130.95°E | 22 | 12 | | |
| | | Jayapura | -2.20°S | 140.76°E | 18 | 86 | | |
| | | **FMA717 total** | | | **40** | **98** | **86** | **148** |
| **2014** | FMA572 | Padang A | -1.27°S | 99.20°E | 16 | 30 | | |
| | | Padang B | -1.30°S | 97.80°E | 45 | 6 | | |
| | | **FMA572 total** | | | **61** | **36** | | |
| | FMA573 | Palabuhanratu B | -9.00°S | 106.00°E | 37 | 52 | | |
| | | Prigi B | -9.00°S | 111.00°E | 43 | 69 | | |
| | | **FMA573 total** | | | **80** | **121** | | |
| | FMA714 | Ambon | -3.86°S | 128.09°E | 48 | 103 | | |
| | | Kendari C | -4.58°S | 129.90°E | 23 | 7 | | |
| | | **FMA714 total** | | | **71** | **110** | | |
| | FMA715 | Gorontolo C | -0.61°S | 123.61°E | 0 | 45 | | |
| | | Kendari B | -2.90°S | 126.50°E | 25 | 32 | | |
| | | Bitung G | 1.45°N | 125.50°E | 2 | 29 | | |
| | | **FMA715 total** | | | **27** | **106** | | |
| | FMA716 | Bitung B | 3.50°N | 125.40°E | 20 | 22 | | |
| | | Bitung C | 2.70°N | 125.50°E | 0 | 18 | | |
| | | **FMA716 total** | | | **20** | **40** | | |
| | FMA717 | Sorong A | 0.25°N | 130.95°E | 34 | 27 | | |
| | | Jayapura | -2.20°S | 140.76°E | 12 | 23 | | |
| | | **FMA717 total** | | | **46** | **50** | | |

Table 5.2. Tentative identifications for parasites

| Host | Dissection code | Tentative identification | Site | Seq. locality | GenBank accession code | Component species |
|---|---|---|---|---|---|---|
| **BET** | *Didymosulcus* type 1 | *Didymocystis bifurcata* | Gill filament | Solomon Islands | MK268210 | Y |
| | *Didymosulcus* type 2 | *Didymozoon longicolle* | Gill filament | Not sequenced | - | Y |
| | *Didymosulcus* type 3 | *Didymocystis* sp. 1 | Gill arch | Ambon | MK268211–12 | N |
| | *Koellikeria* type 1 | *Wedlia globosa* | Stomach wall | Solomon Islands | MK268213 | |
| | | *Wedlia* sp. 1 | Stomach wall | Not sequenced | - | |
| | *Koellikeria* type 2 | *Wedlia* sp. 2 | Liver | Palabuhanratu | MK268214 | N |
| | *Koellikeria* type 3 | *Coeliotrema thynni* | Pyloric caeca | Solomon Islands | MK268215 | |
| | *Koellikeria* type 4 | *Koellikeria* sp. 1 | Intestinal wall | Solomon Islands | MK268216 | Y |
| | *Hatschekia* sp. | *Hatschekia* sp. | Gill | Not sequenced | - | N |
| | *Hirudinella* sp. | *Hirudinella ventricosa* | Stomach | Not sequenced | - | N |
| | *Bolbosoma* sp. | *Bolbosoma* sp. | Gut wall | Not sequenced | - | Y |
| | *Rhadinorhynchus* sp. | *Rhadinorhynchus* sp. | Gut wall & intestine | Not sequenced | - | Y |
| **YFT** | *Didymosulcus* type 1 | *Didymocystis bifurcata* | Gill filament | Not sequenced | - | Y |
| | *Didymosulcus* type 2 | *Didymozoon longicolle* | Gill filament | Not sequenced | - | Y |
| | *Didymosulcus* type 3 | *Didymocystis* sp. 1 | Gill arch | Solomon Islands | MK268217 | N |
| | *Koellikeria* type 1 | *Wedlia bipartita* | Stomach wall (Largest) | Ambon | MK268218–19 | Y |
| | | *Wedlia bipartita* | Stomach wall | Bali | MK268220 | |
| | | *Wedlia orientalis* | Stomach wall (Small) | Solomon Islands | MK268221 | |
| | | *Wedlia globosa* | Stomach wall (Large) | Solomon Islands | MK268222 | |
| | *Koellikeria* type 2 | *Wedlia* sp. 2 | Liver | Palabuhanratu | MK268223 | N |
| | *Koellikeria* type 3 | *Wedlia pylorica* | Pyloric caeca | Ambon | MK268224–25 | Y |
| | | *Wedlia pylorica* | Pyloric caeca | Solomon Islands | MK268226–27 | |
| | | *Wedlia pylorica* | Pyloric caeca | Bali | MK268228 | |
| | *Koellikeria* type 4 | *Koellikerioides intestinalis* | Intestinal wall | Solomon Islands | MK268229–30 | Y |
| | | *Koellikeria* sp. 1 | Intestinal wall | Not sequenced | - | |
| | *Hatschekia* sp. | *Hatschekia* sp. | Gill | Not sequenced | - | N |
| | *Hirudinella* sp. | *Hirudinella ventricosa* | Stomach | Not sequenced | - | N |
| | *Bolbosoma* sp. | *Bolbosoma* sp. | Gut wall | Not sequenced | - | Y |
| | *Rhadinorhynchus* sp. | *Rhadinorhynchus* sp. | Gut wall & intestine | Not sequenced | - | Y |

Table 5.3. Abbreviated summary of parasite abundances (mean numbers per fish) in BET (top) and YFT (bottom), from 2013 and 2014 samples combined. Data are for fish in which gill and/or viscera were examined. To simplify the table, only component parasite species are shown. FMA = Fisheries Management Area; FL = fork length (in cm).

**BET:**

| FMA | Sample size (total) | Mean FL (cm) | *Didymocystis bifurcata* Gills | *Didymozoon longicolle* Gills | *Koellikeria* type 1 Stomach wall | *Koellikeria* type 3 Pyloric caeca | *Koellikeria* type 4 Int. wall | *Bolbosoma* sp. All viscera | *Rhadinorhychus sp.* |
|---|---|---|---|---|---|---|---|---|---|
| Maldives | 29 | 39.4 | 0.89 | **3.22** | 1.45 | 6.24 | 0.28 | 0.10 | 0.03 |
| FMA 572 | 158 | 37.4 | 0.37 | **0.25** | 0.47 | 0.28 | 0.51 | **0.08** | 0.00 |
| FMA 573 | 168 | 36.7 | 1.60 | **0.00** | 1.01 | 2.01 | 0.24 | **0.08** | 0.02 |
| FMA 714 | 157 | 42.3 | 1.22 | 1.19 | 1.69 | 2.59 | 0.39 | 0.19 | 0.00 |
| FMA 715 | 92 | 42.4 | 1.93 | 1.91 | 0.59 | 1.28 | 0.18 | 0.16 | 0.04 |
| FMA 716 | 22 | 46.3 | 3.82 | 1.36 | 1.73 | 0.82 | 0.00 | 0.05 | 0.00 |
| FMA 717 | 86 | 43.8 | 1.38 | **2.84** | 1.21 | 0.47 | 0.20 | 0.18 | 0.02 |
| Solomon Is. | 55 | 42.3 | 4.04 | 1.76 | 1.00 | 2.24 | 0.16 | 0.25 | 0.09 |

**YFT:**

| FMA | Sample size (total) | Mean FL (cm) | *Didymocystis bifurcata* Gills | *Didymozoon longicolle* Gills | *Koellikeria* type 1 Stomach wall | *Koellikeria* type 3 Pyloric caeca | *Koellikeria* type 4 Int. wall | *Bolbosoma* sp. All viscera | *Rhadinorhychus sp.* |
|---|---|---|---|---|---|---|---|---|---|
| Maldives | 52 | 38.0 | 2.16 | **3.96** | 2.08 | 2.08 | 0.10 | 0.15 | 0.02 |
| FMA 572 | 137 | 36.3 | 2.83 | **0.58** | 0.63 | 0.77 | 0.25 | 0.06 | 0.02 |
| FMA 573 | 287 | 36.1 | 2.61 | **0.02** | 1.05 | 1.45 | 0.20 | 0.02 | 0.01 |
| FMA 714 | 255 | 39.4 | 2.45 | 3.14 | 1.96 | 3.64 | 0.20 | 0.07 | 0.00 |
| FMA 715 | 193 | 39.1 | 1.80 | 1.88 | 0.68 | 1.72 | 0.06 | 0.04 | 0.03 |
| FMA 716 | 74 | 40.7 | 8.03 | 3.55 | 1.86 | 2.74 | 0.00 | 0.05 | 0.00 |
| FMA 717 | 148 | 39.1 | 2.14 | **12.54** | 2.58 | 3.63 | 1.56 | **0.25** | 0.02 |
| Solomon Is. | 52 | 37.1 | 4.35 | 4.78 | 0.67 | 2.06 | 0.39 | 0.08 | 0.06 |

Table 5.4. Mean abundance ±SE and prevalence (in parentheses) of parasites infecting bigeye tuna (*Thunnus obesus*) from collection locations in and adjacent to Indonesian waters in 2013 and 2014. Data are for fish in which both gill and viscera material were examined in the same fish. FMA = Fisheries Management Area; FL = fork length (in cm).

| Year | FMA | N | FL (cm) | Parasite species / species type | | | | | | |
|---|---|---|---|---|---|---|---|---|---|---|
| | | | | *Didymocystis bifurcata* | *Didymozoon longicolle* | *Koellikeria* type 1 | *Koellikeria* type 3 | *Koellikeria* type 4 | *Bolbosoma* sp. | *Rhadinorhynchus* sp. |
| **2013** | Maldives | 22 | 37.7±0.5 | 0.91±0.27 (45) | 3.14±2.34 (41) | 1.68±0.66 (36) | 8.09±3.50 (45) | 0.18±0.13 (9) | 0.14±0.14 (5) | 0.00±0.00 (0) |
| | FMA 572 | 75 | 34.9±0.2 | 0.47±0.12 (24) | 0.13±0.06 (8) | 0.73±0.12 (37) | 0.36±0.11 (15) | 0.48±0.17 (17) | 0.04±0.02 (4) | 0.00±0.00 (0) |
| | FMA 573 | 61 | 35.6±0.3 | 1.62±0.29 (66) | 0.00±0.00 (0) | 0.30±0.08 (20) | 3.84±1.86 (38) | 0.31±0.10 (18) | 0.00±0.00 (0) | 0.00±0.00 (0) |
| | FMA 714 | 82 | 41.6±0.4 | 1.16±0.19 (52) | 1.20±0.31 (35) | 1.79±0.24 (63) | 3.15±1.26 (52) | 0.34±0.09 (20) | 0.28±0.06 (26) | 0.00±0.00 (0) |
| | FMA 715 | 50 | 41.7±0.5 | 1.24±0.21 (48) | 1.76±0.46 (34) | 0.71±0.18 (26) | 0.80±0.26 (32) | 0.13±0.06 (12) | 0.21±0.06 (24) | 0.04±0.02 (4) |
| | FMA 716 | 2 | 44.9±1.9 | 9.00±2.00 (100) | 4.00±0.00 (100) | 3.50±1.50 (100) | 1.00±1.00 (50) | 0.00±0.00 (0) | 0.50±0.50 (50) | 0.00±0.00 (0) |
| | FMA 717 | 38 | 41.7±0.6 | 1.78±0.37 (61) | 4.00±0.98 (68) | 0.98±0.23 (42) | 0.55±0.25 (16) | 0.40±0.15 (18) | 0.34±0.12 (13) | 0.03±0.03 (3) |
| | Solomon Is. | 26 | 39.6±0.6 | 6.08±1.06 (77) | 0.00±0.00 (0) | 1.04±0.33 (42) | 3.04±0.77 (62) | 0.31±0.15 (15) | 0.08±0.05 (8) | 0.00±0.00 (0) |
| **2014** | Maldives | 5 | 47.9±1.5 | 0.80±0.80 (20) | 3.60±2.06 (60) | 0.20±0.20 (20) | 0.40±0.40 (20) | 0.00±0.00 (0) | 0.00±0.00 (0) | 0.00±0.00 (0) |
| | FMA 572 | 61 | 40.8±0.3 | 0.34±0.10 (20) | 0.49±0.16 (18) | 0.16±0.06 (11) | 0.20±0.09 (10) | 0.56±0.25 (15) | 0.13±0.05 (11) | 0.00±0.00 (0) |
| | FMA 573 | 80 | 37.8±0.3 | 1.59±0.30 (51) | 0.00±0.00 (0) | 1.65±0.28 (48) | 1.14±0.26 (36) | 0.11±0.04 (9) | 0.11±0.04 (9) | 0.04±0.02 (4) |
| | FMA 714 | 71 | 43.1±0.2 | 1.23±0.34 (34) | 1.17±0.52 (24) | 1.56±0.41 (32) | 1.94±0.49 (31) | 0.45±0.16 (23) | 0.08±0.03 (8) | 0.00±0.00 (0) |
| | FMA 715 | 26 | 43.1±0.3 | 3.81±1.23 (58) | 1.00±0.46 (31) | 0.50±0.26 (15) | 1.77±0.56 (50) | 0.08±0.08 (4) | 0.04±0.04 (4) | 0.00±0.00 (0) |
| | FMA 716 | 20 | 46.5±0.3 | 3.30±1.25 (50) | 1.10±0.51 (30) | 1.55±0.45 (45) | 0.80±0.26 (40) | 0.00±0.00 (0) | 0.00±0.00 (0) | 0.00±0.00 (0) |
| | FMA 717 | 46 | 46.1±0.4 | 1.97±0.51 (57) | 1.67±0.51 (37) | 1.55±0.41 (48) | 0.55±0.17 (15) | 0.06±0.04 (7) | 0.11±0.06 (11) | 0.02±0.02 (2) |
| | Solomon Is. | 28 | 44.9±0.7 | 2.20±0.71 (54) | 3.46±1.31 (46) | 0.79±0.20 (43) | 1.18±0.31 (57) | 0.04±0.04 (4) | 0.43±0.22 (14) | 0.18±0.07 (18) |

Table 5.5. Results for one-way permutational analysis of variance pairwise tests of parasite abundance of bigeye tuna (*Thunnus obesus*) from collection locations in and adjacent to Indonesian waters in 2013 (upper diagonal) and 2014 (lower diagonal) (component species only). The code in the table corresponds to the parasite species that is significantly different among regions at p = 0.01. D1 = *Didymocystis bifurcata*, D2 = *Didymozoon longicolle*, K1 = *Koellikeria* type 1, K3 = *Koellikeria* type 3, K4 = *Koellikeria* type 4, B = *Bolbosoma* sp. Note no significant differences were observed in the abundance of *Rhadinorhynchus* sp. among locations '-' = no result due to small sample size.

| **Region** | Maldives | FMA 572 | FMA 573 | FMA 714 | FMA 715 | FMA 716 | FMA 717 | Solomon Is. |
|---|---|---|---|---|---|---|---|---|
| Maldives | | D2, K3 | D2, K1 | none | K3 | - | K3 | D1, D2 |
| FMA 572 | - | | D1, K1, K3 | D1, D2, K1, K3, B | D1, D2, B | - | D1, D2 | D1, K3 |
| FMA 573 | - | D1, D2, K1, K3 | | D2, K1, B | D2, B | - | D2, K1, B | D1, K1 |
| FMA 714 | - | K1, K3 | D2 | | K1 | - | D2, K1, K3 | D1, D2 |
| FMA 715 | - | D1, K3 | D2, K1 | D1 | | - | D2 | D1, D2, K3 |
| FMA 716 | - | D1, K1, K3 | D2 | none | none | | - | - |
| FMA 717 | - | D1, K1 | D2 | none | K3 | none | | D1, D2, K3 |
| Solomon Is. | - | D1, D2, K1, K3 | D2 | D2 | none | none | K3 | |

Table 5.5. Classification success from random forest modelling on component species.

a) Bigeye tuna 2013

| Region | Eastern Indian Ocean | Indonesian Archipelago | Western Pacific Ocean |
|---|---|---|---|
| Eastern Indian Ocean | 79% | 21% | 0% |
| Indonesian Archipelago | 31% | 61% | 8% |
| Western Pacific Ocean | 29% | 45% | 26% |

b) Bigeye tuna 2014

| Region | Eastern Indian Ocean | Indonesian Archipelago | Western Pacific Ocean |
|---|---|---|---|
| Eastern Indian Ocean | 79% | 19% | 2% |
| Indonesian Archipelago | 51% | 40% | 9% |
| Western Pacific Ocean | 54% | 37% | 9% |

c) Yellowfin tuna 2013

| Region | Eastern Indian Ocean | Indonesian Archipelago | Western Pacific Ocean |
|---|---|---|---|
| Eastern Indian Ocean | 78% | 21% | 1% |
| Indonesian Archipelago | 31% | 66% | 3% |
| Western Pacific Ocean | 22% | 38% | 47% |

d) Yellowfin tuna 2014

| Region | Eastern Indian Ocean | Indonesian Archipelago | Western Pacific Ocean |
|---|---|---|---|
| Eastern Indian Ocean | 32% | 66% | 2% |
| Indonesian Archipelago | 15% | 82% | 3% |
| Western Pacific Ocean | 16% | 64% | 20% |

Table 5.7. Mean abundance ±SE and prevalence (in parentheses) of parasites infecting yellowfin tuna (*Thunnus albacares*) from collection locations in and adjacent to Indonesian waters in 2013 and 2014. Data are for fish in which both gill and viscera material were examined in the same fish. FMA = Fisheries Management Area; FL = fork length (in cm).

| Year | FMA | n | FL (cm) | Parasite species / species type | | | | | | |
|---|---|---|---|---|---|---|---|---|---|---|
| | | | | *Didymocystis bifurcata* | *Didymozoon longicolle* | *Koellikeria* type 1 | *Koellikeria* type 3 | *Koellikeria* type 4 | *Bolbosoma* sp. | *Rhadinorhynchus* sp. |
| **2013** | Maldives | 33 | 35.9±0.5 | 2.61±0.51 (70) | 2.48±0.62 (58) | 2.03±0.42 (64) | 2.88±0.99 (45) | 0.15±0.11 (6) | 0.21±0.09 (15) | 0.00±0.00 (0) |
| | FMA 572 | 68 | 34.7±0.3 | 1.79±0.86 (54) | 0.18±0.10 (6) | 0.78±0.17 (29) | 0.79±0.19 (28) | 0.16±0.07 (9) | 0.09±0.03 (9) | 0.00±0.00 (0) |
| | FMA 573 | 73 | 34.2±0.3 | 5.29±0.97 (79) | 0.05±0.03 (4) | 0.52±0.12 (27) | 1.78±0.32 (56) | 0.18±0.08 (7) | 0.01±0.01 (1) | 0.00±0.00 (0) |
| | FMA 714 | 112 | 36.9±0.3 | 2.71±0.37 (70) | 4.15±0.57 (58) | 1.75±0.33 (49) | 4.48±0.83 (61) | 0.05±0.02 (5) | 0.09±0.03 (8) | 0.00±0.00 (0) |
| | FMA 715 | 78 | 38.2±0.4 | 1.47±0.28 (48) | 2.59±0.53 (42) | 0.65±0.13 (30) | 1.94±0.46 (44) | 0.06±0.03 (3) | 0.08±0.04 (6) | 0.06±0.03 (5) |
| | FMA 716 | 34 | 40.9±0.9 | 14.26±2.22 (94) | 4.82±0.87 (71) | 2.50±0.41 (76) | 0.12±0.08 (6) | 0.00±0.00 (0) | 0.12±0.07 (9) | 0.00±0.00 (0) |
| | FMA 717 | 69 | 37.2±0.3 | 2.38±0.31 (68) | 12.14±1.94 (75) | 1.62±0.50 (41) | 3.93±0.79 (46) | 1.86±0.51 (36) | 0.29±0.07 (22) | 0.03±0.02 (3) |
| | Solomon Is. | 29 | 36.4±0.2 | 0.72±0.19 (41) | 0.31±0.12 (21) | 0.52±0.15 (34) | 1.72±0.43 (48) | 0.03±0.03 (3) | 0.10±0.06 (10) | 0.00±0.00 (0) |
| **2014** | Maldives | 18 | 41.9±0.4 | 1.33±0.40 (56) | 6.67±1.96 (56) | 2.17±0.58 (67) | 0.67±0.29 (28) | 0.00±0.00 (0) | 0.06±0.06 (6) | 0.06±0.06 (6) |
| | FMA 572 | 34 | 40.4±0.3 | 3.12±0.82 (65) | 0.29±0.12 (21) | 0.47±0.25 (15) | 0.82±0.25 (32) | 0.38±0.18 (15) | 0.03±0.03 (3) | 0.00±0.00 (0) |
| | FMA 573 | 121 | 37.2±0.3 | 1.00±0.21 (34) | 0.00±0.00 (0) | 1.55±0.21 (46) | 0.91±0.17 (34) | 0.10±0.04 (7) | 0.03±0.02 (2) | 0.02±0.01 (2) |
| | FMA 714 | 110 | 42.7±0.2 | 1.15±0.39 (19) | 0.86±0.43 (17) | 2.18±0.43 (47) | 2.73±0.58 (42) | 0.34±0.07 (18) | 0.05±0.03 (4) | 0.00±0.00 (0) |
| | FMA 715 | 106 | 39.9±0.4 | 1.97±0.36 (44) | 1.02±0.21 (31) | 0.65±0.12 (30) | 1.42±0.23 (42) | 0.08±0.04 (4) | 0.02±0.02 (1) | 0.00±0.00 (0) |
| | FMA 716 | 40 | 40.6±0.6 | 2.73±0.61 (65) | 2.48±1.13 (38) | 1.33±0.44 (35) | 4.98±1.43 (70) | 0.00±0.00 (0) | 0.00±0.00 (0) | 0.00±0.00 (0) |
| | FMA 717 | 50 | 42.7±0.6 | 1.36±0.37 (36) | 11.84±4.81 (42) | 3.36±0.92 (52) | 1.42±0.29 (44) | 0.04±0.03 (4) | 0.22±0.07 (18) | 0.02±0.02 (2) |
| | Solomon Is. | 23 | 38.0±0.6 | 9.09±2.47 (57) | 10.22±2.85 (52) | 1.09±0.44 (26) | 2.91±1.08 (39) | 0.83±0.53 (17) | 0.04±0.04 (4) | 0.13±0.07 (13) |

Table 5.8. Results for one-way permutational analysis of variance pairwise tests of parasite abundance of yellowfin tuna (*Thunnus albacares*) from collection locations in and adjacent to Indonesian waters in 2013 (upper diagonal) and 2014 (lower diagonal) (component species only). The codes to the parasite species are in the caption to Table 5.5. Note no significant differences were observed in the abundance of *Rhadinorhynchus* sp. among locations.

| **Region** | Maldives | FMA 572 | FMA 573 | FMA 714 | FMA 715 | FMA 716 | FMA 717 | Solomon Is. |
|---|---|---|---|---|---|---|---|---|
| Maldives | | D1, D2, K1 | D2, K1, B | none | K1 | D1, K3 | D2, K4 | D1, D2, K1 |
| FMA 572 | D2, K1 | | D1, K3 | D1, D2, K1, K3 | D2, K3 | D1, D2, K1, K3 | D1, D2, K3, K4, B | none |
| FMA 573 | D2 | D1, D2, K1 | | D1, D2, K1 | D1, D2 | D1, D2, K1, K3 | D1, D2, K4, B | D1 |
| FMA 714 | D2 | D1, K1 | D2, K3, K4 | | K1 | D1, K3 | D2, K4, B | D1, D2 |
| FMA 715 | D2, K1 | none | D2, K1 | D1, K1, K4 | | D1, K1, K3 | D2, K4, B | D2 |
| FMA 716 | K3 | D2, K3 | D1, D2, K3 | D1, D2, K3, K4 | K3 | | D1, K1, K3, K4 | D1, D2, K1, K3 |
| FMA 717 | none | D2, K1 | D2, B | D2, K4, B | D2, K1, B | D1, K3, B | | D1, D2, K4 |
| Solomon Is. | none | D2 | D1, D2 | D1, D2 | D1, D2 | D2 | D1 | |

Table 5.9. Summary of permutational multivariate analysis of variance tests to detect differences among groups of BET and YFT within individual Indonesian Fisheries Management Areas (FMAs). Pairwise test results that are significant at p = 0.01 are highlighted.

| Species | Year | FMA | Groups compared | F | p | df |
|---|---|---|---|---|---|---|
| **BET** | 2013 | FMA 573 | Palabuhanratu A vs. Prigi A | 10.84 | 0.001 | 1, 59 |
| | | FMA 714 | Kendari A vs. Ambon | 4.70 | 0.003 | 1, 73 |
| | | FMA 715 | Gorontalo A vs. Gorontalo C | 0.78 | 0.541 | 1, 30 |
| | | FMA 717 | Sorong A vs. Jayapura | 3.61 | 0.016 | 1, 36 |
| | 2014 | FMA 572 | Padang A vs. Padang B | 2.32 | 0.035 | 1, 59 |
| | | FMA 573 | Palabuhanratu B vs. Prigi B | 1.59 | 0.187 | 1, 78 |
| | | FMA 714 | Kendari C vs. Ambon | 0.97 | 0.411 | 1, 69 |
| | | FMA 717 | Sorong A vs. Jayapura | 5.94 | 0.001 | 1, 44 |
| **YFT** | 2013 | FMA 573 | Palabuhanratu A vs. Prigi A | 3.77 | 0.018 | 1, 71 |
| | | FMA 714 | Kendari A vs. Ambon | 4.65 | 0.008 | 1, 104 |
| | | FMA 716 | Bitung A vs. Bitung D | 1.34 | 0.257 | 1, 32 |
| | | FMA 717 | Sorong A vs. Jayapura | 7.75 | 0.001 | 1, 67 |
| | 2014 | FMA 573 | Palabuhanratu B vs. Prigi B | 0.75 | 0.510 | 1, 119 |
| | | FMA 715 | Kendari B vs. Gorontalo C | 2.21 | 0.063 | 1, 75 |
| | | FMA 715 | Kendari B vs. Bitung G | 2.58 | 0.049 | 1, 59 |
| | | FMA 715 | Gorontalo C vs. Bitung G | 2.38 | 0.059 | 1, 72 |
| | | FMA 717 | Sorong A vs. Jayapura | 12.20 | 0.001 | 1, 48 |

## 5.7 Figures

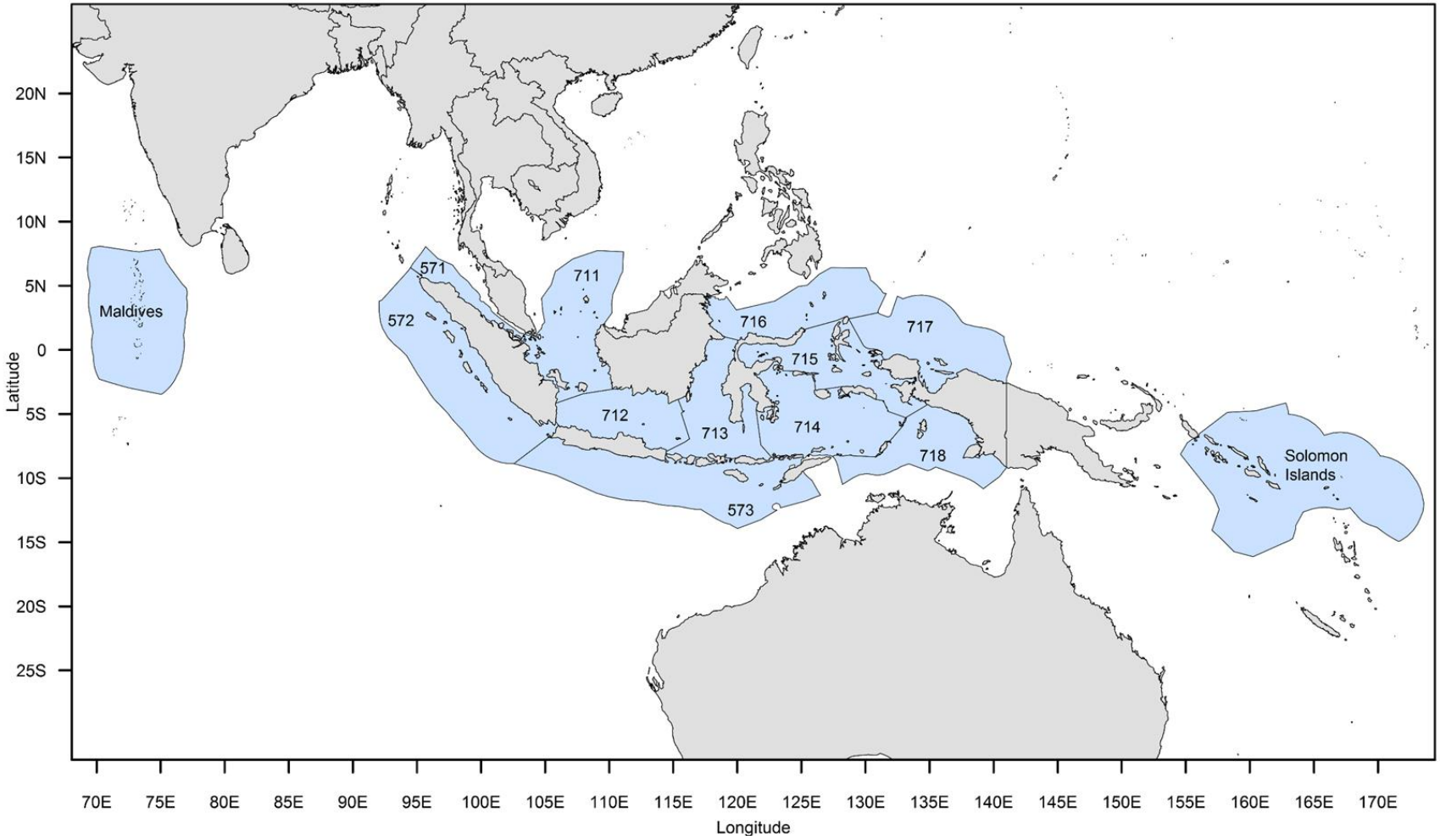


Figure 5.1. Map showing the Indonesian Fisheries Management Areas (FMAs) and the two additional sampling zones.

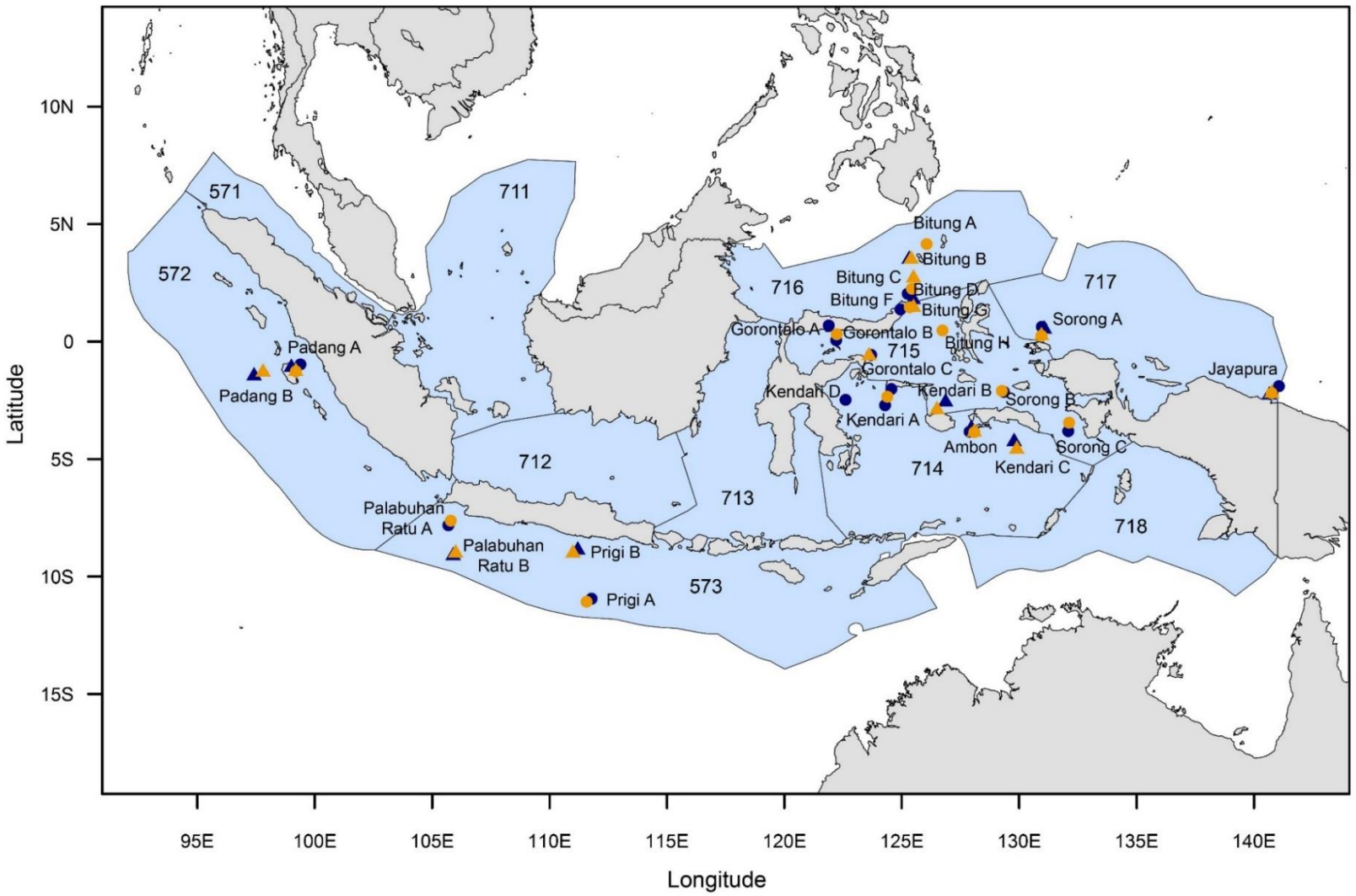


Figure 5.2. Map of Indonesia showing the 'as best known' locations of the catch locations of fish sampled. Blue = BET, orange = YFT. Circles = 2013, triangles = 2014.

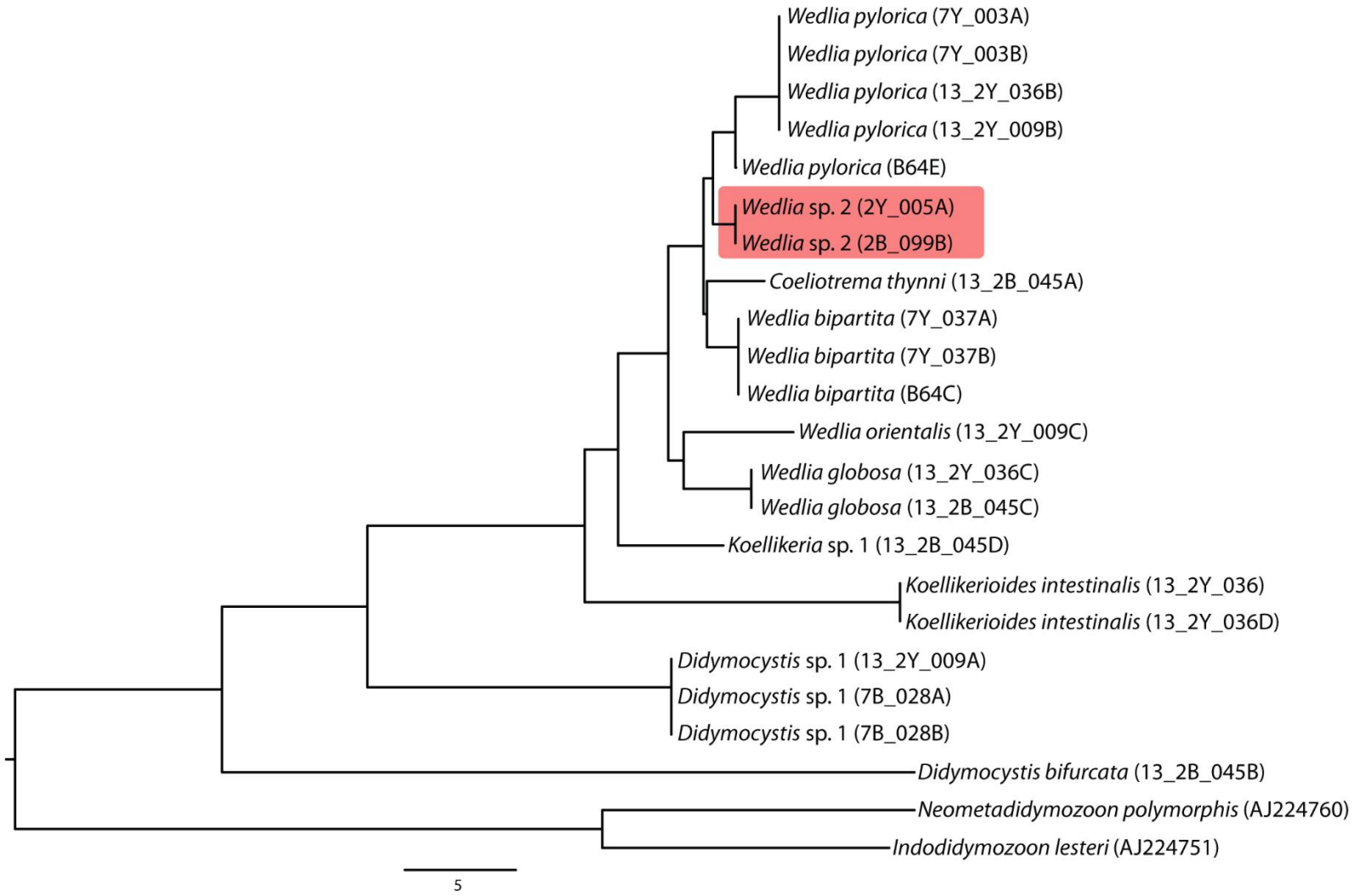


Figure 5.3. Neighbour-joining analyses of the ITS2 sequences of didymozoids from BET and YFT. Highlighted pair is an example of the same parasite species occurring in both tuna species.

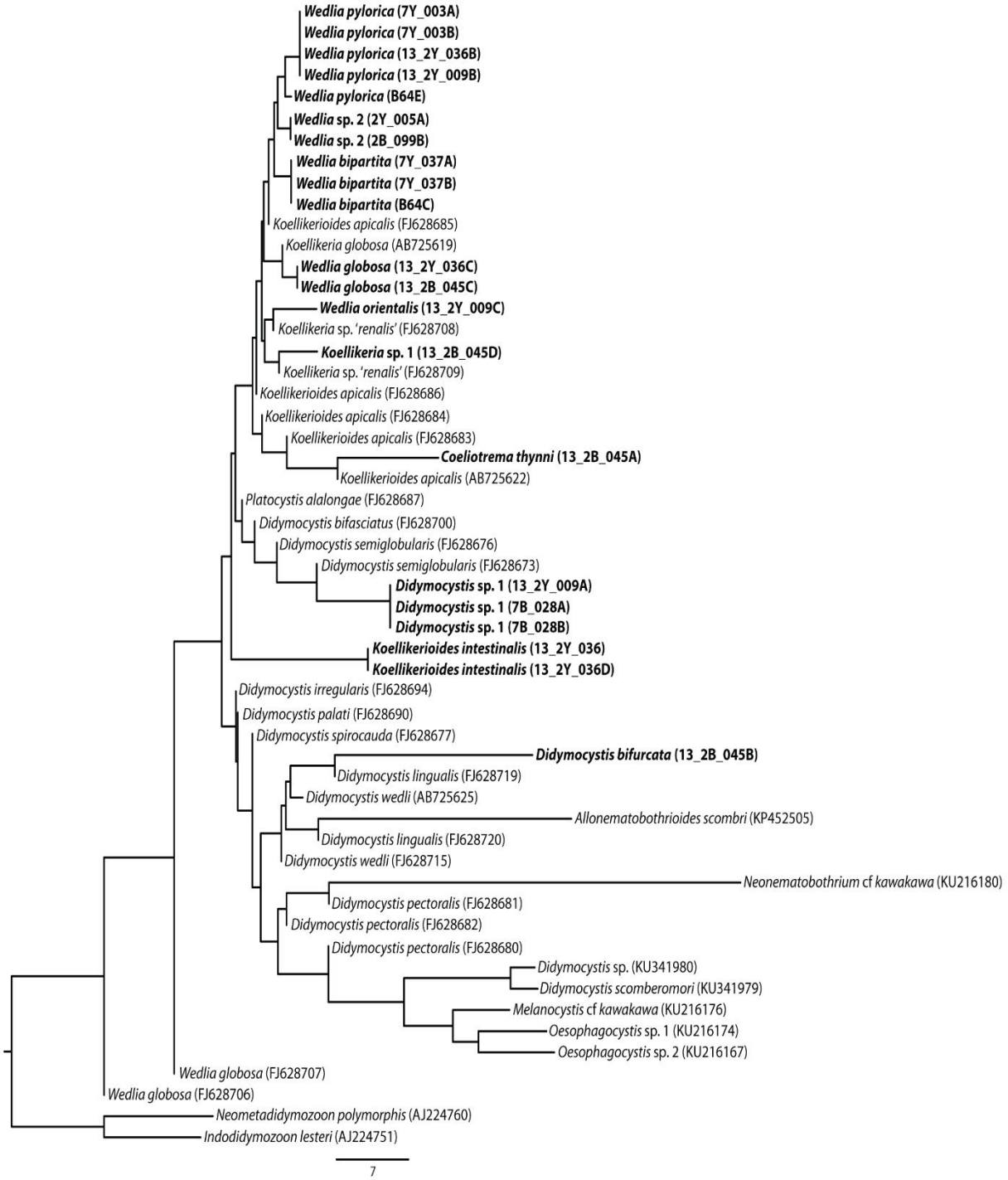


Figure 5.4. Neighbour-joining analyses of the ITS2 sequences derived in this project (bold type) with sequences from GenBank.

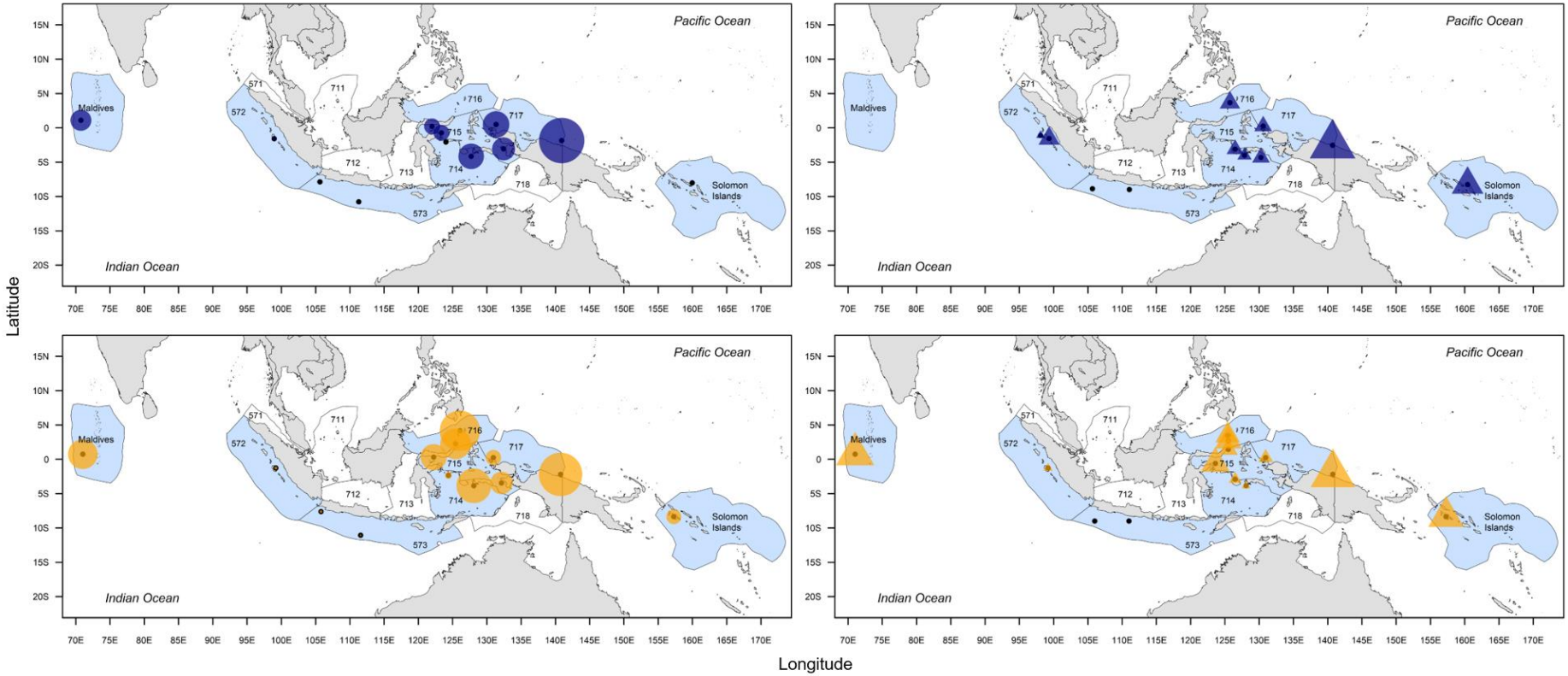


Figure 5.5. Relative prevalence of *Didymozoon longicolle* from samples of bigeye tuna (top row) and yellowfin tuna (bottom row) in 2013 (circles; left column) and 2014 (triangles; right column). Only those locations were >8 fish were dissected are shown. Zero prevalence is indicated by a solid black dot.

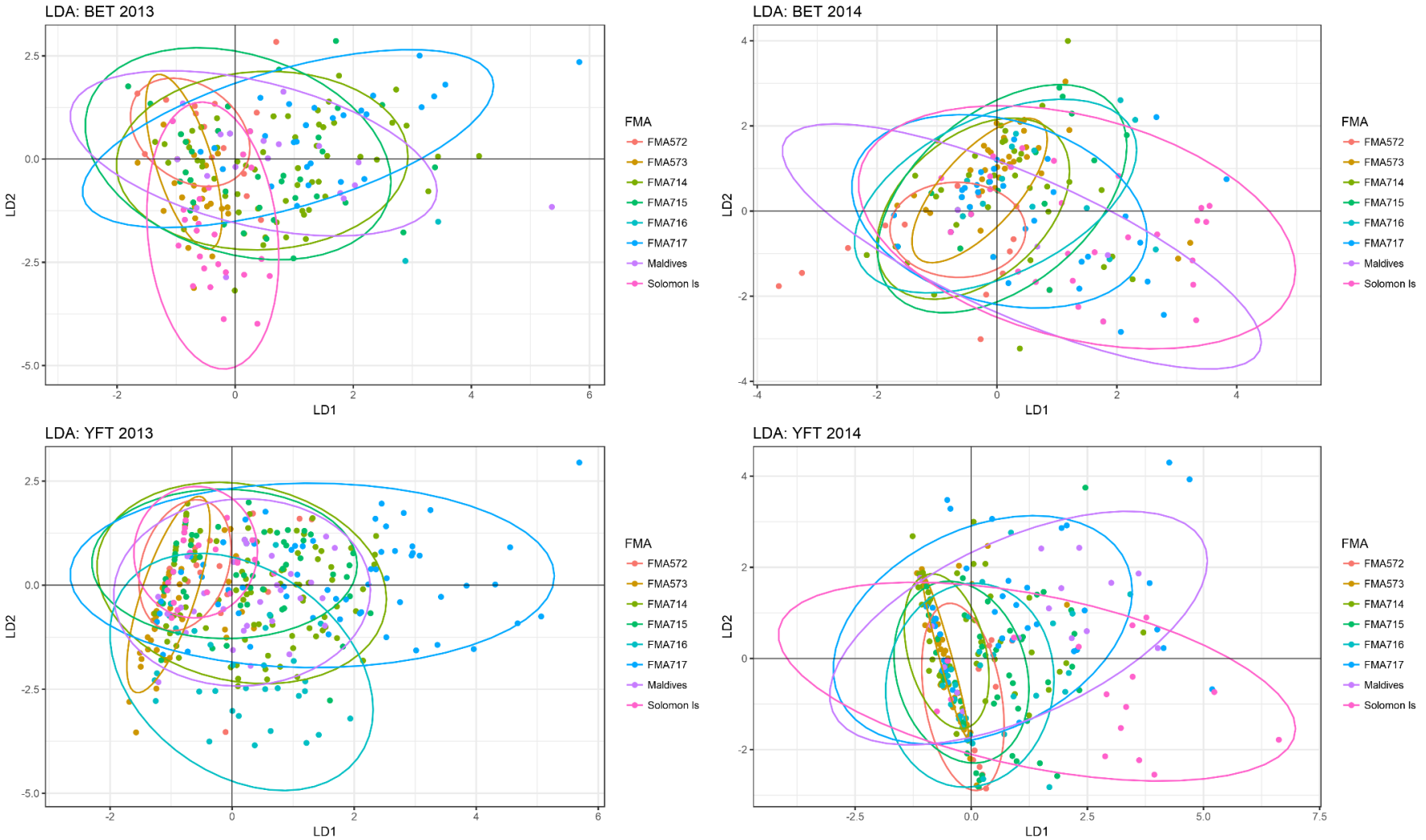


Figure 5.6. Results of Linear Discriminant Analysis (LDA) for BET (*T. obesus*; top) and YFT (*T. albacares*; bottom) for 2013 (left) and 2014 (right) by Fisheries Management Areas (FMAs) showing 95% confidence ellipses. Note the ellipse for BET from FMA716 in 2013 was not drawn due to insufficient sample size.

## 5.8 References (cited in Section 5)

Aguila R. D., Perez S. K. L., Catacutan B. J. N., Lopez G. V., Barut N. C. and Santos M. D. (2015). Distinct yellowfin tuna (*Thunnus albacares*) stocks detected in Western and Central Pacific Ocean (WCPO) using DNA microsatellites. Plos One 10 (12): # e0144568.

Anderson G. R. and Barker S. C. (1998). Inference of phylogeny and taxonomy within the Didymozoidae (Digenea) from the second internal transcribed spacer (ITS2) of ribosomal DNA. Systematic Parasitology 41: 87–94.

Ankenbrand M. J., Keller A., Wolf M., Schultz J. and Förster F. (2015). ITS2 Database V: Twice as much. Molecular Biology and Evolution 32: 3030–3032.

Baudin-Laurencin F. (1971). Crustaces et helmonthes parasites de l'albacore (*Thunnus albacares*) du Golf de Guinée. Documents scientifiques. Centre de Rechercher Oceanographiques Abidjan (ORSTOM), 2: 11–30.

Bush A. O., Lafferty K. D., Lotz J. M. and Shostak J. M. (1997). Parasitology meets ecology on its own terms: Margolis et al. revisited. Journal of Parasitology 83: 575–583.

Cribb T. H., Anderson G. R., Adlard R. D. and Bray R. A. (1998). A DNA-based demonstration of a three-host life-cycle for the Bivesiculidae (Platyhelminthes: Digenea). International Journal for Parasitology 28: 1791–1795.

Dammannagoda S. T., Hurwood D. A. and Mather P. B. (2008). Evidence for fine geographical scale heterogeneity in gene frequencies in yellowfin tuna (*Thunnus albacares*) from the north Indian Ocean around Sri Lanka. Fisheries Research 90:147–157.

Dao H. T., Smith-Keune C., Wolanski E., Jones C. M., Jerry D. R. (2015). Oceanographic currents and local ecological knowledge indicate, and genetics does not refute, a contemporary pattern of larval dispersal for the ornate spiny lobster, *Panulirus ornatus* in the South-East Asian Archipelago. *PLoS One*, 10: e0124568.

Edgar R. C. (2004). MUSCLE: multiple sequence alignment with high accuracy and high throughput. Nucleic Acids Research 32: 1792–1797.

Eveson J. P., Million J., Sardenne F. and Le Croizier G. (2015). Estimating growth of tropical tunas in the Indian Ocean using tag-recapture data and otolith-based age estimates. Fisheries Research 163: 58–68.

Farley J., Clear N., Leroy B., Davis T. and McPherson G. (2010). Age and growth of bigeye tuna (*Thunnus obesus*), from the eastern and western Australian Fishing Zone. Final report 2000/100 to the Fisheries Research and Development Corporation. CSIRO Marine Research, Hobart, Tasmania.

Gordon A. L. (2005). Oceanography of the Indonesian Seas and their throughflow. *Oceanography*, 18(4): 14–27.

Grewe P. M., Feutry P., Hill P. L., Gunasekera R. M., Schaefer K. M., Itano D. G., Fuller D. W., Foster S. D. and Davies C. R. (2015). Evidence of discrete yellowfin tuna (*Thunnus albacares*) populations demands rethink of management for this globally important resource. Scientific Reports 5, 16916. doi: 10.1038/srep16916.

Ishii N. (1935). Studies on the family Didymozoidae Monticelli, 1888. Japanese Journal of Zoology 6: 279–335.

Itano D. G. (2000). The reproductive biology of yellowfin tuna (*Thunnus albacares*) in Hawaiian waters and the western tropical Pacific Ocean: project summary. SOEST-JIMAR # 00-328, pp 69.

Jones J. B. (1991). Movements of albacore tuna (*Thunnus alalunga*) in the South-Pacific - evidence from parasites. Marine Biology 111 (1): 1-9.

Keller A., Schleicher T., Schultz J., Müller T., Dandekar T. and Wolf M. (2009). 5.8S-28S rRNA interaction and HMM-based ITS2 annotation. Gene 430: 50–57.

Køie M., Lester R. J. G. (1985). Larval didymozoids (Trematoda) in fishes from Moreton Bay, Australia. Proceedings of the Helminthological Society of Washington 52: 196–203.

Kusuma D. W., Murdimanto A., Aden L. Y., Sukresno B., Jatisworo D., Hanintyo R. (2017). Sea surface temperature dynamics in Indonesia. IOP Conference Series: Earth and Environmental Science 98: 012038. Doi: 10.1088/1755-1315/98/1/012038.

Lester R. J. G. and Newman L. J. (1986). First rediae and cercariae to be described from heteropods. Journal of Parasitology 72: 195–197.

Lester R. J. G. and MacKenzie K. (2009). The use and abuse of parasites as stock markers for fish. Fisheries Research 97: 1–2.

Lester R. J. G. and Moore B. R. (2015). Parasites as valuable stock markers for fisheries in Australasia, East Asia and the Pacific Islands. Parasitology 142: 36–53.

Lester R. J. G., Barnes A. and Habib G. (1985). Parasites of skipjack tuna, *Katsuwonas pelamis* – fishery implications. Fishery Bulletin 83: 343–356.

Lester R. J. G., Sewell K. B., Barnes A. and Evans K. (1988). Stock discrimination of orange roughy, *Hoplostethus atlanticus*, by parasite analysis. Marine Biology 99: 137–143.

Lester R. J. G., Thompson C., Moss H. and Barker S.C. (2001). Movement and stock structure of narrow-barred Spanish mackerel as indicated by parasites. Journal of Fish Biology 59: 833–842.

Mele S., Merella P., Macias D., Gomez M. J., Garippa G. and Alemany F. (2010). Metazoan gill parasites of wild albacore *Thunnus alalunga* (Bonaterre, 1788) from the Balearic Sea (western Mediterranean) and their use as biological tags. Fisheries Research 102: 305–310. DOI: 10.1016/j.fishres.2010.01.002.

Mele S., Macias D., Gomez-Vives M. J., Garippa G., Alemany F. and Merella P. (2012). Metazoan parasites on the gills of the skipjack tuna *Katsuwonus pelamis* (Osteichthyes: Scombridae) from the Alboran Sea (western Mediterranean Sea). Diseases of Aquatic Organisms 97: 219–225. DOI: 10.3354/dao02421.

Moore B. R., Welch D. J., Newman S. J. and Lester R. J. G. (2012). Parasites as indicators of movement and population connectivity of a non-diadromous, tropical estuarine teleost: king threadfin *Polydactylus macrochir*. Journal of Fish Biology 81: 230–252.

Morgan J. A. and Blair D. (1995). Nuclear rDNA ITS sequence variation in the trematode genus Echinostoma: an aid to establishing relationships within the 37-collar-spine group. Parasitology 111: 609–615.

Nascimento-Justo M. C. and Kohn A. (2012). Notes on helminth parasites of tuna fishes (Scombridae) in Brazil. Revista Mexicana de Biodiversidad 83: 285-290.

Oksanen J., Blanchet F. G., Friendly M., Kindt R., Legendre P., McGlinn D., Minchin P. R., O'Hara R. B., Simpson G. L., Solymos P., Steven M. H. M., Szoecs E. and Wagner H. (2017). Vegan; community ecology package. R package version 2.4-2. https://CRAN.R-project.org/package=vegan

Poulin R. and Kamiya T. (2015). Parasites as biological tags of fish stocks: a meta-analysis of their discriminatory power. Parasitology SI 142:145–155.

R Core Team (2016). R: A language and environment for statistical computing. R Foundation for Statistical Computing, Vienna, Australia. http://www.R-project.org/.

Ripley B., Venables B., Bates D. M., Hornik K., Gebhardt A. and Firth D. (2016). Support functions and datasets for Venables and Ripley's MASS. R package version 7.3. https://cran.rproject.org/web/packages/MASS/MASS.pdf

Rooker J. R., Wells R. J. D., Itano D. G., Thorrold S. R., Lee J. M. (2016). Natal origin and population connectivity of bigeye and yellowfin tuna in the Pacific Ocean. *Fisheries Oceanography*, 25: 277–291.

Sambrook J. and Russell D. W. (2001). *Molecular cloning: A laboratory manual*. Cold Spring Harbor, NY: Cold Spring Harbor Laboratory Press. 2344 pp.

Sardenne F., Dortel E., Le Croiziera G., Million J., Labonne M., Leroy B., Bodin N. and Chassot E. (2015). Determining the age of tropical tunas in the Indian Ocean from otolith microstructures. Fisheries Research 163: 44–57.

Schaefer K., Fuller D., Hampton J., Caillot S., Leroy B. and Itano D. (2015). Movements, dispersion, and mixing of bigeye tuna (*Thunnus obesus*) tagged and released in the equatorial Central Pacific Ocean, with conventional and archival tags. Fisheries Research 161: 336–355. http://dx.doi.org/10.1016/j.fishres.2014.08.018

Tamura K., Stecher G., Peterson D., Filipski A., and Kumar S. (2013). MEGA6: Molecular Evolutionary Genetics Analysis version 6.0. Molecular Biology and Evolution 30: 2725–2729.

Tanabe T. (2001). Feeding habits of skipjack tuna *Katsuwonus pelamis* and other tuna *Thunnus* spp. Juveniles in the tropical western Pacific. Fisheries Science 67: 563–570.

Vande Vusse F. J. (1980). A pelagic gastropod first intermediate host for a hemiuroid trematode. Journal of Parasitology 66: 167-168.

Weng J. S., Lee M. A., Liu K. M., Huang H. H. Wu L. J. (2017). Habitat and behaviour of adult yellowfin tuna (*Thunnus albacares*) in the waters off southwestern Taiwan determined by pop-up satellite archival tags. *Aquatic Living Resources*, 30: 34.

Williams Jr. E. and Bunkley-Williams L. (1996). Parasites of offshore big game fishes of Puerto Rico and the Western Atlantic. Antillean College Press. 382 pp.

Yamaguti S. (1970). The digenetic trematodes of Hawaiian fishes. Keigaku Publishing Co. Ltd, Tokyo, 436 pp.

# 6. Technique 2: Otolith chemistry

Team: Naomi Clear[1], Paige Eveson[1], Craig Proctor[1], Arief Wujdi[2], Matt Lansdell[1], Chris Dietz[3], Jay Thompson[4], and Leonid Danyushevsky[4]

[1]CSIRO Oceans and Atmosphere, Hobart, Tasmania, Australia

[2]Research Institute for Tuna Fisheries, Bali, Indonesia

[3]Central Science Laboratory, University of Tasmania, Sandy Bay, Tasmania, Australia

[4]Centre for Ore Deposit and Earth Sciences, University of Tasmania, Sandy Bay, Tasmania, Australia

*Note: The Tables and Figures for this chapter follow as Sections 6.6 and 6.7 respectively, following the Discussion (Section 6.5).*

## 6.1 Introduction

Elemental concentrations and stable isotopic ratios in fish otoliths can act as natural markers to identify population structures and movements of fish through specific water bodies (Fraile et al. 2016; Wells et al. 2015). In this study we used otoliths to provide information about fidelity to locations and, conversely, to inform us about connectivity, or the degree of exchange between fish populations.

Stable isotopes are non-radioactive forms of elements that are differentiated by their atomic mass. They occur naturally in the tissues of fish and have been measured in blood, muscle, endolymph (fluid surrounding the otoliths) and otoliths (Mulcahy et al. 1979; Schwarcz et al. 1998). Two that have been studied extensively and vary between groups of fish are the isotopes of oxygen (O18:O16) and carbon (C13:C12). These isotopes are deposited in the inorganic crystalline aragonite of otoliths; their ratio in the otolith is determined partially by the surrounding environment and hence these ratios can reflect differences between areas (Dufor et al. 1998; Edmonds et al. 1999).

Oxygen isotopes are thought to be deposited approximately in equilibrium with ambient seawater. They can be used to identify separate water bodies of water in which ambient temperature differs and hence have been used to delineate stocks of a number of fish species (Edmonds and Fletcher 1997; Edmonds et al. 1999; Gao and Beamish 1999; Newman et al. 2000; Stephenson et al. 2001; Shiao et al. 2010; Fraile et al. 2014). The deposition of carbon isotopes in otoliths is more complex; sources include dissolved inorganic carbon and metabolic carbon derived from diet. Their incorporation can be influenced by metabolic rate and oxygen consumption (Thorrold et al. 1997; Schwarcz et al. 1998), ontogenetic changes, increased range of depth distribution (i.e. spending more time in colder water), and dietary shifts (Mulcahy et al. 1979; Radtke et al. 1996; Schwarcz et al., 1998).

Other elements in ambient seawater are incorporated into otoliths, within or onto the calcium carbonate crystal or bonded to the organic matrix (Izzo et al. 2016). In general, the concentration of elements in otoliths can be described as ‘macro’, >10% by weight, such as Ca, C and O; ‘micro’, 100-5000 ppm, including Na, Sr, K, S and Cl; and ‘trace’, less than 50-100 ppm, including Zn, Br, Se, Ni and Pb. Similar to stable isotope ratios, the concentrations of elements deposited in otoliths can reflect ambient water chemistry and they can also be influenced by physiological and behavioural effects. Some otolith elements exist in concentrations close to equilibrium with the surrounding environment, such as Ba (Moore and Simpfendorfer 2014) while other elements are driven more by physiology, including metabolism and growth rates, such as Mg and Mn (DiMaria et al. 2010; Sturrock et al. 2012). Others, such as Sr can be influenced by either or both (Fowler et al. 1995). The nature and extent of physiological control over the incorporation of elements is perhaps the most poorly understood of all the factors influencing otolith chemistry. However Campana et al. (2000) note that if physiologically controlled elements do differ significantly among groups, there is no reason to exclude them from the chemical ‘fingerprint’. In fact, in situations where groups of fish come from different spawning areas but experience the same environmental conditions, those

otolith elements under more physiological control play an important role in differentiating groups (Kerr and Campana 2013).

One further influence on otolith composition in this study is the ability of tunas to elevate their body temperature using vascular counter-current heat exchangers (Carey 1973; Holland et al. 1992), potentially affecting the incorporation of elements and stable isotopes into the otoliths, moving it further from equilibrium with the ambient water. The extent of this ability varies between tuna species and these thermoregulatory mechanisms are less developed in yellowfin tuna compared with bigeye tuna (Dewar et al. 1994; Bernal et al. 2017). However the mechanisms are underdeveloped in very small tunas, which are limited to warmer waters, avoiding incursions into colder water until at least 1.5 – 2 kg in weight (Graham et al. 2007; Kubo et al. 2008; Schaefer et al. 2009). Hence, in the current study, otolith composition may not be confounded by thermoregulation, in particular at the analysis spot at the core region.

Kinetic and metabolic factors and thermoregulation can all influence the incorporation of stable isotopes and elements into otoliths. These influences are not constant over the life of a fish because physiology changes as the fish develops. As a consequence, ontogenetic effects on otoliths mean that stable isotope ratios and elemental concentrations measured at different points on otoliths, i.e. deposited at different life stages of the fish, cannot be directly compared. While all the factors and processes involved in tuna otolith development are not understood, differences in otolith composition between groups of fish can still provide evidence of natal origin and spatial structure (Wells et al. 2012). Otoliths act as a natural tag that can be used to differentiate groups of fish and, because otolith chemistry is believed to be phenotypically controlled, patterns of stock structure and dynamics can be derived even where there is no genetic heterogeneity within the fish sampled. Fish are subject to seasonal and annual changes in environmental conditions and otolith composition can vary within those time scales. The sampling design allowed us to test for inter-annual variability in otolith composition and to minimise ontogenetic effects.

We used stable isotope ratios and element concentrations measured in otoliths that were collected as part of the overall project to address one of the project's key aims (see section 4): namely to investigate if the data support the well-mixed stock hypothesis, currently assumed in the assessment and management of Indonesian tuna fisheries, or if they indicate more spatial structure.

Another overall project objective achieved within the otolith chemistry study was capacity development for Indonesian scientists – we describe the training and involvement of an Indonesian scientist in several stages of the study.

## 6.2 Materials and Methods

The procedures employed for sampling of YFT and BET for the population structure study are covered in Section 4. Sagittal otoliths were sampled from bigeye and yellowfin tuna that were landed at 11 port locations in a narrow sampling period in both 2013 and 2014 (Table 6.1). This generated 44 groups of samples: from 2 species, 11 locations, in 2 years. The otoliths were received and archived at the CSIRO laboratories in Hobart.

### *6.2.1 Otolith Preparation*

From each of the 44 groups, samples for analysis were chosen by size, around the mean of fish length, with the aim to analyse fish that had been spawned at the same time to minimise variation in otolith composition due to ontogeny (Figures 6.1a and 6.1b). Analyses were conducted at two facilities: stable isotope ratios were analysed at the Central Science Laboratory, University of Tasmania (CSL), and elemental chemistry was analysed at the Centre for Ore Deposits and Earth Sciences at the University of Tasmania (CODES). The time required for sample preparation for CODES' samples was greater than that for CSL so we prepared a minimum of 20 samples for CODES

and 25 samples for CSL. There were several groups for which fewer than 20 samples had been collected, e.g. bigeye in Bitung in 2013. For these groups we prepared all otoliths that were available.

Where possible, we chose samples that had two intact otoliths so that one from each pair could be analysed at CSL and the other at CODES, i.e. sister otoliths (from the same fish) were analysed at the two facilities. When one of the pair was broken, distal to the primordium, the intact otolith was used for CSL and the broken otolith for CODES. If both otoliths were broken, distal to the primordium, the otolith with the least material missing was used for CSL. If either otolith was broken through the primordium, the pair were not considered for analysis.

Once chosen for analysis, otoliths were cleaned in milli-Q water, dried and imaged. Images of samples were taken under stereomicroscope and were captured by an iDS digital camera with uEye Cockpit 4.90 software (IDS Imaging Development Systems). Unbroken otoliths were weighed to 2 decimal places of a milligram.

For the stable isotope ratio analysis, whole otoliths were dissolved to determine an isotopic signal from the entire life of the fish. In contrast, the elemental isotope concentrations were measured at particular points along the otoliths using a laser. To achieve this, transverse sections were prepared that contained growth axes from the primordium to the margin.

### 6.2.2 Isotope Analysis

#### Sample processing

Common Isotope Ratio Mass Spectrometer (IRMS) instruments are gas source mass spectrometers, which means that the sample to be analysed is introduced in a gaseous state. This implies that most samples have to be processed before entering the mass spectrometer, so that only a single chemical species enters at a given time. Otoliths are chemically composed of calcium carbonate, mainly aragonite, which has to be converted into carbon dioxide while preserving the isotopic signature of the carbonate (Swart et al. 1991) it derives from.

#### Otolith digestion

Otolith samples are typically acid digested (103% $H_3PO_4$, 50° C, 12 h) until conversion into $CO_2$ is complete. To do so, the otolith is weighed on a high precision balance and then placed into the side finger of the reaction tube (A in Figure 6.2). Then, 5 mL of water free phosphoric acid are added to the main part of the tube (B in Figure 6.2). The tube is then joined with the tube top with a Viton® O-ring (C) and clamp (F) and connected through port E to the vacuum line (valve 1 in Figure 6.3). The whole tube is evacuated for about two hours by opening the valve on the reaction tube top to high vacuum. When properly evacuated, the otolith sample is thrown into the acid by inclining the reaction tube and the latter placed in a water batch at 50° C for 12 hours.

The carbonate-phosphoric acid reaction method was developed for offline chemistry and extraction of isotopically representative $CO_2$ from carbonates (McCrea 1950) and can be described by the following equation:

$$CaCO_3 + H_3PO_4 \leftrightarrow CaHPO_4 + CO_2 + H_2O \qquad \text{(Equation 1)}$$

As can be seen, out of the three oxygen atoms in the carbonate, only two end up in the $CO_2$ gas which will be measured. This causes the isotopic value to change and the measurement has to be corrected accordingly, as discussed in a later section.

#### Clean up of sample gas

Once the acid reaction has reached its equilibrium state, the resulting sample gas ($CO_2$) has to be purified. To do so, the reaction tube is removed from the water bath and connected to the vacuum line. After evacuating the connection, the valve on top of the reaction tube is opened and the

sample gas frozen into a first cold trap on the line (Figure 6.3), containing liquid nitrogen at -196° C. Non-condensable reaction by-products are pumped away after measuring their amount by taking a pressure reading on the Pirani gauge.

The sample gas is then thawed and frozen into the cold finger, also at -196° C. During this step, the gas passes through an intermediate cold trap, immersed into an acetone/$N_{2\ liq.}$ mixture at -94° C. This assures removal of any traces of water still present in the sample. After closing off the cold finger section of the vacuum line (valves 7-10, Figure 6.3, the sample is heated up to room temperature and a pressure reading is taken on the Baratron Vacuum Gauge. This measure indicates the yield, which is the amount of $CO_2$ gas produced by the acid digestion of the particular sample. Subsequently, a collection tube is attached onto the line, immersed in liquid nitrogen and frozen into it by opening valve 9. After that, the valve on top of the collection tube is closed, the latter detached from the vacuum line and the clean gas inside is now ready to be attached to the sample port of the mass spectrometer for measurement. Samples are flagged when non-condensables are high or the yield is out of the expected range.

**Measurement**

The resulting purified $CO_2$ is then transferred to the Isotope-Ratio Mass Spectrometer for measurement. In our case this is a dual inlet system (VG Optima), where the sample gas is alternated rapidly with a standard gas of known isotopic composition. A total of six of these measurements are then compared to yield a result and its corresponding analytical error (precision). The mass spectrometer for isotopic measurements generally consists in an ion source, a flight tube surrounded by a magnet and a detection system capable of measuring ions.

The ion source converts a part of the sample gas into charged ions, these are then accelerated over a potential in the kilo-volt range to produce a bundled beam which can be injected into a bended flight tube. The flight tube is situated within a strong magnetic field, causing a separation of the ion beam in components according to their mass-to-charge ratio (m/z). Due to their weight, heavier ion beams are bent in a bigger radius than lighter ones (see Figure 6.3). The current (concentration) of each separated ion beam is then measured using a 'Faraday cup' (or multiplier detector).

For carbon dioxide measurements, the by far most intense beam is at mass 44, representing $^{12}C^{16}O_2$, this is gas containing the most abundant isotopes of carbon and oxygen. At mass 45, we expect the carbon-12 isotope to be substituted by carbon-13 ($^{13}C^{16}O_2$) and similarly, at mass 46 one oxygen-16 to be substituted by an oxygen-18 isotope ($^{12}C^{16}O^{18}O$).

Fluctuations in the performance of the ion source make a classical calibration of an isotope concentration versus response in a single mass channel hard, if not impossible. These fluctuations will affect the whole ion beam (all masses) in the same way and therefore cancel out when the ratio of a minor to mayor beam is recorded. For this reason, the raw data for oxygen and carbon are the ratios m/z46 and m/z45, respectively, to m/z44.

**Corrections**

As can be seen from Equation 1, the $CO_2$ liberated by the acid reaction accounts for only 2/3 of the oxygen in the solid carbonate. An isotopic fractionation occurs, where the acid-liberated $CO_2$ is about 10 – 11 per mil (‰) heavier than the original carbonate, depending on the mineral and reaction temperature.

In order to correct for this effect when calculating the isotopic composition of the carbonate solid, an acid fractionation factor ($\alpha_{CO2(ACID)\text{-}otolith}$) appropriate for the reaction temperature and for the specific carbonate mineral was applied. As the reaction relies on an equilibrium state rather than on a reaction proceeding to completion, this equilibrium can be expressed as follows:

$$\delta_{true} = (\delta_{measured} - 1000*(E\text{-}1)/E) + K * (T_{Reaction} - T_{Standard})$$

being the equilibrium constant, or Acid Fractionation Factor (AAF), for calcite and the applied conditions:

E = 1.01025, K = 0.04; $T_{Reaction}$ = 50º C and $T_{Standard}$ = 25º C

The raw data is subjected to a number of instrumental corrections such as subtracting the amplifier zero readings and abundance sensitivity correction.

When analysing $CO_2$, different isotopic species of the same element (isotopologues) can produce a contribution at certain masses and a further correction must be made (Brand et al. 2010). The most commonly applied one is the Craig Correction, taking into account that international standard PDB has a contribution of approximately 6% at mass 45 due to $^{17}O$ isotope ($^{12}C^{16}O^{17}O$ instead of $^{13}C^{16}O_2$). Similarly, 0.2% of mass 46 is derived from isotopic species containing $^{13}C$ and $^{17}O$, but not $^{18}O$. Conversion of delta 45 values into delta 13 can then be expressed as:

$$\delta\,^{13}C = 1.067\,\delta(45/44) - 0.0338\,\delta\,^{18}O$$

and

$$\delta\,^{18}O = 1.0010\,\delta\,(46/44) - 0.0021\,\delta\,^{13}C$$

**Data Quality Assurance**

Raw data correction, calibration of isotope data and post run data correction protocols follow general principles that have been reviewed for example by Werner and Brand (Werner and Brand 2001), Most importantly, they are based on the `IT principle', referring to `Identical Treatment' of sample and reference material.

Isotopic differences can be measured most precisely when small, therefore the used Reference Materials should bracket the range of isotopic composition of the samples to be measured.

And even though the precision obtained with dual inlet systems by comparing the ion current ratios of the gases in both reservoirs a number of times is with approximately 0.01‰ very high, the same does not apply to the long-time accuracy of these measurements due to instrumental drifts. These can have multiple causes, including isotopic change of the reference gas in the dual inlet system during an analysis sequence, build-up of water or other contaminants, changing conditions of the mass spectrometer, deterioration of ion source conditions and many more.

In each run of 12 samples and four standards were processed at the start of the run plus one at the end, followed by a measurement of the zero enrichment. Traces for $\Delta$45/44 and $\Delta$46/44, ion currents, precision for the six combined sample/reference measurements and instrumental parameters (e.g. analyser and inlet vacuum, bellow positions at target beam etc.) were checked after each sample measurement, with the sample still in the bellow. The measurement was repeated if any anomaly was detected at this stage.

Data was then corrected for the usual isobaric interferences modified for a triple collector mass spectrometer and for any drift, e.g. caused by fractionation in the reference gas during the run. Figure 6.6 depicts an example for such a correction for the oxygen isotope, including the formula obtained for a linear fit and the square of the corresponding regression coefficient.

The error for these analyses is <0.1‰ as indicated by replicate analyses of internal standards.

**Reporting**

Isotope data reported as ‘delta’ values (δ) are ratios that relate the isotopic composition of the sample to that of a standard. Delta values are said to be either heavier (enriched) or lighter (depleted) than a standard and given as per mil (‰) difference (δ) compared to a standard. Delta

values are given as per mil (‰) difference (δ) compared to a standard. The result is multiplied by 1000 simply to make the resulting ratio more 'meaningful'.

$$\delta^{18}O = \left[ \frac{\left(\frac{^{18}O}{^{16}O}\right)_{sample}}{\left(\frac{^{18}O}{^{16}O}\right)_{standard}} - 1 \right] \times 1{,}000$$

For example, if a sample is said to have a delta value of +5 ‰ δ $^{18}$O, then it is 5 parts in 1000 enriched in $^{18}$O compared with the standard. If it has a delta value of -5 ‰ δ $^{18}$O then it is 5 parts in 1000 depleted in $^{18}$O.

The measured isotopic composition has to be converted and reported on an internationally accepted reference scale to enable accurate comparison of results. For $\delta^{13}$C and $\delta^{18}$O from carbonates, this is usually the Vienna Pee Dee Belemnite (VPDB) scale. This is a cretaceous marine fossil, which $\delta^{13}$C value was defined to be zero. Since this original Reference Material has exhausted more than two decades ago, Relative $^{13}$C/$^{12}$C values (d$^{13}$C) of carbonate are now expressed in per mill relative to VPDB by assigning a value of +1.95‰ exactly to NBS 19 calcite (Friedman at al. 1982). The Commission on Atomic Weight and Isotopic Abundances of the International Union of Pure and Applied Chemistry (IUPAC) recommends reporting of $^{18}$O/$^{16}$O values (d$^{18}$O) of carbonate either relative to VPDP or VSMOW scale.

Standard Mean Ocean Water (SMOW) consists of mixed distilled ocean waters collected from different spots around the globe. Respective values can be calculated using the following conversion:

$$\delta\,^{18}O_{SMOW} = \delta\,^{18}O_{PDB} * E + 1000*(E-1) \qquad \text{(Equation 2)}$$

being the equilibrium constant E = 1.03086.

In this study, two Certified Reference Materials (NBS 18 and NBS 19) and two inter-laboratory standards (ANU M1 and ANU PRM2) were used, their assigned values are given in Table 6.2.

### Post-run data evaluation protocols

Final results were given as valid if the precision of the measurement was better than 0.045 for the mean value of the six single measurements. A high non-condensable measure (NC) during sample clean-up may have several causes, such as an air leak during digestion or clean up, transfer line not evacuated or dirty sample, e.g. organic material attached. Some of these would affect the isotopic composition of the sample gas (e.g. air leak) and others not (e.g. organic contamination). Results for samples flagged with high NC were given as valid if their values were within 1.5 standard deviations of the other results obtained for a specific sampling site and tuna species. Given that $CO_2$ from air has $\delta^{13}$C and $\delta^{18}$O of ca -8 ‰ and +1 ‰, respectively, we would have to expect a shift to heavier values when otolith derived carbonate is contaminated with atmospheric $CO_2$.

A given otolith weight should produce a reproducible yield of carbon dioxide after digestion. This relation was checked over the whole study, as exemplified in Figure 6.5. A yield lower than expected could be due to a not totally digested sample (e.g. stuck to tube wall), partly sample loss during clean up, or impurities in the carbonate matrix, a high yield may be caused by an air leak, carbonate

contamination, crossover or an air leak during digestion or trapping. Again, some of these events may affect the isotopic results while others not.

Isotopic results for yield outliers were discarded or accepted following the same criteria than those applied for samples with high NC values. For these reasons, only 4 out of a total of 1123 samples were rejected. Isotopic outliers with no indication of any error during the analytical procedure were included in the further data treatment.

### 6.2.3 Otolith Proportion Index

Because the stable isotope technique digests the entire otolith, there is potential for this to affect the isotopic measurements obtained. We would expect the effect, if any, to be minimal since the remaining material of a broken otolith should still have isotope signal deposited throughout its life and hence from every location in which the fish has spent time. However, to be sure, we investigated whether the isotope values differed according to the amount of otolith present.

To determine whether the isotope values differed according to the amount of otolith present, we developed an index of "otolith proportion" (OPI) to quantify the amount of the otolith that was present for analysis.

The otoliths of small tuna are delicate and easily broken during sampling and cleaning. The break usually occurs at the rostral tip, the thinnest part of the otolith where new calcium carbonate is deposited. To estimate total length of broken otoliths, we examined a set of whole (unbroken) otoliths, measuring total length (TL) and the length along the primordium to post rostrum axis (PPL) (Figure 6.6). The linear relationship between TL and PPR was calculated for each species and this equation used to determine TL for broken otoliths (Figures 6.7, 6.8 and 6.9).

Otolith proportion index was then calculated using the following:

Otolith Proportion Index (OPI) = PL/ETL, where

PL is the length of the broken otolith,

ETL is the estimated length if the otolith was whole.

We examined stable isotope results to determine if there were significant differences between results for intact, whole, otoliths and those that were broken. We fitted linear regressions with either $\delta^{18}O$ or $\delta^{13}C$ as the independent variable and OPI as the explanatory variable to see if there was a significant relationship, for YFT and BET separately (Figure 6.10). The slope did not differ significantly from zero in any of the models (p-values >0.10). Thus, in our analyses of the stable isotope data (as described in Section 6.2.2), we made no distinction between partial and whole otoliths.

Histograms of the OPI values for BET and YFT are given in Figure 6.11, where a value of 1 indicates whole otoliths. The lowest OPI is 0.62 for BET and 0.65 for YFT.

**Left and right otolith equivalence**

To test for equivalence in the stable isotopes of left and right otoliths sampled from the same fish, we examined results from the analysis of pairs of otoliths at CSL. Ten fish were chosen for this study: 5 from each of the 2 tuna species in the ACIAR project; and the samples of each species were from 2 locations (Figures 6.12 and 6.13).

A paired t-test was run on the stable isotope ratios measured in 20 otoliths to determine whether there was a statistically significant mean difference between the values measured in sister otoliths.

There were no statistical differences between left and right otoliths for oxygen or carbon (Tables 6.3 – 6.5).

### 6.2.4 Elemental Composition Analysis

Unlike the stable isotope ratio analysis, during which the whole otolith was dissolved to determine an isotopic signal from the entire life of the fish, elemental concentrations were measured at 4 points along otolith sections. These points provided a chemical signal at particular stages in the fish's life:

1) 10 – 20 days from the primordium (beginning of life);

2) at the first inflection, when the fish was 30 – 40 days old,

3) inside the margin, covering material deposited approximately 2 weeks before capture which, in fish of around 40 cm, was when the fish was 3 – 4 months old;

4) a replicate of point 1 but on the other (dorsal) side of the primordium.

Using the results of the daily age analysis (see Section 4.4.2), an age at each of the 4 CODES analysis points was estimated, and a measurement of the width of increments at the four positions was made (Figure 6.14 and Table 6.6). This allowed a calculation of how many days were covered by the 29 micron laser spot. Increment width was highest at positions 1 and 2, with the laser only covering 2 - 3 days, while at the margin the laser covered around 2 weeks.

To prepare otoliths for CODES analysis, they were embedded in epoxy resin — EpoFix resin and hardener— and left to harden for a minimum of 24 hours. The resulting resin blocks containing the specimens were sectioned on an Accutom rotary saw with Buhler diamond-edged blades to produce transverse sections that contained the primordium and were approximately 0.8 mm thick. During cutting, Milli-Q water was used as a coolant and run across the blade and specimen.

The resulting sections were ground down on one side by-hand to expose the growth axis using two progressively-finer grades of silicon carbide wet-and-dry paper (1000 and 2400 grit) that were lubricated with Milli-Q water. The sections were then turned over and adhered permanently to glass slides using resin. The grinding was repeated on the other side of the section using the two grades of wet-and-dry paper; then polishing was done with 5 µm aluminium oxide lapping film. As the laser was predicted to create a 50 µm crater, we aimed to polish the section until the primordium lay 25 µm below the surface. To achieve this, we used a compound microscope fitted with both transmitted and incident lighting, which allowed focussing both on the surface and within the section and hence we could determine how far the primordium was below the surface of the section. During the polishing stage of preparation, the section was checked regularly under the microscope until the correct depth was reached. After each stage of grinding and polishing the mounts were cleaned ultrasonically for 3 minutes: one minute in each of 3 beakers of Milli-Q water.

Further sample preparation and the analyses of elemental composition were carried out at CODES. Individual otolith sections were mounted in 1" round epoxy mounts fitting 5 otoliths per mount (Figure 6.16). Epoxy was used to fix the otoliths (already thin-sectioned and fixed to glass) in the round. Any epoxy that accidently covered the otolith was gently polished away with 1200 grit and polished with 0.3 micron alumina oxide powder using high purity methanol. Samples were degassed overnight in a vacuum to remove any water vapour.

**Instrumentation**

Laser ablation: Resonetics RESOLution S-155 system with a Coherent 110 Compex Pro ArF excimer laser operating at 193nm wavelength and a ~20ns pulse width Mass spectrometer: Agilent 7900 Inductively Coupled Plasma Mass Spectrometer (ICP-MS).

### Analytical Conditions

Samples are put in to a large format laser ablation two volume cell (Muller 2009) that can accommodate 20 one inch rounds (Figure 6.16). The ablation cell is sealed and evacuated of all atmospheric air using a series of evacuations and backfilling with helium. Atmospheric air is known to cause higher interferences (oxide formation) as well as more change in the signal intensity with time (i.e. drift), so minimizing air is best practice.

Ablation takes place in a helium atmosphere flowing at 0.35 l/min. The otoliths are ablated at 10Hz repetition rate, a laser energy of ~3.5 J/cm2, ~30 micron spot for 45 seconds. Prior to each ablation the ICP-MS collects 30 seconds of 'gas blank' that subtracted from the signal during the ablation. During the ablation process the sample is vaporized and sent into the ICP-MS. Argon gas used normally fed into an ICP-MS, so the helium is combined with argon directly after the ablation site, the latter of which is flowing at 1.05 l/min. Helium is used in the ablation cell as it gives a smaller particle size distribution, less element fractionation and more sensitivity (Eggins 1998)

Standards analysed with otoliths are the NIST610 (Jochum 2011), BCR-2g – a basaltic glass, and MACS-3 – a synthetic carbonate pressed powder. BCR-2g and MACS-3 are from the United States Geological Survey. Standards are run approximately every hour to correct for instrument drift.

Isotopes measured are $^{7}$Li, $^{23}$Na, $^{24}$Mg, $^{31}$P, $^{39}$K, $^{43}$Ca, $^{55}$Mn, $^{56}$Fe, $^{57}$Fe, $^{63}$Cu, $^{65}$Cu, $^{85}$Rb, $^{88}$Sr, $^{137}$Ba, $^{208}$Pb with dwell times for each mass being between 20 and 30 milliseconds. The instrument sequentially measures intensities on each of these peaks starting at $^{7}$Li and finishing at $^{208}$Pb and then repeated. So the instrument will collect a reading of all these masses every 0.48 seconds leading to 178 measurements per isotope per measurement (this included both signal and the 'gas blank').

### Quantification

One issue with laser ablation is that different materials will ablated at different rates based on density and colour (among other factors). For example, a fish otolith with the exact same concentration of an element (e.g Sr) as that of a silicate glass will have different signal intensities (counts per second or cps) due to the different amount of material ablated. To account for this, the element of interest (Sr) is normalized to another element (internal standard element) that we know the concentration of (Longerich 1996). The assumption is that the element we know or can assume the concentration of (Ca in this case) behaves in the same way as the element of interest (Sr). This is generally true, however some elements will behave slightly differently and this is known as 'element fractionation' and is one of the major limitations to LA-ICP-MS. Normalizing elements to an internal standard also minimizes the effects of the signal drop off during ablation so that while the signal may drop off by 50%, the ratio of an element to the internal standard is relatively constant (Figure 6.17).

Data processing is done in a Microsoft Excel macro-based workbook developed in the Earth Science department at the University of Tasmania. Calculations are done using the equations of Longerich (1996). An example equation is shown for Sr in equation 1:

$$((^{43}Ca_{cps\text{-}smp}/^{88}Sr_{cps\text{-}smp}) / (Ca_{ppm\text{-}smp}/Sr_{ppm\text{-}smp})) = ((^{43}Ca_{cps\text{-}std}/^{88}Sr_{cps\text{-}std}) / (Ca_{ppm\text{-}std} / Sr_{ppm\text{-}std}))$$

Equation 1: PPM calculation formula based on Longerich (1996). "cps-smp" is the measured intensity (in counts per second) of a given isotope in the sample. "cps-std" is the measured intensity (in counts per second) of a given isotope in the standard. "ppm-smp" is the concentration of a given element in the sample. "ppm-std" is the concentration of a given element in the std.

As an example from the most recent session on February 16$^{th}$, 2016, otolith 195-1 Sr concentrations are calculated by re-arranging the formula above and using the NIST610 standard:

$43Ca_{cps\text{-}smp}$ =756255

$88Sr_{cps\text{-}smp}$ = 3203940

$Ca_{ppm\text{-}smp}$= 400400

$Sr_{ppm\text{-}smp}$ = unknown

$43Ca_{cps\text{-}std}$ = 123385 (from file A001)

$88Sr_{cps\text{-}std}$ = 748484 (from file A001)

$Ca_{ppm\text{-}std}$ = 81475

$Sr_{ppm\text{-}std}$ = 515.5

Re-arranging equation 1 gives:

$Sr_{ppm\text{-}smp} = Ca_{ppm\text{-}smp} / (( Ca_{ppm\text{-}std} / Sr_{ppm\text{-}std}) / (43Ca_{cps\text{-}std}/88Sr_{cps\text{-}std}) * (43Ca_{cps\text{-}smp}/88Sr_{cps\text{-}smp})$

$Sr_{ppm}$ = 400400 / ((81475/515.5)/(123385/748484)*(756255/3203940)) = 1767 ppm.

This value will differ slightly from the reported value in the results sheet since we take the drift corrected average (Sr/Ca cps ratio) of all NIST610 analyses. Additionally a secondary standard correction is done using BCR-2g and MACS-3 where concentrations are corrected to the accepted values for these materials. This is done to ensure accurate calibration and assess instrument performance by how well the two standards quantify relative to their published values.

Errors are propagated through calculations and include counting statistic errors from the element of interest and the internal standard element in both the standard and unknown as well as errors related to the drift correction. Errors are reported at 1 sigma level.

Detection limits are calculated based on Longerich (1996) using three times the standard deviation of the background in the 30 second gas blank for each analysis. This standard deviation value is then applied as a ratio to the internal standard element (Ca) and ppm is calculated as above. In this case the detection limit is a function primarily of the standard deviation of the background as well as the intensity of the internal standard. For elements with low level backgrounds (e.g. Sr) the background has many zeros and it becomes difficult to estimate the background accurately in only 30 seconds as there can often only be one 'count' on the detector in that time. Therefore the average detection limit of all the samples is also reported as this is more representative of the true detection limit.

### 6.2.5 Data processing

For both the stable isotope and element data, any value that was more than 4 SDs from the mean for a particular stable isotope/element and species (and otolith position in the case of the element data) was considered an outlier and omitted from further analyses. Assuming a normal distribution, the expected number of samples that would fall outside 4 SDs from the mean is approximately 1 in 10,000. For the isotope data, there were no $\delta^{13}C$ outliers and only 6 $\delta^{18}O$ outliers (3 for YFT and 3 for BET; Figure 6.18). The element data had a greater number of outliers with 101 over all elements, both species and all otolith positions. $^{7}Li$ had the most outliers with 33, whereas $^{39}K$ had no outliers (Table 6.7; Figure 6.19 a-b).

For the element composition data, there were a few elements for which a value was not obtained for some samples at one or more otolith positions, possibly because the amount of the element present was too small to be detected by the machine. Specifically, $^{56}Fe$ and $^{208}Pb$ had no value in over half of the sample-position combinations and therefore these elements were eliminated from further analyses. For $^{65}Cu$, $^{85}Rb$ and $^{55}Mn$, there were 193, 94 and 2 sample-position combinations, respectively, out of a total of 3419 for which the element did not have a value. Rather than imputing a value that may be incorrect, we chose to leave these as null, meaning that these samples will be left out of any analyses that use the elements and positions for which they are null. For most

elements, the distribution of values for a given species and otolith position are right-skewed, so we log-transformed the data to make them more closely follow a normal distribution, since this is an assumption of almost all of the statistical analyses performed (see next section, Statistical Analyses).

Figure 6.20 shows a map of where the samples used in the statistical analyses of the stable isotope and elemental composition data were collected for YFT and BET separately.

### 6.2.6 Statistical analyses

Data from the stable isotope analysis and elemental composition analysis were investigated separately to determine whether differences existed between samples collected from different Fishery Management Areas (FMAs; see Figure 6.20), as well as those collected from the two outlier sites, Maldives and Solomon Islands. Note that for convenience, we refer to the Maldives and Solomon Islands as FMA 111 and FMA 999 respectively, even though they are not true FMAs. Initially, simple summary statistics and plots were used to look for broad patterns in the data and do a preliminary comparison amongst FMAs. Subsequently, univariate and multivariate statistical models were used to more formally compare data amongst FMAs.

For the elemental composition data[10], prior to looking for differences among FMAs, we first investigated how the data for each element compared between the four different otolith positions (using paired t-tests of equivalence, as well as calculating correlations), as this would guide how we proceeded with further analyses. The results showed significant differences in the data for almost all elements and positions (see Results section 6.3), so in subsequent analyses, the element data were analysed for each otolith position separately.

Univariate analysis of variance (ANOVA) models were fit to the data from each stable isotope and element separately with FMA, season and their interaction as covariates. For the element data, the models were also fitted to the data from each otolith position separately. We ran the ANOVAs using (i) all FMAs, and (ii) leaving out the Maldives (FMA 111) and Solomon Islands (FMA 999) to see if differences existed within just the Indonesian archipelago.

Quadratic discriminant analyses (QDA) were also carried out on both the stable isotope and element data with FMA as the grouping variable. QDA is a type of classification analysis that is useful in determining whether a set of variables (in our case, either the stable isotope variables or the element variables) is effective in predicting group membership (i.e. which FMA a sample belongs to). QDAs were run for each species and season separately since the ANOVA results showed a significant season effect for both the stable isotope data and most elements in the elemental composition data, and for the elemental composition data, separate QDAs were also run for each otolith position. For the element data, we also ran QDAs using different subsets of elements to try and determine a set of elements that was most useful for distinguishing between FMAs; we used results from the ANOVAs, as well as correlations between elements, to help guide our choice of subsets to try. Thus, for the stable isotope data, 4 models were run (2 species x 2 seasons); whereas for the element data, 16 models were run (2 species x 2 seasons x 4 otolith positions) for each subset of elements tried. We used leave-one-out cross-validation to determine classification success rates. In order to determine how much better the classification success rate is than random (e.g., with only two areas, you would expect to classify 50% of the samples to the correct area simply by chance, even if the explanatory variables were not at all informative about area), we also randomized the FMAs and re-ran the QDAs, and we repeated this 1000 times.

We chose to use QDA rather than linear discriminant analyses (LDA) because LDA makes the assumption that the covariance matrices between groups (FMAs in our case) are equivalent, and in

[10] *Recall that the element data are log-transformed in all analyses (see Section 6.2.5).*

most cases this assumption was not met for our data based on Box's M-tests for homogeneity of covariance matrices (performed in R using the function *boxM* in package *biotools*).

For QDA, we needed to specify prior probabilities of a sample belonging to each FMA. Most commonly, either equal or proportional (i.e., proportional to the number of samples in each FMA) prior probabilities are assumed (noting that these would be the same if sample sizes were the same among all FMAs). Equal priors assume that a sample has an equal prior probability of belonging to any FMA, whereas proportional priors assume that a sample has a greater probability of belonging to an FMA with a larger sample size (which would be true if sampling was proportional to the population). Since sampling was not done in proportion to population size in our study, we used equal prior probabilities.

## 6.3 Results

### *6.3.1 Stable isotope results*

Sample sizes by species, season and FMA used in the stable isotope analyses after data processing (see Section 6.2.5) are given in Table 6.8. As for the element data, the sample sizes range in size since some FMAs incorporate more of the sample catch locations than others, and FMA 716 only has 2 BET samples in 2013 since very few BET were caught in this area in 2013.

Boxplots comparing the data by species and season (Figure 6.21) show that BET has higher values for both isotopes than YFT, and that for a given species, $\delta^{18}O$ is, on average, higher in 2014 than 2013. Looking at the data for each species broken down by FMA and season (Figures 6.22 and 6.23), we see that the difference in $\delta^{18}O$ values between seasons is largely driven by the western-most FMAs, particularly 111 (Maldives) and 572. Although both isotopes vary quite a lot within each FMA (this is particularly true for $\delta^{13}C$ for YFT), there are still noticeable differences between some areas. In general, the $\delta^{18}O$ values are highest[11] in the easternmost FMAs, whereas the $\delta^{13}C$ values are highest in the western most areas.

Because there are only two stable isotopes in our dataset, it is possible to visualize the data using scatterplots (Figures 6.24 and 6.25). The amount of variability within FMAs is large, however differences amongst FMAs are still apparent in the raw data, and more so when the data are plotted as means and standard errors. In particular, for YFT and BET, FMA 111 (Maldives) tends to have the largest $\delta^{18}O$ values, whereas FMA 999 (Solomon Islands) tends to have the highest $\delta^{13}C$ values. Within the Indonesian archipelago, the patterns are more species and season specific. For example, for BET in both seasons, the easternmost FMAs in the archipelago (FMA 716 and 717) group together and have higher $\delta^{13}C$ values on average than other areas in the archipelago (Figure 6.25). This is somewhat true for YFT in 2013 as well, but not in 2014 (Figure 6.24). Patterns in the data are quite consistent between seasons for BET, but less so for YFT.

Results from more formal statistical comparisons using ANOVAs are given in Table 6.9. The ANOVAs run using data from all FMAs confirm that, for YFT and BET, both isotopes differ significantly among FMAs. $\delta^{18}O$ differs significantly between seasons for both species, whereas $\delta^{13}C$ does not differ significantly between seasons for BET and only marginally for YFT ($p = 0.013$). The results for the ANOVAs leaving out the two outlier sites (FMAs 111 and 999) are very similar (Table 6.9), with the only exception being that the FMA:Season interaction is no longer significant in the $\delta^{18}O$ model for BET.

Results from running QDA models with FMA as the group variable and $\delta^{18}O$ and $\delta^{13}C$ as the explanatory variables, using leave-one-out cross-validation, are summarized in the Tables 6.10 and

[11] *Technically, amounts of isotopes are normally reported as "heavier/lighter" rather than "higher/lower", but for the purposes of this report we have used the latter.*

6.11. Table 6.10 gives the overall classification success rates (i.e., % of samples classified to the FMA where they were captured); and Table 6.11 gives the more detailed classification results by FMA, in order to see where the classification errors are made and if there are any consistent patterns.

The overall classification success rates are ~30% for YFT in both seasons and 36-40% for BET; these rates are much better than with randomized FMAs, for which the mean success rate from 1000 bootstraps ranges from 11.0 to 14.5% (Table 6.10). The classification results broken down by FMA (Table 6.11) show that the highest numbers generally occur along the diagonal of the tables, which means that samples are often correctly classified to the FMA where they were captured. Numbers tend to get smaller further away from the diagonal, meaning that samples which are not classified to the FMA where they were captured tend to be classified to adjacent or nearby FMAs.

In order to visualize the QDA classification results, Figure 6.26 shows plots of $\delta^{13}C$ vs $\delta^{18}O$ for YFT and BET in 2014 with the points colour-coded by predicted FMAs for comparison with the data colour-coded by observed FMAs (as in the top right panel of Figures 6.24 and 6.25). Given the large degree of variability and overlap in the stable isotope values among FMAs, the models do a reasonable job of assigning samples to groups corresponding to their observed FMAs.

### 6.3.2 Element composition results

Sample sizes by species, season and FMA used in the element analyses after data processing (see Section 6.2.5) are given in Table 6.12.The sample sizes range in size since some FMAs incorporate more of the sample catch locations than others (see Figure 6.20). For FMA 716, there are only 2 BET samples in 2013 because this FMA includes only the Bitung sample locations from which very few BET samples were obtained in 2013 (see Table 4.1).

For most elements, the data differed significantly between otolith positions for both YFT and BET (Figure 6.27). The position that has the highest or lowest values is not consistent between elements (for example, for $^{7}Li$, $^{23}Na$ and $^{24}Mg$, the lowest values tend to be for position 3, but for $^{88}Sr$ and $^{137}Ba$ the lowest values tend to be for position 2); however, the pattern for a given element is consistent between YFT and BET. For a couple of elements ($^{39}K$ and $^{85}Rb$) the data look quite similar between otolith positions, but boxplots do not take into account the fact that data from the different positions are not independent since they came from the same otoliths. Thus, a better way to compare the data between otolith positions is using paired t-tests to compare the data for a given element and species between any two otolith positions. Results from the paired t-tests show there are only a few cases, particularly for YFT, where there was not a significant difference (Table 6.13). Somewhat surprisingly, there were not more cases for which the data at positions 1 and 4 (both representing spots near the primordium) were not statistically equivalent.

Even though the data differs significantly between different otolith positions for most elements, the data may still be strongly correlated. For both YFT and BET, $^{23}Na$, $^{39}K$ and $^{88}Sr$ tend to be highly correlated between all otolith positions, and most elements tend to be highly correlated between otolith position 1 and 4 (Table 6.14). Thus, even though for most elements the data from the two positions near the primordium are not statistically equivalent, they are strongly correlated.

Boxplots were used to visually compare the data for each species by FMA and season. Only results for otolith position 1 (Figures 6.28 and 6.29) and position 3 (Figures 6.30 and 6.31) are shown[12]. Which elements vary the most amongst FMAs and also between seasons depends on the species and the otolith position. For example: $^{23}Na$, $^{39}K$ and $^{85}Rb$ appear quite variable between FMAs as

[12] *For many of the element concentration analyses, only results for positions 1 and 3 are shown since these represent the times near birth and capture, and are most useful for addressing whether there is evidence that a fish has moved long distances between these times. Note position 4 is also near the primordium, but on the dorsal rather than ventral side. As positions 2 and 3 are on the ventral side of the primordium, we opted to use position 1 for the "primordium point" to represent the time near birth.*

well as seasons for both species and otolith positions; $^{31}$P, $^{88}$Sr and $^{137}$Ba are reasonably variable amongst FMAs but similar between seasons; and $^{55}$Mn is highly variable between FMAs and seasons at position 3 (for both species) but not at position 1.

Results from more formal statistical comparisons using ANOVAs are given in Table 6.15. Again only results for otolith positions 1 and 3 are presented. We concentrate first on the results for the ANOVAs run using data from all FMAs. Regardless of species or otolith position, most elements differ significantly among FMAs, with the most common exceptions being: (i) $^{65}$Cu, which does not differ significantly between FMAs in any case except YFT position 1, and (ii) $^{7}$Li, which does not differ for YFT position 3 or BET position 1, and only marginally for BET position 3. Most elements also differ significantly between seasons, and have a significant FMA:Season interaction, but there are more exceptions and less consistencies across species and otolith positions. However, there are 3 elements, $^{23}$Na, $^{39}$K and $^{85}$Rb, for which all covariates are significant in all of the ANOVAs (i.e., for both species and otolith positions).

The results for the ANOVAs leaving out the two outlier sites (FMAs 111 and 999) are very similar (Table 6.16) with the only cases where an element no longer differs significantly amongst FMAs being $^{24}$Mg for YFT position 3, $^{39}$K for BET positions 1 and 3, and $^{88}$Sr for BET position 3. These results suggest it is not just the two outlier sites causing FMA to be a significant factor in the models, but rather that significant differences exist within the Indonesian archipelago.

The ANOVA results show that differences do exist in the elemental composition of samples from different FMAs, however the data only needs to differ between two or more areas in order for FMA to be a significant factor. The power to distinguish samples between FMAs is much greater if multiple elements are used, which is why we also used QDA. We initially ran the QDAs using all elements as explanatory variables, but based on the ANOVA results, we tried sequentially leaving out $^{65}$Cu and $^{7}$Li. Omitting these two elements gave consistently good results for both species and all otolith positions. We tried further reductions in elements, but the results varied a lot depending on the species and the otolith position (as we would expect based on the boxplots and ANOVAs). Rather than choosing a different subset of elements for each species and otolith position combination, we have opted to present and discuss results from the QDAs using all elements except $^{65}$Cu and $^{7}$Li. In order to summarize the results, we calculated the leave-one-out cross-validation success rates over all FMAs (Table 6.16). Across all species, otolith positions and seasons, the classification success rates range from 28.4% (BET 2014 position 4) to 50.8% (BET 2013 position 3), which are much better than with randomized FMAs, for which the mean success rate from 1000 bootstraps ranges from 12.2 to 14.5% (Table 6.16). Across the board, the classification success rates are higher in 2013 than 2014. Within a season, they are lowest for otolith position 2 and highest for position 3, with the exception of BET in 2014.

More detailed classification results broken down by FMA are presented for both species and seasons for otolith positions 1 and 3 (Table 6.17; see footnote below), in order to see where the classification errors are made and if there are any consistent patterns. The highest numbers generally occur along the diagonal of the tables, which means that samples are often correctly classified to the FMA where they were captured. Numbers tend to get smaller further away from the diagonal, meaning that samples which are not classified to the FMA where they were captured tend to be classified to adjacent or nearby FMAs. These general trends are true for both otolith positions 1 and 3, even though the overall classification success rate is smaller for position 1 (with the exception of BET 2014). We might have expected the classification success rates to be highest for the outlier sites, FMA 111 (Maldives) and FMA 999 (Solomon Islands), and while this is often true, there are many exceptions. For the same species and otolith position, the results can vary quite a lot between the two seasons; this is particularly true for the Solomon Islands (FMA 999) where the classification success rate is much lower in 2014 than 2013 for both species and both otolith positions.

## 6.4 Discussion

In this study, otolith chemistry has identified structure among the YFT and BET populations in the Indonesian archipelago. Applying discriminant function analysis to both the stable isotopes and elemental chemistry data sets, fish were often correctly classified to the FMA where they were captured, and when this was not the case, they tended to be classified to adjacent or nearby FMAs. This may indicate that fish generally did not move large distances between birth and capture (estimated to be at 3 – 4 months of age). However, this could also simply be due to the ocean environments being more similar amongst FMAs that are closer in proximity, in which case, even if fish remained in the same FMA between birth and capture, their otolith chemistry would still be more similar to nearby FMAs than to distant ones. While these two scenarios are not distinguishable with the data we have available (to do so would require data on the ocean chemistry of these regions in the two seasons for which we have otolith samples), in either case they suggest that these fish did not moved large distances in their first few months of life.

This could be further explored using the elemental composition data, for which data are measured at multiple otolith positions. If fish have remained within the same FMA between birth and capture, then the classification of samples to the FMAs where they were captured should be equally good using data from all otolith positions. However, if fish have moved substantially, such that they have spent time in multiple FMAs, then we would expect classification success rates to be best using data from the otolith position near the margin, since this position represents roughly two weeks in the last month of a fish's life (during which time the fish was likely to be in the FMA of capture). In comparison, we would expect classification results for the otolith position near the primordium to be worse than for the margin position, since this position represents several days in the first two weeks of a fish's life, at which time the element composition would not be expected to match the location of capture. Classification rates to the capture FMA were in fact higher at the margin than at the primordium for YFT in 2013 and 2014 and for BET in 2013. In 2014, the BET classification rate at the margin was 36.6% and slightly higher, 39.2%, at the primordium. A complication is that the data at the primordium may be influenced by maternal effects (e.g. Ruttenberg et al. 2005), in which case the lower classification rate at the primordium may not actually reflect fish movement, but instead reflect differences in maternal effects between fish.

Following on from the above discussion, if we assume that fish were in the FMA where they were caught during the few weeks prior to capture, then the elemental composition data at the margin should provide a "signature" for each FMA; i.e., the level of variability observed amongst fish captured in the same FMA should reflect the amount of variability that can be expected even for fish that have not moved. Thus the success rate for classifying fish to the FMA where they were captured that was obtained using the margin data should be the highest that can be achieved for fish that have not moved. The fact that the classification rate can be quite low at the margin for some seasons and regions presumably reflects that the chemistry of the ocean is more difficult to distinguish amongst regions in some seasons (e.g., due to the ocean chemistry at different regions being more similar to each other, or having greater variability such that differences are harder to detect). For example, consider BET in 2014: using element data from the margin, the classification success rate for fish caught around the Solomon Islands (FMA 999) was only 30.0% (6 out of 20), compared to 63.6% in 2013, and 2 fish were classified to the Maldives (FMA 111), from which we know they could not have travelled within such a short timeframe. This indicates that the otolith chemistry for BET around the Solomon Islands in 2014 overlapped significantly with the otolith chemistry for BET from other regions, presumably due to the ocean chemistry at the Solomon Islands being less distinguishable from other FMAs in this year. This hypothesis is supported by the fact that the classification success rate for YFT caught at the Solomon Islands (FMA 999) using margin data was also lower in 2014 than 2013.

Overall, the otolith chemistry results for both tuna species provide evidence that, in their first 3 – 4 months of life, fish are unlikely to have moved great distances, and many fish are likely to have

remained within the same FMA. We cannot say for certain whether some fish could have moved between the outlier sites (Maldives and Solomon Islands) and the Indonesian archipelago; a reasonable number of fish from the outlier sites were classified to the nearest FMAs within the archipelago (using both the stable isotope data and elemental composition data), but as noted above, this could just indicate the ocean chemistry being similar at these sites and not fish movement.

We observed significant differences in the otolith chemistry data ($\delta^{18}O$ and many elements) between 2013 and 2014 for both species and most locations. As discussed in the Introduction, ambient temperature can affect stable isotope levels in seawater, and thus their levels in fish otoliths. If the water temperature at a given location changed between seasons, then this could explain at least some of the observed differences in $\delta^{18}O$. To investigate, we extracted sea surface temperature (SST) within a +/-1.5 degree square of each sample location over the 6 months prior to the sampling date, and compared the average with the average $\delta^{18}O$ and $\delta^{13}C$ values at those locations. We found that SST was lower in 2014, and correspondingly, the $\delta^{18}O$ values were higher (heavier) at almost all locations. We did not find a consistent relationship between SST and $\delta^{13}C$.

The otolith chemistry data collected during this study could be a valuable resource to investigate the relationship between the otolith chemical fingerprint of groups of tuna and oceanographic parameters. In addition examining the elemental chemistry and stable isotopes in the otoliths of older BET and YFT could be an important next step for understanding how otolith chemistry is affected by ontogeny, and for identifying movements of fish beyond the first few months of life.

## 6.5 Tables

Table 6.1. Otoliths collected during the ACIAR project during two rounds

| Location | Bigeye tuna | | | Yellowfin tuna | | |
|---|---|---|---|---|---|---|
| | 2013 | 2014 | Total | 2013 | 2014 | Total |
| Ambon | 57 | 61 | 118 | 91 | 104 | 195 |
| Bitung | 4 | 23 | 27 | 99 | 95 | 194 |
| Gorontalo | 60 | 0 | 60 | 96 | 66 | 162 |
| Jayapura | 12 | 26 | 38 | 80 | 66 | 146 |
| Kendari | 50 | 91 | 141 | 100 | 103 | 203 |
| Maldives | 44 | 49 | 93 | 73 | 111 | 184 |
| Padang | 122 | 94 | 216 | 101 | 102 | 203 |
| Palabuhanratu | 102 | 102 | 204 | 101 | 100 | 201 |
| Prigi | 35 | 43 | 78 | 92 | 101 | 193 |
| Solomon Islands | 75 | 51 | 126 | 81 | 107 | 188 |
| Sorong | 99 | 71 | 170 | 97 | 106 | 203 |
| All locations | 660 | 611 | 1271 | 1011 | 1061 | 2072 |

Table 6.2: Isotopic composition of CRM's and LRM's applied in this study.

| CRM | ϱ $^{13}C_{PDB}$ | ϱ $^{18}O_{VPDB}$ | matrix |
|---|---|---|---|
| | | | |
| NBS-18 | -5.01 | -23.20 | carbonitite |
| NBS-19 | 1.95 | -2.20 | limestone |
| ANU-M1 | 1.32 | -6.05 | calcite |
| ANU-PRM2 | 0.72 | -17.41 | calcite |
| Ref: IAEA Values 10/2012 | | | |

Table 6.3. Probability table from t-test for carbon and oxygen isotopes

| Isotope | df | *t*-value | P(T<=t) two-tail | significance |
|---|---|---|---|---|
| δ $^{13}$C | 9 | 0.372708815 | 0.717991148 | NS |
| δ $^{18}$O | 9 | -0.012660605 | 0.990174778 | NS |

Table 6.4. Probability statistics for carbon isotopes

| δ $^{13}$C | N | Mean | StDev | SE Mean |
|---|---|---|---|---|
| left | 10 | -10.46 | 0.379 | 0.120 |
| right | 10 | -10.41 | 0.392 | 0.124 |
| difference | | -0.05 | -0.013 | -0.004 |

Table 6.5. Probability statistics for oxygen isotopes.

| δ $^{18}$O | N | Mean | StDev | SE Mean |
|---|---|---|---|---|
| left | 10 | -2.5385 | 0.177 | 0.056 |
| right | 10 | -2.5396 | 0.227 | 0.072 |
| difference | | 0.0011 | -0.016 | -0.050 |

Table 6.6. Ages, increment widths and temporal coverage of laser points 1 - 4.

| Point number | Position on otolith section | Approximate age at the position | Width of increments (microns) | Number of daily increments covered by laser point |
|---|---|---|---|---|
| 1 | 65 microns from primordium along ventral (long arm) | 2 weeks | 14 - 27 | 2 - 3 days |
| 2 | At first inflection, 30 microns in from the corner | 1 month | 15 - 29 | 2 - 3 days |
| 3 | At the margin, 60 microns from the edge | 3 - 4 months | 2 - 4 | 2 weeks |
| 4 | 65 microns from primordium along dorsal (short arm) | 2 weeks | Not measured | 2 - 3 days |

Table 6.7. Number of outliers for each element, by species and otolith position.

| Species | Position | $^{7}$Li | $^{23}$Na | $^{24}$Mg | $^{31}$P | $^{39}$K | $^{55}$Mn | $^{65}$Cu | $^{85}$Rb | $^{88}$Sr | $^{137}$Ba |
|---|---|---|---|---|---|---|---|---|---|---|---|
| BET | 1 | 5 | 2 | 1 | 0 | 0 | 0 | 2 | 1 | 0 | 2 |
| BET | 2 | 5 | 0 | 6 | 2 | 0 | 1 | 4 | 1 | 0 | 3 |
| BET | 3 | 2 | 1 | 3 | 1 | 0 | 0 | 1 | 0 | 1 | 1 |
| BET | 4 | 5 | 2 | 0 | 0 | 0 | 1 | 0 | 1 | 0 | 1 |
| YFT | 1 | 4 | 1 | 2 | 0 | 0 | 1 | 2 | 1 | 1 | 0 |
| YFT | 2 | 2 | 2 | 3 | 1 | 0 | 0 | 1 | 0 | 1 | 3 |
| YFT | 3 | 4 | 0 | 2 | 1 | 0 | 0 | 1 | 0 | 2 | 0 |
| YFT | 4 | 6 | 1 | 1 | 0 | 0 | 0 | 2 | 0 | 0 | 1 |
| | **Total** | **33** | **9** | **18** | **5** | **0** | **3** | **13** | **4** | **5** | **11** |

Table 6.8. Sample sizes by species, season and FMA used in the stable isotope analyses.

| | **BET** | | **YFT** | |
|---|---|---|---|---|
| **FMA** | | | | |
| | 2013 | 2014 | 2013 | 2014 |
| 111 | 25 | 24 | 24 | 26 |
| 572 | 27 | 25 | 31 | 25 |
| 573 | 49 | 50 | 50 | 52 |
| 714 | 53 | 31 | 55 | 32 |
| 715 | 37 | 22 | 40 | 70 |
| 716 | 2 | 21 | 23 | 18 |
| 717 | 28 | 50 | 39 | 31 |
| 999 | 37 | 25 | 25 | 25 |
| **Total** | **258** | **248** | **287** | **279** |

Table 6.9. Results from ANOVA models fit to the data from each isotope and species separately with FMA, season and FMA:Season interaction as covariates. Models were run (i) using all FMAs, and (ii) excluding FMAs 111 and 999, which correspond to the two outlier sites. Shown are p-values from tests of significance for each covariate. Shaded cells mark covariates that are NOT significant at level 0.05.

| Species | FMA option | Isotope | FMA | Season | FMA:Season |
|---|---|---|---|---|---|
| **YFT** | All | $\delta^{18}O$ | 0 | 0 | 0 |
| | | $\delta^{13}C$ | 0 | 0.013 | 0 |
| | Exclude 111 & 999 | $\delta^{18}O$ | 0 | 0 | 0 |
| | | $\delta^{13}C$ | 0 | 0.016 | 0 |
| **BET** | All | $\delta^{18}O$ | 0 | 0 | 0.044 |
| | | $\delta^{13}C$ | 0 | 0.233 | 0.850 |
| | Exclude 111 & 999 | $\delta^{18}O$ | 0 | 0 | 0.893 |
| | | $\delta^{13}C$ | 0 | 0.391 | 0.603 |

Table 6.10. Overall classification success rates (% correct over all FMAs) from the leave-one-out cross-validation QDAs run on the isotope data for each species and season separately.[1] For comparison, the mean, minimum and maximum classification success rates from 1000 bootstraps with randomized FMAs are also given.

| | | | % Correct from randomized FMAs | | |
|---|---|---|---|---|---|
| Species | Season | % Correct | Min | Mean | Max |
| **YFT** | 2013 | 32.4 | 1.4 | 11.6 | 27.9 |
| | 2014 | 29.4 | 1.4 | 11.0 | 25.1 |
| **BET** | 2013 | 36.3 | 2.3 | 13.4 | 29.3 |
| | 2014 | 40.3 | 0.8 | 11.4 | 33.9 |

[1]Results derived from the following call in R:

qda(FMA ~ O18 + C13, data=d, CV=TRUE, prior=rep(1/n.fma,n.fma))

where d contains the isotope data for the species and season being modelled, CV=TRUE means to use cross-validation, and n.fma=8 is the number of FMAs in the model, used to set equal prior probabilities for all FMAs.

Table 6.11. Classification tables from leave-one-out cross-validation QDAs run on the isotope data for each species and season separately. Rows are the observed FMAs and columns are the predicted FMAs. Note for BET 2013, there were too few samples in FMA 716 for this area to be included in the models.

**YFT, 2013**

| | 111 | 572 | 573 | 714 | 715 | 716 | 717 | 999 | % correct |
|---|---|---|---|---|---|---|---|---|---|
| 111 | 20 | 2 | 0 | 0 | 0 | 0 | 0 | 2 | 83.3 |
| 572 | 1 | 21 | 0 | 5 | 0 | 4 | 0 | 0 | 67.7 |
| 573 | 1 | 11 | 8 | 3 | 6 | 8 | 5 | 8 | 16.0 |
| 714 | 3 | 21 | 9 | 9 | 5 | 6 | 0 | 2 | 16.4 |
| 715 | 2 | 6 | 12 | 6 | 5 | 3 | 2 | 4 | 12.5 |
| 716 | 0 | 7 | 2 | 1 | 1 | 6 | 0 | 6 | 26.1 |
| 717 | 1 | 6 | 6 | 0 | 3 | 4 | 9 | 10 | 23.1 |
| 999 | 0 | 1 | 0 | 0 | 1 | 5 | 3 | 15 | 60.0 |

**YFT, 2014**

| | 111 | 572 | 573 | 714 | 715 | 716 | 717 | 999 | % correct |
|---|---|---|---|---|---|---|---|---|---|
| 111 | 19 | 5 | 1 | 0 | 0 | 0 | 0 | 1 | 73.1 |
| 572 | 4 | 15 | 0 | 3 | 0 | 1 | 2 | 0 | 60.0 |
| 573 | 1 | 6 | 7 | 9 | 4 | 17 | 7 | 1 | 13.5 |
| 714 | 0 | 6 | 1 | 8 | 2 | 7 | 8 | 0 | 25.0 |
| 715 | 3 | 8 | 6 | 20 | 2 | 18 | 10 | 3 | 2.9 |
| 716 | 0 | 2 | 2 | 5 | 0 | 7 | 2 | 0 | 38.9 |
| 717 | 3 | 2 | 1 | 5 | 0 | 2 | 11 | 7 | 35.5 |
| 999 | 0 | 1 | 0 | 4 | 0 | 1 | 6 | 13 | 52.0 |

**BET, 2013**

| | 111 | 572 | 573 | 714 | 715 | 716 | 717 | 999 | % correct |
|---|---|---|---|---|---|---|---|---|---|
| 111 | 17 | 4 | 0 | 0 | 2 | – | 0 | 2 | 68.0 |
| 572 | 5 | 15 | 2 | 0 | 5 | – | 0 | 0 | 55.6 |
| 573 | 2 | 9 | 13 | 3 | 17 | – | 5 | 0 | 26.5 |
| 714 | 7 | 6 | 13 | 1 | 21 | – | 2 | 3 | 1.9 |
| 715 | 4 | 4 | 2 | 2 | 23 | – | 2 | 0 | 62.2 |
| 716 | – | – | – | – | – | – | – | – | – |
| 717 | 4 | 2 | 2 | 0 | 13 | – | 0 | 7 | 0.0 |
| 999 | 2 | 1 | 1 | 1 | 6 | – | 2 | 24 | 64.9 |

Table 6.11 continued

| BET, 2014 | | | | | | | | | |
|---|---|---|---|---|---|---|---|---|---|
| | 111 | 572 | 573 | 714 | 715 | 716 | 717 | 999 | % correct |
| 111 | 22 | 1 | 0 | 0 | 1 | 0 | 0 | 0 | 91.7 |
| 572 | 2 | 19 | 3 | 0 | 0 | 1 | 0 | 0 | 76.0 |
| 573 | 0 | 12 | 16 | 3 | 8 | 8 | 3 | 0 | 32.0 |
| 714 | 1 | 0 | 10 | 6 | 3 | 8 | 0 | 3 | 19.4 |
| 715 | 1 | 0 | 8 | 2 | 3 | 8 | 0 | 0 | 13.6 |
| 716 | 0 | 0 | 1 | 2 | 0 | 13 | 3 | 2 | 61.9 |
| 717 | 3 | 2 | 5 | 4 | 0 | 24 | 6 | 6 | 12.0 |
| 999 | 1 | 0 | 1 | 1 | 0 | 7 | 0 | 15 | 60.0 |

Table 6.12. Sample sizes by species, season and FMA used in the elemental composition analyses. Note that FMA 111 refers to the Maldives and 999 to the Solomon Islands.

| | BET | | YFT | |
|---|---|---|---|---|
| **FMA** | 2013 | 2014 | 2013 | 2014 |
| 111 | 22 | 19 | 20 | 21 |
| 572 | 20 | 22 | 24 | 22 |
| 573 | 40 | 43 | 43 | 41 |
| 714 | 41 | 24 | 46 | 27 |
| 715 | 27 | 17 | 33 | 55 |
| 716 | 2 | 19 | 22 | 16 |
| 717 | 24 | 37 | 30 | 24 |
| 999 | 22 | 20 | 22 | 20 |
| Total | 198 | 201 | 240 | 226 |

Table 6.13. P values from paired t-tests between element data from pairs of otolith positions (e.g., P1-2 denotes position 1 vs 2). Shaded cells indicate no significant difference at level 0.05.

| **BET** | P1-2 | P1-3 | P1-4 | P2-3 | P2-4 | P3-4 |
|---|---|---|---|---|---|---|
| Li7 | 0 | 0 | 0 | 0 | 0 | 0 |
| Na23 | 0 | 0 | 0.182 | 0 | 0 | 0 |
| Mg24 | 0 | 0 | 0 | 0 | 0 | 0 |
| P31 | 0 | 0 | 0 | 0.404 | 0 | 0 |
| K39 | 0 | 0.001 | 0 | 0.260 | 0.807 | 0.513 |
| Mn55 | 0 | 0 | 0 | 0.843 | 0 | 0 |
| Cu65 | 0 | 0 | 0 | 0 | 0 | 0 |
| Rb85 | 0 | 0 | 0 | 0.004 | 0 | 0 |
| Sr88 | 0 | 0 | 0.383 | 0 | 0 | 0 |
| Ba137 | 0 | 0 | 0.001 | 0 | 0 | 0.042 |

| **YFT** | P1-2 | P1-3 | P1-4 | P2-3 | P2-4 | P3-4 |
|---|---|---|---|---|---|---|
| Li7 | 0 | 0 | 0 | 0 | 0 | 0 |
| Na23 | 0 | 0 | 0.004 | 0 | 0 | 0 |
| Mg24 | 0 | 0 | 0 | 0 | 0 | 0 |
| P31 | 0 | 0 | 0 | 0 | 0 | 0 |
| K39 | 0 | 0.73 | 0.001 | 0 | 0 | 0.042 |
| Mn55 | 0 | 0 | 0 | 0 | 0 | 0 |
| Cu65 | 0 | 0 | 0 | 0 | 0 | 0 |
| Rb85 | 0 | 0 | 0.1 | 0 | 0 | 0 |
| Sr88 | 0 | 0.03 | 0.989 | 0 | 0 | 0.02 |
| Ba137 | 0 | 0 | 0 | 0 | 0 | 0 |

Table 6.14. Correlations between element data from pairs of otolith positions (e.g., P1-2 denotes position 1 vs 2). Shaded cells indicate correlations >0.5.

| **BET** | P1-2 | P1-3 | P1-4 | P2-3 | P2-4 | P3-4 |
|---|---|---|---|---|---|---|
| Li7 | 0.17 | 0.22 | 0.48 | 0.22 | 0.39 | 0.27 |
| Na23 | 0.66 | 0.52 | 0.71 | 0.56 | 0.64 | 0.49 |
| Mg24 | 0.45 | 0.43 | 0.56 | 0.33 | 0.42 | 0.32 |
| P31 | 0.38 | 0.27 | 0.48 | 0.38 | 0.43 | 0.20 |
| K39 | 0.84 | 0.68 | 0.89 | 0.78 | 0.81 | 0.69 |
| Mn55 | 0.25 | 0.16 | 0.52 | 0.29 | 0.22 | 0.23 |
| Cu65 | 0.37 | 0.38 | 0.61 | 0.34 | 0.40 | 0.38 |
| Rb85 | 0.80 | 0.68 | 0.85 | 0.74 | 0.78 | 0.67 |
| Sr88 | 0.39 | 0.13 | 0.60 | -0.01 | 0.32 | 0.09 |
| Ba137 | 0.11 | 0.15 | 0.67 | 0.07 | 0.10 | 0.16 |

| **YFT** | P1-2 | P1-3 | P1-4 | P2-3 | P2-4 | P3-4 |
|---|---|---|---|---|---|---|
| Li7 | 0.11 | 0.21 | 0.36 | 0.19 | 0.30 | 0.25 |
| Na23 | 0.58 | 0.54 | 0.69 | 0.49 | 0.58 | 0.45 |
| Mg24 | 0.34 | 0.20 | 0.52 | 0.31 | 0.38 | 0.26 |
| P31 | 0.39 | 0.13 | 0.41 | 0.30 | 0.42 | 0.28 |
| K39 | 0.83 | 0.69 | 0.90 | 0.80 | 0.82 | 0.70 |
| Mn55 | 0.26 | 0.22 | 0.56 | 0.34 | 0.27 | 0.35 |
| Cu65 | 0.33 | 0.22 | 0.45 | 0.39 | 0.40 | 0.24 |
| Rb85 | 0.75 | 0.69 | 0.83 | 0.77 | 0.73 | 0.70 |
| Sr88 | 0.29 | 0.08 | 0.48 | 0.13 | 0.13 | 0.20 |
| Ba137 | 0.25 | 0.11 | 0.64 | 0.02 | 0.13 | 0.21 |

Table 6.15. Results from ANOVAs fit to the data from each element, species and otolith position separately with FMA, Season and FMA:Season (F:S) interaction as covariates. Models were run (i) using all FMAs, and (ii) excluding FMAs 111 and 999 (the outlier sites). Shown are p-values from tests of significance for each covariate. Shaded cells mark covariates that are NOT significant at level 0.05.

| | | | All FMAs | | | FMAs 111 & 999 excluded | | |
|---|---|---|---|---|---|---|---|---|
| Species | Position | Element | FMA | Season | F:S | FMA | Season | F:S |
| **YFT** | 1 | Li7 | 0.0030 | 0 | 0 | 0.0184 | 0 | 0 |
| | | Na23 | 0 | 0 | 0 | 0.0001 | 0 | 0 |
| | | Mg24 | 0 | 0.0888 | 0.0024 | 0.0115 | 0.3816 | 0.0117 |
| | | P31 | 0.0006 | 0.0015 | 0.7800 | 0.0089 | 0.0009 | 0.9807 |
| | | K39 | 0 | 0 | 0 | 0 | 0 | 0 |
| | | Mn55 | 0 | 0.0073 | 0.0942 | 0.0003 | 0.0026 | 0.0964 |
| | | Cu65 | 0.0074 | 0.0003 | 0.4687 | 0.0025 | 0.0078 | 0.4698 |
| | | Rb85 | 0 | 0 | 0 | 0 | 0 | 0 |
| | | Sr88 | 0.9732 | 0.6189 | 0.0018 | 0.9169 | 0.8199 | 0.0198 |
| | | Ba137 | 0 | 0.3968 | 0.1248 | 0 | 0.5923 | 0.0689 |
| **YFT** | 3 | Li7 | 0.2112 | 0.6819 | 0.0002 | 0.472 | 0.962 | 0 |
| | | Na23 | 0 | 0 | 0 | 0 | 0 | 0 |
| | | Mg24 | 0.0302 | 0 | 0 | 0.1473 | 0 | 0 |
| | | P31 | 0.0739 | 0.2408 | 0.0704 | 0.1100 | 0.2796 | 0.1431 |
| | | K39 | 0 | 0 | 0 | 0 | 0 | 0 |
| | | Mn55 | 0 | 0 | 0 | 0 | 0 | 0 |
| | | Cu65 | 0.6189 | 0 | 0.1459 | 0.494 | 0 | 0.4162 |
| | | Rb85 | 0 | 0 | 0 | 0 | 0 | 0 |
| | | Sr88 | 0 | 0.0001 | 0 | 0 | 0.0001 | 0 |
| | | Ba137 | 0 | 0.8431 | 0.0271 | 0 | 0.9442 | 0.0294 |
| **BET** | 1 | Li7 | 0.4926 | 0.7878 | 0.0643 | 0.5248 | 0.9130 | 0.2410 |
| | | Na23 | 0 | 0 | 0 | 0 | 0 | 0.0002 |
| | | Mg24 | 0 | 0.0666 | 0.0986 | 0 | 0.3680 | 0.1793 |
| | | P31 | 0 | 0.4807 | 0.1708 | 0.0001 | 0.3605 | 0.1097 |
| | | K39 | 0 | 0 | 0 | 0.2122 | 0 | 0 |
| | | Mn55 | 0 | 0.8384 | 0.1301 | 0 | 0.8511 | 0.0718 |
| | | Cu65 | 0.1024 | 0.0037 | 0.0574 | 0.0427 | 0.0196 | 0.0516 |
| | | Rb85 | 0 | 0 | 0 | 0.01 | 0 | 0 |
| | | Sr88 | 0.0063 | 0.3634 | 0.0487 | 0.055 | 0.2448 | 0.0198 |
| | | Ba137 | 0 | 0.0066 | 0.0016 | 0 | 0.0330 | 0.0022 |
| **BET** | 3 | Li7 | 0.0182 | 0.0073 | 0.6272 | 0.0283 | 0.0346 | 0.4139 |
| | | Na23 | 0 | 0 | 0.0015 | 0.0153 | 0 | 0.0004 |
| | | Mg24 | 0 | 0 | 0.3568 | 0 | 0.0005 | 0.3697 |
| | | P31 | 0 | 0.4615 | 0.0008 | 0 | 0.5595 | 0.0371 |
| | | K39 | 0.0039 | 0 | 0 | 0.1676 | 0 | 0 |
| | | Mn55 | 0 | 0 | 0.0021 | 0 | 0 | 0.5988 |

| | | | | | | | |
|---|---|---|---|---|---|---|---|
| | Cu65 | 0.8826 | 0.1654 | 0.3653 | 0.9451 | 0.6254 | 0.4747 |
| | Rb85 | 0.0001 | 0 | 0 | 0.0281 | 0 | 0 |
| | Sr88 | 0.0001 | 0.0001 | 0.0067 | 0.0002 | 0.0003 | 0.1126 |
| | Ba137 | 0 | 0.4732 | 0.3577 | 0 | 0.7105 | 0.8972 |

Table 6.16. Overall classification success rates (% correct over all FMAs) from the leave-one-out cross-validation QDAs run on the element data for each species, otolith position and season separately.[1] For comparison, the mean, minimum and maximum classification success rates from 1000 bootstraps with randomized FMAs are also given.

| | | | | % Correct from randomized FMAs | | |
|---|---|---|---|---|---|---|
| Species | Position | Season | % Correct | Min | Mean | Max |
| **YFT** | 1 | 2013 | 35.2 | 3.8 | 12.3 | 21.2 |
| | | 2014 | 31.9 | 5.2 | 12.4 | 22.5 |
| | 2 | 2013 | 34.6 | 5.6 | 12.2 | 22.6 |
| | | 2014 | 28.8 | 5.4 | 12.6 | 21.5 |
| | 3 | 2013 | 50.4 | 3.0 | 12.2 | 23.1 |
| | | 2014 | 46.7 | 4.6 | 12.9 | 24.4 |
| | 4 | 2013 | 47.4 | 3.9 | 12.2 | 22.4 |
| | | 2014 | 30.8 | 6.2 | 13.0 | 21.3 |
| **BET** | 1 | 2013 | 43.5 | 6.2 | 14.5 | 26.4 |
| | | 2014 | 39.2 | 5.0 | 12.7 | 23.1 |
| | 2 | 2013 | 36.1 | 5.7 | 13.8 | 23.2 |
| | | 2014 | 31.3 | 4.5 | 12.6 | 23.2 |
| | 3 | 2013 | 50.8 | 5.8 | 14.4 | 24.9 |
| | | 2014 | 36.6 | 5.2 | 12.2 | 21.5 |
| | 4 | 2013 | 36.8 | 4.7 | 14.1 | 25.9 |
| | | 2014 | 28.4 | 3.1 | 12.5 | 23.2 |

[1]Results derived from the following call in R:

qda(FMA ~ log($^{23}$Na)+log($^{24}$Mg)+log($^{31}$P)+log($^{39}$K)+log($^{55}$Mn)+log($^{85}$Rb) +log($^{88}$Sr)+log($^{137}$Ba), data=d, CV=TRUE, prior=rep(1/n.fma,n.fma))

where d contains the element data for the species, position and season being modelled, CV=TRUE means to use cross-validation, and n.fma=8 is the number of FMAs in the model, used to set equal prior probabilities for all FMAs.

Table 6.17. Classification tables from leave-one-out cross-validation QDAs run on the element data for each species, otolith position and season separately. Only results for positions 1 and 3 are shown. Rows are the observed FMAs and columns are the predicted FMAs. Note for BET 2013, there were too few samples in FMA 716 for this area to be included in the models.

**YFT, Position 1, 2013**

| | 111 | 572 | 573 | 714 | 715 | 716 | 717 | 999 | % correct |
|---|---|---|---|---|---|---|---|---|---|
| 111 | 7 | 2 | 3 | 2 | 3 | 2 | 1 | 0 | 35.0 |
| 572 | 4 | 7 | 2 | 4 | 1 | 1 | 2 | 1 | 31.8 |
| 573 | 1 | 11 | 9 | 10 | 7 | 2 | 3 | 0 | 20.9 |
| 714 | 2 | 4 | 7 | 14 | 10 | 1 | 5 | 3 | 30.4 |
| 715 | 2 | 3 | 1 | 8 | 12 | 5 | 2 | 0 | 36.4 |
| 716 | 2 | 0 | 0 | 4 | 2 | 10 | 2 | 2 | 45.5 |
| 717 | 1 | 3 | 5 | 3 | 4 | 3 | 8 | 2 | 27.6 |
| 999 | 0 | 0 | 0 | 0 | 0 | 1 | 4 | 16 | 76.2 |

**YFT, Position 1, 2014**

| | 111 | 572 | 573 | 714 | 715 | 716 | 717 | 999 | % correct |
|---|---|---|---|---|---|---|---|---|---|
| 111 | 9 | 0 | 1 | 3 | 2 | 1 | 4 | 1 | 42.9 |
| 572 | 0 | 11 | 2 | 1 | 0 | 3 | 3 | 1 | 52.4 |
| 573 | 0 | 7 | 7 | 3 | 7 | 1 | 4 | 5 | 20.6 |
| 714 | 3 | 0 | 4 | 7 | 5 | 5 | 2 | 1 | 25.9 |
| 715 | 1 | 1 | 3 | 12 | 18 | 5 | 10 | 4 | 33.3 |
| 716 | 2 | 0 | 0 | 4 | 2 | 5 | 3 | 0 | 31.3 |
| 717 | 2 | 1 | 0 | 6 | 6 | 1 | 6 | 2 | 25.0 |
| 999 | 3 | 3 | 3 | 1 | 1 | 0 | 0 | 5 | 31.3 |

**YFT, Position 3, 2013**

| | 111 | 572 | 573 | 714 | 715 | 716 | 717 | 999 | % correct |
|---|---|---|---|---|---|---|---|---|---|
| 111 | 15 | 3 | 2 | 0 | 0 | 0 | 0 | 0 | 75.0 |
| 572 | 0 | 10 | 8 | 3 | 1 | 0 | 1 | 0 | 43.5 |
| 573 | 2 | 9 | 20 | 5 | 6 | 0 | 1 | 0 | 46.5 |
| 714 | 0 | 1 | 8 | 18 | 10 | 3 | 3 | 0 | 41.9 |
| 715 | 0 | 4 | 8 | 4 | 11 | 2 | 4 | 0 | 33.3 |
| 716 | 0 | 0 | 0 | 2 | 1 | 11 | 5 | 3 | 50.0 |
| 717 | 0 | 0 | 2 | 4 | 2 | 4 | 15 | 2 | 51.7 |
| 999 | 0 | 0 | 0 | 2 | 0 | 0 | 1 | 18 | 85.7 |

Table 6.17 Continued

**YFT, Position 3, 2014**

| | 111 | 572 | 573 | 714 | 715 | 716 | 717 | 999 | % correct |
|---|---|---|---|---|---|---|---|---|---|
| 111 | 15 | 1 | 2 | 2 | 1 | 0 | 0 | 0 | 71.4 |
| 572 | 1 | 9 | 0 | 4 | 1 | 0 | 2 | 0 | 52.9 |
| 573 | 2 | 0 | 10 | 5 | 6 | 2 | 1 | 0 | 38.5 |
| 714 | 1 | 1 | 2 | 9 | 11 | 0 | 2 | 1 | 33.3 |
| 715 | 1 | 0 | 11 | 8 | 22 | 10 | 1 | 1 | 40.7 |
| 716 | 1 | 0 | 2 | 1 | 7 | 4 | 0 | 0 | 26.7 |
| 717 | 0 | 0 | 1 | 4 | 1 | 2 | 16 | 0 | 66.7 |
| 999 | 0 | 0 | 1 | 0 | 3 | 0 | 2 | 7 | 53.8 |

**BET, Position 1, 2013**

| | 111 | 572 | 573 | 714 | 715 | 716 | 717 | 999 | % correct |
|---|---|---|---|---|---|---|---|---|---|
| 111 | 7 | 1 | 7 | 4 | 1 | – | 0 | 1 | 33.3 |
| 572 | 1 | 10 | 7 | 1 | 1 | – | 0 | 0 | 50.0 |
| 573 | 1 | 8 | 17 | 2 | 6 | – | 4 | 2 | 42.5 |
| 714 | 5 | 0 | 7 | 14 | 11 | – | 2 | 1 | 35.0 |
| 715 | 3 | 0 | 6 | 5 | 8 | – | 4 | 1 | 29.6 |
| 716 | – | – | – | – | – | – | – | – | – |
| 717 | 2 | 1 | 4 | 2 | 1 | – | 13 | 1 | 54.2 |
| 999 | 1 | 0 | 2 | 1 | 0 | – | 2 | 15 | 71.4 |

**BET, Position 1, 2014**

| | 111 | 572 | 573 | 714 | 715 | 716 | 717 | 999 | % correct |
|---|---|---|---|---|---|---|---|---|---|
| 111 | 6 | 0 | 2 | 6 | 0 | 0 | 3 | 2 | 31.6 |
| 572 | 0 | 11 | 6 | 0 | 2 | 1 | 1 | 1 | 50.0 |
| 573 | 3 | 8 | 19 | 0 | 0 | 4 | 4 | 3 | 46.3 |
| 714 | 3 | 0 | 2 | 9 | 2 | 3 | 4 | 1 | 37.5 |
| 715 | 1 | 1 | 2 | 3 | 4 | 2 | 4 | 0 | 23.5 |
| 716 | 0 | 1 | 2 | 3 | 2 | 6 | 2 | 3 | 31.6 |
| 717 | 2 | 0 | 4 | 5 | 5 | 3 | 15 | 3 | 40.5 |
| 999 | 0 | 0 | 0 | 4 | 0 | 4 | 4 | 8 | 40.0 |

Table 6.17 Continued

**BET, Position 3, 2013**

| | 111 | 572 | 573 | 714 | 715 | 716 | 717 | 999 | % correct |
|---|---|---|---|---|---|---|---|---|---|
| 111 | 11 | 2 | 1 | 5 | 1 | – | 0 | 0 | 55.0 |
| 572 | 1 | 9 | 5 | 1 | 1 | – | 0 | 2 | 47.4 |
| 573 | 1 | 5 | 23 | 4 | 3 | – | 0 | 3 | 59.0 |
| 714 | 0 | 3 | 9 | 19 | 9 | – | 1 | 0 | 46.3 |
| 715 | 0 | 1 | 1 | 5 | 14 | – | 6 | 0 | 51.9 |
| 716 | – | – | – | – | – | – | – | – | – |
| 717 | 0 | 1 | 5 | 3 | 3 | – | 6 | 3 | 28.6 |
| 999 | 0 | 3 | 1 | 2 | 0 | – | 2 | 14 | 63.6 |

**BET, Position 3, 2014**

| | 111 | 572 | 573 | 714 | 715 | 716 | 717 | 999 | % correct |
|---|---|---|---|---|---|---|---|---|---|
| 111 | 7 | 2 | 1 | 7 | 0 | 0 | 1 | 0 | 38.9 |
| 572 | 0 | 9 | 3 | 1 | 1 | 1 | 3 | 2 | 45.0 |
| 573 | 1 | 4 | 19 | 2 | 2 | 3 | 6 | 3 | 47.5 |
| 714 | 0 | 0 | 5 | 8 | 3 | 5 | 3 | 0 | 33.3 |
| 715 | 0 | 2 | 4 | 7 | 0 | 0 | 2 | 0 | 0.0 |
| 716 | 2 | 1 | 4 | 3 | 1 | 5 | 1 | 0 | 29.4 |
| 717 | 1 | 4 | 8 | 4 | 0 | 1 | 16 | 3 | 43.2 |
| 999 | 2 | 2 | 3 | 0 | 0 | 0 | 7 | 6 | 30.0 |

## 6.6 Figures

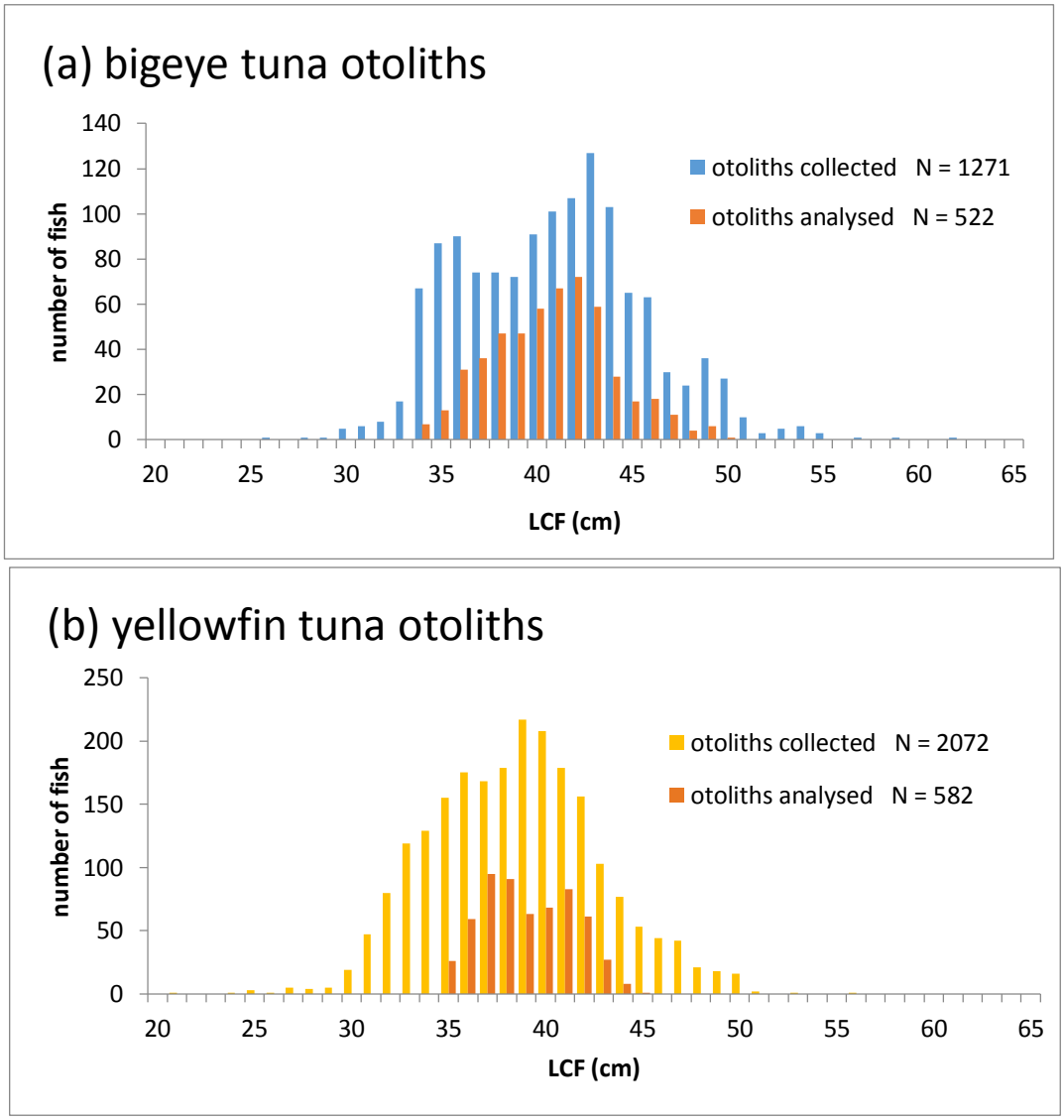


Figure 6.1. (a) Bigeye tuna and (b) yellowfin tuna otoliths collected during the ACIAR project sampling and the subset of otoliths chosen for analysis.

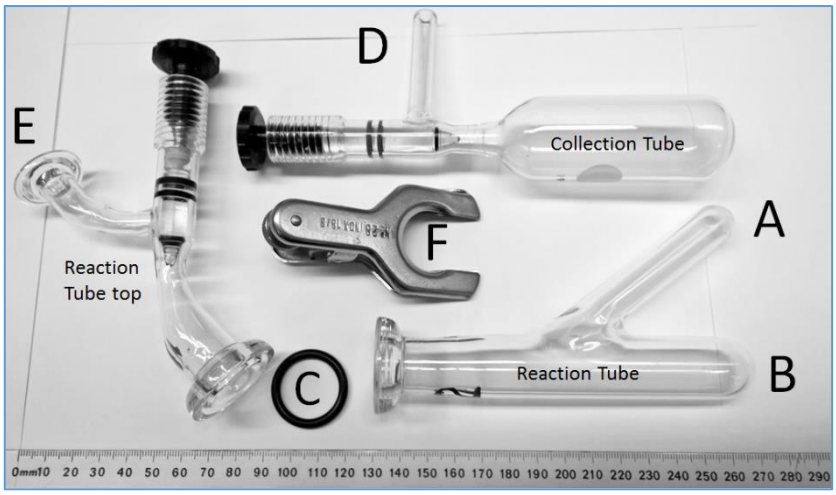


Figure 6.2. Glassware used for otolith digestion.

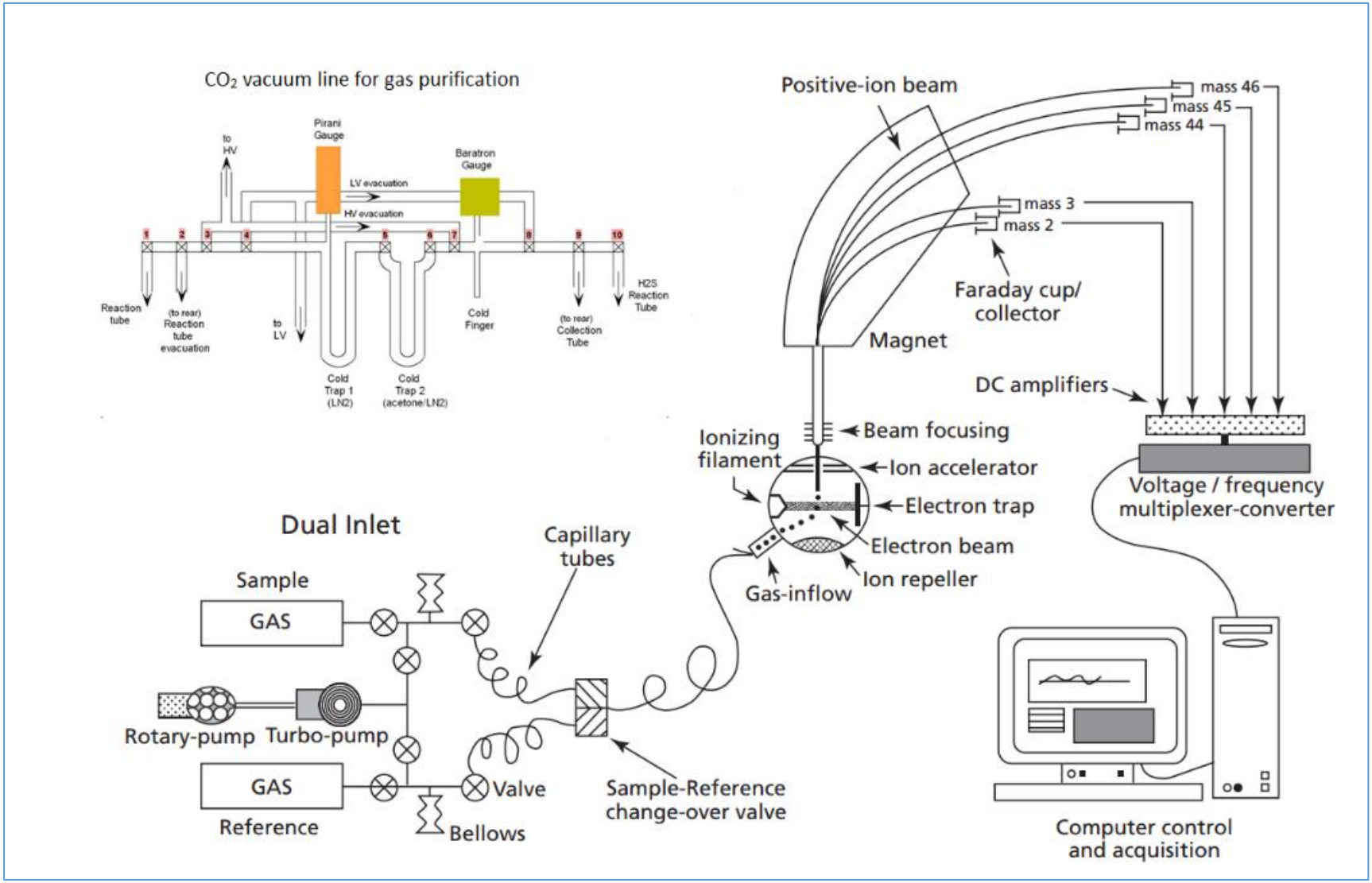


Figure 6.3. Setup of an isotope-ratio mass spectrometer measuring $CO_2$.

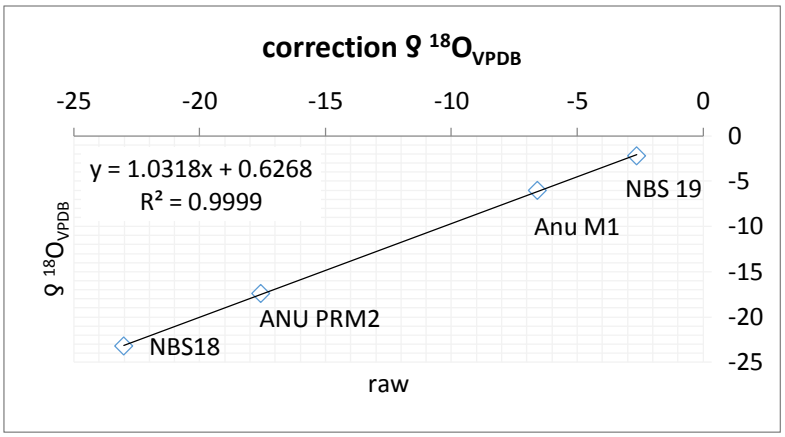


Figure 6.4. Example for oxygen data correction using international and inter-laboratory standard materials.

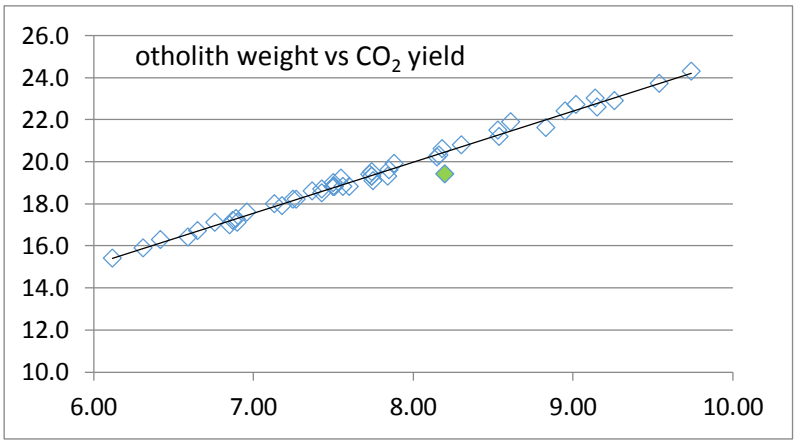


Figure 6.5. Linear relationship between otolith weight [in mg] and amount of $CO_2$ produced [in mbar] during digestion. The data point marked in green is an outlier with a yield smaller than expected.

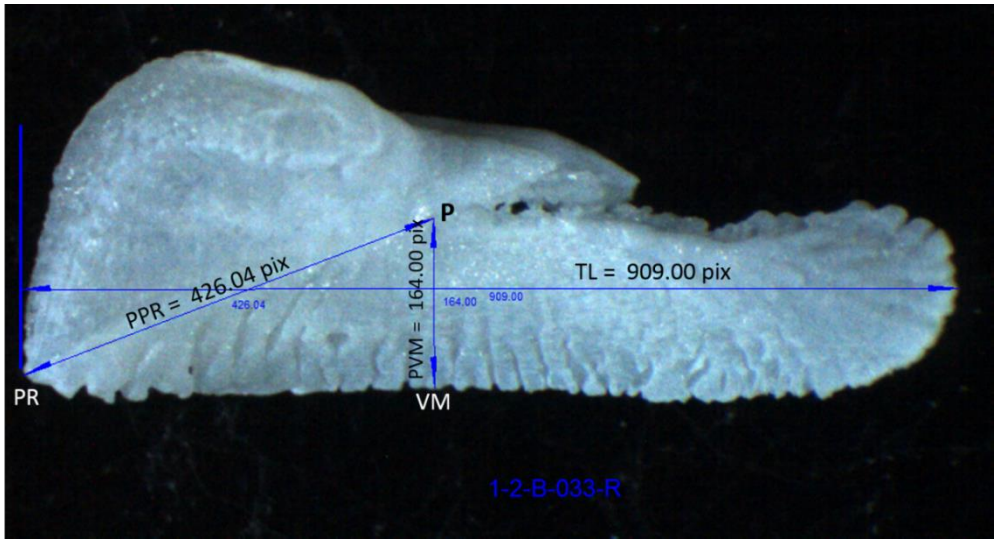


Figure 6.6. Image of a whole otolith from a bigeye tuna showing the areas used to calculate the otolith proportion index: primordium (P), post rostrum (PR), rostrum (R), length (TL) and primordium to post rostrum (PPR).

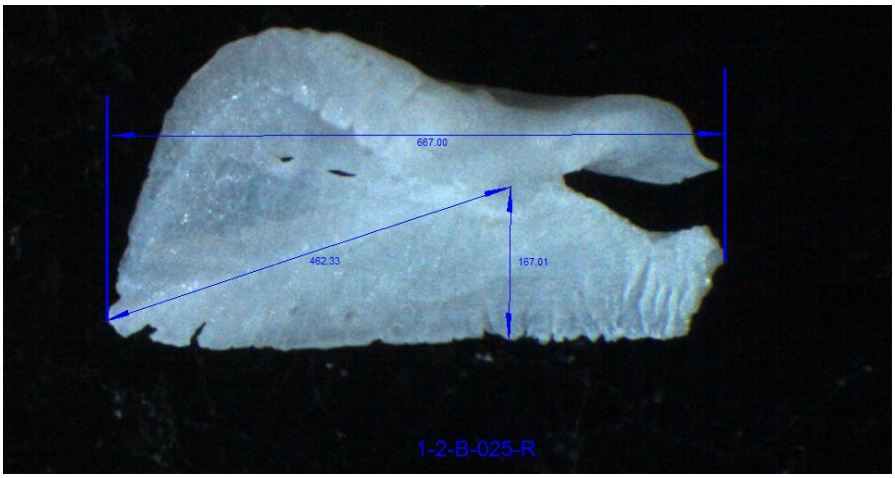


Figure 6.7. Image of a broken otolith from a bigeye tuna, indicating a partial length of 667 pixels.

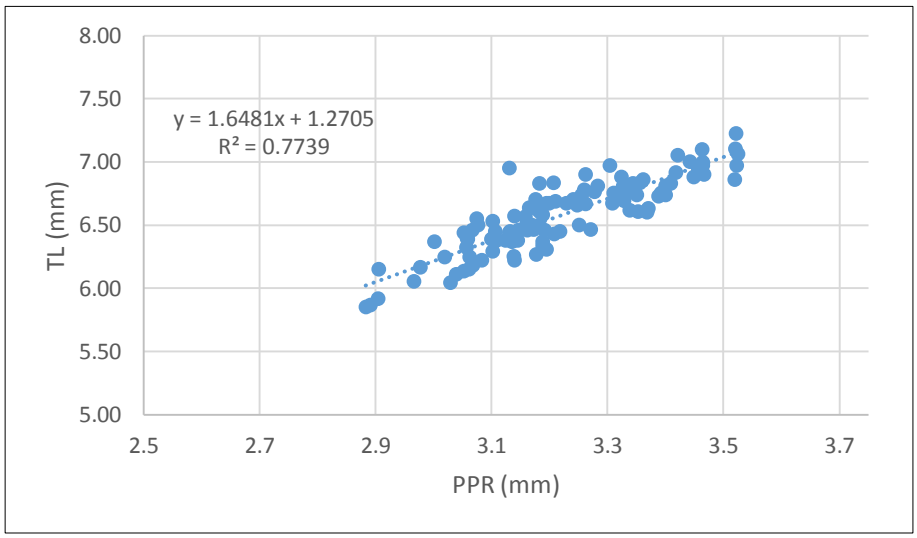


Figure 6.8. The relationship between total length and primordium-post rostrum length for YFT.

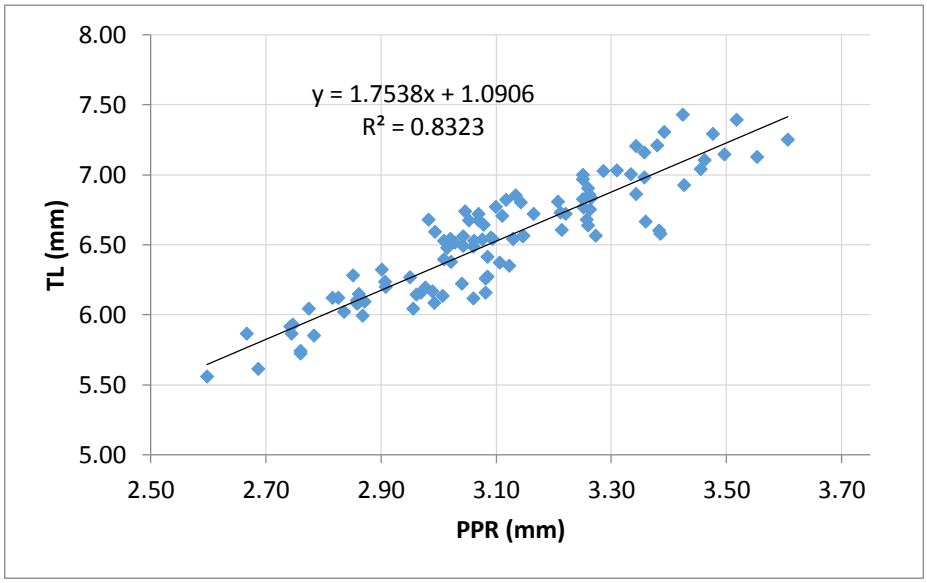


Figure 6.9. The relationship between total length and primordium-post rostrum length for BET.

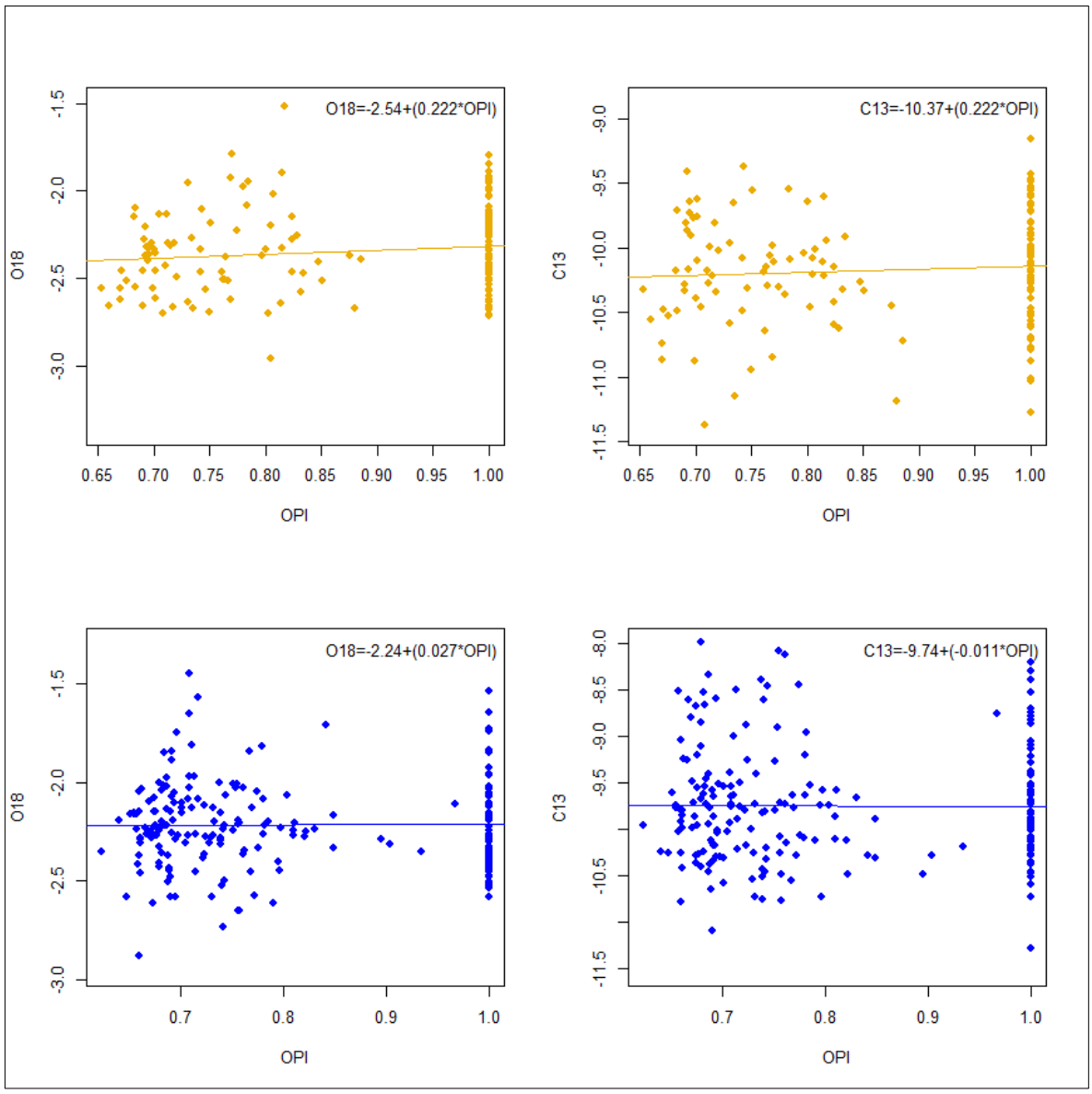


Figure 6.10. Plots of $\delta^{18}O$ (labelled as O18) and $\delta^{13}C$ (labelled as C13) versus OPI for YFT (top row) and BET (bottom row). The linear regression fit is shown, and the fitted equation given in the top right corner.

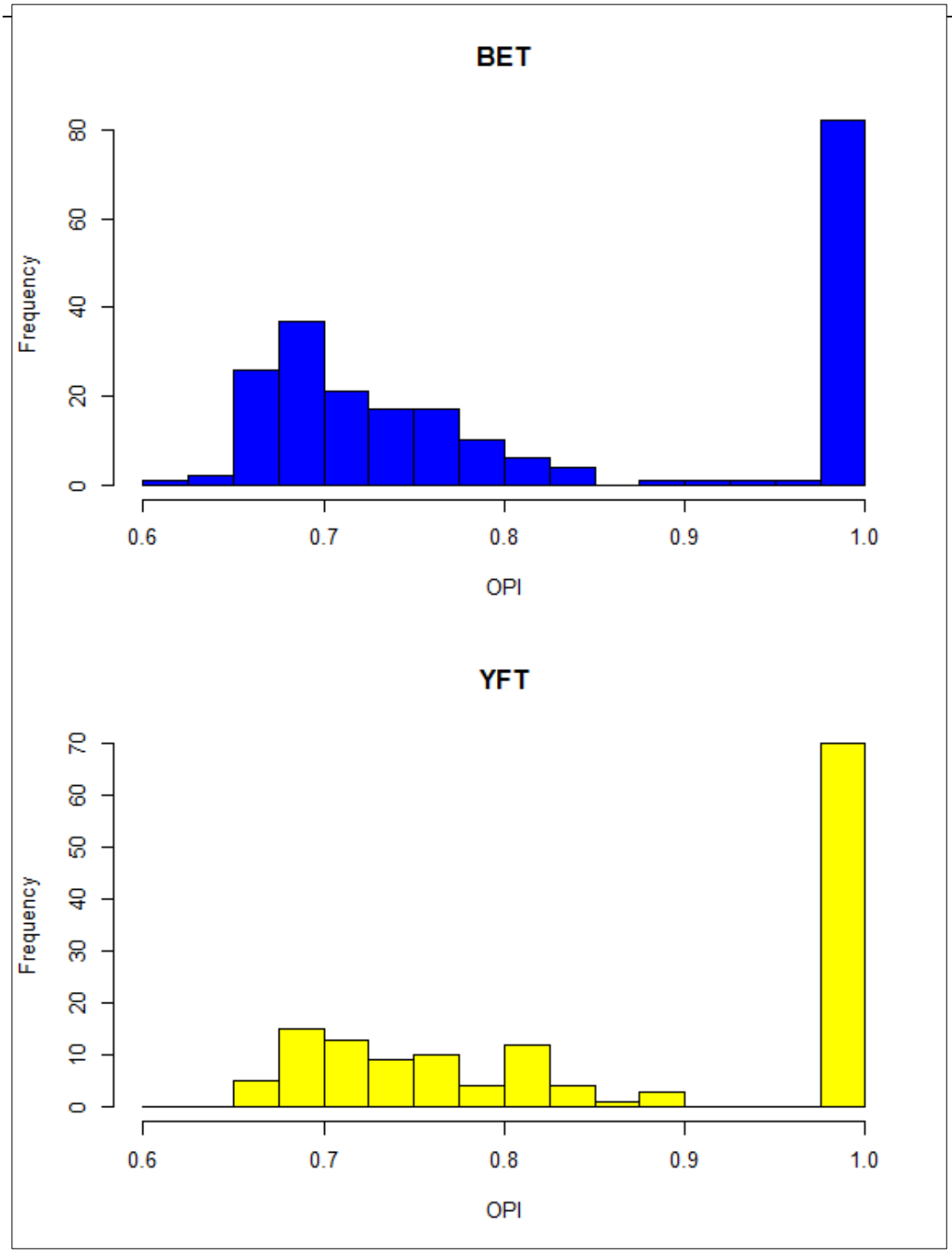


Figure 6.11. Histograms of otolith proportion index (OPI) values calculated for the BET and YFT samples.

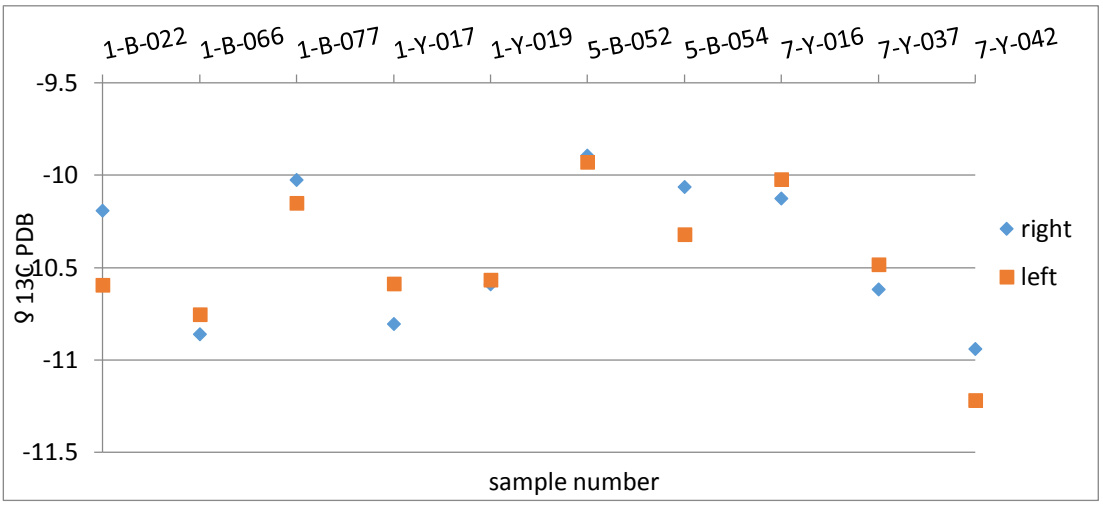


Figure 6.12. Comparison of δ $^{13}$C PDB values for left and right otoliths.

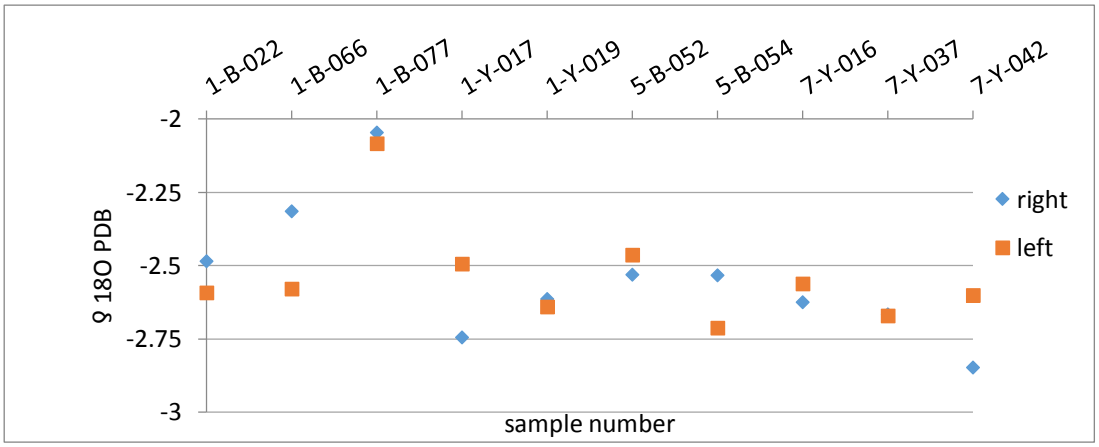


Figure 6.13. Comparison of δ $^{18}$0 PDB values for left and right otoliths.

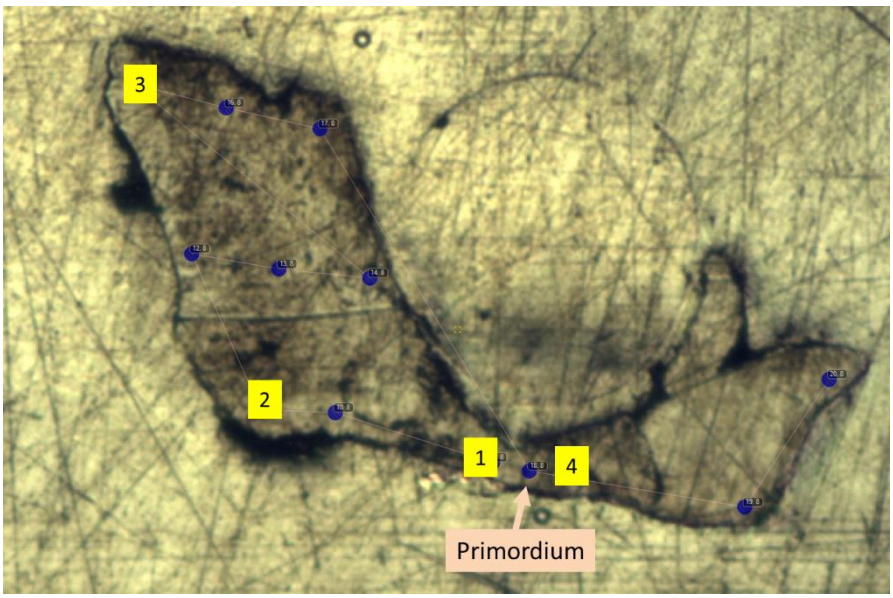


Figure 6.14. Positions of laser points 1 - 4, along otolith sections.

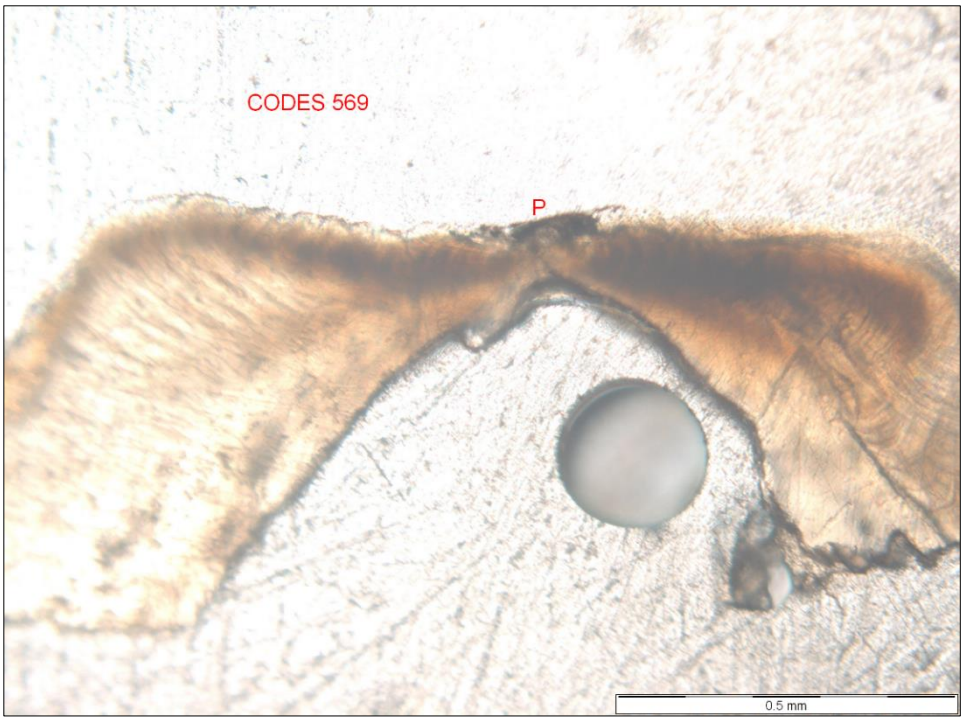


Figure 6.15. Tuna otolith section that has been ground down to expose the primordium (P) and the growth increments either side.

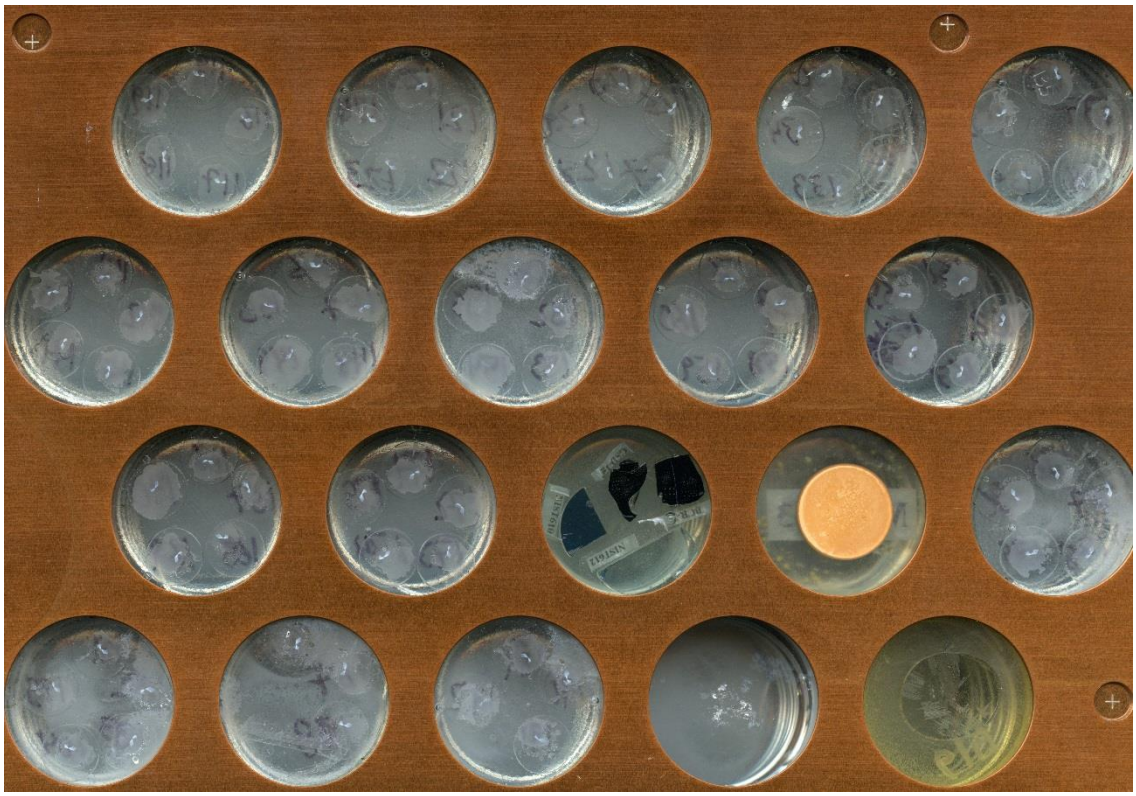

Figure 6.16. A holder with sixteen 1-inch rounds, each holding 5 otolith sections. The remaining positions in the holder contain reference standards.

Laser Ablation cell used in study

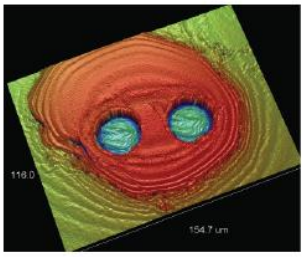

Optical profiler image of ablatoin crater in the mineral zircon. Crater formed after 12 seconds of ablation and is ~ 4 microns in depth by 29 microns in diameter.

Quadrupole ICP-MS instrument used in study.

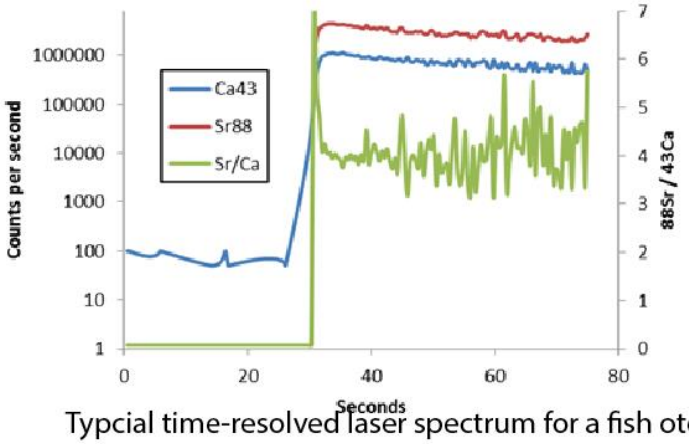


Typcial time-resolved laser spectrum for a fish otolith analysis. Note that the isotope intensities are in log scale while the ratio is linear scale.

Figure 6.17. Diagram showing equipment used in study and the steps involved in data collection.

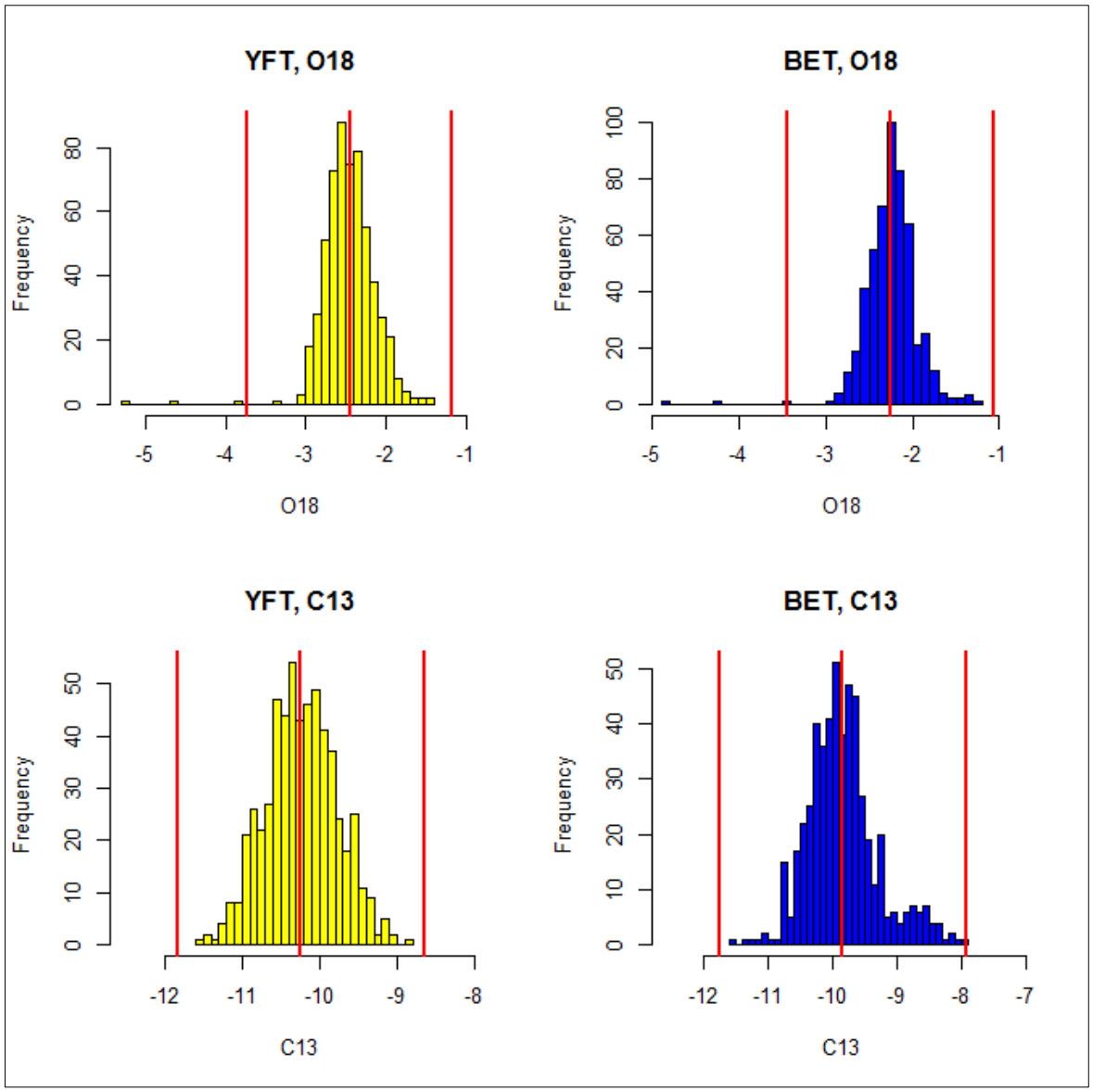


Figure 6.18. Distribution of $\delta^{18}O$ (O18) and $\delta^{13}C$ (C13) values for YFT and BET. Vertical red lines show the mean +/- 4 standard deviations; any values outside this range were considered outliers and omitted from further analyses.

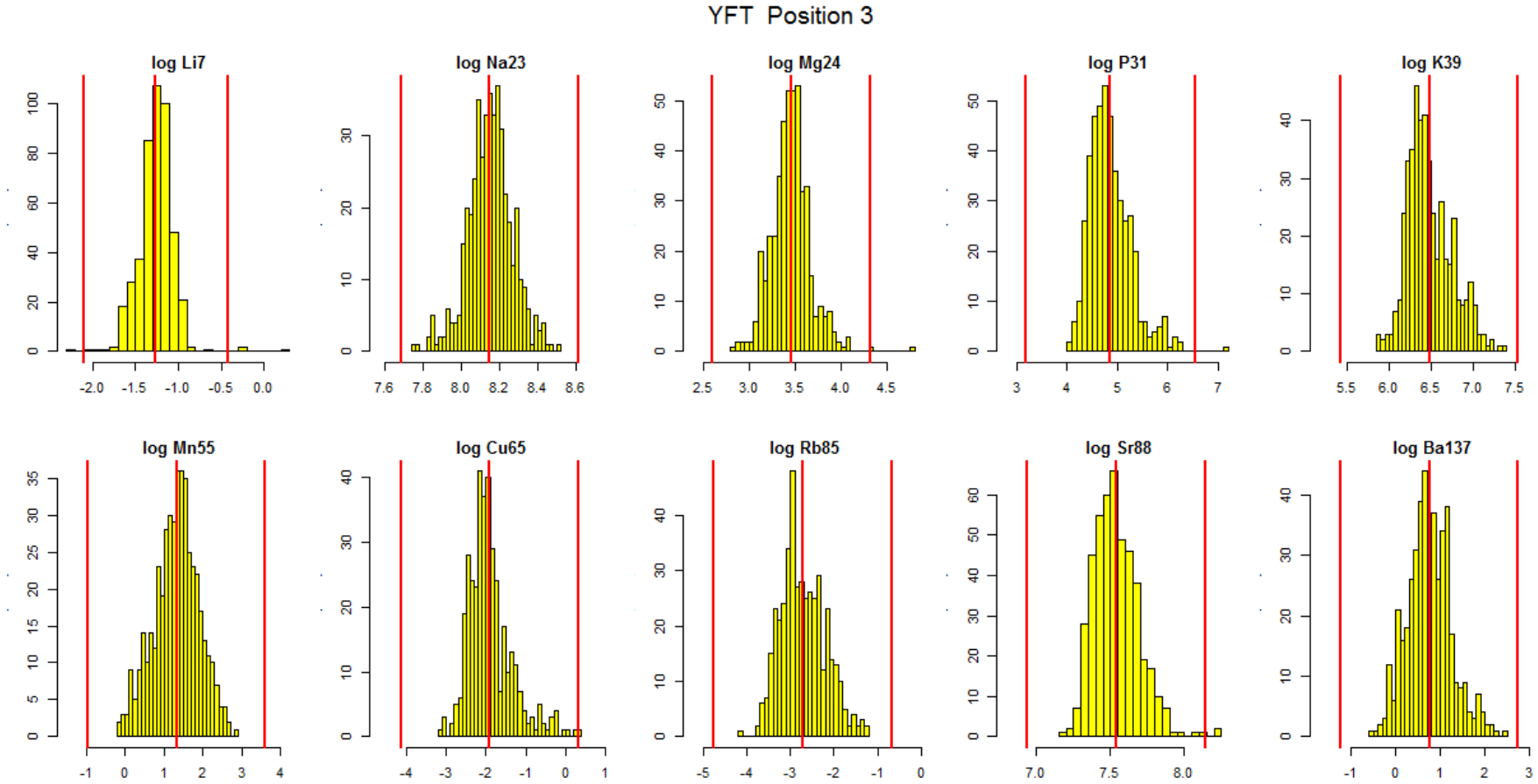


Figure 6.19a. Distribution of log-transformed element concentration values at otolith position 3 for YFT. Vertical red lines show the mean +/- 4 standard deviations; any values outside this range were considered outliers and omitted from further analyses. Note that only otolith position 3 is shown for brevity, but plots look similar for other positions.

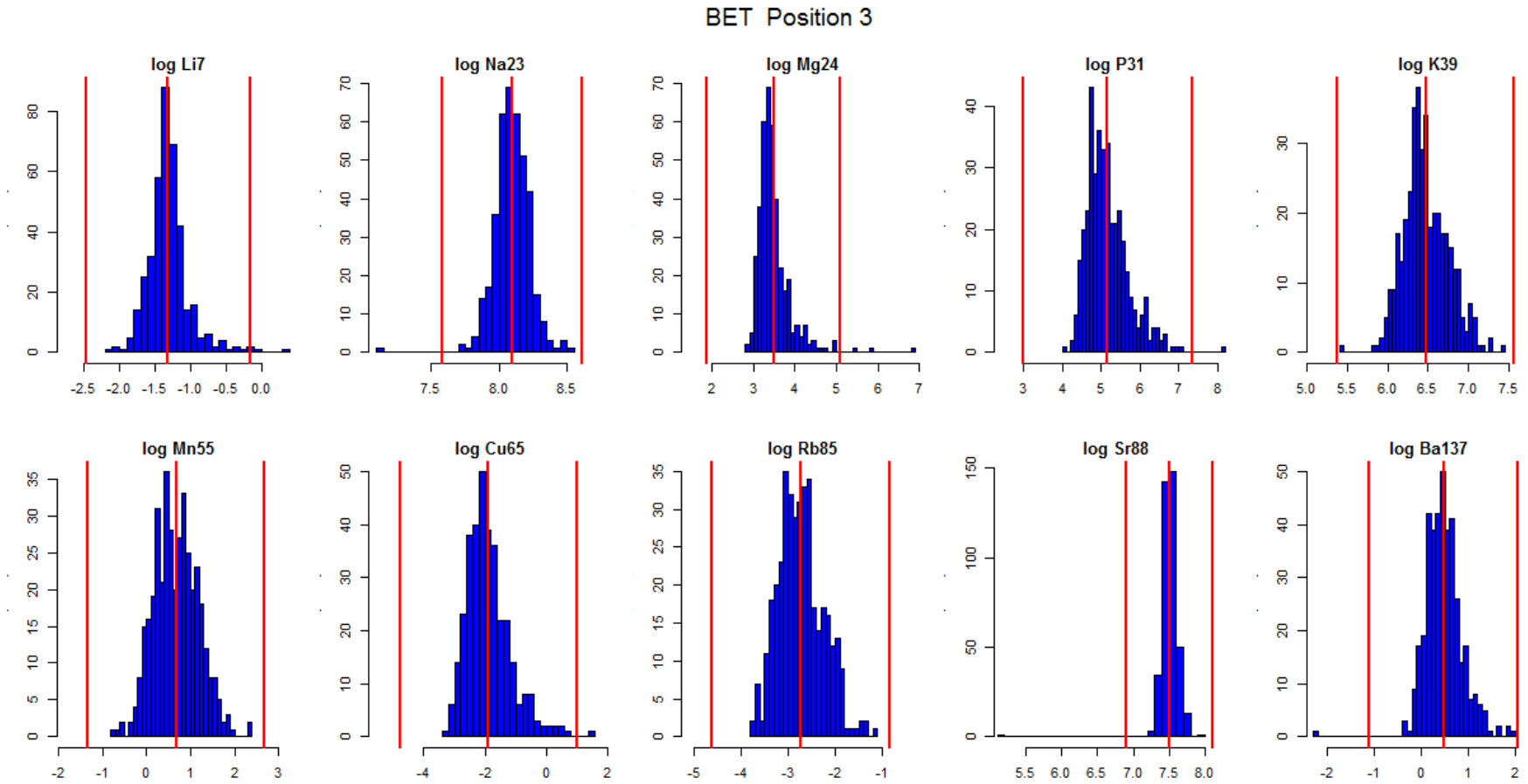


Figure 6.19b. Distribution of log-transformed element concentration values at otolith position 3 for BET. Vertical red lines show the mean +/- 4 standard deviations; any values outside this range were considered outliers and omitted from further analyses. Note that only otolith position 3 is shown for brevity, but plots look similar for other positions.

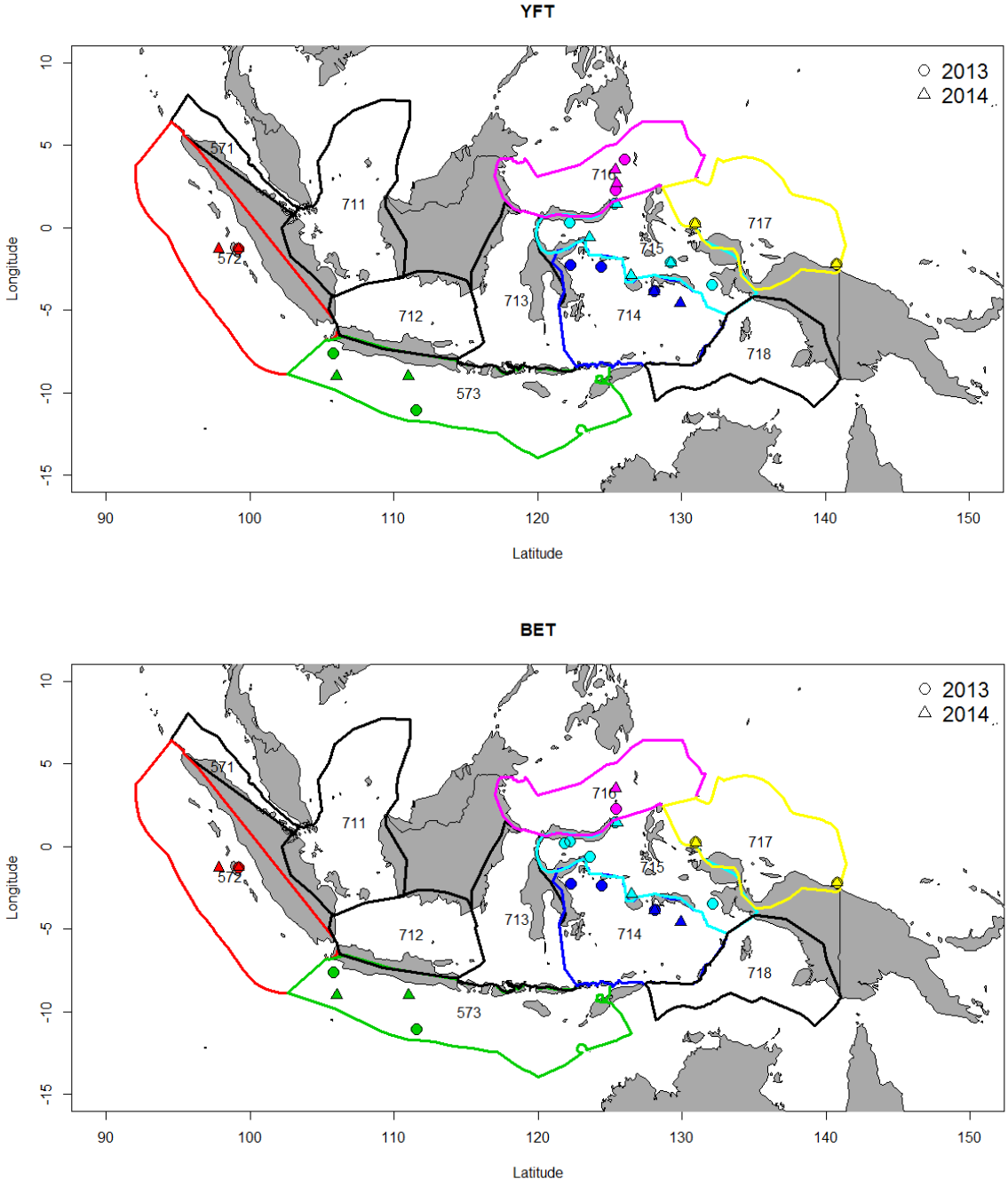


Figure 6.20. Locations where samples used in statistical analyses of the otolith stable isotope and elemental composition data were collected, colour-coded by Fisheries Management Areas (FMAs). Note that the two outlier sites, Maldives and Solomon Islands (which have been assigned FMA codes 111 and 999), are not shown.

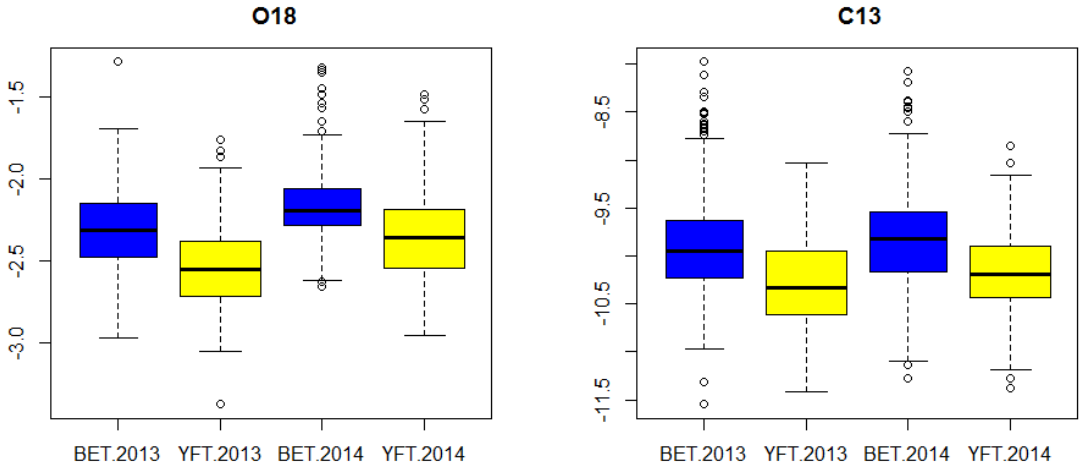


Figure 6.21. Boxplots comparing the stable isotope data, $\delta^{18}O$ (labelled as O18) and $\delta^{13}C$ (labelled as C13), by species and season.

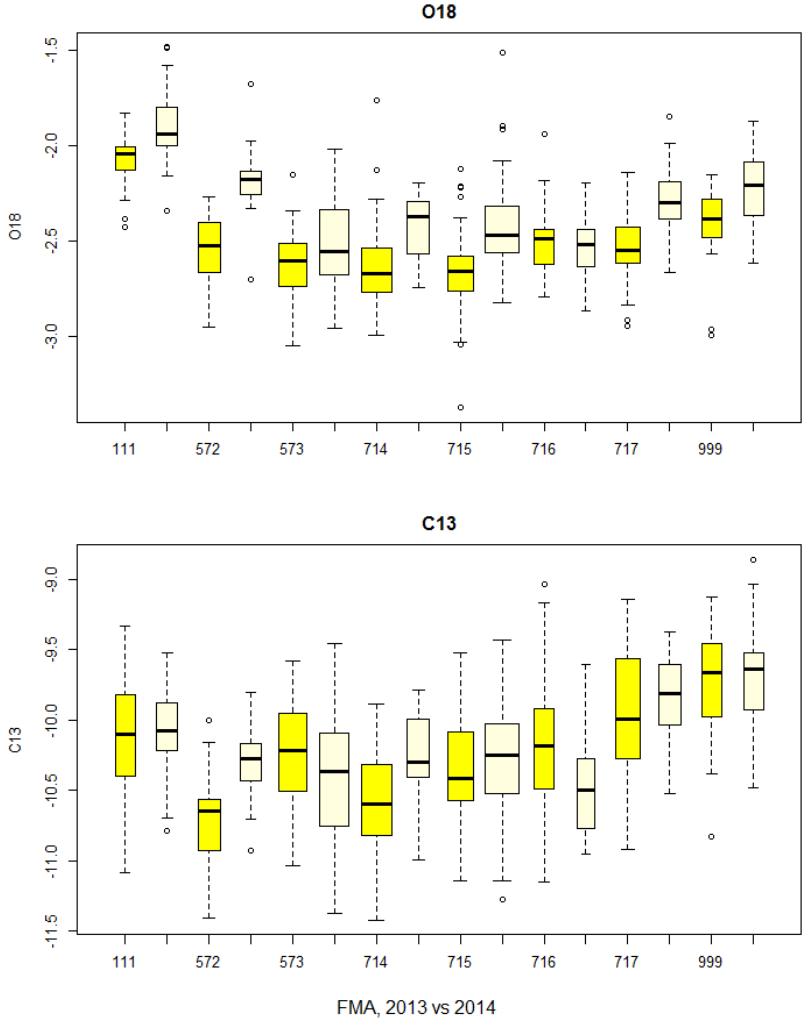


Figure 6.22. Boxplots comparing the stable isotope data, $\delta^{18}O$ (labelled as O18) and $\delta^{13}C$ (labelled as C13) for YFT, by FMA and season. Dark yellow corresponds to 2013 and light yellow to 2014.

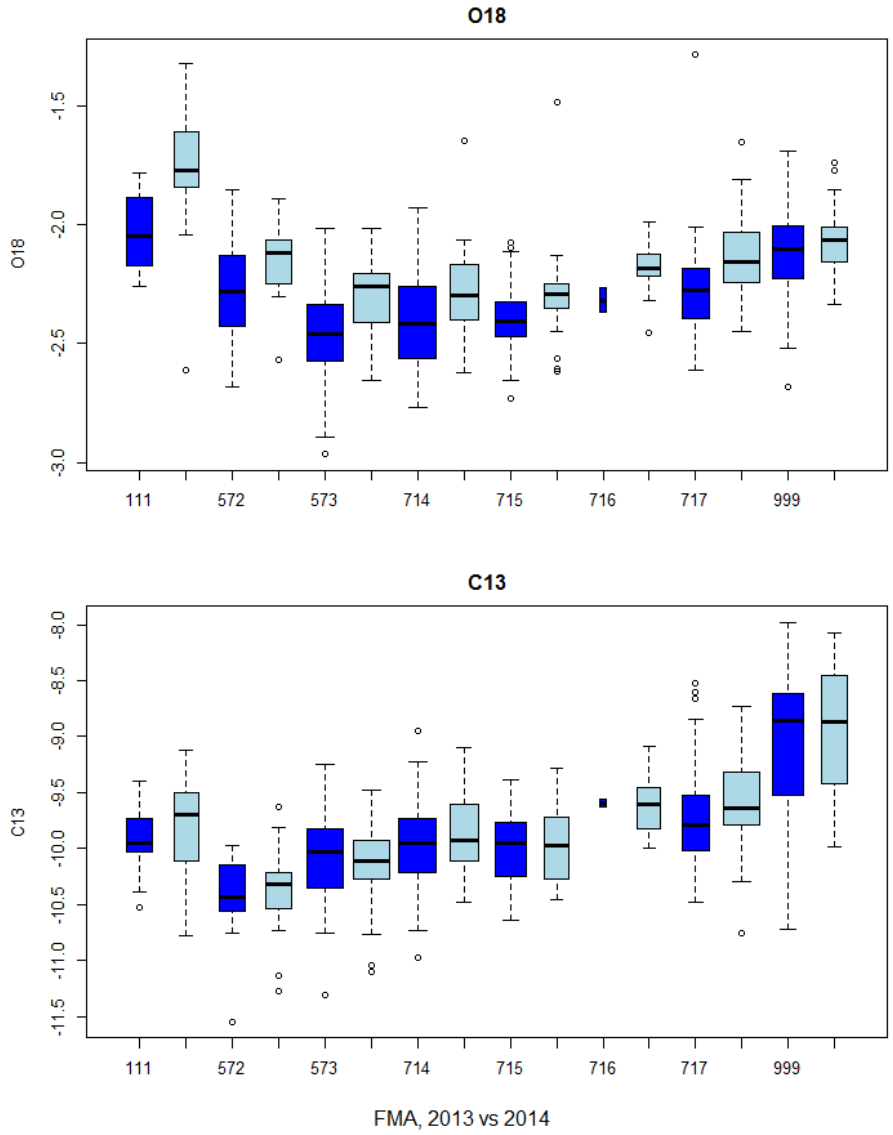


Figure 6.23. Boxplots comparing the stable isotope data, $\delta^{18}O$ (labelled as O18) and $\delta^{13}C$ (labelled as C13) for BET, by FMA and season. Dark blue corresponds to 2013 and light blue to 2014.

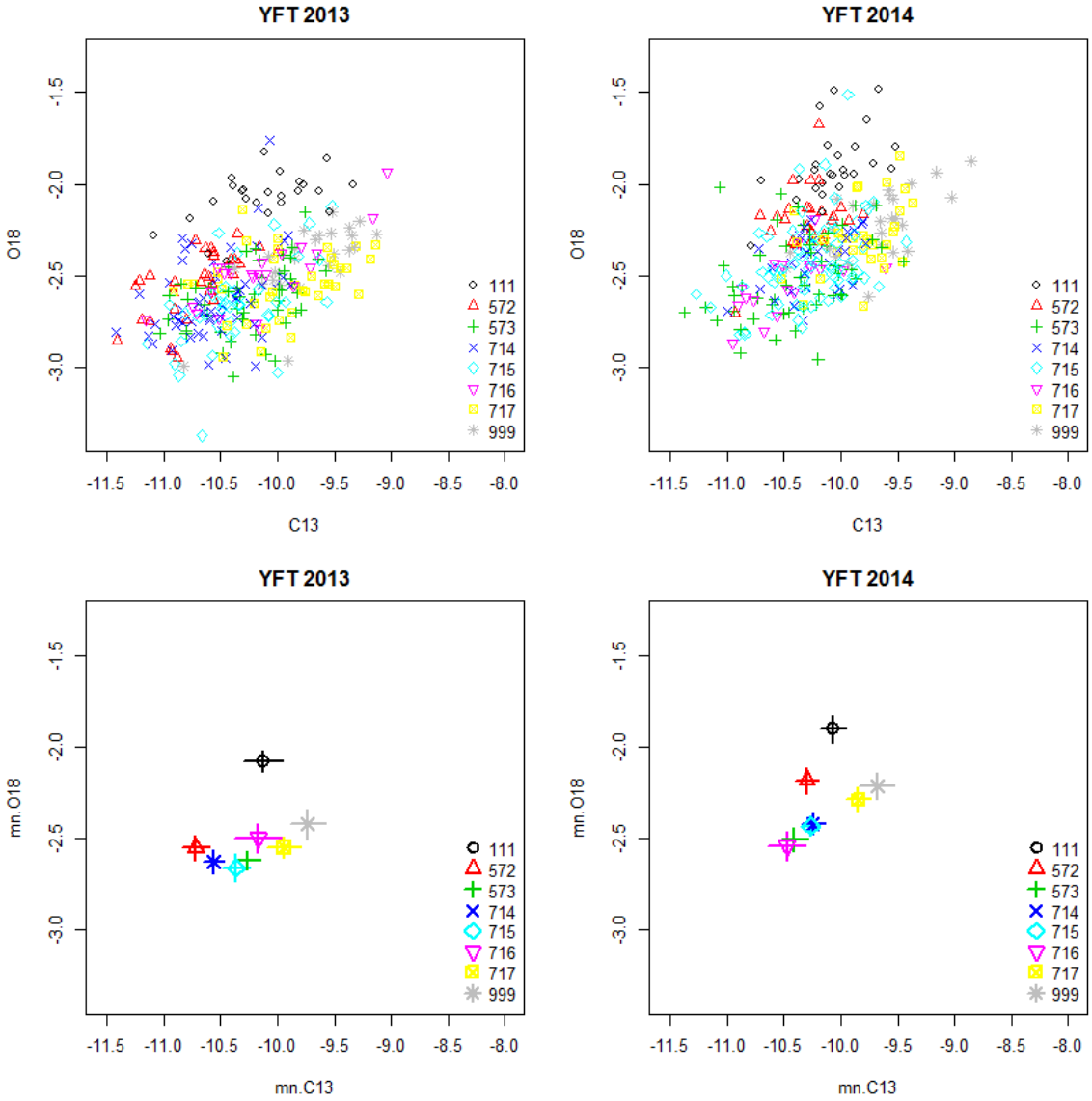


Figure 6.24. Scatterplots of $\delta^{13}C$ (labelled as C13) vs $\delta^{18}O$ (labelled as O18) for YFT by season, colour-coded by FMA. The top plots show the raw data so that the variability within and overlap between FMAs can be seen. The bottom plots show the mean values +/- 2 standard errors.

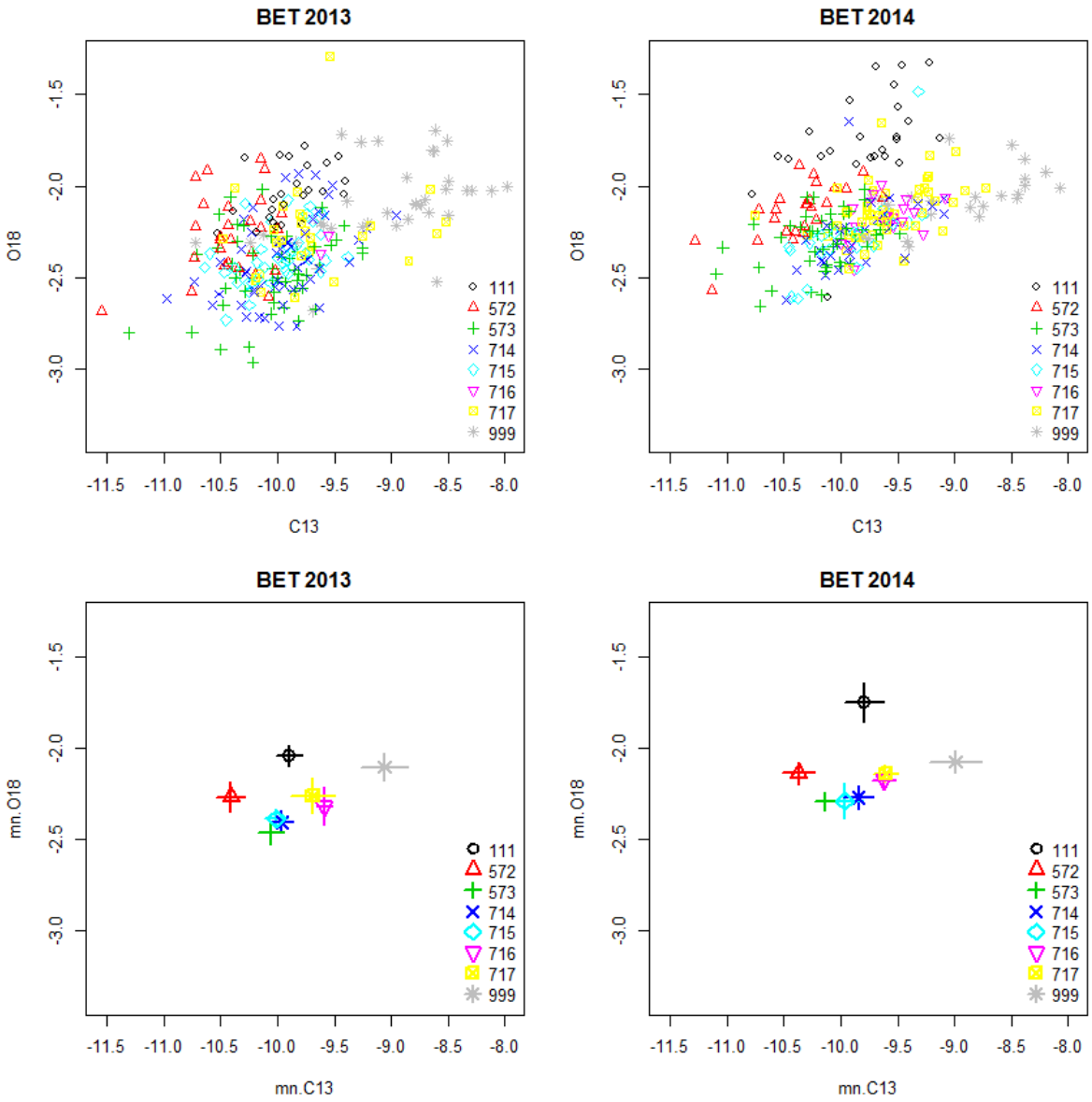


Figure 6.25. Scatterplots of $\delta^{13}C$ (labelled as C13) vs $\delta^{18}O$ (labelled as O18) for BET by season, colour-coded by FMA. The top plots show the raw data so that the variability within and overlap between FMAs can be seen. The bottom plots show the mean values +/- 2 standard errors.

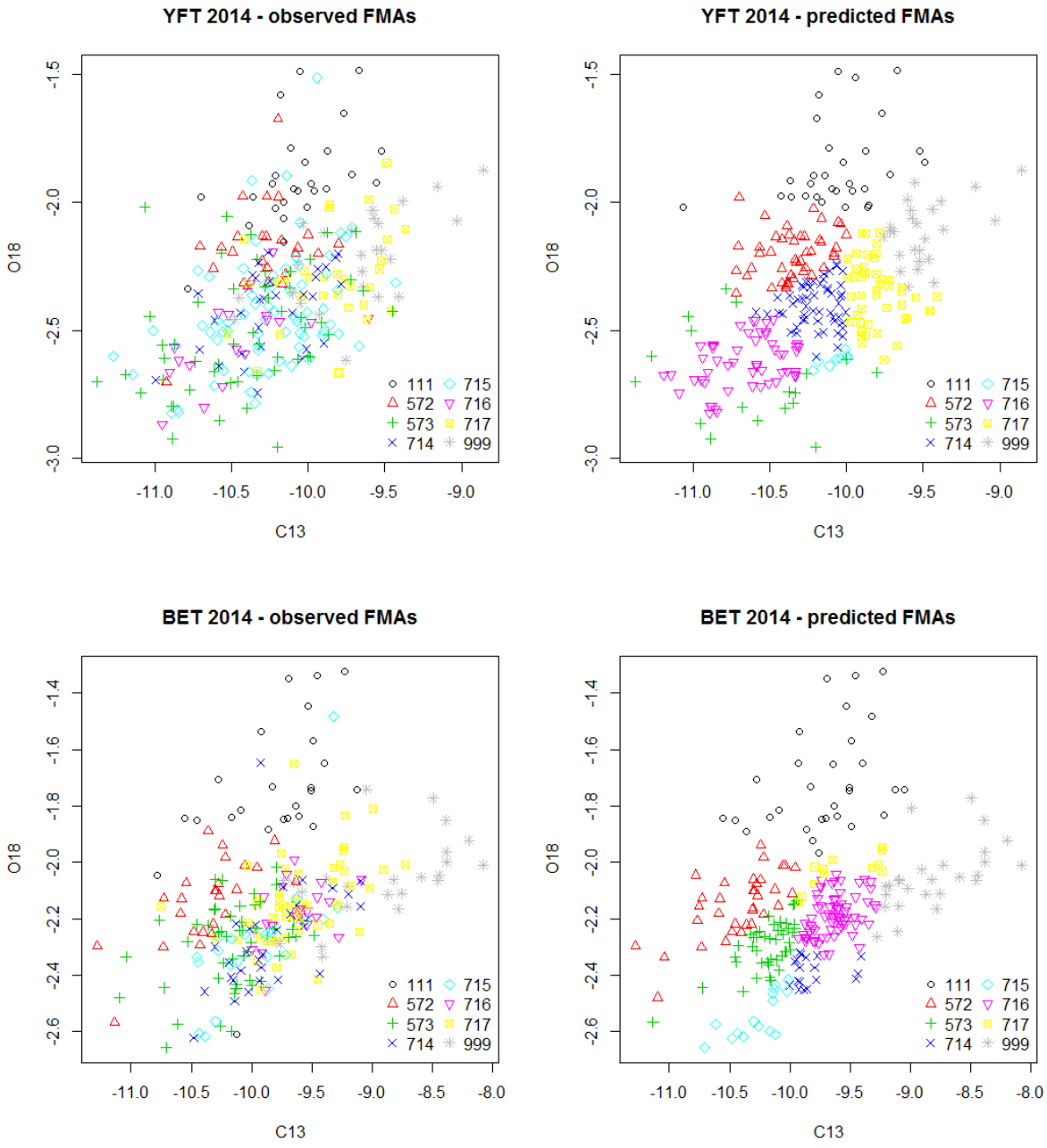


Figure 6.26. Scatterplots of $\delta^{13}C$ (labelled as C13) vs $\delta^{18}O$ (labelled as O18) for YFT (top row) and BET (bottom row) in 2014, where the data have been colour-coded by observed FMAs on the left and by QDA-predicted FMAs on the right.

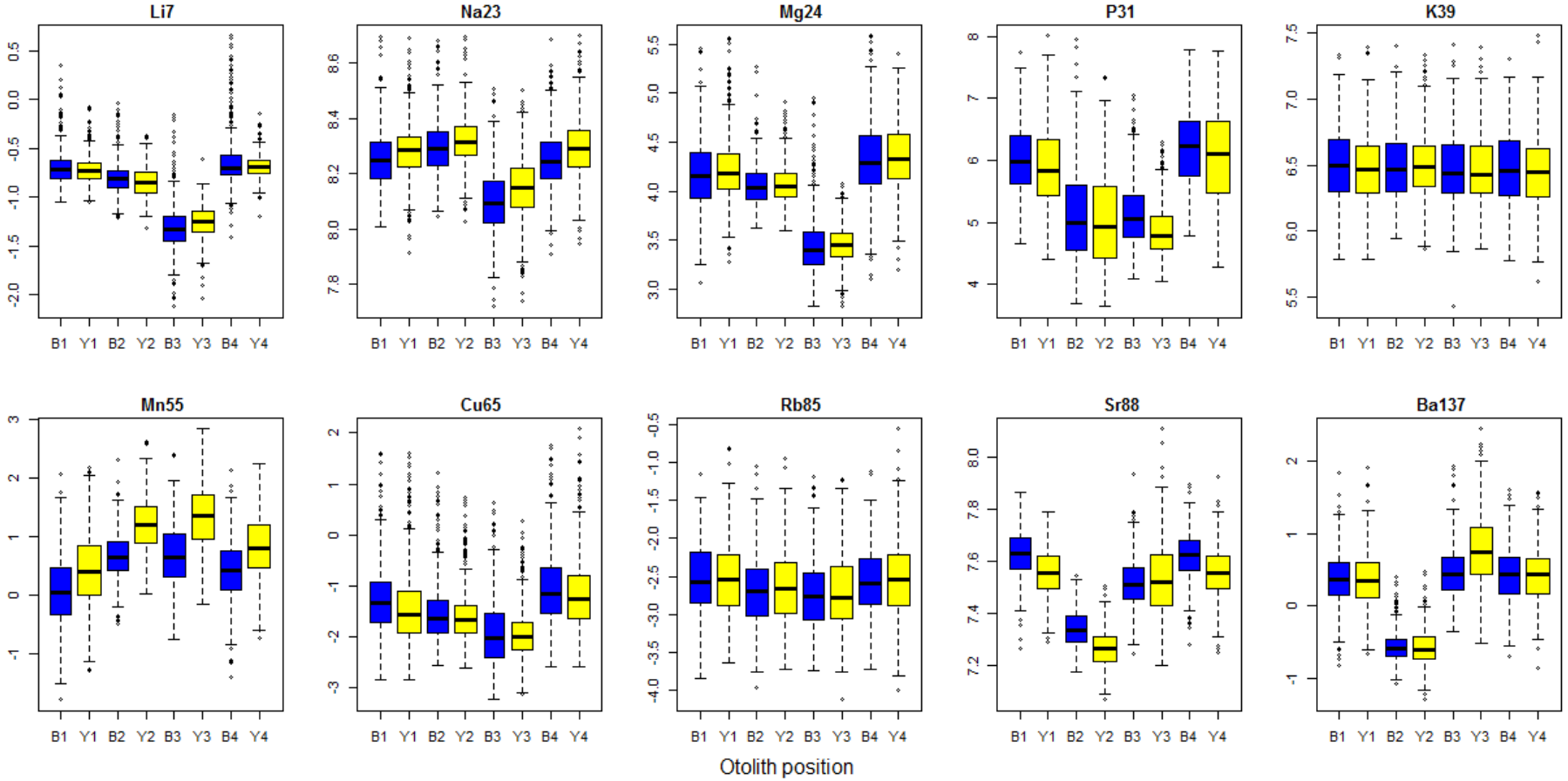


Figure 6.27. Boxplots comparing the element data (log-transformed) between otolith positions for BET (blue) and YFT (yellow). B1 denotes BET, position 1, Y1 denotes YFT position 1, etc.

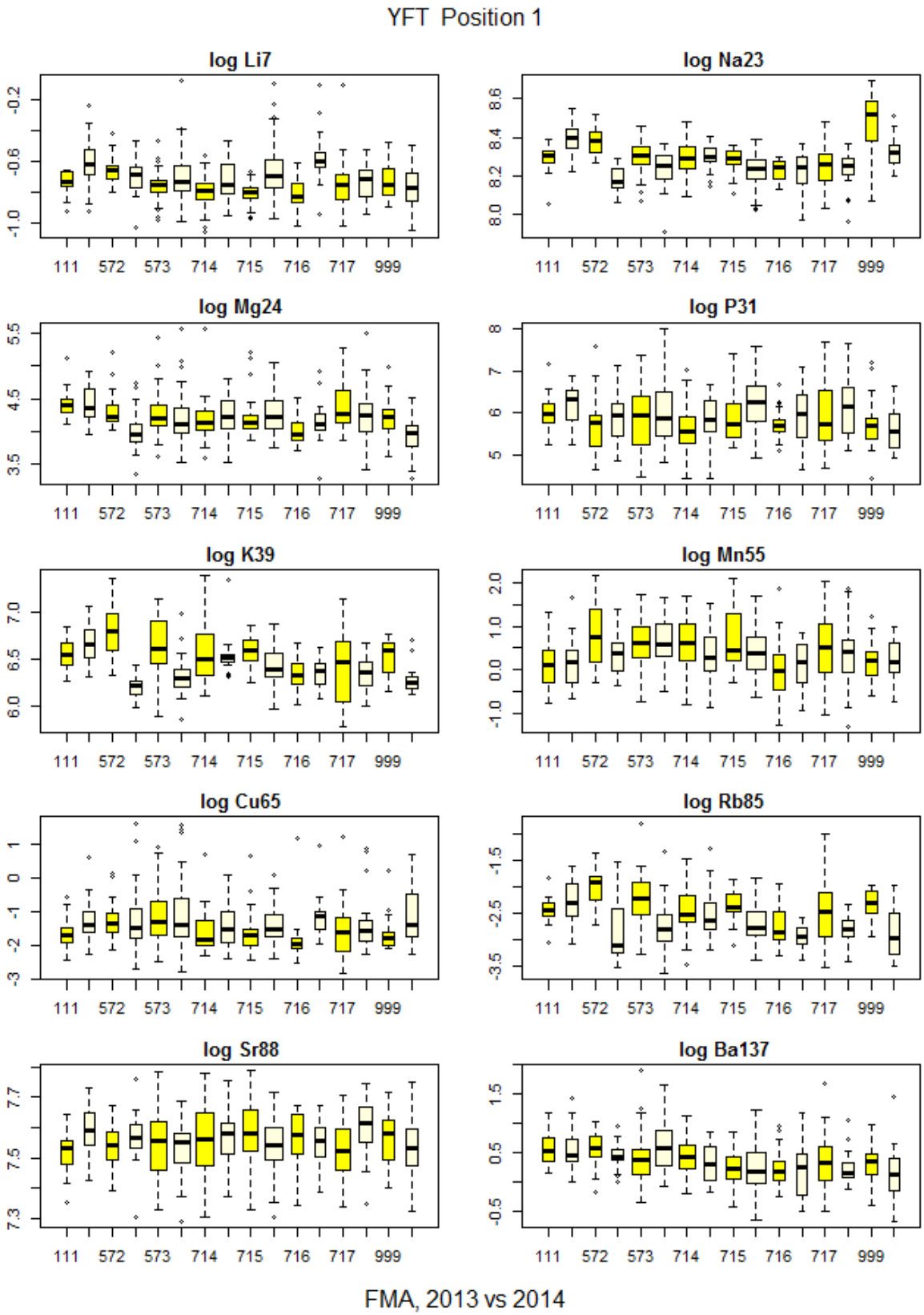


Figure 6.28. Boxplots of the log-transformed element data for YFT at otolith position 1, split by FMA and season, where dark yellow corresponds to 2013 and light yellow to 2014.

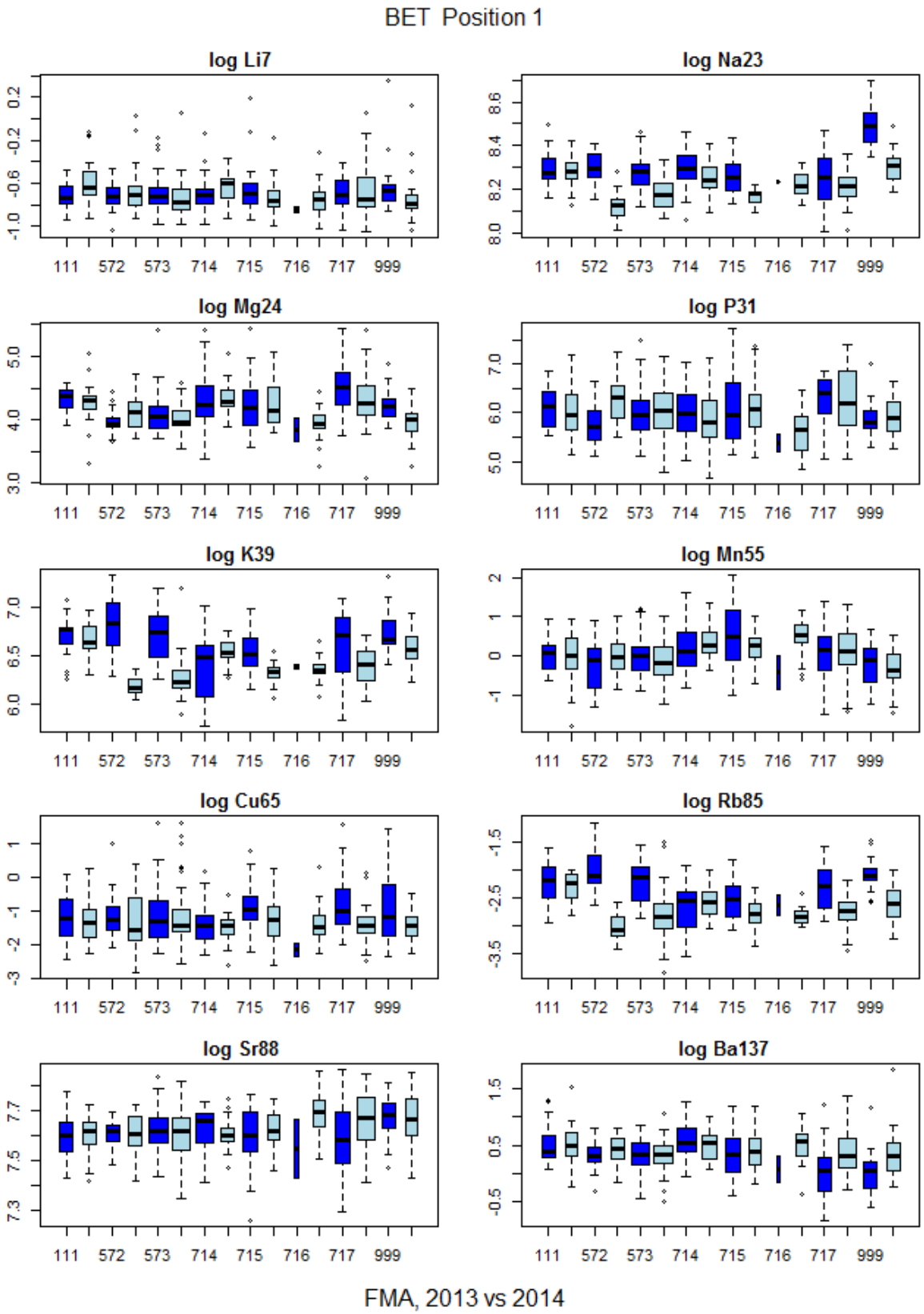


Figure 6.29. Boxplots of the log-transformed element data for BET at otolith position 1, split by FMA and season, where dark blue corresponds to 2013 and light blue to 2014.

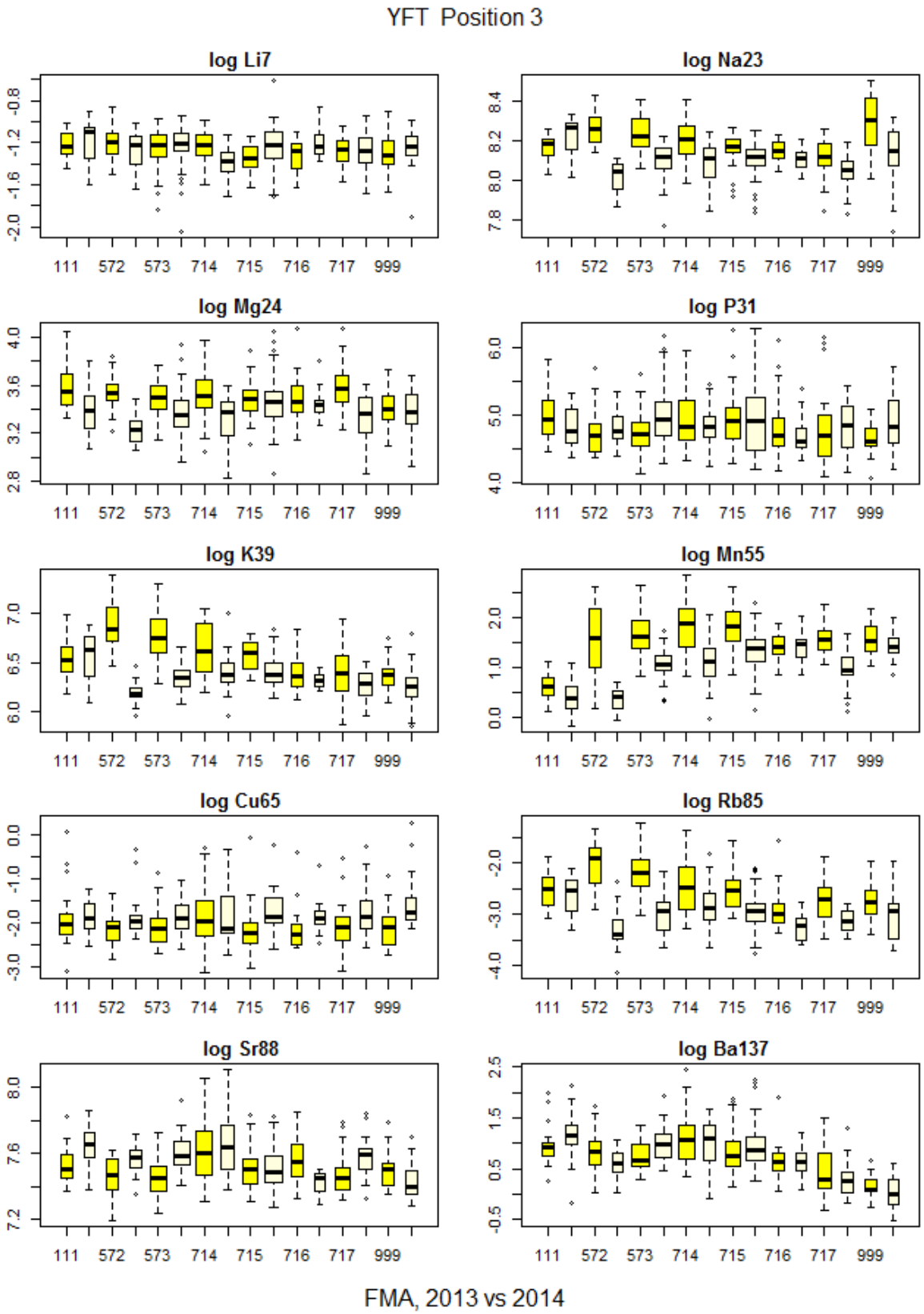


Figure 6.30. Boxplots of the log-transformed element data for YFT at otolith position 3, split by FMA and season, where dark yellow corresponds to 2013 and light yellow to 2014.

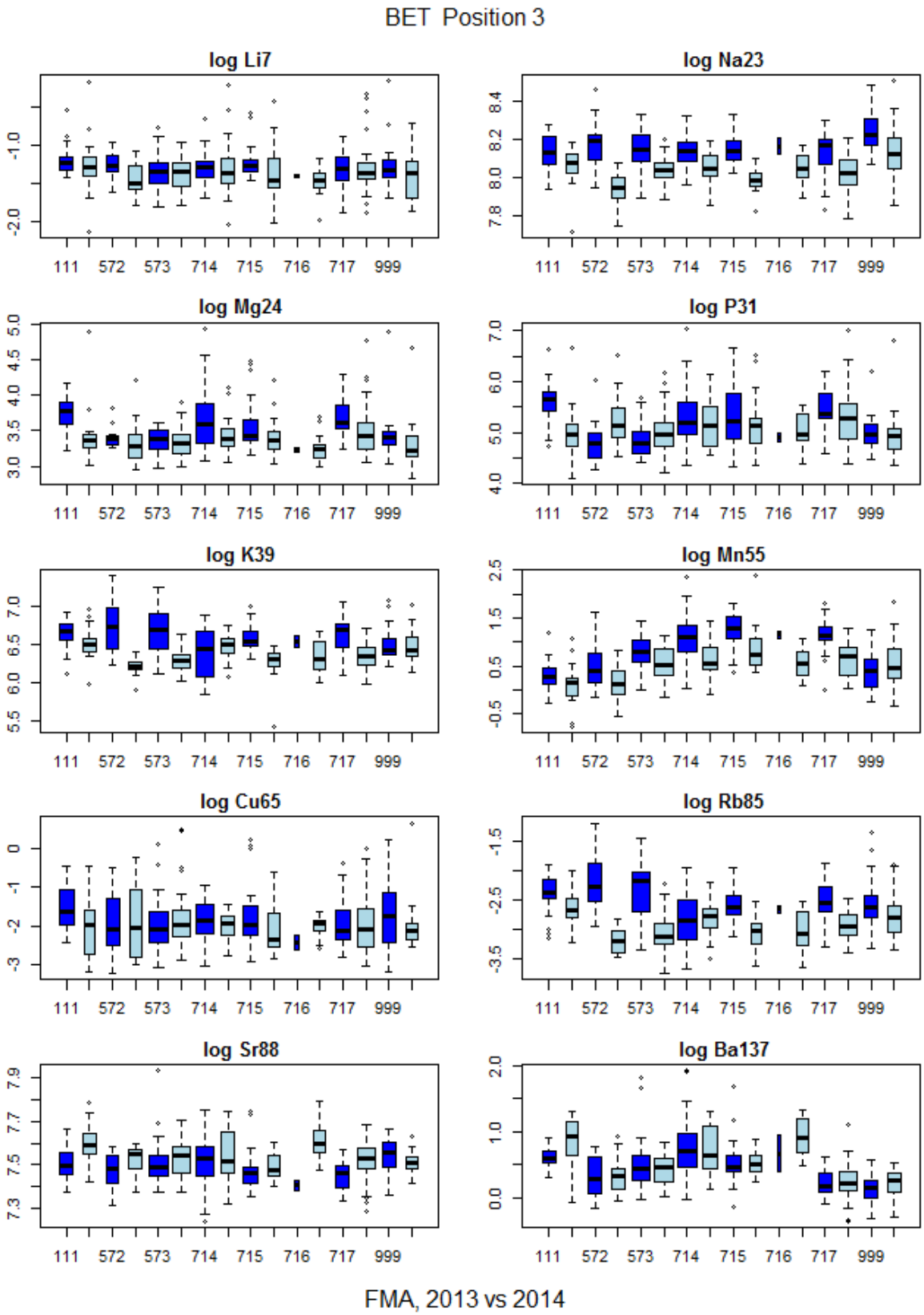


Figure 6.31. Boxplots of the log-transformed element data for BET at otolith position 3, split by FMA and season, where dark blue corresponds to 2013 and light blue to 2014.

## 6.7 References (cited in Section 6)

Bernal D., Brill R. W., Dickson K. A. and Shiels H. A. (2017). Sharing the water column: physiological mechanisms underlying species-specific habitat use in tunas. Reviews in Fish Biology and Fisheries 27: 843–880.

Brand W.A., Assonov S.S. and Coplen T.B. (2010). Correction for the $^{17}O$ interference in $\delta(^{13}C)$ measurements when analyzing $CO_2$ with stable isotope mass spectrometry (IUPAC Technical Report). Pure and Applied Chemistry 82 (8): 1719.

Campana S. E., Chouinard G. A., Hanson J. M., Frechet A. and Brattey J. (2000). Otolith elemental fingerprints as biological tracers of fish stocks. Fisheries Research 46: 343–357.

Carey F. G. (1973). Fishes with warm bodies. Scientific American 228: 36–44.

Dewar H., Graham J. B., and Brill R. W. (1994). Studies of tropical tuna swimming performance in a large water tunnel. Journal of Experimental Biology 192: 33–44.

DiMaria R. A., Miller J. A. and Hurst T. P. (2010). Temperature and growth effects on otolith elemental chemistry of larval Pacific cod, *Gadus microcephalus*. Environmental Biology of Fishes 89:453–462.

Dufor V., Pierre C. and Rancher J. (1998). Stable isotopes in fish otoliths discriminate between lagoonal and oceanic residents of Tairo Atoll (Tuamoto Archipelago, French Polynesia). Coral Reefs 17: 23–28.

Edmonds J. S. and Fletcher W. J. (1997). Stock discrimination of pilchards *Sardinops sagax* by stable isotope ratio analysis of otolith carbonate. Marine Ecology Progress Series 152[1-3]: 241–247.

Edmonds J. S., Steckis R. A., Moran M. J., Caputi N. and Morita M. (1999). Stock delineation of pink snapper and tailor from Western Australia by analysis of stable isotope and strontium/calcium ratios in otolith carbonate. Journal of Fish Biology 55[2]: 243–259.

Eggins S. M., Kinsley L. P. J. and Shelley J. M. G. (1998). Applied Surface Science 127–129: 278–286.

Fowler A. J., Campana S. E., Jones C. M. and Thorrold S. R. (1995). Experimental assessment of the effect of temperature and salinity on elemental composition of otoliths using laser ablation ICPMS. Canadian Journal of Fisheries and Aquatic Sciences 52: 1431–1441.

Fraile I., Arrizabalaga H. and Rooker J. R. (2015). Origin of Atlantic bluefin tuna (*Thunnus thynnus*) in the Bay of Biscay. *ICES Journal of Marine Science* 72 (2): 625–634.

Fraile I., Arrizabalaga H., Santiago J., Goñi N., Arregi I., Madinabeitia S., R., Wells R. J. D. and Rooker J. R. (2016). Otolith chemistry as an indicator of movements of albacore (*Thunnus alalunga*) in the North Atlantic Ocean. *Marine and Freshwater Research* 67: 1002–1013.

Friedman I., O'Neil J. and Cebula G. (1982). Two new carbonate stable isotope standards. Geostandard Newslett. 6: 11.

Gao Y. and Beamish R. J. (1999). Isotopic composition of otoliths as a chemical tracer in population identification of sockeye salmon (*Oncorhynchus nerka*). Canadian Journal of Fisheries and Aquatic Sciences 56: 2062–2068.

Graham B. S., Grubbs D., Holland K. and Popp B. N. (2007). A rapid ontogenetic shift in the diet of juvenile yellowfin tuna from Hawaii. Marine Biology 150: 647–658.

Holland K., Brill R., Chang R., Sibert J. and Fournier D. (1992). Physiological and behavioural thermoregulation in bigeye tuna (*Thunnus obesus*). Nature 358: 410–412.

Izzo C., Doubleday Z., A. and Gillanders B., M. (2016). Where do elements bind within the otoliths of fish? Marine and Freshwater Research 67: 1072–1076.

Jochum K. P., Weis U., Stoll B., Kuzmin D., Yang Q., Raczek I., Jacob D. E., Stracke A., Birbaum K., Frick D. A., Günther D. and Enzweiler J. (2011). Geostandards and Geoanalytical Research 35: 397–429.

Kerr L. A. and Campana S. E. (2014). Chemical Composition of Fish Hard Parts as a Natural Marker of Fish Stocks. *In*, Cadrin, S. X., Kerr, L. A. and Mariani, S. Stock Identification Methods: Applications in Fishery Science, p. 205–234.

Kubo T., Sakamoto W., Murata O. and Kumai H. (2008). Whole-body heat transfer coefficient and body temperature change of juvenile Pacific bluefin tuna *Thunnus orientalis* according to growth. Fisheries Science 74: 995–1004.

Longerich H. P., Jackson S. E. and Gunther D. (1996). Journal of Analytical Atomic Spectrometry 11: 899–904.

McCrea J.M. (1950). On the isotopic chemistry of carbonates and a Paleo-temperature scale. Journal of Chemical Physics 18: 849.

Moore B. R, and Simpfendorfer C. A. (2014). Assessing connectivity of a tropical estuarine teleost through otolith elemental profiles. Marine Ecology Progress Series 501: 225-238.

Mulcahy S. A., Killingly J. S., Phleger C. F. and Berger W. H. (1979). Isotopic composition of otoliths from a benthopelagic fish, *Coryphaenoides acrolepis*, Macrouridae: Gadiformes. Oceanologica Acta 2[4]: 423–427.

Muller W., Shelley M., Miller P. and Broude S. (2009). Journal of Analytical Atomic Spectrometry 24: 209–214.

Newman S. J., Stekis R. A., Edmonds J. S., and Lloyd J. (2000). Stock structure of the goldband snapper *Pristipmoides mutlidens* (Pisces: Lutjanidae) from the waters of northern and western Australia by stable isotope ratio analysis of sagittal otolith carbonate. Marine Ecology Progress Series 198: 239–247.

Radtke R. L., Showers W., Moksness E. and Lenz P. (1996). Environmental information stored in otoliths: Insights from stable isotopes. Marine Biology 127 (1): 161–170.

Ruttenberg BI, Hamilton SL, Hickford MJH, Paradis GL, Sheehy MS, Standish JD, Ben-Tzvi , Warner RR. (2005). Elevated levels of trace elements in cores of otoliths and their potential for use as natural tags. Marine Ecology Progress Series 297: 273–281.

Schaefer K. M., Fuller D. W. and Block B. A. (2009).Vertical movements and habitat utilization of skipjack (*Katsuwonus pelamis*), yellowfin (*Thunnus albacares*), and bigeye (*Thunnus obesus*) tunas in the equatorial eastern Pacific Ocean, as ascertained through archival tag data. In: Nielsen J.L., Arrizabalaga H., Fragoso N., Hobday A., Lutcavage M., Sibert J. (eds.), Reviews: Methods and Technologies in Fish Biology and Fisheries, Vol. 9, Tagging and Tracking of Marine Animals with Electronic Devices. Springer Publication, pp. 121–144.

Schwarcz H. P., Gao Y., Campana S., Browne D., M. Knyf M. and Brand U. (1998). Stable carbon isotope variations in otoliths of Atlantic cod (*Gadus morhua*). Canadian Journal of Fisheries and Aquatic Sciences 55: 1798–1806.

Shiao J-C., Wang S-W., Yokawa K., Ichinokawa M., Takeuchi Y., Chen Y-G. and Shen C-C. (2010). Natal origin of Pacific bluefin tuna *Thunnus orientalis* inferred from otolith oxygen isotope composition. Marine Ecology Progress Series 420: 207–219.

Stephenson P. C., Edmonds J. S., Moran M. J. and Caputi N. (2001). Analysis of stable isotope rations to investigate stock structure of red emperor and rankin cod in northern Western Australia. Journal of Fish Biology 58: 126–144.

Sturrock A. M., Trueman C. N., Darnaude A. M. and Hunter E. (2012). Can otolith elemental chemistry retrospectively track migrations in fully marine fishes? Journal of Fish Biology 81: 766–795.

Swart P. K., Burns S. J. and Leder J. J. (1991). Fractionation of the stable isotopes of oxygen and carbon in carbon dioxide during the reaction of calcite with phosphoric acid as a function of temperature and technique. Chemical Geology 86: 89.

Thorrold S. R., Campana S. E., Jones C. M. and Swart P. K. (1997). Factors determining δ13C and δ18O fractionation in aragonitic otoliths of marine fish. Geochimica et Cosmochimica Acta 61: 2909.

Wells R. J. D., Rooker J. R. and Itano, D. G. (2012). Nursery origin of yellowfin tuna in the Hawaiian Islands. Marine Ecology Progress Series 461: 187–196.

Wells R. J. D., Kinney M. J., Kohin S., Dewar H., Rooker J. R. and Snodgrass O. E. (2015). Natural tracers reveal population structure of albacore (*Thunnus alalunga*) in the eastern North Pacific. ICES Journal of Marine Science 72 (7): 2118–2127.

Werner R. A. and Brand W. A. (2001). Referencing strategies and techniques in stable isotope ratio analysis. Rapid Communications in Mass Spectrometry 15: 501.

# 7. Technique 3: Genetics

Team: Peter Grewe[1], Matt Lansdell[1], Muhammad Taufik[2], Peta Hill[1], Scott Foster[3], and Thierry Gosselin[4].

[1]CSIRO Oceans and Atmosphere, Hobart, Tasmania, Australia

[2]Research Institute for Marine Fisheries, Cibinong, West Java, Indonesia

[3]CSIRO Data61, Hobart, Tasmania, Australia

[4]Department of Biology, Laval University, Quebec, Canada

*Note: The Figures for this chapter follow as Section 7.4, following the Results and Discussion (Section 7.3).*

## 7.1 Introduction

Examination of stock connectivity in the Indo-Pacific region for BET and YFT through analyses of genetic population structuring has often led to reporting of ambiguous results. Researchers have either concluded lack of genetic differentiation for these species on large geographic scales (thousands of kilometres) or the finding of population subdivision in quite limited geographical range on the scale of hundreds of kilometres. Past studies, which have used a variety of genetic marker techniques (including protein electrophoresis, mitochondrial DNA, DNA microsatellites), have predominantly cited a combination of three general reasons to explain inconclusive results (i.e. lack of genetic differentiation): i) inadequate numbers of individuals collected from each sample site; ii) lack of resolution due to the type of DNA markers used in the analysis; or iii) presence of sufficient gene flow among sampling locations that prevents development of significant population differentiation. The approaches used in this project's study aimed to overcome the shortcomings of previous studies by initially addressing the first of these two points that appear to be mainly technical issues as a result of financial constraints, genetic marker resolution, or insufficient geographic and temporal sampling coverage. We chose to use single nucleotide polymorphism (SNP) analysis, the most modern DNA profiling approach that showed potential for demonstrating differentiation in YFT and BET where previous state of the art techniques of mitochondrial DNA and DNA microsatellite analysis had failed to do so. We also hoped to shed light on the addressing the third point (i.e., sufficient gene flow preventing population differentiation) through examination of two quite distant outlier populations where the potential of connectivity was suspected to be much lower than that expected within the Indonesian archipelago.

## 7.2 Methodology

### *7.2.1 Sample collection and DNA Isolation*

Biopsies of white muscle were obtained from individuals close to the main dorsal fin and preserved in RNAlater® (Life Technologies) for shipment to laboratory for DNA extraction. Representative individuals from each of the sampling location and species were chosen from the total sample pool collected for the project (Table 7.1). Approximately 15mg of tissue was subsampled from these biopsies and used for DNA extractions. Total genomic DNA was isolated using one of two protocols; either a Machery Nagel Nucleo-Mag bead based DNA isolation kit or a CTAB protocol, a Phenol-Chloroform based method described by Grewe *et al*. (1993). The bead based extractions were performed on an Eppendorf EP-Motion-5075 robotic liquid handling station. DNA aliquots were shipped to Diversity Array Technologies in Canberra where DNA complexity reduction and library construction was performed prior to sequencing that was used to generate genotype data for each individual.

Table 7.1. Locations and numbers of individual bigeye (BET) and yellowfin (YFT) chosen for the genetic analysis.

| Sampling location | BET | | YFT | |
|---|---|---|---|---|
| | 2013 | 2014 | 2013 | 2014 |
| Maldives | 44 | 48 | 50 | 46 |
| Padang | 48 | 48 | 46 | 46 |
| Palabuhanratu | 48 | 48 | 46 | 46 |
| Prigi | 36 | 43 | 58 | 51 |
| Ambon | 48 | 48 | 46 | 46 |
| Kendari | 48 | 48 | 46 | 46 |
| Gorontalo | 48 | 1 | 46 | 88 |
| Bitung | 4 | 23 | 90 | 71 |
| Sorong | 31 | 48 | 63 | 46 |
| Jayapura | 16 | 34 | 78 | 60 |
| Solomon Islands | 48 | 48 | 46 | 46 |

### 7.2.2 DArTseq genotyping

The sequencing protocols used incorporated a DArT-Seq proprietary next generation sequencing methodology. DArTseq™ represents a combination of DArT complexity reduction methods and next generation sequencing platforms (Kilian et al. 2012; Courtois et al. 2013; Raman et al. 2014; Cruz et al. 2013). This represents a new implementation of sequencing complexity with reduced representations (Altshuler et al. 2000) and more recent applications of this concept on the next generation sequencing platforms (Baird et al. 2008; Elshire et al. 2011). Similar to DArT methods based on array hybridisations, the technology is optimized for each organism and application by selecting the most appropriate complexity reduction method (both the size of the representation and the fraction of a genome selected for assays). Four methods of complexity reduction were tested in tuna (data not presented) and the PstI-SphI method selected. DNA samples were processed in digestion/ligation reactions principally as per Kilian et al. (2012) but replacing a single PstI-compatible adaptor with two different adaptors corresponding to two different Restriction Enzyme (RE) overhangs. The PstI-compatible adapter was designed to include Illumina flow cell attachment sequence, sequencing primer sequence and "staggered", varying length barcode region, similar to the sequence reported by Elshire *et al*. (2011). The reverse adapter contained a flow cell attachment region and an SphI-compatible overhang sequence.

Only "mixed fragments" (PstI-SphI) were effectively amplified by PCR. PCR conditions consisted of an initial denaturation at 94°C for 1 min followed by 30 cycles of 94°C for 20 sec, 58°C for 30 sec and 72°C for 45 sec, with a final extension step at 72°C for 7 min. After PCR, equimolar amounts of amplification products from each sample of the 96-well microtiter plate were bulked and applied to cBot (Illumina) bridge PCR, followed by sequencing on an Illumina Hiseq2000. The sequencing (single read) was run for 77 cycles.

Sequences generated from each lane were processed using a proprietary DArTseq analytical pipeline (DArT-Soft14 version). In the primary pipeline, the FASTQ files were first processed to filter away poor-quality sequences, applying more stringent selection criteria to the barcode region compared to the rest of the sequence. In that way the assignments of the sequences to specific samples carried in the "barcode split" step were very reliable. Approximately 2,000,000 sequences per barcode/sample were identified and used in marker calling. Finally, identical sequences were collapsed into "fastqcall files". These files were used in the secondary pipeline for DArTseq PL's proprietary SNP and SilicoDArT (presence/absence of restriction fragments in representation) calling

algorithms (DArTsoft14). For the current study only co-dominant SNP-DArT markers were used for population analysis.

### 7.2.3 Genotype Data Analysis

The DArT sequencing data set used to generate individual genotypes for population analysis was obtained using the DArTsoft14 pipeline. Individual locus sequences consisted of 75bp fragments containing one or more polymorphic SNPs. When multiple polymorphisms were found on the same 75bp fragment (RAD contig), a single SNP was randomly chosen to represent that locus to avoid linkage disequilibrium between close loci. Loci were further eliminated from population analysis by excluding loci where call rate (individuals scored for a locus) was less than 90% of individuals with a genotype scored per population and where minor allele frequencies (MAF) of individual loci were less than 5%. Departure from Hardy-Weinberg equilibrium (HWE) was tested for each locus within each sampling location using the "HWE.test.genind" function in the Adegenet R package 45 and the false discovery rate method was applied to control for multiple comparison testing 46. Additional filtering was done to eliminate identical individuals. As part of this process we also calculated individual paired relatedness to determine whether individuals had been allocated to correct species or not. All ambiguously labelled individuals were eliminated from population analysis testing.

The resulting genotype data set was analysed using two different methods. The first method used an R-package program (stockR), that implemented a strategy for robustly identifying genetically distinct groups or putative stocks within the data set (Foster et al. 2018). The methods implemented in stockR are directly targeted at finding breeding groups, unlike some commonly-used statistical methods. Genetic relatedness among all individuals was used to cluster them into "K" different groups via a particular statistical mixture model, using a latent variable for the group membership of each individual fish. The most pertinent output of the modelling was an assignment of each fish to one of "K" genetically related groups over a range of seven different levels (K=2 to 8 groups). The proportions of the different K-groups at each fishing port were plotted to provide a visual interpretation of the overall spatial distribution of the different defined genetic groups. A cross-validation was performed to estimate percentage of likely correct assignment to each "K" cluster group. The higher the percentage of correct assignments, the more support the data has for that amount of grouping. The cross-validation was performed by examining the genetic cluster that each individual was assigned using the full data set, and then to hold a random group of individuals out and re-performing the analysis (we held out a fifth of the data). A total of 100 hold-out sets were evaluated for each number of groups (K). The cross-validation statistic was defined to be the number of held-out fish that were re-assigned to the same group. The number of correctly reassigned fish is measured by the sum of the posterior probability of group membership. This process is performed for each of K=2 to K=8 putative genetic groups.

The second genetic analysis used a measure of $F_{ST}$ genetic relatedness to estimate and define genetically related distance between pairs of sites. These values were then used to produce a tree dendrogram by an unweighted pair group method analysis (UPGMA). Branch node positions were tested using a bootstrap method (10,000 replicates) to determine tree robustness.

## 7.3 Results and Discussion

Sampling effort for both species permitted a reasonably robust testing of connectivity for both BET and YFT. Target sample sizes ($n \geq 46$) analysed for YFT were achieved for all 11 sites in both years (with the exception of Sorong in 2014, n = 36). Achieving target samples sizes for the BET analysis, proved to be more difficult due to rare occurrence of this species in the overall catches at each site. Despite this, overall sampling effort was considered sufficient for both species with at least 9 of 11 sites yielding $\geq$ 30 individuals per site in each year. Interestingly, the filtering of genotype data revealed only a small number (< 4) individuals where tissues from an individual had been sampled

multiple times but labelled as a different fish. This duplication may either have happened during sampling on-site or during sub-sampling at the lab. The low frequency of occurrence did not affect sampling strategy robustness for the overall analysis and one individual from each of the duplicate pairs was eliminated from final population analysis. Duplicate DNA was also intentionally run from some individuals as an internal quality control check. These were also eliminated from the final population analysis. During the quality control filtering of the data, a few individuals (< 12 total from 3 sites) were discovered that had been mislabelled the wrong species. Species identification of individuals, which were tested using mitochondrial DNA markers, were confirmed to have been mislabelled as the incorrect species and were subsequently eliminated from consideration in the population analysis. Again, removal of these individuals had no impact on the overall statistical precision of the analysis as they were present at such a very low frequency of the overall sampling effort.

Genetic analysis of single nucleotide polymorphisms (SNPs) for both bigeye (BET) and yellowfin (YFT) tuna samples revealed interesting patterns of connectivity among the 11 sampling locations examined. Most importantly, for both species the pattern of connectivity appeared to be temporally stable for each of the sampling years. For each species, two types of analysis were applied to examine patterns of connectivity and stock. The first method compared genetic relatedness among all individuals grouping them into "K" different levels of genetic clusters. This analysis was done without giving information about prior groupings or sampling location and gave an assignment of each individual to one of "K" genetically related groups. A total of seven different levels (K = 2 to 8) of clustering or groupings were examined and the proportion of individuals in each genetic group was then plotted for each sampling site (Figures 7.1 & 7.2 for BET and YFT respectively). Cross-validation at various groups of K were analysed to determine the percentage of repeatable assignment at a given number of K groupings. This cross-validation analysis revealed a substantial drop from 85% at K=3 to 70% at K=4 for BET (Figure 7.3 -left) and for YFT from 86% (K=2) to 74% (K=3) (Figure 7.3 - right). Thus, for the purposes of this summary document we have only presented the K = 3 for BET and K=2 for YFT. clustering analysis (Figures 7.1 & 7.2).

The analysis of BET appears to demonstrate restricted connectivity between Indian Ocean (Maldives, Padang, Palabuhanratu, Prigi) and Pacific Ocean (Sorong, Jayapura, Solomon Islands). Samples from the central Indonesian sites (Kendari, Ambon, Gorontalo, Bitung) appear to have limited connectivity to both areas with geographically adjacent sites showing greatest similarity to each other. The second analysis produced a tree dendrogram that used $F_{ST}$ genetic relatedness estimates to define a level of differentiation between pairs of sites. Interestingly, the tree analysis also supported results from stockR, in that sites geographically close to each other also appeared to be more similar genetically (Figure 7.4).

In general, $F_{ST}$ values were greater among BET than those observed among YFT sites. However, while YFT appears to be less differentiated than BET, there is still a marked difference observed between samples from the central Indian Ocean (Maldives) and those of Western Pacific origin (Jayapura, Solomon Islands). Interestingly, internal Indonesian sites (Ambon, Kendari, Gorontalo, Bitung) show very limited if any differentiation from the western Pacific sites (Jayapura, Solomon Islands) which may be an indication of higher genetic connectivity for YFT than BET in this region (Figure 7.5). This pattern of differentiation among the sampling location regions may be an indication of limited gene flow between central and eastern Indian Ocean sampling regions with more pronounced gene flow among central Indonesian and Western Pacific sampling regions. Additional sampling among these areas will certainly help to further resolve this hypothesis.

The genetic subdivision observed by the current study has revealed more structure than previously described for YFT in the Indo-Pacific region by some studies (Ward et al. 1997; Appleyard et al. 2001; Grewe and Hampton 1998; Davies et al. 2014). In retrospect, these previous studies, which used mtDNA and DNA microsatellite markers, were incapable of the genetic resolution offered by DArT-Seq analysis as demonstrated by Grewe et al. (2015). While the genetic resolution was able to reveal the

presence of structure among the sampling sites, the putative stock structure appears to be more complex and not as differentiated as other studies have purported on smaller geographic scales than examined by our study (Diaz-Jaimes and Uribe-Alcocer 2006; Dammannagoda et al. 2008). Our data appears to demonstrate presence of multiple (at least 2 – 3) genetically distinct groups within each sampling location. A variety of hypotheses could explain this observation, with perhaps the simplest explanation being that the fish sampled in this study were 4 – 5 months of age and therefore already at a point where mixing of genetically differentiated spawning locations could have occurred. Further examination of genetic data obtained from a sample of larvae or ripe and running adults would be required to further address this hypothesis.

In summary, the connectivity for BET and YFT in the Indo-Pacific region of Indonesia was assessed through analysis using a genetic clustering approach to group individuals, as well as examination of $F_{ST}$ measure genetic relatedness among sampling locations. Analysis of the distribution of genetic cluster groups for both BET and YFT among the sampling sites appears to demonstrate presence of subtle genetic structure of at least 2 or 3 genetic groupings. There is a geographic partitioning of the groups among the sampling locations that appears to be positively correlated with proximity of sampling locations and could indicate clinal genetic variation consistent with an isolation by distance model. The most differentiated populations are on the extreme ends of our sampling distribution and represent central Indian Ocean versus Western Pacific Ocean regions. Support for this outcome was observed in the tree-based examination of genetic relatedness ($F_{ST}$) among sampling locations. The geographic partitioning of the sampling locations appears to have a strong genetic basis that was temporally stable over the two years of the project. Further sampling of additional sites and additional year classes will help to provide further support for both temporal stability and geographic connectivity with respect to regions and may lead to additional clues as to the origin of major spawning locations. The data generated by this project is consistent with the presence of multiple genetic groups. This information can now be used to guide future sampling strategies to further elucidate the genetic patterning and examine population structure in these two important tuna species.

## 7.4 Figures

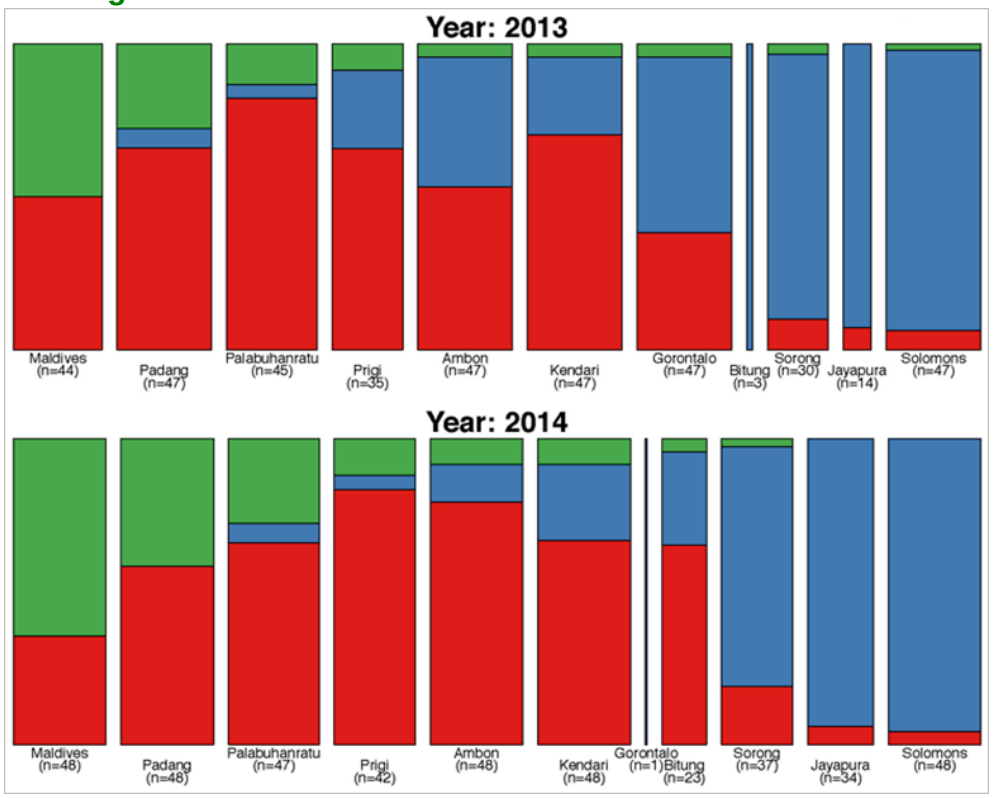


Figure 7.1. Proportion at each sampling site of BET clustered into three genetically partitioned groups (K = 3). Sample sizes for each location and time point are indicated in parentheses.

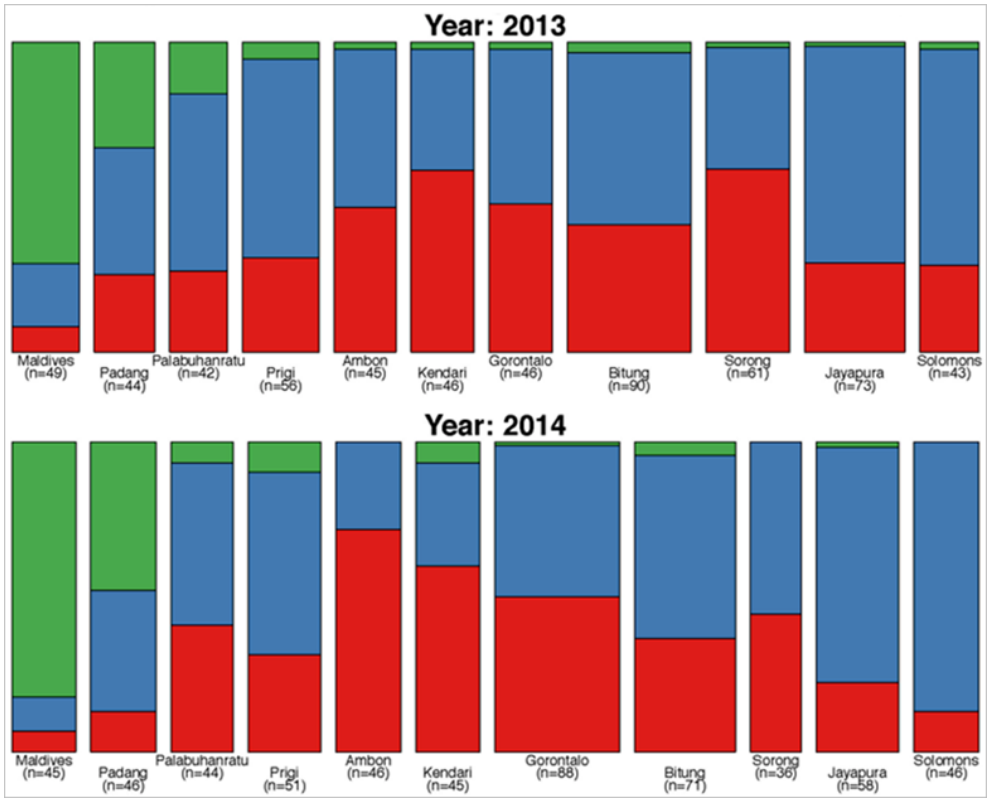


Figure 7.2. Proportion at each sampling site of YFT clustered into two genetically partitioned groups (K = 2). Sample sizes for each location and time point are indicated in parentheses.

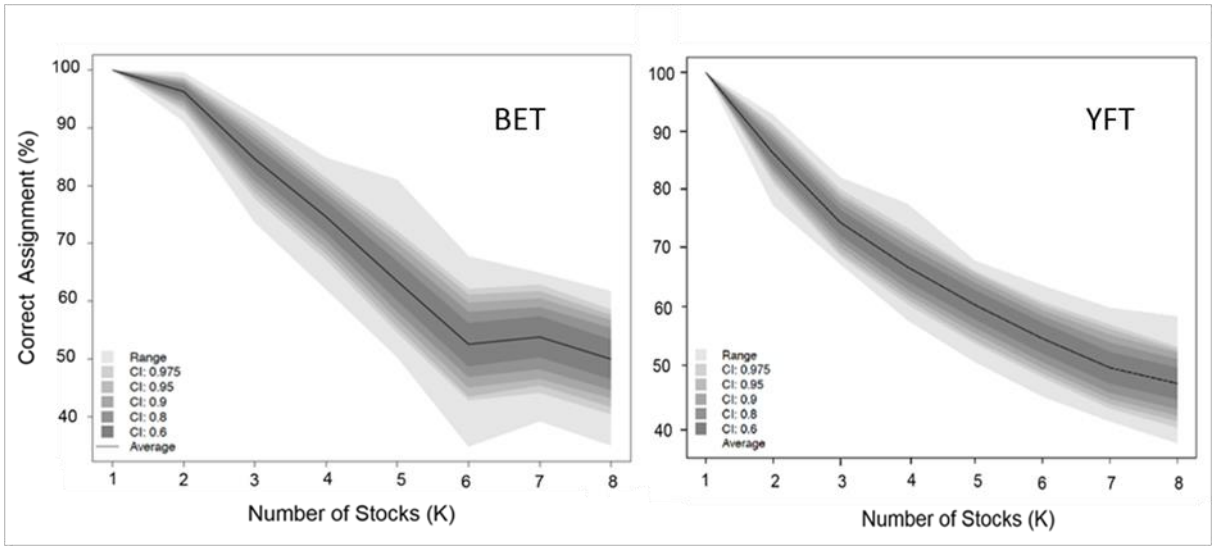


Figure 7.3. Cross-validation percent correct assignment (y-axis) of an individual to its original K-group given the number of K genetic groups under consideration (x-axis), for BET (left) and YFT (right). Shaded regions indicate confidence intervals surrounding assignment estimates.

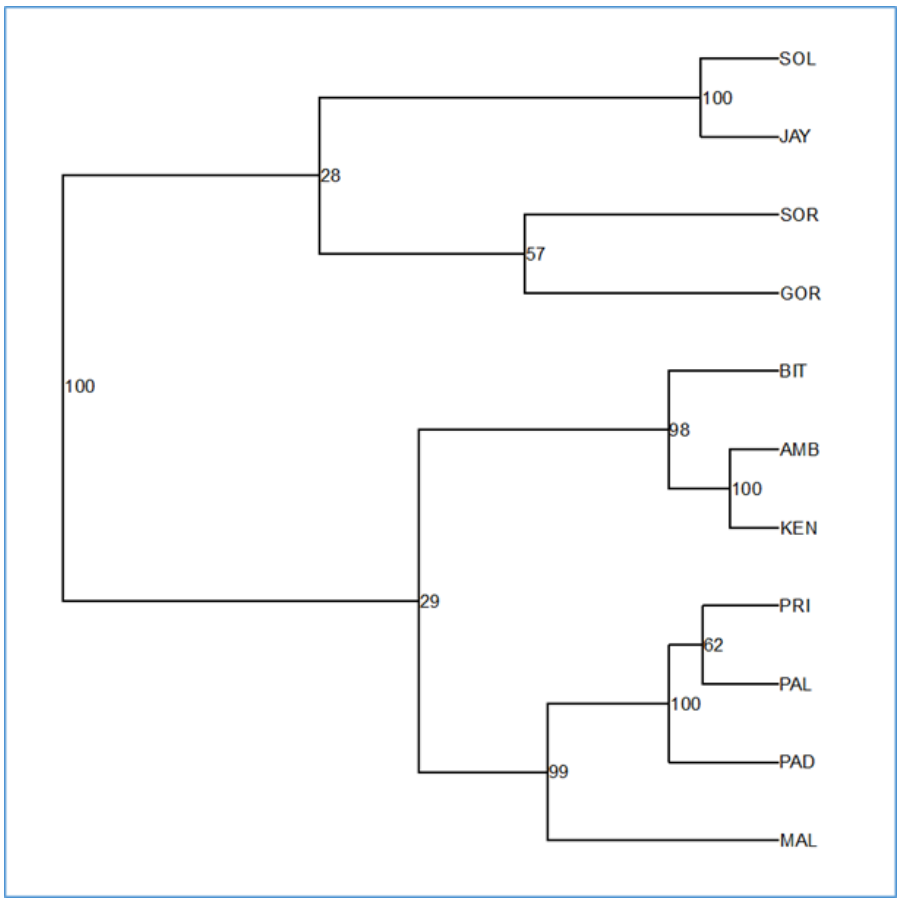


Figure 7.4. BET: Tree of genetic relatedness of each sample location, based on similarity as calculated using $F_{ST}$ measure of genetic differentiation between pairs of sample locations. Bootstrap values of reproducibility percentage are indicated for each node of the dendogram.

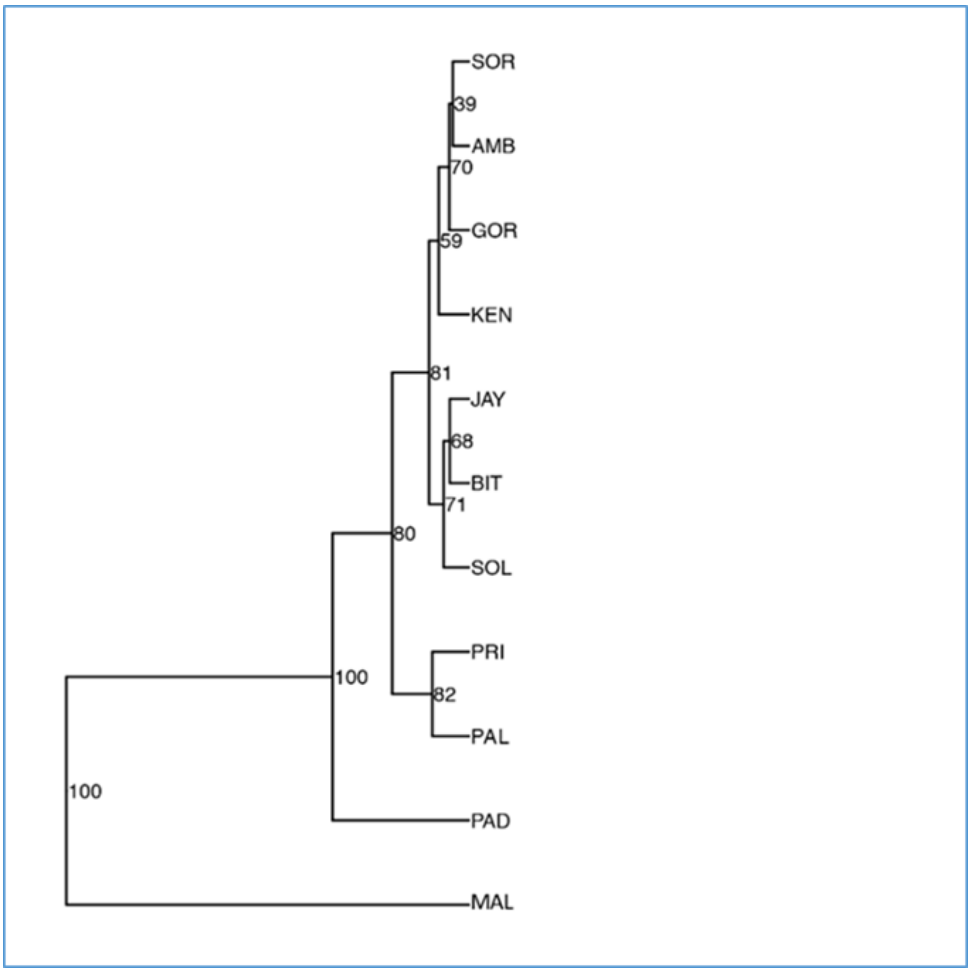


Figure 7.5. YFT: Tree of genetic relatedness of each sample location, based on similarity as calculated using $F_{ST}$ measure of genetic differentiation between pairs of sample locations. Bootstrap values of reproducibility percentage are indicated for each node of the dendrogram.

## 7.5 References (cited in Section 7)

Allendorf F. W., Hohenlohe P. A. and Luikart G. (2010). Genomics and the future of conservation genetics. Nat. Rev. Genet. 11, 697–709.

Altshuler D., Pollara V. J., Cowles C. R., Van Etten W. J., Baldwin J., Linton L. and Lander E. S. (2000). An SNP map of the human genome generated by reduced representation shotgun sequencing. Nature 407, 513-516.

Anon (2014). Commission for the Conservation and Management of Highly Migratory Fish Stocks in the Western and Central Pacific Ocean. Scientific Committee. Regular Session (10th : 2014 : Majuro, Marshall Islands). Tenth regular session, Majuro, Marshall Islands, 6-14 August 2014 : summary report. -- Majuro, Marshall Islands : Western and Central Pacific Fisheries Commission, 2014. 229 pp.

Appleyard S., Grewe P., Innes B., and Ward R. (2001). Population structure of yellowfin tuna (*Thunnus albacares*) in the western Pacific Ocean, inferred from microsatellite loci. Marine Biology 139, 383-393.

Baird N. A., Etter P. D., Atwood T. S., Currey M. C., Shiver A. L., Lewis Z. A., Selker E. U., Cresko W. A. and Johnson E. A. (2008). Rapid SNP discovery and genetic mapping using sequenced RAD markers. Plos One 3, e3376.

Beaumont M.A. and Nichols R.A. (1996). Evaluating loci for use in the genetic analysis of population structure. Proceedings of the Royal Society of London Series B: Biological Sciences 263, 1619-1626.

Benjamini Y. and Hochberg Y. (1995). Controlling the false discovery rate: a practical and powerful approach to multiple testing. Journal of the Royal Statistical Society Series B (Methodological) 57, 289-300.

Bekkevold D., FishPopTrace Consortium, Helyar S. J., FishPopTrace Consortium, Limborg M. T., FishPopTrace Consortium, Nielsen E. E., FishPopTrace Consortium, Hemmer-Hansen J., FishPopTrace Consortium, Clausen L. A. W., FishPopTrace Consortium, Carvalho G. R., FishPopTrace Consortium (2015). Gene-associated markers can assign origin in a weakly structured fish, Atlantic herring, ICES Journal of Marine Science, 72, 1790–1801.

Courtois B., Audebert A., Dardou A., Roques S., Ghneim- Herrera T., Droc G., Frouin J., Rouan L., Goze E., Kilian A., Ahmadi N. and Dingkuhn M. (2013). Genome-wide association mapping of root traits in a japonica rice panel. PloS one 8, e78037.

Cruz V.M.V., Kilian A. and Dierig D.A. (2013). Development of DArT marker platforms and genetic diversity assessment of the US collection of the new oilseed crop *Lesquerella* and related species. PloS one 8, e64062.

Dammannagoda S. T., Hurwood D. A. and Mather P. B. (2008). Evidence for fine geographical scale heterogeneity in gene frequencies in yellowfin tuna (*Thunnus albacares*) from the north Indian Ocean around Sri Lanka. Fish. Res. 90, 147–157.

Davey J. W., Hohenlohe P. A., Etter P. D., Boone J. Q., Catchen J. M. and Baxter M. L. (2011). Genome-wide genetic marker discovery and genotyping using next-generation sequencing. Nat. Rev. Genet. 12, 499–510.

Davies N., Shelton H., Hampton J., and McKenzie S. (2014). Stock assessment of the yellowfin tuna in the western and central Pacific Ocean. WCPFC-SC10-2014/SA- WP-04.

Diaz-Jaimes P. and Uribe-Alcocer M. (2006). Spatial differentiation in the eastern Pacific yellowfin tuna revealed by microsatellite variation. Fisheries Science 72, 590-596.

Elshire R. J., Glaubitz J. C., Sun Q., Poland J. A., Kawamoto K., Buckler E. S. and Mitchell S. E. (2011). A robust, simple genotyping-by-sequencing (GBS) approach for high diversity species. PloS one 6, e19379.

Ely B., Viñas J., Alvarado Bremer J. R., Black D., Lucas L., Covello K., Labrie A. V. and Thelen E. (2005). Consequences of the historical demography on the global population structure of two highly migratory cosmopolitan marine fishes: the yellowfin tuna (*Thunnus albacares*) and the skipjack tuna (*Katsuwonus pelamis*). BMC Evolutionary Biology 5(1), 19.

Foster S.D., Feutry P., Grewe P., Berry O., Hui F. K. C., and Davies C. (2018). Reliably discriminating stock structure with genetic markers: Mixture models with robust and fast computation. . Mol Ecol Resour. 2018;00:1–16. https://doi.org/10.1111/1755-0998.12920

Grewe P. M., Krueger C. C., Aquadro C. F., Bermingham E., Kincaid H. L., and May B. (1993). Mitochondrial DNA variation among lake trout (*Salvelinus namaycush*) strains stocked into Lake Ontario. Can. J. Fish. Aquatic. Sci. 50, 2397-2403.

Grewe P. M. and Hampton J. (1998). An assessment of bigeye (*Thunnus obesus*) population structure in the Pacific Ocean, based on mitochondrial DNA and DNA microsatellite analysis. School of Ocean and Earth Science and Technology Publication 98-05, Joint Institute for Marine and Atmospheric Research Contribution 98-320.

Grewe P. M., Feutry P., Hill P. L., Gunasekera R. M., Schaefer K. M., Itano D. G., Fuller D. W., Foster S. D., Davies C. R. (2015). Evidence of discrete yellowfin tuna (*Thunnus albacares*) populations demands rethink of management for this globally important resource. Scientific Reports, 5, 16916. doi:10.1038/srep16916.

Hampton J. and Fournier D.A. (2001). A spatially disaggregated, length-based, age-structured population model of yellowfin tuna (*Thunnus albacares*) in the western and central Pacific Ocean. Marine and Freshwater Research 52, 937-963.

Hauser L. and Ward R. D. (1998). Population identification in pelagic fish: the limits of molecular markers. In: Advances in molecular biology (ed Carvalho G.R.). IOS Press.

Itano D. G and Holland K. N. (2000). Movement and vulnerability of bigeye (*Thunnus obesus*) and yellowfin tuna (Thunnus albacares) in relation to FADs and natural aggregation points. Aquatic Living Resources 13, 213-223.

Jombart T. (2008). adegenet: a R package for the multivariate analysis of genetic markers. Bioinformatics 24, 1403-1405.

Kilian A., Wenzl P., Huttner E., carling J., Xia L., Blois H., Caig V., Hller-Uszynska K., Jaccoud D., Hopper C., Aschenbrenner-Kilian M., Evers M., Peng K., Cayla C., Hok P. and Uszynski G. (2012). Diversity arrays technology: a generic genome profiling technology on open platforms. In: Data Production and Analysis in Population Genomics (eds Pompanon F. and Bonin A.). Springer Nature Switzerland.

Langley A., Wright A., Hurry G., Hampton J., Aqorua T. and Rodwell L. (2009). Slow steps towards management of the world's largest tuna fishery. Marine Policy 33, 271-279.

Nielsen E. E., Cariani A., Aoidh E. M., Maes G. E., Milano I., Ogden R., Taylor M., Hemmer-Hansen J., Babbucci M., Bargelloni L., Bekkevold D., Diopere E., Grenfell L., Helyar S., Limborg M. T., Martinsohn J. T., McEwing R., Panitz F., Patarnello T., Tinti F., Van Houdt J. K. J., Volckaert F. A. M., Waples R. S., FishPopTrace c., Albin J. E. J., Vieites Baptista J. M., Barmintsev V., Bautista J. M., Bendixen C., Bergé J.-P., Blohm D., Cardazzo B., Diez A., Espiñeira M., Geffen A.J., Gonzalez E., González-Lavín N., Guarniero I., Jeráme M., Kochzius M., Krey G., Mouchel O., Negrisolo E., Piccinetti C., Puyet A., Rastorguev S., Smith J. P., Trentini M., Verrez-Bagnis V., Volkov A., Zanzi A., and Carvalho G. R. (2012). Gene-associated markers provide tools for tackling illegal fishing and false eco-certification. Nature Communications 3, 851.

Palsbøll P. J., Berube M. and Allendorf F. W. (2007). Identification of management units using population genetic data. Trends in Ecology & Evolution 22, 11-16.

Palumbi S. R. (1994). Genetic divergence, reproductive isolation, and marine speciation. Annual Review of Ecology and Systematics, 547-572.

Peterson B. K., Weber J. N., Kay E. H., Fisher H. S. and Hoekstra H. E. (2012). Double Digest RADseq: An inexpensive method for De Novo SNP discovery and genotyping in model and non-model species. Plos One 7, e37135.

Pritchard J. K., Stephens M. and Donnelly P. (2000). Inference of population structure using multilocus genotype data. Genetics 155, 945-959.

Qiu F.and Miyamoto M. M. (2011). Use of nuclear DNA data to estimate genetic diversity and population size in Pacific Bluefin and Yellowfin Tuna (*Thunnus orientalis* and *T. albacares*). Copeia 2011, 264-269.

Raman H., Raman R., Kilian A., Detering F., Carling J., Coombes N., Diffey S., Kadkol G., Edwards D., McCully M., Ruperao P., Parkin I. A. P., Batley J., Luckett D. J. and Wratten N. (2014). Genome-wide delineation of natural variation for pod shatter resistance in Brassica napus. PloS one 9, e101673.

Royce W. F. (1964). A morphometric study of yellowfin tuna *Thunnus albacares* (Bonnaterre). Fish Bull 63, 395-443.

Schaefer K. M. (1991). Geographic variation in morphometric characters and gill raker counts of yellowfin tuna Thunnus albacares from the Pacific Ocean. Fishery Bulletin 89, 289-297.

Schaefer K. M. (1992). An evaluation of geographic and annual variation in morphometric characters and gill-raker counts of yellowfin tuna, *Thunnus albacares*, from the Pacific Ocean. Inter-American Tropical Tuna Commission bulletin 20, 133-163.

Schaefer K. M. (2009). Stock structure of bigeye, yellowfin, and skipjack tunas in the eastern Pacific Ocean. Inter-Amer Trop Tuna Comm, Stock Assess Rep 9, 203-221.

Schaefer K. M., Fuller D. W. and Block B. A. (2011). Movements, behavior, and habitat utilization of yellowfin tuna (*Thunnus albacares*) in the Pacific Ocean off Baja California, Mexico, determined from archival tag data analyses, including unscented Kalman filtering. Fisheries Research 112, 22-37.

Scoles D. and Graves J. E. (1993). Genetic analysis of the population structure of yellowfin tuna, *Thunnus albacares*, from the Pacific Ocean. Fishery Bulletin US 91, 690-698.

Sibert J.and Hampton J. (2003). Mobility of tropical tunas and the implications for fisheries management. Marine Policy 27, 87-95.

Waples R. S. (1998). Separating the wheat from the chaff: patterns of genetic differentiation in high gene flow species. Journal of Heredity 89, 438-450.

Waples R. S. and Gaggiotti O. (2006). What is a population? An empirical evaluation of some genetic methods for identifying the number of gene pools and their degree of connectivity. Molecular Ecology 15, 1419-1439.

Ward R.D. (2002). Genetics of fish populations. In: Handbook of Fish Biology and Fisheries, Volume 1: Fish Biology (eds Hart P. J. B and Reynolds J. D.). Blackwell Science.

Ward R. D., Elliott N. G., Grewe P. M. and Smolenski A. J. (1994). Allozyme and mitochondrial DNA variation in yellowfin tuna (*Thunnus albacares*) from the Pacific Ocean. Marine Biology 118, 531-539.

Ward R. D., Elliott N. G., Innes B. H., Smolenski A. J. and Grewe P. M. (1997). Global population structure of yellowfin tuna, *Thunnus albacares*, inferred from allozyme and mitochondrial DNA variation. Fishery Bulletin 95, 566-575.

Willette D. A., Allendorf F. W., Barber P. H., Barshis D. J., Carpenter K. E., Crandall E. D., Cresko W. A., Fernandez-Silva I., Matz M. V., Meyer E., Santos M. D., Seeb L. W. and Seeb J. E. (2014). So, you want to use next-generation sequencing in marine systems? Insight from the Pan-Pacific Advanced Studies Institute. Bulletin of Marine Science 90, 79-122.

# 8. General Discussion

This study's primary goal was to investigate presence or absence of structure in YFT and BET populations across Indonesia's oceanic waters (both archipelagic and non-archipelagic) and the degree of connectivity of those populations to adjacent regions in the Indian and Western Pacific Oceans. The outcomes were to assist Indonesia and international partners (primarily through the RFMOs) in developing management measures on appropriate geographic scales for these two important tuna species. The study was intended as a first exploration of the population structure and not entered into with expectation of a comprehensive, fully definitive outcome, especially given that the resources of the project limited the study to one life-history stage; juvenile tunas of average 4 – 5 months of age.

The investigation employed the three techniques – genetics (using next generation sequencing), otolith chemistry (analyses of stable isotopes and elemental chemistry), and parasites (characterisations of parasite species and abundances). This multi-technique approach was considered the best way of having 'a strong first look' at the degree of population structure, recognising that each of these techniques have strengths and limitations for providing definitive answers. We thought that by employing the three techniques together, as had been done earlier by others (Buckworth et al. 2007; Welch et al. 2009), the likelihood of achieving an informative and useful 'picture' of the degrees of movement and connectivity of the tunas across a broad geographic range was high.

The three techniques have provided outcomes that overall are in agreement. The outcomes of the genetics analyses suggest at least 2 or 3 genetic groupings ("a subtle genetic structure") for both species of tuna and with clines of genetic variation across the geographic range, consistent with an isolation by distance model. Within the BET samples there were three reliably identifiable genetic groups and two such groupings among the YFT samples, and the groupings for both species appeared temporally stable, with similar patterns evident for the 2013 and 2014 samples. The most significant differentiation, based on the DNA profiles, was between the fish from the two outlier locations, Maldives (central Indian Ocean) and the Solomon Islands (western Pacific Ocean).

The outcomes from the parasites characterisations and otolith chemistry analyses concur with the genetics outcomes in suggesting multiple populations for both species across the geographic range of the study. The patterns of prevalence and abundance of didymozoid parasites suggested limited to no movement of fish westwards from the Indonesian archipelago into the eastern and central Indian Ocean, and also very restricted movement from the Western Pacific Ocean westwards into the Indonesian archipelago. Therefore, the outcomes from the parasites indicated at least three groups (populations) based on the YFT and BET dissected in the study, and overall the patterns were similar from both the 2013 and 2014 samples. A higher number of significant differences in parasite abundances across the range was observed for YFT compared to BET, a result possibly influenced by more YFT having been sampled and by parasites being more abundant in YFT in general. However, it could also indicate that juvenile YFT show more regional fidelity than BET.

The overall outcome from the otolith chemistry analyses, using both stable isotopes and elemental chemistry, was that YFT and BET had not moved large distances in their first 4 – 6 months of life. Based on discriminant function analyses of both otolith chemistry data sets, the majority of fish were classified to the FMAs where they had been captured or to nearby FMAs. The differentiation of fish sampled at the outlier sites (Maldives and Solomon Islands) from those sampled within the Indonesian FMAs was not as strong for either species compared to that for the genetics and parasites (e.g. a small percentage of fish sampled at these outlier regions were classified to Indonesian FMAs based on their otolith chemistry). This is due in part to the nature of otoliths, with each of the measured stable and elemental isotopes occurring in all otoliths, and the nature of otolith chemistry data, which are continuous rather than being a discrete measure of presence or absence (such as the parasite data). In addition, there are many factors that can influence the otolith data, such as

ontogenetic effects, maternal effects and water chemistry. For example, widely separated sampling regions with similar ocean environments could result in similar otolith chemistry, without any mixing of fish between the regions. More information about oceanography and these other factors would be required to draw stronger conclusions.

Examination of the spatial dynamics of these two tuna species, which were based on mark-recapture tagging studies of juveniles similar to the size and age to those in the current study, have shown mixed results with respect to regional fidelity. Tagging studies carried out in the Western and Central Pacific Oceans, and including fish tagged in Indonesian archipelagic waters (Schaefer et al. 2015; SPC 2012), showed low levels of long-distance movements (> 500 nmi) from points of release. Similarly, movements of YFT and BET, tagged in Western Pacific regions (including Solomon Islands) to east of Indonesia, into Indonesian EEZ waters were also observed to be at low level (SPC 2012). In contrast, large scale tagging of YFT and BET in the western Indian Ocean showed a higher proportion of long distance movements (average distances travelled of 710 nmi and 657 nmi for YFT and BET respectively) and lower levels of regional fidelity (Hallier and Million 2009).

The outcomes of this study are a useful contribution to the discussions and planning around current development of harvest strategies and regional management for Indonesia's tuna fisheries. They further confirm that there is no or low level of mixing of stocks of both species between the Indian and Western Pacific Oceans. The results also suggest meta-populations with some degree of regional fidelity may well exist within the Indonesian archipelago, and therefore should be considered in scenarios of regional management, at level of FMA or other scales. Further research, especially on older fish, appears to be highly desirable.

# 9. Conclusions

- The results for the three techniques that were, overall, consistent, suggesting multiple populations for both species across the geographic range;
- The outcomes of the genetics analyses suggested at least 2 or 3 genetic groupings ("a subtle genetic structure") for both YFT and BET, with clines of genetic variation across the geographic range;
- The patterns of prevalence and abundance of parasites suggested limited to no movement of fish (both species) westwards from the Indonesian archipelagic waters (IAW) into the eastern and central Indian Ocean, and also little movement from the Western Pacific Ocean westwards into the Indonesian archipelago. These results indicate at least three groups (populations) for each species, and the overall patterns were similar across years;
- The overall outcome from the otolith chemistry analyses, using both stable isotopes and elemental chemistry, was that the YFT and BET had not moved large distances in their first 4 - 6 months of life;
- These conclusions need to be qualified by the fact that the population structure study was based on samples from young-of-the-year tuna and the assumption that these individuals had not migrated substantial distances from the areas in which they were spawned. Further studies on other life history stages (ideally mature fish, and/or larvae) are required to substantiate, or refute, these conclusions;
- These results suggest that the current national and regional governance arrangements are likely to be consistent with the structure and connectivity of YFT and BET populations. That is, the Indian and Western Central Pacific Oceans being managed as separate stocks, by the respective Commissions, and IAW having higher connectivity (as indicated by estimates of gene flow) with adjacent WCPO waters, than with EIO waters;

- With respect to structure and connectivity in IAW, the results do not allow firm conclusions to be drawn on the appropriate scale of assessment management of its tuna fisheries within IAW (by FMA, multiple FMAs, or other scale). However, given the scale of movements documented from previous conventional tagging studies and the estimated level of gene-flow among neighbouring FMAs in IAW (713,714,715) and those bordering the WCPO (716, 717) reported here, it is likely that connectivity between these FMAs for both species is sufficiently high that they should be assessed and managed as a single management unit, consistent with current arrangements;
- An important outstanding question, which is not adequately resolved by this study, is the level of connectivity between IAW and adjacent areas of the WCPO. This connectivity is an important component of estimating the contribution of recruitment and adult biomass in the different areas to the populations overall and the relative impacts and sustainability of harvests in each area. Addition sampling over a number of years and use of other methods, such as Close-kin Mark Recapture have the potential to address this question directly;
- The population structure study engaged participating Indonesian scientists in planning, design and execution of large-scale field sampling, new methods in genetics, otolith chemistry, otolith morphology, and parasite characterisations, and for four of them this included substantial training in Australian institutions. Individual scientists have already been using these new skills to participate in new projects, both independently and as part of new collaborative projects with CSIRO.

## Appendix 1 Sampling protocol

# ACIAR PROJECT FIS/2009/059

# SAMPLING PROTOCOL
# FOR POPULATION STRUCTURE STUDY


Australian Government
Australian Centre for
International Agricultural Research



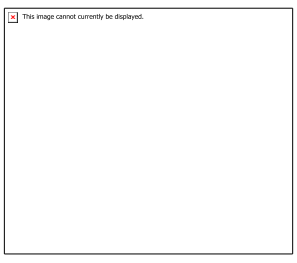

# Contents

# 1. Introduction

In August 2012 Research Centre for Capture Fisheries (RCFMC) commenced a 4 year collaboration project with CSIRO Marine and Atmospheric Research (CSIRO) on tuna fisheries; a next phase project as follow-on to earlier Australia – Indonesia collaborations in tuna fisheries research, spanning more than 20 years. The project, ***"Developing research capacity for management of Indonesia's pelagic fisheries resources"***, is co-funded by Australian Centre for International Agricultural Research (ACIAR) and CSIRO, with in-kind contributions from RCFMC. The overall aim of the project is to improve Indonesia's capacity to assess and manage its tuna fisheries by addressing key information gaps with particular reference to yellowfin tuna (YFT), *Thunnus albacares*, and bigeye tuna (BET), *Thunnus obesus*, and, in the course of doing so, to improve Indonesia's pelagic fisheries research capacity.

The objectives of the abovementioned project fall within three primary components:

1. Defining the population structures of tunas in Indonesia's archipelagic waters and connectivity to populations in adjoining regions;
2. Assessing and characterising Indonesia's tuna fisheries that are based around Fish Aggregating Devices (FADs), and;
3. Communication of the project's findings and recommendations.

This manual of sampling protocols is specifically relevant to the population structure study and the objectives of this study are as follows:

1. Using three independent, complementary techniques - genetics, otolith (ear bones) chemistry and parasite loads, to determine the degree of population structure and connectivity of the tunas over a wide geographical range;
2. Advise, in consultation with the relevant Regional Fisheries Management Organisations, on the implications of the results of the above investigation for approaches to assessment and management of fisheries harvesting these stocks;
3. Provide capacity development for Indonesian scientists in the aforementioned analytical techniques.

# 2. Sampling objectives and priorities

The plan for the first round of sampling for the population structure study includes sampling YFT and BET from nine locations across Indonesia (Figure 1) and from at least two 'outlier' locations in the Indian and Western Pacific Oceans. The primary objective is to obtain sufficient samples of both species, from each location, to enable statistically robust investigation of the level of variation in genetic characters, otolith chemistry, and parasites within and between samples. Four key priorities of the plan are as follows:

1. **To standardise, to as highest level as possible, in all sampling techniques**, to minimise the possibility of introducing 'artificial' variations in the results of the analyses through differences in sampling methods between sampling teams;
2. **To maximise the quality** of fish sampled, the quality of samples obtained, and the quality of the samples on arrival from the field to the laboratory;

3. **To collect the samples from all sampling locations, simultaneously**, in as short time-window as possible, to minimise temporal variability;
4. **To ensure all samplers, before going to the field, are competent and confident in methods of identification of juvenile YFT and BET.** The importance of this cannot be overstated.

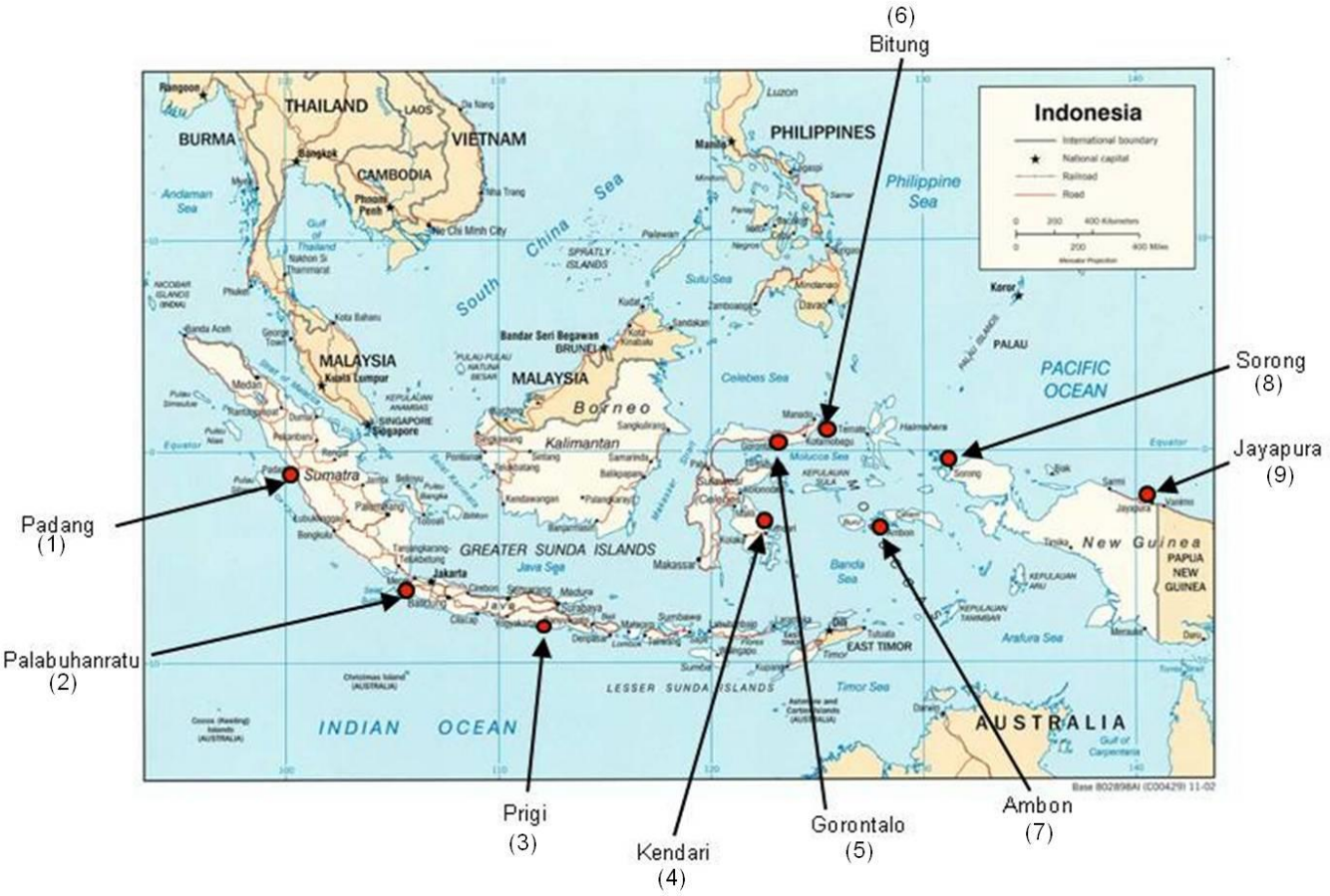


**Figure 1.** The 9 sampling locations in Indonesia.

# 3. Protocols for obtaining the fish

- Ideally, **prior arrangements** will have been made with fishers and/or fishing companies at each location, with assistance of local contacts, to maximise the likelihood of access to good quality fish, and remove the need to go through auction process. The best situation would be prior arrangement with fishing skipper(s) so that the small fish are sorted by species at sea and placed into boxes or crates for ready access and purchase on arrival into port;
- **Sampling teams need to be able to hand-pick the fish** wherever possible, to ensure best quality and size of fish;
- **Our target size range is 30 – 50 cm LCF** (i.e. 0+ fish). If you have access to smaller fish (e.g. 20 – 29cm), in good condition, these can be included.
- **The project has budget to purchase the fish**, but after the biological samples are taken the fish are no longer needed. Prior to sampling, discussions should be had with local fisheries authorities and/or port authorities to determine to whom the fish can be donated (e.g. local charity or local community association). Some fish

can be given to local staff who have provided assistance, but donating to local community will help build good relationships;
- Ideally, after purchase, the fish will be put **as soon as possible into crushed ice**, in polystyrene boxes (either borrowed or purchased at the fishing port), or placed into a cool-room (not freezer) if available;
- Ideally the fish **will be obtained as early as possible in the day** to allow time for the biological sampling during remainder of the morning – afternoon;
- As much information as possible about how and where the fish were caught needs to be obtained. This is to be recorded on the Tuna Sampling Data Sheets.

# 4. Facilities for biological sampling

For the benefit of you, as samplers, but also for achieving the best quality samples, it is important you establish a good base for your biological sampling after arrival at each location. Ideally, the facility you use as your 'lab' will be located not too far from the fish landing place e.g. in a space within the fishing port, or a facility provided by Port Authority or by a fishing company. Your lab could also be a space onboard a fishing vessel, if you have a good relationship with the skipper who sold you the fish!

Your facility for biological sampling should include the following:
- Sufficient space for you and your team to work comfortably, and sufficient space for the fish boxes and your sampling equipment;
- Ideally a table or bench to allow you to work on the fish without having to bend over;
- Sufficient light so you can see what you are doing;
- Sufficient shade and ventilation so you can breathe and don't get too hot!
- Ready access to clean water, for washing your knives, scalpels, tweezers, and for washing your hands.

# 5. Biological sampling procedures

The following is the recommended order of steps in your biological sampling. Keeping to this order is important for the standardisation of sampling across locations and across sampling teams.

## 5.1 Confirming species ID

It is critically important that you confirm the species ID of every fish prior to the samples being taken from that fish. This should be done with both external features and internal examination of liver and swim-bladder. Yellowfin and bigeye tunas can be easily misidentified at small size, particularly if the fish have lost condition since capture and external markings have faded. A combination of characters should be checked to ensure correct identification.

**See Appendix for extracts from the David Itano guides**[13] for identification of yellowfin and bigeye at small size.

[13] *Itano, D. (2004) Manual for the identification of yellowfin and bigeye tunas in fresh condition. For the 17th Meeting of the Standing Committee of Tuna and Billfish, Majuro, Marshall Islands (9 to 18 August 2004), Working Group on Fishing Technology, INF-FTWG -5*

## 5.2 Tuna Sampling Data Sheet

The Tuna Sampling Data Sheet (see example in Appendix 1) is your main system of recording. **Please use a new sheet for each new batch of fish that you sample**, and a separate sheet for each species. The sheets will already be labelled with "YELLOWFIN" or "BIGEYE". A **"batch"** may be a sample of fish you have obtained from one vessel, or possibly a sample you have obtained from a vessel owner or fishing company and may be mixed catch from more than one vessel. On the reverse side of the sheet there is space to record more detailed information about the source of the fish in each batch. This information is very important, as it may help with understanding any differences that we see in the analyses, among and between samples.

## 5.3 Specimen number, vials, and labels

Among all the information that you record on the Tuna Sampling Data Sheet and on the on the sample vials and on the labels for each sample, **the Specimen number is the most important**. Errors in recording the Specimen Nos. can be a disaster for the project.

The specimen numbering system we will use for this 2nd round of sampling for the project is **a simple code: The location number - 2 (for round 2).- the species ("Y" or "B") - the fish no.(3 digits).**

As example, if you are sampling the 24th yellowfin tuna in Kendari (which has location no. 4 – see full list of numbers below), its Specimen No. will be "4-2-Y-024". If you are sampling the 43rd bigeye tuna in Jayapura (which has location no. 9), its specimen number will be "9-2-B-043".

This system of numbering will mean each sampling team can generate their specimen numbers independent of the other teams, but it does rely on the sampling teams knowing the last Specimen No. to be assigned for each species at their sampling locations.

The Indonesian sampling location numbers are as follows (moving West to East):

1 – Padang

2 – Palabuhanratu

3 – Prigi

4 – Kendari

5 – Gorontalo

6 – Bitung

7 – Ambon

8 – Sorong

9 – Jayapura

Other Indonesian locations, already used for parasites preliminary training:
10 – Kedonganan (fish caught south of Lombok), 11 – Muara Baru (fish caught south of Sumbawa)

Outlier Sites: 12 – Maldives, 13 – Solomon Islands.

Ideally, your genetics sample vials and the BEEM capsules for otoliths should be labelled

with Specimen Numbers **BEFORE you begin a sampling session**. This will make your sampling sessions much more efficient and will reduce the likelihood of errors in the specimen numbering system.

It is important that the vials are labelled **by engraving the specimen number into the plastic** using a strong, sharp pointed instrument (e.g. the tip of your solid-blade scalpel) **and then over-written in black permanent pen**. The numbers and letter should be large and clear to read. If needed, the number can be written as two lines (Figure 2). This method of labelling makes the number easy to read but also ensures the number will never be lost. Permanent pen can rub-off with time or be lost in accidental spillages of solvents such as alcohol.

The engraving process is tedious but is worth the effort, because any loss of specimen numbers on the vials will be a disaster!

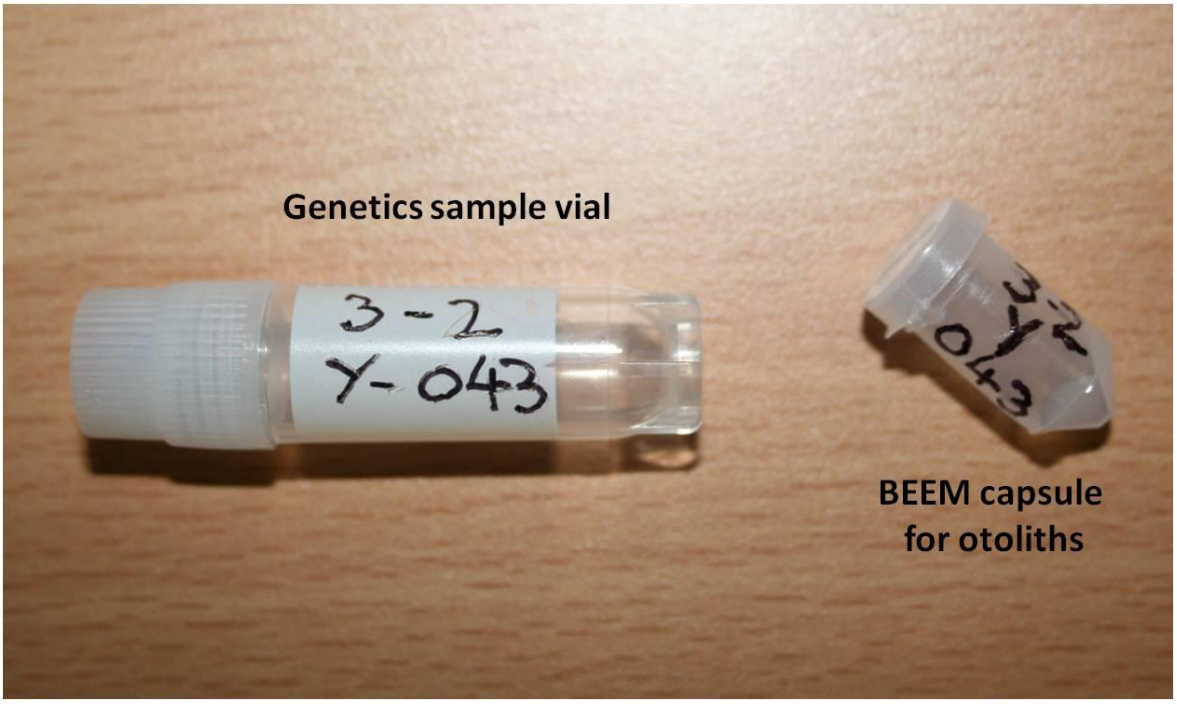


**Figure 2.** Illustrating the 2ml genetics sample vials ("cryo-vials") and polyurethane BEEM capsules for the otoliths. The Specimen Number is engraved into the vial and capsule and over-written in black permanent marker. "3-2-Y-043" means Location 3 (i.e. Prigi)-2nd time of sampling-Yellowfin-fish no. 43.

## 5.4 Measuring the fish

Measure the length (Length to Caudal Fork) of the fish to nearest half centimetre, using the ruler provided and record on the Tuna Sampling Data Sheet. The ruler should be taped down flat to whatever 'lab' bench you are using, and the fish measured on top of the ruler.

## 5.5 Sample for genetics

The **highest priority** in the taking of a sample for the genetics analyses is **to ensure there is no cross-contamination between samples**. Remember to only use bottled water (e.g. Aqua) for cleaning all instruments.

The following is the recommended procedure:

1. Clean one side of the fish using fresh tissues moistened with clean water to remove any blood and/or mucous on the skin;
2. Using a good sharp knife, make an incision on the cleaned side of the fish;


3. Take a slice of tissue that is about 1.5-2.5cm wide and no more than 5mm thick;


*This thinner slice (1.5cm wide ) is OK at 3mm thick*

*This thicker slice is OK about 1-2cm wide*

*Thicker slice BUT, NO more than 5mm thick!*

4. Transfer the muscle tissue sample direct **to the pre-labelled genetics sample vial**, again ensuring there is no contamination from your fingers at the mouth of the vial or on the inside of the vial lid. Push onto tube and trim away excess;

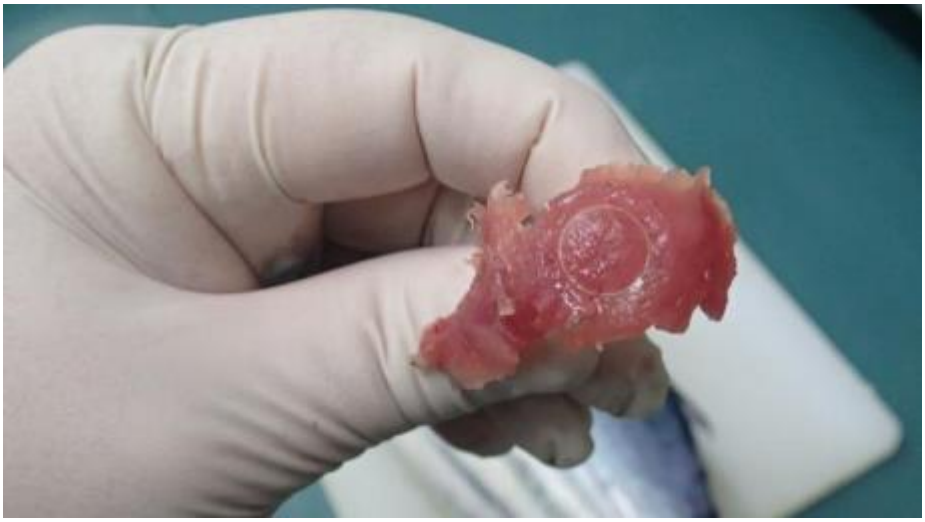

5. Move the muscle sample to the base of the vial, using a clean, blunt instrument and then, using a dropper pipette, top up the vial with **RNAlater buffer** but leave an air gap of about 5mm at the top so the buffer does not overflow. To avoid any chance of cross-contamination, ensure that the end of the pipette does not make contact with the muscle sample;

*Nicely trimmed, now Push the tissue disc into the tube a bit*

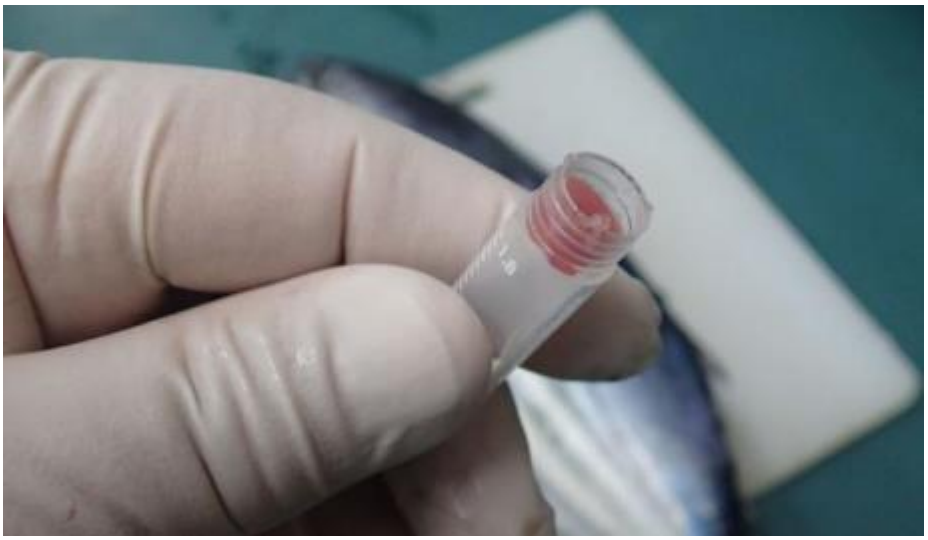

Push the tissue right down into the tube so that it is immersed in buffer, then tighten the cap onto tube.

6. Seal the vial with the lid and check that the information on the vial is correct, and tick the "Genetics sample" column on your Tuna Sampling Data Sheet to indicate a sample has been taken for that fish;
7. Place the sample vial onto ice, in a closed container (e.g. small cool-box or polystyrene box), **ensuring that the samples remain in order**.
8. At the end of the sampling session, the samples should be transferred to the Sample vial box. You will have a separate Sample vial box for each species and boxes for each of your sampling locations. **Do not mix the samples by species or locations.**
9. After the samples have been transferred to the Sample vial boxes, the boxes, with lids securely closed, should be placed on ice. The samples need to be kept cool, at < 4$^{o}$C, for at least the first 24hrs. After this time the samples can be transported at room temperature. For longer term storage, the samples should be stored in a refrigerator at 4 – 8 $^{o}$C.

## 5.6 Samples for parasites

The **highest priority** for the samples to be taken from each fish for the parasites **is to keep the samples as cold as possible** following dissection, and placed into a freezer at earliest opportunity. The steps should be as follows:

1. **Remove one complete gill 'basket'or the gills as two pieces** (individual left and right sides). Place into a ziplock plastic bag, accompanied by a waterproof-paper label onto which you have written clearly in pencil the date of sampling, the Specimen No., and the fish length (the latter useful as a cross-check);
2. **Remove the complete viscera** including the stomach, intestine, pyloric caeca and liver (Figure 5). Place into another ziplock bag accompanied by a matching label to that described above;
3. Staple the gill sample bag and the viscera sample bag together, to provide a complete sample-set for each fish. This is very important for later, when the samples are being examined in the laboratory;
4. Make sure both ziplock bags are properly closed, **and then freeze as soon as possible**. This is particularly important for the viscera sample as it will begin to degrade quickly if left unfrozen. If you have to wait until the sampling session is over before gaining access to a freezer, keep the samples buried in crushed ice during the sampling session;
5. Record onto the Tuna Sampling Data Sheet a "G" and "S" in the "Parasites column to confirm samples taken;
6. Use a larger ziplock bag to keep the samples from one batch of fish together, removing as much air as possible from the bags before closing them, to keep volume to a minimum.

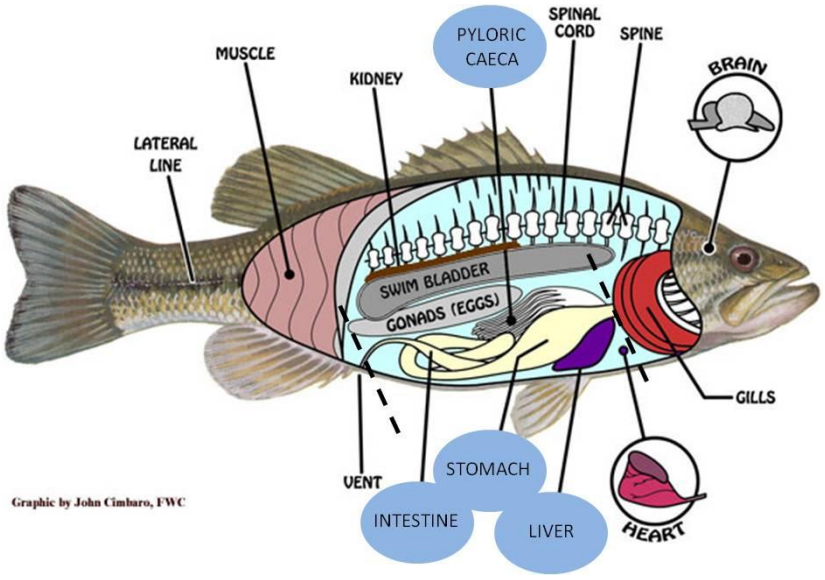


**Figure 5.** Illustrating the intestinal related organs (highlighted blue) to remove for the parasites sample: stomach, pyloric caeca, intestine, and liver. Modified from graphic of John Cimbaro (FWC).

## 5.7 Samples for otolith chemistry

Removal of otoliths from small tunas may appear difficult to you at first, but once you have done a few fish, you will quickly develop the skill. The trick is learning the feel and even the sound of the otoliths as you reach down into the bone cavities with your tweezers. In most cases you will use these senses, rather than relying on seeing the otoliths, to remove them from the cavities in which they lie.

It is important to wear surgical gloves during otolith removal and cleaning, to avoid contaminating the otolith surface with salts from your fingers. Cross-contamination between otoliths can also occur so washing your gloves between each fish will minimise the risk of this. Remember to only use bottled water (e.g. Aqua) for cleaning all instruments an your hands.

The recommended steps are as follows:

1. Lay the fish on its side on the plastic chopping board provided in your kit;
2. Using the sharp knife from your kit, and taking great care not to cut yourself, make vertical cut (dorsal – ventral) **at a point one eye-diameter distance from the posterior edge of the eye**, down to the level of an imaginary horizontal line across from the top of the eyes ( Figure 6). It is critically important that this vertical cut is no closer to the eyes than the one eye-diameter distance**. If you cut too close, you will cut right through the otoliths**!;
3. Then make a second cut; an almost horizontal cut at the level of the top of the eyes, but with a slight angle down (no more than $10^{o}$ from horizontal) towards the tail, to intersect with your first cut ( Figure 6);
4. You can now raise the top of the head, exposing the brain. This is called by some fisheries scientists the **"lifting-the-lid" technique of otolith removal** ( Figure 7);
5. Carefully move aside the brain tissue with your tweezers from the posterior area of the brain region. Do not discard the brain tissue, just in case you inadvertently entrap an otolith among that tissue while moving it. You may need to go through it later if you can't locate one or both of the otoliths!;

6. Using the fine pointed tweezers from your sampling kit, locate the otolith on the left or right, sitting in its cavity at the base of the brain-case. As mentioned above, you can feel and sometimes hear the otolith against the points of the tweezers;
7. Being careful not to crush the otolith, gently grasp the otolith with the tweezers and raise it from the fish;
8. Using a combination of the tweezers and your fingers, **very gently clean all the adhering tissue from around the otolith**. A clean tissue may also help to remove the tissue and fluid. Once the otolith is clean, place it onto the dark background provided in your kit, while you proceed to remove the second otolith;
9. The otoliths from these small tunas (Figure 8) are very fragile and it is likely that, even with care, you will unavoidably break some of the otoliths during removal from the fish or through cleaning. In most cases, **we can still use these broken otoliths, so retain all the pieces**;
10. Place the otoliths into the pre-labelled BEEM capsule (Figure2), after first checking that the Spec. No. on the capsule matches the Spec. No. for that fish on the Tuna Sampling Data Sheet (which of course should be the same number as that used for the genetics and parasite samples from that fish);
11. Record on the Tuna Sampling Data Sheet in the "Otoliths" column, using "L" & "R" to indicate whether you were successful in removing one or both otoliths;
12. Cap the BEEM capsule and place it into the Otolith sample box provided (1 box per species per sampling location), keeping the samples in the order sampled. Do not mix samples by species or by location.

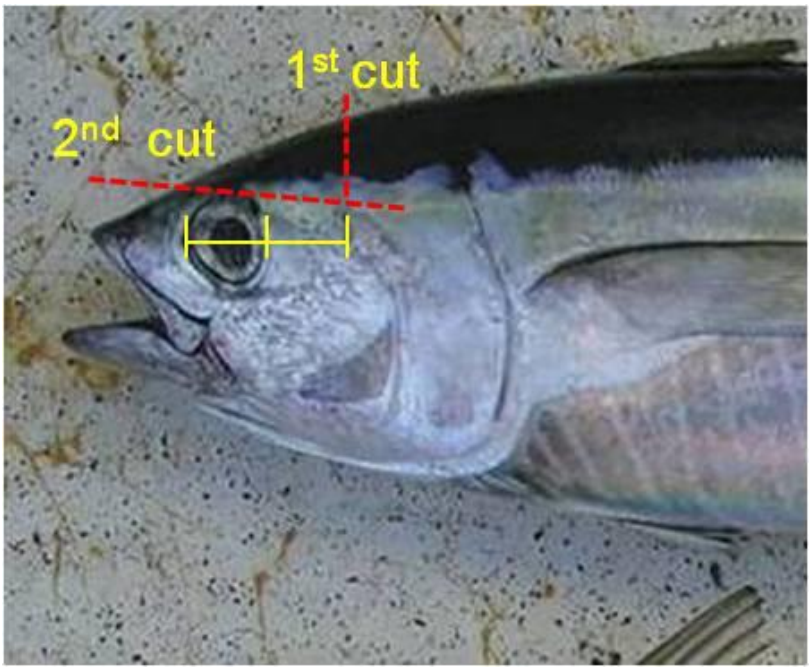


**Figure 6.** 'Lifting-the-lid' technique. 1st cut is made vertical, at one eye-diameter distance from rear margin of the eye. 2nd cut is almost horizontal at level of top of the eye.

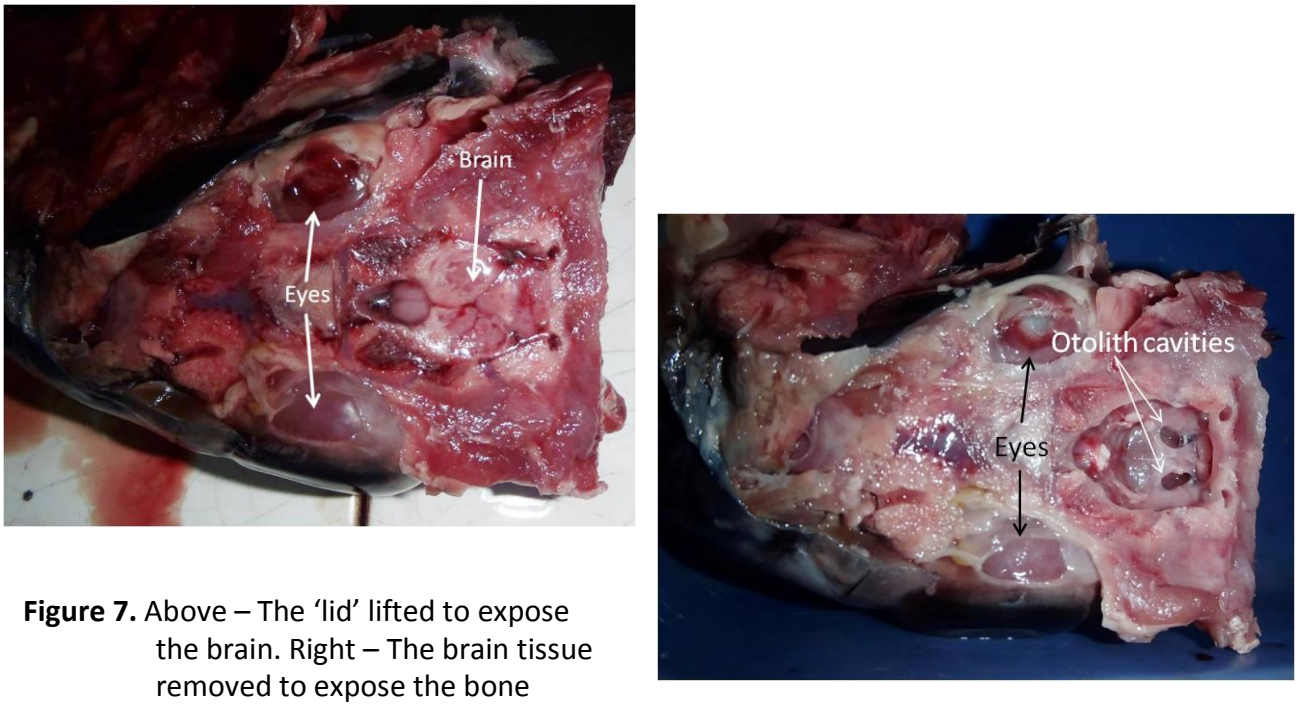


**Figure 7.** Above – The 'lid' lifted to expose the brain. Right – The brain tissue removed to expose the bone cavities in which the otoliths lie.

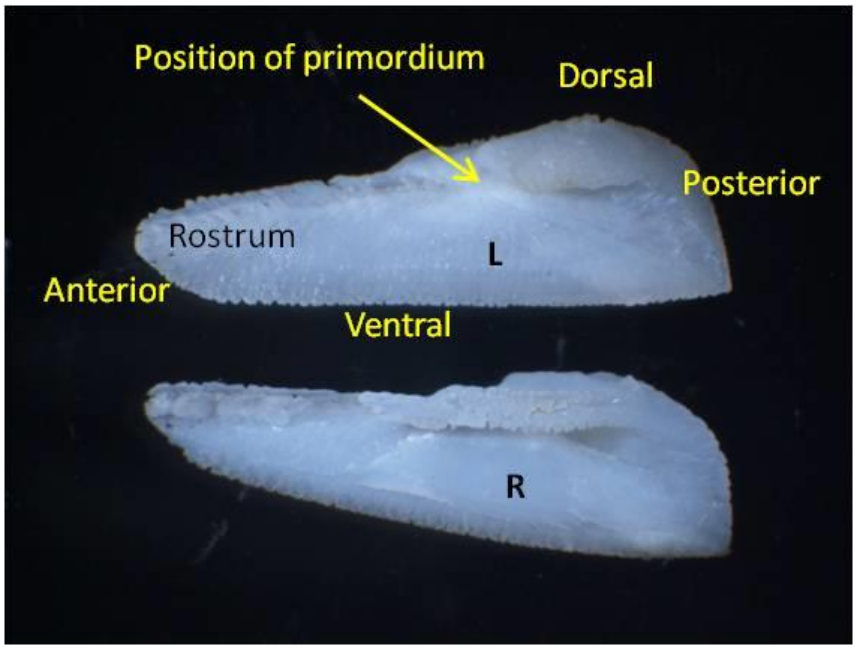


**Figure 8.** Left (L) and right (R) sagitta otoliths from a southern bluefin tuna. The otoliths from yellowfin and bigeye tunas are of a very similar shape to these and the rostrums (the anterior, 'pointed' projections, in otoliths of small tunas are delicate and easily broken.

# 6. Transporting frozen samples

The following are important recommendations for the transport of your frozen samples (i.e. samples collected for parasite analyses):

- If the cool-box is at room-temperature, it must be cooled before the samples are placed inside for transport. This can be done by cooling with crushed-ice or

by placing the cool-box into a freezer room or cool-room (e.g. the type used by fish processing company) for at least 30 minutes;

- The samples should be packed into the cool-box, surrounded by 'blue-ice' blocks which have been pre-frozen;
- All remaining space in the cool-box, between the samples and the blue-ice can be filled with balls of newspaper. These balls should also be pre-cooled;
- The lid of the cool-box should then be taped shut to prevent accidental opening during transport;
- Ideally, the cool-box should not be opened until the samples are ready to be transferred to the freezer at RIMF or to another freezer.

# 7. Appendix

Extracts from David Itano's manual[14] of identification of yellowfin and bigeye tunas:

- pectoral fin short, just reaching insertion of second dorsal fin
- pectoral fin thicker, stiffer and rounded at tip

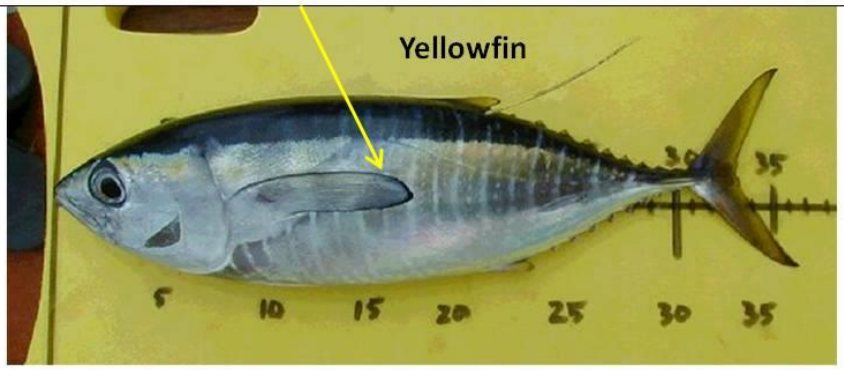


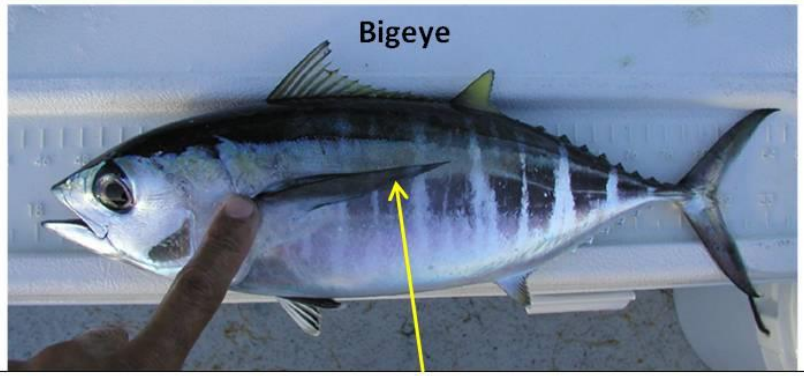


- pectoral fin slightly longer reaching second dorsal fin
- pectoral fin thin, flexible and pointed at the tip

[14] *Itano, D. (2004) A handbook for the identification of yellowfin and bigeye tunas in fresh condition. 17th Meeting of the Standing Committee on Tuna and Billfish, Majuro, Marshall Islands (9-18 August 2004), Fishing Technology Working Group, INF-FTWG-5.*

**Yellowfin (~ 33 cm)**

- Short, blunt pectoral fin
- Closely spaced markings of lines and rows of dots in chevron pattern extending to insertion of pectoral fin
- Shorter, smaller head, small, round eye
- Yellowish tail


**Bigeye (~ 34 cm)**

- Longer, pointed pectoral fin
- Irregular, white lines across body
- Large head, deep body, large eye
- Dusky colored tail

Larger fish
(approx 40 – 45cm LCF).

YFT (upper), BET (lower).
Very fresh condition.

## Internal characteristics

### 1. Liver shape and appearance

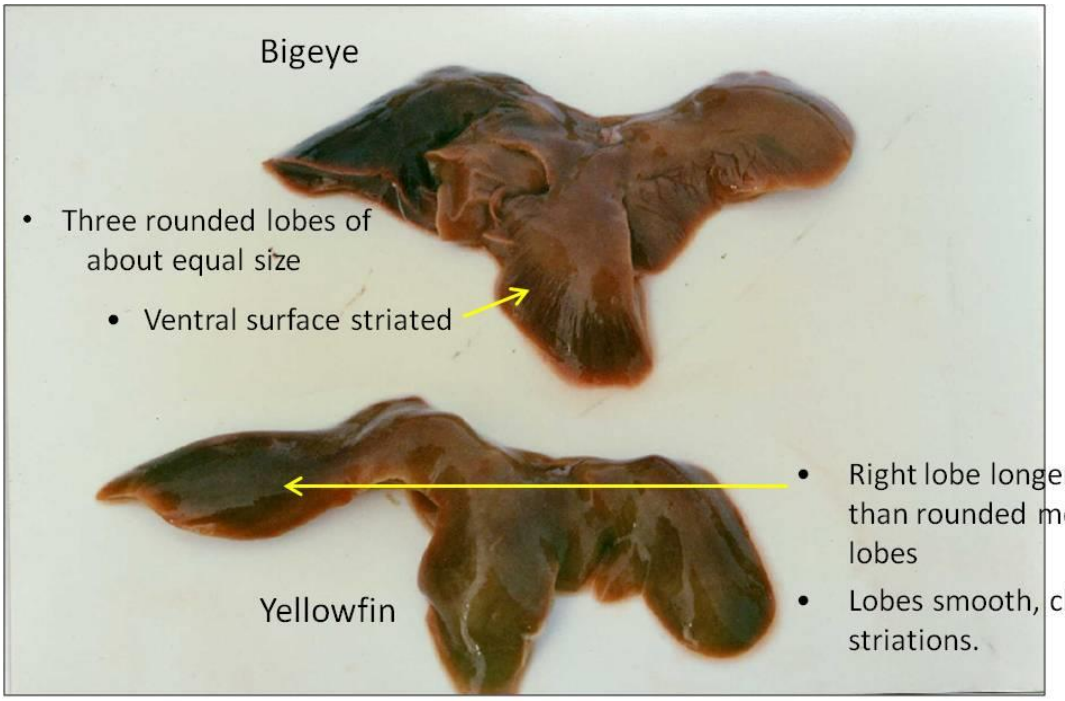


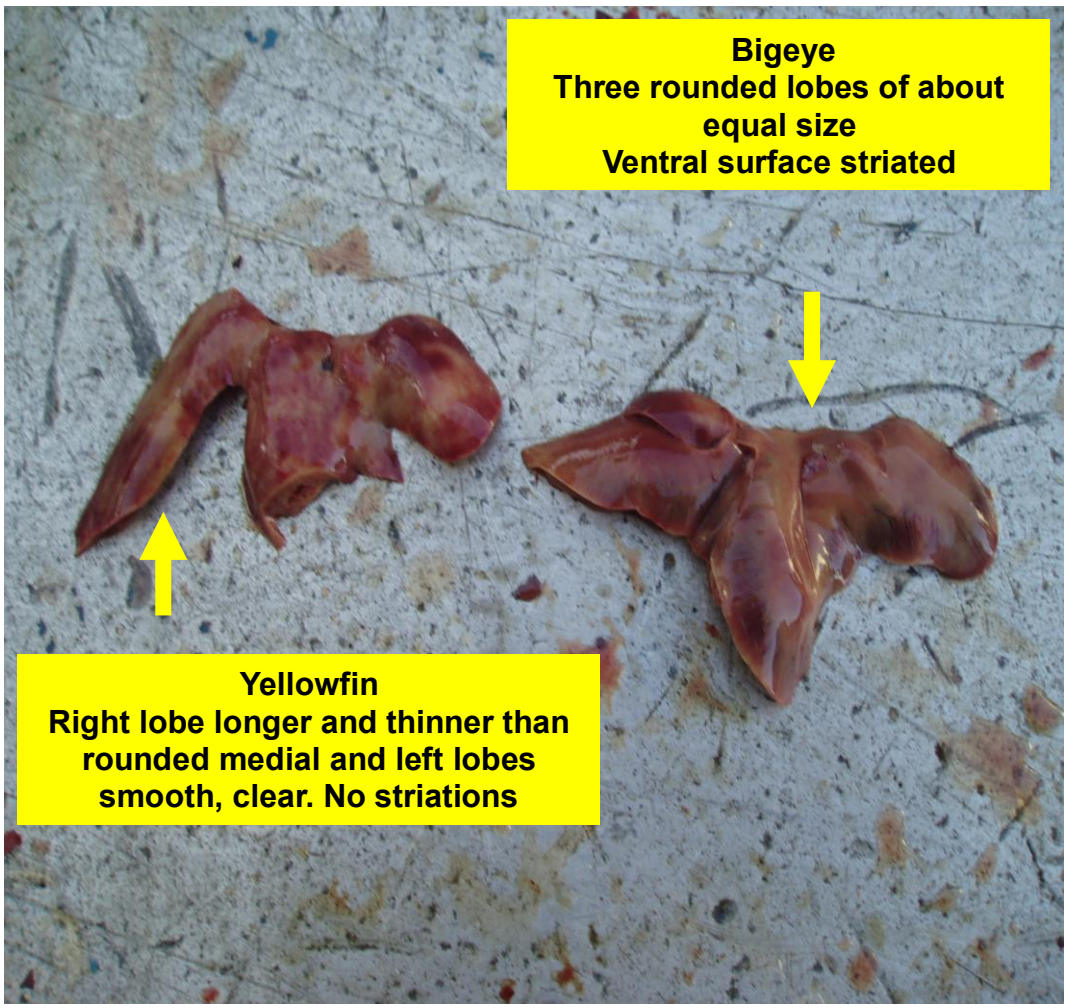

## Swim-bladder

- occupies almost entire body cavity
  - large, conspicuous, often inflated



- only in anterior half of body cavity
  - inconspicuous, usually deflated or slightly inflated

**Note:** In cases where the swim-bladder is fully or partially deflated, it is still possible to see the swim-bladder tissue and determine its length relative to the body cavity.

The fish you will be sampling for this population study are likely to have been in storage for at least 1 – 2 days and body markings will be faded and disappearing. However, in most cases it should still be possible to see some characteristic features, as in the example illustrated below for two fish of approx 45cm LCF:

YFT - Lines slightly curved, are evenly spaced and separated by rows of spots extending to below pectoral fin, still obvious and easy to recognize;

BET - Irregular vertical pale lines on bigeye have faded, but can still be recognized.

Here the length of the pectoral fins, the size of the eyes, and size of the head (relative to overall body size) are also useful in confirming the ID.

# Appendix 2 RNAlater recipe

**Recipe for an RNAlater-like buffer solution (for 1.5 litres):**

935 ml of autoclaved, MilliQ water (or good quality distilled water)

700 g Ammonium sulfate

Stir until dissolved

Add 25 ml of 1 M Sodium Citrate

And 40 ml of 0.5 M EDTA

Adjust to pH 5.2 using concentrated sulphuric acid, $H_2SO_4$ (about 20 drops= 1 ml)

Store at room temperature